Molecular and Cellular Characterization of Human Embryonic Stem Cell Derived Hepatocytes

Jenna L. Voellinger

A dissertation

submitted in partial fulfillment of the

requirements for the degree of

Doctor of Philosophy

University of Washington

2015

Reading Committee:

Edward J. Kelly, Chair

Yvonne S. Lin

Kenneth E. Thummel

Program Authorized to Offer Degree:

Pharmaceutics

University of Washington

Abstract

Molecular and Cellular Characterization of Human Embryonic Stem Cell Derived Hepatocytes

Jenna L. Voellinger

Chair of the Supervisory Committee:

Associate Professor Edward J. Kelly

Department of Pharmaceutics

Primary human hepatocytes are commonly used to evaluate liver drug metabolism and toxicity. Pluripotent stem cell derived hepatocytes (SCDHs) have the potential to overcome access and function-related limitations associated with primary hepatocytes. However, in order for SCDHs to become routinely used in preclinical drug metabolism and toxicity screening, they must demonstrate reproducible activity of drug metabolism proteins, particularly the oxidative CYP enzymes, and at a level comparable to that of primary human hepatocytes.

The work presented in this dissertation explores the potential of SCDHs to be used as an *in vitro* pre-clinical model for drug metabolism studies. Namely, we focus on further identifying how similar SCDHs are to primary human hepatocytes with regard to drug-metabolizing enzymes. Moreover, we performed genotype profiling on the commonly used human embryonic

stem cell lines (hESCs) to further identify their utility in pharmacogenetic screening. In addition, we investigated the miRNA expression profile of SCDHs to identify miRNA candidates that could improve the maturity of SCDHs.

Our data showed that SCDHs are immature compared to primary human hepatocytes in terms of the expression and activity of drug-metabolizing enzymes, notably the CYP enzymes. We found that SCDHs more closely resemble fetal hepatocytes regarding expression of hepatocyte markers, drug-metabolizing enzymes, transporters, and transcription factors. This translated into minimal CYP activity for only CYPs 1A and 3A when examining metabolite formation. In addition, we show that the miRNA expression profile of SCDHs compared to stem cells, cryopreserved hepatocytes and human liver tissue indicates global changes associated with immaturity in SCDHs. Taken together, our findings provide a more thorough characterization of SCDHs with regards to their use in drug metabolism studies, and provide insight into a possible mechanism to enhance the maturity and functionality of SCDHs. Additional studies are warranted to further evaluate the effect of the miRNAs identified here on the differentiation of hepatocytes.

Table of Contents

List of Figures

List of Tables

Acknowledgements

First and foremost I would like to thank my doctoral advisor, Dr. Edward Kelly, for his tireless effort and passion for my scientific and personal growth. He has helped me to grow tremendously as a scientist, I could not have had a better mentor.

To my thesis reading and doctoral supervisory committee members Drs. Thummel, Lin, Shen, and Kavanagh, and previous committee members Drs. Bloedow and Campbell, I wish to express my gratitude for their guidance, support, and scientific curiosity. They have vastly contributed to my personal and scientific growth.

I wish to thank Dr. Catherine Lockhart for her help generating the figures in Chapter 1. She is an immensely talented graphic designer, and I am so very thankful that she shared her skills with me.

I would like to thank our collaborator Dr. David Hay and members of his lab, especially Sebastian Greenhough and Dagmara Szkolnicka, for hosting me in their lab and teaching me their differentiation technique.

I would like to thank the University of Washington Center for Ecogenetics and Environmental Health Functional Genomics and Proteomics Facility Core for running both the DMET plus chip array and the microRNA microarray. I would especially like to thank Dr. Theo Bammler and James MacDonald for their help on the statistical analyses.

To the faculty of the Pharmaceutics and Medicinal Chemistry departments, I wish to thank you for fostering an environment of collegiality and intense scientific learning. I am proud to have had the opportunity to learn from such talented scientists and teachers.

Dedication

To my husband, Adam: I sincerely thank you for your love, support and encouragement. I would not have made it through graduate school without you.

To my parents, Mark and Beatrix, and my brother, Eric: Thank you for your unconditional love, support, and encouragement in everything I do.

Chapter 1

Introduction: Stem Cells and Drug Metabolism

The work presented in this chapter has been previously published

in

New Horizons in Predictive Drug Metabolism and Pharmacokinetics (2015) 152-176.

DOI 10.1039/9781782622376

1.1 Introduction

Stem cells have a high self-renewal capability and can give rise to any type of mature cell in the body making them a very attractive target for researchers in regenerative medicine. While there is excitement surrounding the possibilities of stem cell research, this field is still in its infancy. The field of human pluripotent stem cell research is centered on two cell sources, embryonic stem cells (ESCs) and induced pluripotent stem cells (iPSCs). Research with ESCs began first with mouse ESCs in the early 1980's [1, 2], and was followed by establishment of the first human ESC lines in 1998 [3]. Due in part to ethical concerns regarding development of ESC lines, interest arose in ways to develop pluripotent stem cells from somatic cells or other non-embryonic sources. A breakthrough in this area occurred in 2006, when a group from Kyoto University, led by Shinya Yamanaka, were able to demonstrate that a combination of four retrovirally delivered factors, Oct4, Klf4, Sox2 and cMyc, could reprogram mouse fibroblasts to pluripotency; they termed these cells induced pluripotent stem cells, or iPSCs [4]. They shortly followed this work a year later with demonstration that the same four factors could also reprogram human fibroblasts to pluripotency [5]. Development of iPSCs now allows the possibility of generating cell lines matched to specific patients, which can be used to study genetic diseases or as a source for regenerative medicine [6]. Just six years after publication of his work on cellular reprogramming, Shinya Yamanaka and Sir John Gurdon were awarded the 2012 Nobel Prize in Physiology or Medicine [6]. This demonstrates the robustness of this approach, its rapid acceptance in the stem cell field, and vast potential for research [6].

Since the establishment of human pluripotent stem cells lines, both ESCs and iPSCs, there have been some forays into their use for regenerative medicine. For example, the use of ESC-derived oligodendrocyte progenitor cells to treat spinal cord injury. Geron Corporation was

the first to gain US Food and Drug Administration (FDA) approval for a Phase I clinical trial involving ESCs in 2009. This trial tested GRNOPC1, their human ESC-derived oligodendrocyte progenitor cells for acute spinal cord injury [7, 8]. This was viewed as an important milestone in the field of regenerative medicine. Unfortunately, Geron stopped their trial prematurely putatively for business reasons [9]. Following Geron's pioneering trial, other clinical trials have been initiated to examine human ESC-based therapies, most notably with ESC-derived retinal pigmented epithelial cells. As of September 2014, there are 8 clinical trials involving human ESC therapies listed with ClinicalTrials.gov (www.ClincalTrials.gov). Of these 8 trials, 7 involve human ESC-derived retinal pigmented epithelial cells for therapy in Stargardt's macular dystrophy, dry age-related macular degeneration, and wet age-related macular degeneration (www.ClincalTrials.gov). The eighth trial is set to examine human ESC-derived cardiac progenitor cells in patients with severe heart failure (www.ClinicalTrials.gov). While iPSCs offer the potential for patient-derived cell lines to be used in regenerative medicine, there have been concerns regarding their safety, namely the oncogenic potential of the factors used for reprogramming, once injected back into the patient. Nonetheless, in September 2014, the first iPSC-derived cells (retinal pigmented epithelium) were injected into a human patient with macular degeneration in Japan [10]. Results of this trial may hold implications for future approval of iPSC-based cell therapies.

Not only do stem cells offer invaluable opportunities for regenerative medicine, they have vast potential as tools for *in vitro* assays conducted in the drug discovery and development process. Because stem cells can theoretically differentiate into any cell type, they can be used as cell models in drug screening, for both efficacy and toxicity [11]. The advent of iPSCs also allows the development of cell lines from individuals with diverse genetic backgrounds to study

specific disease etiology, or genetic effect on drug metabolism [11]. In addition, stem cells can be used to replace primary cell types in metabolism and toxicity testing, for example stem cell derived hepatocytes in drug metabolism screening and stem cell derived cardiomyocytes in toxicity screening. The purpose of this chapter is to provide an overview of the current state of stem cell technologies regarding their use in drug metabolism screening, with an emphasis on stem cell derived hepatocytes (SCDHs).

1.2 Human Pluripotent Stem Cells

Stem cells are defined as cells that can self-renew and have the ability to generate cells of a specific tissue and associated function through the process of differentiation [12]. Within the genre of stem cells there are 4 main classification types based on the potency of the stem cell, or types of cells that can be produced upon differentiation. This includes the totipotent stem cell, pluripotent stem cell, multipotent stem cell, and unipotent stem cell [13]. Totipotent stem cells are the most versatile; they can differentiate into any and all cell types, including extraembryonic cell types which are necessary for implantation and development of the embryo such as the placenta. Totipotent stem cells are the only type that can independently give rise to a complete organism. Pluripotent stem cells fall one step below totipotent cells; they can differentiate into any cell type except the extraembryonic cell types. Pluripotent stem cells can form any cell type derived from one of the three embryonic germ layers; the ectoderm, mesoderm and endoderm, as illustrated in Figure 1.1. Multipotent stem cells are a more specialized type of stem cell that can differentiate only into a limited range of cell types derived from a specific lineage. For example, hematopoietic stem cells give rise to all types of blood cells and are considered multipotent cells. Unipotent stem cells can differentiate only into one mature cell type. Spermatogenic stem cells

are unipotent stem cells because they can only form sperm cells. The main sources of pluripotent human stem cells in regenerative medicine include embryonic stem cells and induced pluripotent stem cells. In this chapter we will focus our discussion on the use and application of pluripotent stem cells.

The discovery of human pluripotent stem cells has resulted in an emerging field of research that holds promise for both bench research to develop models of human disease and to test new drugs in development, as well as in regenerative medicine to develop cells and tissues for transplant and treatment of diseases [14]. While the discovery of mouse embryonic stem cells occurred in the early 1980's [1, 2], it was not until 1998 that the first human embryonic stem cells (hESCs) were isolated [3]. These hESCs displayed the key characteristics of pluripotency, mainly they could be maintained and expanded in culture, and could generate derivatives from all three embryonic germ layers and form teratomas *in vivo* [3]. This was followed by development of induced pluripotent stem cells (iPSCs), first from mouse embryonic fibroblasts in 2006, and then from human fibroblasts in 2007 [4, 5]. Formation of iPSCs was achieved through retroviral transduction of four factors, or pluripotency genes, Oct4, Sox2, c-Myc, and Klf4 [4, 5]. The resulting iPSCs morphologically resembled hESCs, were able to proliferate in culture, differentiate into cells from all three embryonic germ layers *in vitro*, and form teratomas *in vivo* [4, 5]. A second group also published on the generation of iPSCs in 2007 via lentiviral transduction of human fibroblast cells with the factors Oct4, Sox2, Nanog and Lin28 [15]. The development of iPSC lines opens more doors for regenerative medicine, as well as medical research, with the possibility of creating iPSC lines from specific patients for autologous transplant or patients with various disease or genetic backgrounds for study.

1.2.1 Stem Cell Derived Cardiomyocytes

Stem cells have a high self-renewal capability and can give rise to any cell in the body making them a very attractive target for researchers in regenerative medicine. While there is significant excitement surrounding the possibilities of stem cells in applications ranging from Parkinson's disease to spinal cord injury to organ transplants, this field is still in its infancy. One area with perhaps the most advanced research and application potential in terms of *in vitro* systems is the use of stem cell derived cardiomyocytes for cardiotoxicity screening such as QT prolongation, a leading cause of market withdrawal of prescription medications [16, 17]. A common test used to screen for cardiotoxicity is the ability of the compound to inhibit the cardiac hERG (human ether-a-go-go related gene) channel, which is predictive of QT prolongation [18]. Currently used preclinical models for screening of cardiotoxicity have limited predictive clinical utility [16]. These models include: engineered cell lines expressing the hERG channel, isolated, arterially perfused rabbit ventricular wedge preparations, canine purkinje fibers, and arrhythmia rates in animals [18, 19]. While human primary cardiomyocytes make a better *in vitro* model, they are generally not used because of limited access and quality [16, 18]. Due to these limitations for cardiotoxicity testing, there has been extensive work optimizing the differentiation of hESCs into cardiomyocytes. Stem cell derived cardiomyocytes exhibit functional synchronization of contraction allowing studies of cell-to-cell coupling, signal transduction and repolarization characteristics [18]. They also survive for a prolonged period of time in culture, allowing for examination of both acute effects such as hERG channel inhibition and long-term effects such as ion channel trafficking [18]. Compared to mature cardiomyocytes, stem cell derived cardiomyocytes generally exhibited similar responses to several drugs in safety testing studies; reviewed in Wobus and Loser (2011) [19]. Though there are promising results for the

utility of stem cell derived cardiomyocytes as an *in vitro* model, there are still concerns and reservations, including the purity of the stem cell derived cardiomyocyte population, maturity of the cells, and cost to produce large numbers of the cells [18, 19]. Despite these concerns, there are commercially available stem cell derived cardiomyocytes from companies such as Cellular Dynamics International [20]. A study conducted in 2013 utilizing stem cell derived cardiomyocytes from Cellular Dynamics was able to demonstrate relevant pharmacology and good correlations to current functional cardiac electrophysiological assays using 10 compounds with cardiovascular toxicity effects, supporting the use of stem cell derived cardiomyocytes for electrophysiological cardiac safety screening [21]. The potential of human embryonic stem cell derived cardiomyocytes in a regenerative medicine capacity has also been demonstrated using non-human primates. A study that employed a non-human primate model of myocardial ischemia showed that intra-myocardial delivery of human embryonic stem cell derived cardiomyocytes could remuscularize substantial amounts of the infarcted heart [22]. However, from a safety standpoint, they did observe non-fatal ventricular arrhythmias in the non-human primates that received the hESC-derived cardiomyocytes [22]. Due to the extensive progress made with stem cell derived cardiomyocytes and insufficiencies with current preclinical models to predict cardiotoxicity, there is extensive interest in their routine use and application in drug safety screening. To this end, in July 2013, a meeting was held by the Cardiac Safety Research Consortium and the Health and Environmental Sciences Institute to discuss new approaches to assess drug-induced proarrhythmic risk, which included the use of electrophysiological tests with stem cell derived cardiomyocytes [23, 24]. This demonstrates one application of a stem cell technology to enhance pharmaceutical development.

1.3 Drug Metabolism

Drug metabolism is an important area of study in drug development, as metabolism is a main way drugs are eliminated from the body. Drugs can be eliminated from the body as either the unchanged parent compound or as metabolites [25]. Usually metabolism of drugs results in inactivation of the compound and renders the compound more water soluble to allow for fascile excretion from the body; however, metabolism can also result in the generation of a toxic metabolite. Because of this, preclinical screening of drug metabolism is a fundamental component of the drug development process and is used to predict drug bioavailability, drug-drug interactions, and toxicity. Pharmaceutically-based drug-drug interactions occur when one drug affects the pharmacokinetics of another, or in other words, if one drug changes the absorption, distribution, metabolism or excretion (ADME) of another [26, 27]. Inhibition and induction of drug-metabolizing enzymes can both alter the metabolism of a drug, representing two major reasons for such drug-drug interactions [25].

The main family of enzymes responsible for drug metabolism is the Cytochrome P450s (CYPs). The CYPs are a superfamily of hemoprotein enzymes that primarily catalyze oxidation reactions [28]. It is a large and diverse family of enzymes with 57 functional isozymes in humans. However, it is the members of just three subfamilies (CYP1, CYP2 and CYP3) that are primarily responsible for most metabolic clearance of drugs [29]. They are expressed in numerous tissues, with the main drug-metabolizing CYPs being highly expressed in the primary tissues responsible for drug metabolism – the intestine, liver and kidney. The liver is the most versatile of these organs and, thus, key to drug metabolism and clearance. Accordingly, when evaluating drug metabolism, the hepatic CYPs in particular are extensively studied. The liver, along with the intestine, also plays a crucial role in “first-pass metabolism” of orally

administered compounds. Orally administered compounds are absorbed in the intestinal mucosa where they are delivered to the liver via the portal vein before entering the general blood circulation. This first-pass of compounds through the intestine and liver can result in extensive metabolism of the compound before it enters general circulation, having a major effect on a drug's bioavailability and pharmacological response. This also means that the liver may be exposed to high concentrations of orally dosed drugs and their metabolites, posing a risk for liver toxicity [25]. Some CYPs are also highly polymorphic, and this genetic variation can play a role in therapeutic failure and drug toxicity risk [26, 30]. Variation in the CYP genes can result in enzymes with no functional capacity, enzymes with altered functional capacity, or enzymes with altered expression level. For each polymorphic gene these alterations result in a range of observed phenotypes classified as poor metabolizers (PMs), intermediate metabolizers (IMs), extensive metabolizers (EMs) and ultrarapid metabolizers (UMs) [26, 30]. The CYP with the most variation identified to date is CYP2D6, with more than 63 functional gene alleles (www.cypalleles.ki.se/cyp2d6.htm), including polymorphisms that result in gene deletion (PM), defective splicing (PM or IM) and gene duplication (UM).

Because metabolism plays a crucial role in both the efficacy and toxicity of drugs, it is important to identify the metabolites formed and the enzymes responsible for metabolism [25]. Usually, a drug is metabolized by several competing pathways and the contributing fractions will depend on the relative rates of each parallel pathway. Importantly, it's known that the fraction of dose metabolized by specific enzymes, such as the CYPs, is a major determinant in predicting drug-drug interactions and is essential for understanding the impact of polymorphisms in drug metabolizing enzyme genes on total drug clearance [25, 26]. Because blood drug or metabolite concentrations drive pharmacologic effect, the metabolic profile of a new chemical entity can be

determined *in vitro* and this data is now routinely included in IND (Investigative New Drug) evaluation documents. It is also used to determine the most appropriate follow up clinical studies to assess drug-drug interactions [26]. Reaction-phenotyping involves the use of multiple systems in combination to determine the major metabolic pathways responsible for drug metabolism and clearance. This includes purified recombinant proteins, microsomal membrane and other subcellular fractions, primary hepatocytes, coupled with selective chemical inhibitors, inhibitory antibodies, and probe substrates [26, 31]. Probe substrates are useful in determining the inhibitory potential of a new chemical entity toward specific CYPs. CYP reaction-phenotyping is used to estimate the fraction of a drug cleared by all the CYPs (f_m) and the contribution of each individual CYP ($f_{m,CYP}$) [26]. This data can then be used to predict the magnitude of a drug interaction and the impact of a CYP polymorphism on the pharmacokinetic profile and pharmacological action of the drug. It can also be used to help design more effective clinical studies, so as to avoid therapeutic failure and unexpected toxicity [26]. In addition, the spectrum, reactivity and abundancy of a given metabolite is important, as defined by the FDA's Safety Testing of Drug Metabolites guidance, or MIST [32]. The goal of MIST is to assess circulating metabolite exposure, as the metabolites may have pharmacological activity or toxicity risks. This is determined in part from *in vitro* drug metabolism profiling in combination with animal studies and clinical trials. It is important to have a thorough understanding of the ADME properties of a new chemical entity, including the role of CYPs in the overall clearance of the drug, accurate *in vitro* CYP reaction-phenotype data, metabolic clearance by non-CYP enzymes, renal clearance and biliary clearance [26]. It is also known that some CYP enzymes are susceptible to induction. This induction has been observed primarily in the liver although it has been described for other tissues as well, notably the intestine [26, 33]. Enzyme induction results

in increased metabolic elimination of the drug and therefore reduced plasma concentration of the parent compound. In order to assess the potential for a drug interaction due to enzyme induction one needs knowledge of the enzymes and their contribution to the metabolic elimination of the drug candidate [26].

While the CYP enzymes are the predominant family involved in drug metabolism, there are other enzymes that may play a significant role in the metabolic clearance of a drug. These include the flavin-containing monooxygenases (FMOs), monoamine oxidase, epoxide hydrolase, glutathione S-transferases (GSTs), sulfotransferases (SULTs), methyltransferases, N-acetyltransferases (NATs), and UDP-glucuronyltransferases (UGTs) [31]. Unlike with the CYPs, *in vitro* phenotyping experiments for these other enzymes are less well established and there are fewer selective probe substrates and inhibitors available [26, 31, 34].

1.3.1 Tissues

Again, although the liver is the main organ responsible for drug metabolism there are other tissues with significant expression of the CYPs and other drug metabolizing enzymes that should also be considered when evaluating a drug's first-pass and overall metabolic clearance and may be particularly important in terms of localized toxicity [26]. The two other organs most commonly involved in drug metabolism along with the liver are the intestine and the kidney. These three organ systems and their role in drug clearance are discussed below.

1.3.1.1 Liver

The liver possesses the highest expression levels of drug-metabolizing CYPs, making it the most important organ for the metabolism, detoxification and elimination of drugs, and the

focus of drug optimization and safety studies [25, 26]. Metabolism in the liver plays a key role in determining plasma drug concentration and half-life [25]. Hepatocytes are the main cell type within the liver, comprising about 80% of the liver volume and are the cell type where the drug metabolizing enzymes, such as the CYPs, are principally found [25]. Hepatocytes are polarized cells with a blood-facing sinusoidal membrane and bile-facing cannalicular membrane, as shown in Figure 1.2B. Each of these membranes expresses specific transporters that facilitate movement of drugs into and out of the cell. Transporters expressed on the sinusoidal membrane can affect access of the drug to the drug metabolizing enzymes within the hepatocyte, and transporters on the canalicular membrane affect biliary excretion. The drug metabolizing CYPs are found primarily in the endoplasmic reticulum of hepatocytes. CYP3A4 is the major hepatic microsomal CYP in humans in terms of both abundance and broad substrate specificity [26]. However, CYP1A2, 2A6, 2B6, 2C8, 2C9, 2C19, 2D6 and 2E1 are also present in the liver ER and contribute to drug metabolism (Figure 1.2B) [26, 28]. With regards to screening for drug metabolism activity in the liver, *in vitro* systems include recombinant enzymes, human liver microsomes, S9 fractions, liver slices and primary hepatocytes [26]. Each of these systems has their own advantages and disadvantages, so generally multiple different systems are used when evaluating the metabolic profile of a new chemical entity. The data from these various *in vitro* systems is then integrated to determine the overall metabolism profile [26]. Animal studies are also a useful complement to these *in vitro* human assays. However, they are not always an accurate model of human metabolic capacity because of inter-species differences in enzyme expression and function [35]. Ultimately, *in vivo* human ADME data is needed to both confirm the *in vitro* data and to help place the *in vitro* data in the appropriate clinical context [26].

In vitro characterization of drug metabolism involves kinetic analysis of the metabolite formation rate. The model used most often was developed by Michaelis and Menten [28, 36]: (Equation 1.1)

$$v = \frac{Vmax*S}{Km+S} \quad (1.1)$$

in which v is the velocity, or rate of metabolism and S is the substrate concentration. Vmax is the maximal reaction velocity and is directly proportional to the total enzyme concentration. Km is the Michaelis constant, it represents the affinity of the substrate for the enzyme and is mathematically equated to the substrate concentration at which half maximal velocity (Vmax) is attained [28]. When the substrate concentration is much smaller than Km, which is true for most drugs *in vivo*, v is approximately linearly dependent on substrate concentration, and the ratio Vmax/Km, known as the intrinsic clearance (Clint), represents the maximum efficiency of the metabolic process [28, 36]. Intrinsic clearance is used for extrapolating *in vitro* data to the *in vivo* situation. It acts operationally as a proportionality constant between the rate of drug metabolism (v) and drug concentration at the enzyme active site. If a drug is biotransformed into multiple metabolites then the net Clint is the sum of the individual Clint for each pathway [28]. The *in vitro* intrinsic clearance is scaled to predict the total *in vivo* intrinsic clearance and a liver model, such as the well-stirred model (Equation 1.2), can be used to predict the *in vivo* hepatic clearance [28, 36, 37].

$$CLh = Q * \frac{fu*Clint}{Q+(fu*Clint)} \quad (1.2)$$

in which Q is liver blood flow and f_u is the fraction unbound in blood.

There are a number of *in vitro* systems that can be used to characterize drug metabolism. For example, recombinant enzymes, these are typically created by over-expression of a single

enzyme gene, most commonly in insect cells. Due to the fact that these are singly expressed enzymes they are valuable for identifying the role of a particular enzyme in a compound's metabolism, but are not that useful for characterizing the relative rates of drug metabolism via multiple pathways or sequential metabolism [38, 39]. One needs to keep in mind that they are an artificial system, where the enzyme is typically over-expressed at levels far higher than what is found in native tissue and requires the addition of co-factors [26]. Reaction-phenotyping with recombinant CYP systems is routinely done and can be used to determine kinetic parameters such as single enzyme Km and Vmax [26]. Human liver microsomes are one of the most commonly used *in vitro* systems. These are endoplasmic reticulum (ER) vesicles and as such only contain enzymes expressed in the ER, including the CYPs, FMOs and UGTs [28, 38, 39]. S9 fractions contain both microsomal and cytosolic fractions [39]. However, again, cofactors required for the enzymes must be added to the incubation in order to observe activity, and these fractions are not ideal for examining sequential phase I/phase II metabolism [38, 39]. For example, to examine UGT activity, a detergent must be added to create pores in the membrane so drug may access the active site of the enzyme, resulting in a non-physiological representation of UGT activity [38, 39]. Hepatocytes are superior for studying sequential and/or parallel oxidative and conjugative reactions [28]. In addition, while any of these systems can be used to study inhibition, cell systems such as hepatocytes are the only systems in which to study induction and its effects on the metabolic profile. This whole cell system is also ideally suited for evaluating the role of transporters and potential for transporter-mediated drug interactions. Indeed, sandwich cultured primary hepatocytes are considered the gold standard for determining liver CYP induction [25]. Hepatocytes cultured in the sandwich configuration, between collagen or collagen and Matrigel™, morphologically resemble hepatocytes, maintain metabolism, and form

canalicular membrane networks also providing a means to evaluate liver specific transporters (See Figure 1.2B) [25, 40, 41]. Along these lines, a US FDA draft Guideline to Industry recommends induction studies be performed with hepatocytes obtained from a minimum of three individuals in order to minimize inter-individual differences in responses [42].

In summary, the metabolism of a drug by the liver is evaluated using a combination of *in vitro* systems, such as recombinant enzyme systems, human liver microsomes and/or primary hepatocytes. These results are compared for an overall assessment of metabolic fate, in particular, the role of CYP-mediated metabolism [26]. The FDA guidance "Drug interaction studies – study design, data analysis, and implications for dosing and labeling" highlights the use of human hepatocytes in determining the metabolic profile of a new chemical entity, and if the data indicates CYP enzymes contribute >25% to the total clearance of the compound then studies using human liver microsomes or recombinant enzymes should be performed to identify the individual CYP enzymes responsible for metabolism [42]. It is important in pre-clinical drug development to identify and understand the major pathways of metabolism in order to predict potential drug-drug interactions and potential for liver toxicity [27].

1.3.1.2 Intestine

Although the liver is the main drug metabolizing organ, other tissues express drug-metabolizing enzymes and extra hepatic metabolism is thought to be important for some compounds. For example, metabolism in the intestine contributes to first-pass elimination of orally administered compounds, and is thus a determinant of a drug's oral bioavailability. It's also important to have a clear understanding of the metabolites generated in specific tissues like the intestine to predict potential toxicity in that tissue. Transcellular absorption of orally

administered drugs occurs through enterocytes, the mature absorptive columnar epithelial cells that are part of the mucosal lining in the intestine. The enterocytes have an apical membrane which faces the lumen, where the intestinal villi face and absorption from the GI tract occurs, and a blood facing basolateral membrane, illustrated in Figure 1.2A. Enterocytes also express significant levels of drug metabolizing enzymes, such as CYPs and UGTs (Figure 1.2A).

The main CYP enzyme expressed in the intestine is CYP3A, calculated to account for about 80% of the CYP content based on total immunoquantified P450s, and interestingly is expressed in a gradient along the length of the small intestine, with expression being the highest in the duodenum, followed by the jejunum and lastly the ileum [43-45]. Other CYP enzymes expressed in the small intestine include CYP2C9, 2C19, 2D6 and 2J2 [26]. Although CYP3A is the most abundant CYP in both the liver and small intestine, the total mass of CYP3A in the small intestine is estimated to be only about 1% of that in the liver [45]. This difference in total mass can be in part attributed to the low yield of microsomal protein from the small intestine compared to the liver, and because the localization of the CYPs in the small intestine is restricted to the enterocytes in the villus tip cells, which only account for a small fraction of the total intestinal cell population [44]. In addition, the liver is about twice as large as the small intestine by weight (about 1.5 kg vs. 0.7 kg) [44]. Based on CYP content, levels of CYP3A4 have been estimated at 350 pmol/mg microsomal protein in the liver and 70-160 pmol/mg microsomal protein in the small intestine [44, 46]. Comparison of two other studies show CYP3A content to be closer in range, at 96 pmol/mg microsomal protein in the liver and about 50 pmol/mg microsomal protein in the small intestine [45, 47]. Although CYP3A content in the small intestine may be just a fraction of that in the liver based on total mass, the fact that CYP3A's contribution to total CYP content in the intestine is double that in the liver (80 vs. 40%) coupled

with relatively similar microsomal content, substantiates the small intestine as an important site for first-pass drug metabolism [45, 47].

Similar to the process for determining metabolism in the liver, recombinant enzyme systems of the CYPs known to be expressed in the intestine are used to help understand their potential role in intestinal drug metabolism. In addition, several cell lines have been used to study intestinal drug permeability and biotransformation; this includes primary enterocytes and the immortalized human colon carcinoma cell lines Caco-2 and LS180 cells [43]. While primary enterocytes are metabolically competent, their viability is limited in culture [48]. Caco-2 cells are the more commonly used colon carcinoma cell line for screening drug permeability because they form tight inter-cellular junctions and develop polarized membranes. Caco-2 cells do not express most CYP enzymes constitutively, particularly CYP3A4, which is the main CYP expressed in the small intestine [48-50]. They also lack the nuclear receptor PXR (pregnane X receptor), that mediates the induction of several CYPs by some xenobiotic compounds. However, Caco-2 cells can be induced to express a low level of CYP3A4 by treatment with 1α,25-dihydroxy vitamin D_3, a process mediated by the vitamin D receptor (VDR) [49]. Alternatively, one can use CYP3A4-transfected Caco-2 cells, but this introduces the limitations of an artificial system.

As in the liver, induction of drug metabolizing enzymes and drug transporters in the intestine may lead to drug interactions. LS180 cells have been shown to constitutively express PXR and VDR and, thus, are suitable for studying the regulation of intestinal CYP enzymes and transporters, such as CYP3A4 and p-glycoprotein (P-gp) [51, 52]. Unfortunately, LS-180 cells do not form tight junctions and cannot be used to assess intestinal bioavailability. Another *in vitro* system used to study intestinal drug metabolism is precision-cut slices, these are very small

intestinal cut slices of tissue from different species, allowing for evaluation of species differences in intestinal metabolism [43, 48, 53]. However, access to intestinal tissue for these slices is limited. Overall, there is a lack of robust intestinal cell-based models for simultaneously assessing drug permeability, drug metabolism, DDIs and drug toxicity [43]. Generation of enterocytes from human pluripotent stem cells would in theory offer a human based *in vitro* system to evaluate all cellular functions critical to the prediction of intestinal drug disposition *in vivo*.

There has been limited work on developing protocols for differentiation of pluripotent stem cells to enterocyte or intestinal cells, though what has been attempted shows promising results. The small intestine is a unique organ with a highly regenerative luminal epithelium that turns over about once a week. This self-renewal is driven by intestinal stem cells (or adult stem cells) that reside in the crypt. These cells move up along the villi as they mature, essentially sloughing off the older cells at the tip of the villi [54]. These adult stem cells located in the intestinal crypt can be isolated from human surgical, or biopsy, specimens and used to develop *ex vivo* 3-D enteroid cultures [55-57]. While these represent a promising pre-clinical model, its use is limited by access to human intestinal tissue. For this reason, intestinal cells derived from human embryonic and induced pluripotent stem cells may offer a more convenient solution. To date, most pluripotent stem cell derived intestinal work has been conducted by Dr. Wells' group at Cincinnati Children's Hospital. This group has shown formation of human intestinal organoids (HIOs) from both embryonic and induced pluripotent stem cells that form mature human intestinal epithelium with crypt-villus architecture [58-60]. Their HIOs express the intestinal markers CDX2, SOX9 and KLF5, and they develop crypt-villus architecture with cells expressing LGR5 and ASCL2 (markers of the adult intestinal stem cell population) [58, 59, 61].

The differentiation takes 35 days and involves the factors activin A, Wnt3a, fibroblast growth factor 4 (FGF4), Noggin, Rspondin1 and epidermal growth factor (EGF) [58, 59]. They also were able to show that taking the HIOs and then transplanting them under the kidney capsule of immune compromised mice for 6 weeks before removal allows them to further mature [58]. Additionally, these HIOs have been shown to support replication of a gastrointestinal virus, rotavirus, indicating they are a biologically relevant model of the intestine [62]. While these organoids recapitulated many markers of mature intestine, there has been no assessment to date of drug-metabolizing enzyme functions. Thus, it is unclear, whether such a system would have utility for *in vitro* drug metabolism profiling. In conclusion, more work needs to be done on characterizing stem cell derived intestinal cells in terms of drug metabolizing enzymes and transporters in order for them to be a useful *in vitro* system for preclinical drug metabolism profiling.

1.3.1.3 Kidney

The kidney is a main route for drug excretion, but it can also play a key role in drug metabolism. Along with the intestine and liver, the kidney also expresses significant levels of various drug-metabolizing enzymes, such as some of the CYPs and UGTs, as well as drug transporters (Figure 1.2C). The main cell type in the kidney where drug metabolism and transport occurs is the renal proximal tubule epithelial cell (PTEC). These cells have a polarized blood facing basolateral membrane and an apical membrane which transports compounds into the collecting duct of the kidney to become part of the urine filtrate, illustrated in Figure 2C. In addition, PTECs are known to express CYP3A5 as opposed to CYP3A4 as in the liver [43, 63, 64]. CYP3A5 is a highly polymorphic enzyme, such that the majority of Caucasians (about

85%) do not express functional CYP3A5 protein [65]. The primary variant responsible for this phenotype is *CYP3A5*3*, an intronic SNP which results in improperly spliced mRNA and a truncated protein [65, 66]. To evaluate drug metabolism in the kidney, *in vitro* systems are used in combination with *in vivo* data from animal studies. For *in vitro* systems, immortalized cell lines such as LLC-PK1 (a pig kidney epithelial cell line) and MDCK (Madine Darby Canine Kidney) cells are commonly used, however these are non-human cells and do not fully recapitulate the *in vivo* renal state [43, 67]. Some human renal epithelial cell lines are also available for research purposes, including the HK-2 proximal tubule cell line [68, 69]. However, the HK-2 cell line has been shown to lack expression of some key drug transporters, including OAT1, OAT3 and OCT2, limiting their use as an *in vitro* model of human kidney [69].

There is a clear need to better understand the impact of kidney disease on drug disposition (including metabolism) [63]. Not only does kidney disease affect renal drug clearances, but it also affects the clearance of drugs that are eliminated by the liver and intestine [63]. For the kidney, there is still a lack of *in vitro* models that accurately resemble the *in vivo* kidney, particularly one with compromised function. Development of protocols to generate various cells of the kidney from human pluripotent stem cells would have considerable potential as an *in vitro* model to examine drug metabolism and transport within the kidney and also to study the effects of kidney disease on drug disposition. To gain a better understanding of the kidney's role in drug disposition and toxicity, development of 3D microphysiological systems (or a kidney-on-a-chip) would also be greatly beneficial [70]. For this type of system, stem cell derived renal tubular cells, along with the other cell types of the kidney, would provide a consistent human cell source for manipulation in 3D or microphysiological systems to more accurately model renal functions.

As with the intestine, there has been limited work to date on development of stem cell derived renal cells. The kidney is one of the more complex organs in terms of lineage specification. Kidney formation involves an interaction between two different populations derived from intermediate mesoderm, metanephric mesenchyme and ureteric bud [71]. The metanephric mesenchyme differentiates into the epithelial cells of the kidney (such as the renal tubule cells) and the ureteric bud forms the collecting duct system [71]. Studies examining generation of kidney cells from human pluripotent stem cells have mostly utilized activin A, retinoic acid and BMP7 in the differentiation process [72-76]. One study that classified the differentiated cells as being proximal tubular like cells utilized BMP2 and BMP7 in the differentiation protocol, followed by flow cytometry sorting for aquaporin1 positive cells [76]. More recent protocols have also employed the small molecule CHIR99021, a glycogen synthase kinase-3β inhibitor [77-79]. While these reports demonstrate generation of metanephric mesenchyme and renal proximal tubule like cells, more work needs to be done to develop protocols that definitively yield homogenous populations of renal tubule cells for evaluating the expression and activity of the drug metabolizing enzymes and transporters.

1.4 Stem Cell Derived Hepatocytes

Primary human hepatocytes are isolated from liver organs deemed unsuitable for transplantation or via liver biopsy [16]. For *in vitro* screening, primary human hepatocytes are the most physiologically relevant model, given their expression of phase I and II drug-metabolizing enzymes as well as transporters, under the right conditions. Thus, human hepatocytes have become an integral component for studying drug metabolism and toxicity [16]. While microsomes are still a favored model for high throughput screening, they are increasingly

being replaced or complemented with primary human hepatocytes [80]. However, the utility of human hepatocytes is hampered by donor availability, unpredictable inter-donor variability, lack of cell proliferation and a decline in characteristic hepatic functions over time [16, 81]. Pluripotent stem cells have a high self-renewal capability and can give rise to any cell in the body, including hepatocytes. Hepatocytes derived from stem cells may provide a useful *in vitro* model for drug metabolism, pharmacogenetic, CYP inducibility, and toxicity studies to complement or replace currently available primary/cryopreserved human hepatocytes. In addition, there is a critical need to be able to accurately model human organ systems *in vitro*, such as the liver, to improve our understanding of drug efficacy and safety during drug development. Stem cell derived hepatocytes may provide a more readily available source of cells with quantitatively appropriate and predictable functions for manipulation in 3D or microphysiological systems to more accurately model the liver, or other organ systems.

1.4.1 Differentiation

Hepatocytes derived from hESCs or iPSCs represent an attractive alternative to bypass the limitations associated with primary hepatocytes. The aim of differentiation is to recapitulate natural development *in vitro* within a culture dish using various combinations of growth factors. For the liver this means directing the cells first towards the endoderm pathway, then to the hepatic lineage and finally into mature hepatocytes. There have been several groups reporting the differentiation of human pluripotent stem cells, both hESCs and more recently iPSCs, into hepatocytes. One of the first able to demonstrate this were researchers from Geron Corporation in 2003 [82]. While differentiation efficiencies (based on percentages of cells expressing hepatocyte markers such as albumin) were low to begin with there has been marked

improvement in this area. Earlier protocols often relied on spontaneous differentiation of stem cells through formation of embryoid bodies (3-dimensional multicellular aggregates), a contributing factor to low differentiation efficiencies [82, 83]. More recent protocols now rely on directed differentiation using set combinations of various factors, contributing to the increase in differentiation efficiency [84-86]. There have been a number of various factors used in differentiation protocols in an attempt to recapitulate normal liver development. This differentiation process is therefore broken down into a number of stages, with varying combinations of factors used. The total time to differentiate hepatocytes varies between protocols, ranging from 13 to 32 days [82, 83, 86-98]. A few factors that are common to most protocols include activin A, Wnt3, dimethyl sulfoxide (DMSO), hepatocyte growth factor (HGF), oncostatin M (OSM) and dexamethasone. In addition, other groups have reported transduction of transcription factors along with growth factor treatment as an efficient process for generating SCDHs [90-92]. Takayama et al. have reported transduction of FOXA2 and HNF1α with an adenovirus vector in combination of step-wise culture with growth factors including Activin A, bone morphogenetic protein 4 (BMP4), fibroblast growth factor 4 (FGF4), HGF, OSM to generate SCDHs [90, 91]. More recently, small molecules have also been used to generate SCDHs [99]. Other protocols have also investigated 3D culture of cells, such as spheroids and bioreactors, to enhance hepatocyte differentiation [89, 93, 100, 101].

In summary, there are several protocols available for generating SCDHs. While most of these protocols share common factors, there are differences. Protocols published in journals such as Current Protocols in Stem Cell Biology and Nature Protocols are an easy and convenient way to understand every step in a lab's differentiation process, especially to evaluate differentiation protocols side by side [86, 102]. Before they can be used for *in vitro* metabolite

profiling, the differentiation protocols that yield the most reliable, reproducible hepatocyte like cells must be identified and thoroughly evaluated. In addition, these protocols must be easily scalable and cost-efficient to be implemented in an industry setting.

1.4.2 Stem Cell Derived Hepatocytes For Studying Drug Metabolism

The biggest limitation in the field of SCDHs to date is the inability to reproducibly generate mature hepatocytes with high levels of functional drug metabolizing enzymes. It should be noted that lack of mature differentiated cells is not unique to SCDHs and a lack of functional maturity has been observed across various cell types, remaining a problem in the stem cell field in general [103]. For SCDHs to be used as an *in vitro* assay platform to determine metabolite profiles, this is something that must be overcome.

While there have been a number of publications addressing this issue, there is still an overall inability to obtain mature hepatocytes that possess fully functional CYP activity. Currently, to evaluate stem cell derived hepatocyte function, there is a repeating pattern of criteria used including: gene expression profiling, immunocytochemistry and western blotting of specific markers; indocyanine green staining; glycogen accumulation; and albumin secretion. While most groups acknowledge the importance of functional drug-metabolizing enzymes, such as the CYPs, in hepatocytes, few groups have actually assessed functional activity, and not all using the gold standard of human primary hepatocytes as the comparator. Most groups generally utilize flourescence-based resorufin and P-glo assays to assess CYP activity; only a few studies have utilized LC/MS and compared CYP activity to primary hepatocytes [85, 88, 91, 104]. There is also a large amount of variability between studies. For example, in studies reporting on CYP3A, activity can vary from 0-90% of that seen with human primary hepatocytes [87, 88,

105-108]. This wide range of results could be due to multiple factors, including the different stem cell lines used, the protocol used and/or the quality of primary hepatocytes used for comparison [105]. Selected studies examining functional drug metabolism are summarized in Table 1.1. In one example, LC/MS was utilized to assess activity of four major drug-metabolizing CYPs (CYP1A2, 2C9, 3A4 and 2D6). Results from this study indicated CYP activity comparable to primary hepatocytes for CYPs1A2 and 2D6, indicating the SCDHs obtained in this study do express some functional CYP enzymes [88]. In addition, some published reports have characterized the metabolic capacity, as well as inductive potential of certain CYP enzymes, most using the ethoxyresorufin-O-deethylase (EROD) assay for CYP1A activity. However, when comparing stem cell derived hepatocyte CYP activity data using either resorufin assays [82, 83, 106] or LC/MS [88, 91], to primary hepatocytes, all demonstrate lower activities in SCDHs than primary hepatocytes, further supporting the need for increasing the efficiency of differentiation protocols.

At the heart of the situation is the fact that the majority of studies have reported SCDHs as still expressing α feto-protein (AFP), a protein that is highly expressed in fetal hepatocytes, but is dramatically down-regulated after birth such that healthy adult livers typically do not express AFP. Another marker for fetal liver is the preferential expression of CYP3A7, rather than the dominant adult isoform, CYP3A4. Other commonly used markers include other CYPs, transcription factors, albumin (ALB), alpha-1 antitrypsin (AAT), CK18, and CK19 (a marker of biliary cells and hepatic progenitor cells). Results with these markers together indicate a mixed or immature population of cells. Overall, there is significant need for improvement in the generation and characterizion of SCDHs, particularly with regards to their metabolic capacity as it compares to primary hepatocytes.

While there is evidence that SCDHs do express CYPs and other drug metabolizing enzymes, they still seem to be at immature levels (below human primary hepatocytes). Additionally, the cells still express markers typical of fetal hepatocytes, such as AFP. Whether that poses a problem in terms of use in metabolite profiling and toxicity testing remains to be seen; indeed it could be one of the reasons for insufficient CYP activity. While it would be optimal for SCDHs to express functional drug-metabolizing enzymes at the same level as cryopreserved and primary hepatocytes, as long as the expression and activity is reproducible and scalable, it may not be necessary. For example, if CYP3A4 content in SCDHs is consistently 50% of primary hepatocytes, that can be accounted for in the *in vitro* metabolite profile with a scaling factor.

Finally, significant work needs to be done to optimize a singular differentiation protocol for industry use that produces consistent and functional hepatocytes. To help in identifying and optimizing a protocol for SCDHs, there appears to be a need to develop standard endpoint assays for determining hepatocyte differentiation and function, and standard comparators such as primary hepatocytes (which should be validated on their own) to aid in comparing various differentiation protocols so that protocols that are efficient, reproducible and robust for drug metabolism and toxicity screening can be further developed [105].

1.5 Conclusions

Stem cells have a high self-renewal capability and can give rise to any cell in the body, making them a very attractive target for researchers in regenerative medicine, as well as drug discovery and development. As new chemical entities move into the lead-optimization phase, ADME and drug-drug interaction data should be collected primarily from human models [25].

Stem cell derived culture systems offer a promising new tool for ADME studies, adding to our available human derived pre-clinical models. The three major organ systems involved in drug metabolism include the liver, intestine and kidney. Tissue specific cells generated from pluripotent stem cells for all three of these organs would be very useful for drug metabolism screening. There has been extensive research on stem cell derived hepatocytes for this purpose, and while there is evidence that SCDHs do express CYPs and other drug metabolizing enzymes, they remain at immature levels. Overall there is still need for improvement in generating and characterizing SCDHs, particularly with regards to their metabolic capacity as it compares to primary hepatocytes. While there has not been as much focus on stem cell derived enterocytes or renal proximal tubules, research in both of these areas shows promise. Overall, there is still a need to evaluate each of these cell systems for drug metabolizing enzyme and transporter activities before they could be used routinely for preclinical screening during drug development. In addition, there is a critical need to be able to accurately model these human organ systems *in vitro*, such as with 3D or microphysiological systems, to improve drug efficacy and safety assessment during drug development. Stem cells would make for a consistent human cell source for culturing in a 3D or microphysiological system that more accurately recapitulates organ function. Such systems have vast potential to advance the development of new therapeutic agents, enhancing the safety and efficacy of products approved for the market. The following hypotheses and specific aims address some of the model deficiencies cited above and take us a step closer to the desired goal.

1.6 Hypothesis and Specific Aims

Hypothesis 1: *Hepatocytes derived from human pluripotent stem cells are comparable to primary hepatocytes.*

Aim 1.1: To differentiate hESCs into hepatocytes. Cells will be generated using an existing protocol from our collaborator, Dr. David Hay (Chapter 2) [84].

Aim 1.2: Evaluate stem cell derived hepatocytes for down-regulation of typical stem cell markers and up-regulation of hepatocyte markers. This will be done through immunocytochemistry and gene expression profiling (Chapter 2 and 3).

Aim 1.3: Evaluate the metabolic capacity of stem cell derived hepatocytes using a CYP cocktail assay. Enzyme activity will be measured in comparison to cryopreserved human hepatocytes utilizing two cocktail mixtures assessing CYPs 2C9, 3A, 1A, 2D6, 2A6, 2E1, 2C8, 2C19, and 2B6 (Chapter 3).

Aim 1.4: To quantify microRNA expression in adult liver and stem cell derived hepatocytes and identify microRNAs modulating the differentiation/maturation of hepatocytes. microRNA profiles in hESCs, adult liver, and SCDHs obtained from Aim 1.1 will be compared. Results will be used to optimize the differentiation protocol for generating hepatocytes (Chapter 4).

Hypothesis 2*: Stem cell derived hepatocytes recapitulate genotype-phenotype properties of CYP450 enzymes.*

Aim 2.1: Collect and genotype PBMCs from used Pall filters for the major polymorphisms found in drug-metabolizing enzymes. PBMCs will be banked and genotyped for major polymorphisms in the drug-metabolizing CYPs (Chapter 5).

Aim 2.2: Identify donors with distinct CYP3A5 genotypes for iPSC generation and validation. PBMC donors identified as CYP3A5 expressors versus non-expressors (*1 vs. *3/*3) will be

selected for i.) iPSC generation, ii.) differentiation to hepatocytes and evaluation of metabolic capacity utilizing midazolam (Chapter 5).

Aim 2.3: Establish a proof-of-concept utilizing NIH-approved hESC lines and CYP2D6. Available NIH-approved hESC lines will be genotyped for major polymorphisms in CYP2D6. These cell lines will then be stratified into predicted CYP2D6 phenotypes, i.e. PM, IM, EM, UM, and differentiated into hepatocytes. The metabolic capacity of these SCDHs will be evaluated and compared to cryopreserved hepatocytes identified as corresponding to CYP2D6 PM, IM, EM, UM (Chapter 2).

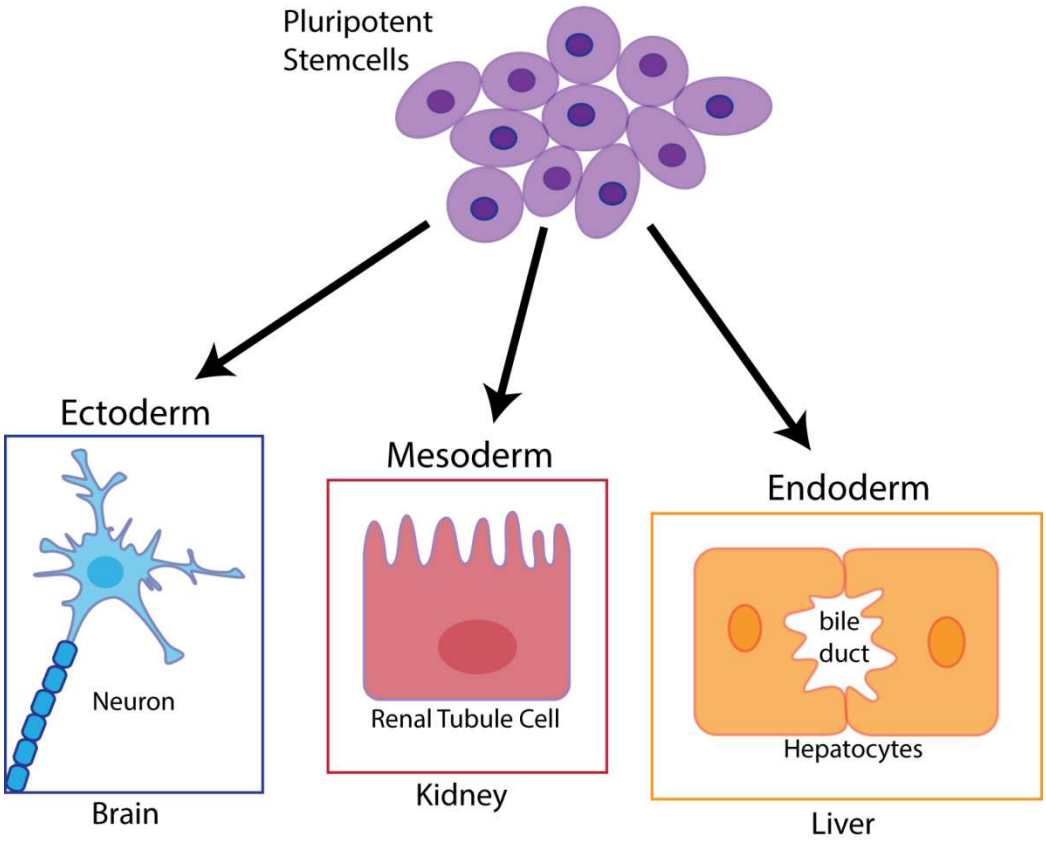

Figure 1.1. Pluripotent stem cells. Pluripotent stem cells can transform into cells from all three embryonic germ layers, the ectoderm, mesoderm and endoderm. Representative tissue and cell types from each of these germ layers are illustrated here. Neurons of the brain are derived from the ectoderm lineage; renal tubule cells of the kidney are derived from the mesoderm lineage; hepatocytes of the liver are derived from the endoderm lineage.

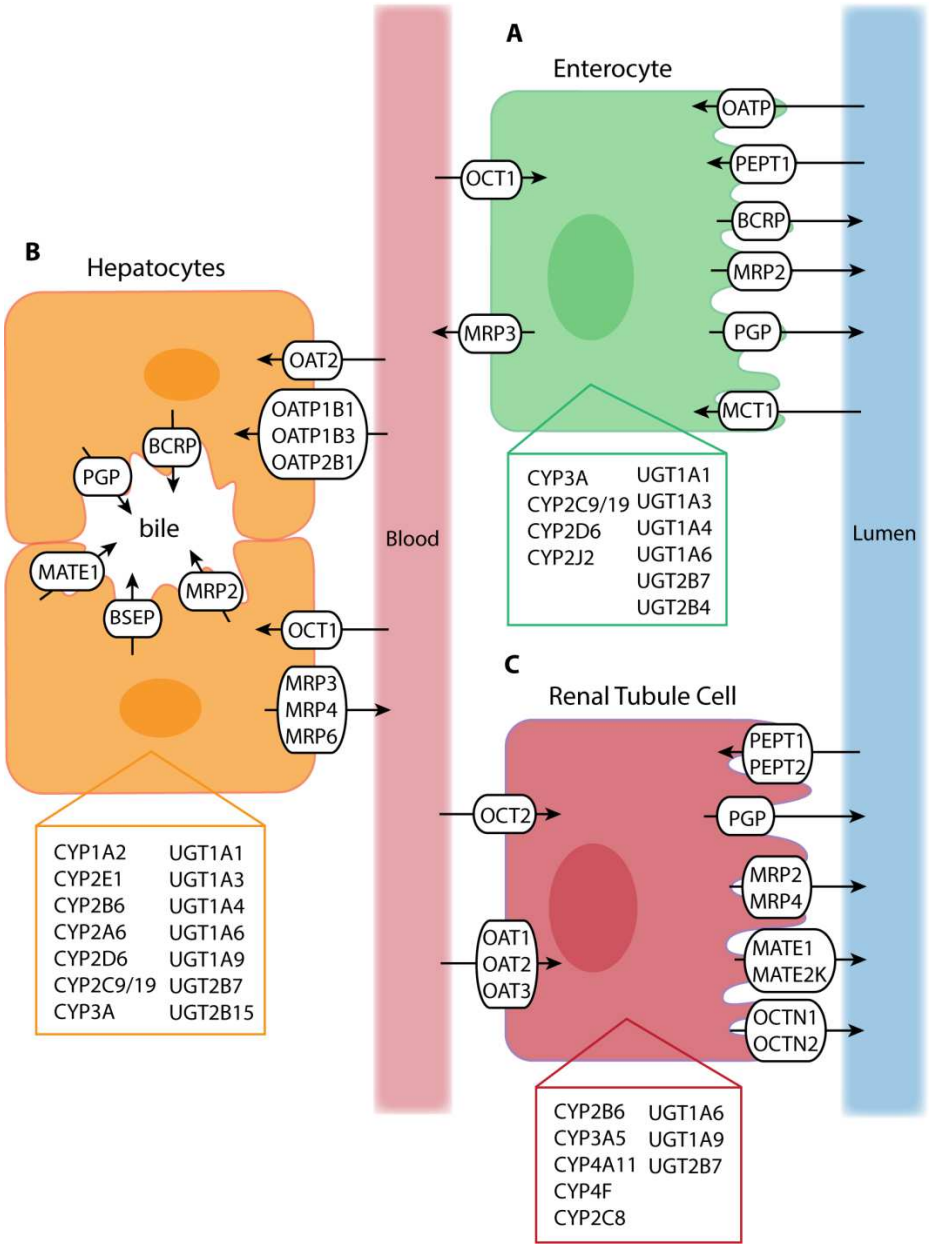

Figure 1.2. Cell types responsible for drug metabolism and transport. The three main organ systems often considered important in drug metabolism are the intestine, liver and kidney. The cell types in each of these tissues where drug-metabolizing enzymes and transporters are located are shown here. These include (A) enterocytes for the intestine, (B) hepatocytes for the liver, and (C) renal tubule epithelial cells for the kidney. For each cell type, the main transporters, CYPs and UGTs are shown.

Table 1.1. Summary of published metabolic activity in stem cell derived hepatocytes.

EROD = Ethoxyresorufin-O-deethylase; HPLC = High performance liquid chromatography; LC/MS = Liquid chromatography/Mass Spectrometry; 3-MC = 3-methylcholanthrene; BNF = β-naphthoflavone; hPH = human primary hepatocytes; SCDH = Stem cell derived hepatocytes.

Reference	Assay	Evaluation	Result
Rambhatla L. et al, 2003	EROD for CYP1A2	Basal activity compared to induced using 3-MC for SCDH and hPH	SCDHs exhibited 3-6 fold induction hPH exhibited 3 fold induction
Duan Y. et al, 2007	EROD for CYP1A2	Basal activity compared to induced using 3-MC for SCDH and hPH	SCDHs exhibit 11 fold induction hPH exhibit 32 fold induction
Ek M. et al, 2007	EROD for CYP1A2	Basal activity	No activity detected in SCDHs
Hay DC. et al, 2007	HPLC	Incubate SCDHs with Rifampin and Testosterone with or without Ketoconazole	No comparison to basal activity prior to rifampin incubation Peak detected that was absent in the presence of inhibitor
Hay DC., Zhao D. et al, 2008	LC/MS	Incubate cells with a cocktail of tolbutamide, bufuralol, phenacetin and midazolam Compare to HepG2 cells	SCDHs metabolize phenacetin and bufuralol similar to HepG2 cells; midazolam metabolism higher than HepG2 but not significant; tolbutamide metabolism in SCDHs but not HepG2 cells
Hay DC., Fletcher C. et al, 2008	EROD for CYP1A2	Basal activity	CYP1A2 activity detected, no comparison to other cell lines
Basma H. et al, 2009	EROD for CYP1A2 HPLC	CYP1A2 basal activity compared to induced using BNF CYP3A basal activity compared to induced using phenobarbital Compare to hPH	SCDHs exhibit inducible CYP1A2 activity at approximately 25-30% of that in hPH SCDHs form 6β-hydroxytestosterone comparable to hPH
Brolen G. et al, 2010	LC/MS	Incubate cells with phenacetin, midazolam or diclophenac Compare to HepG2 cells	Phenacetin metabolite levels similar to HepG2 cells; midazolam metabolite levels slightly higher than HepG2 cells; diclofenac metabolite levels higher than HepG2 which exhibited no activity
Duan Y. et al, 2010	LC/MS	Incubate cells with either phenacetin,	Phenacetin and bufuralol metabolite levels similar to hPH; midazolam and

		midazolam, bufuralol or diclofenac Compare to hPH	diclofenac metabolite levels lower than hPH
Sullivan GJ. et al, 2010	p450 Glo Assay	CYP3A4, CYP1A2 in SCDHs	Luminescent activity detected in SCDHs
Takayama K. et al, 2012	LC/MS	Incubate SCDHs with one of 9 substrates: phenacetin, bupropion, paclitaxel, tolbutamide, S-mephenytoin, bufuralol, midazolam, testosterone, hydroxyl coumarin (test for glucuronidation) Compare to hPH	Metabolite formation as follows, as percent compared to hPH: Acetaminophen – 6.7% Hydroxybupropion – 3.0% 6α-hydroxypaclitaxel – 21.6% Hydroxytolbutamide – 15% 4'-hydroxymephenytoin – 1.7% 1'-hydroxybufuralol – 2.4% 1'-hydroxymidazolam – 2.2% 6β-hydroxytestosterone – 24% 7-hydroxycoumarin glucuronide – 42%

Chapter 2

Pharmacogenetic Profiling of Select Commonly Used Human Embryonic Stem Cell Lines

2.1 Abstract

Background Primary human hepatocytes are commonly used to evaluate liver drug metabolism and toxicity. To overcome issues associated with primary hepatocytes researchers are investigating the potential of pluripotent stem cells as an alternative or complementary source of hepatocytes. Stem cell derived hepatocytes (SCDHs) may also provide an improved system for evaluating genotype-phenotype relationships, e.g. cytochrome P450 (CYP) gene polymorphisms and their impact on drug metabolism and toxicity.

Methods To demonstrate the utility of SCDHs in pharmacogenetic screening, we genotyped the five commonly used WiCell® human embryonic stem cell lines (hESC), H1, H7, H9, H13 and H14 using the Affymetrix DMET™ Plus chip array.

Results One CYP enzyme with documented polymorphic adverse drug reactions is CYP2D6. With regard to CYP2D6 gene copy number variation, we found H1 has only one gene copy, which also harbors the *CYP2D6*41* splicing defect, predictive of a CYP2D6 poor/intermediate metabolizer. We identified no CYP2D6 gene duplications, indicating no representative ultra-rapid metabolizer. The H7 and H14 lines are heterozygous for the non-functional *CYP2D6*4* variant resulting in a predicted intermediate metabolizer phenotype. In addition, we compared the penetrance of the *CYP2D6*41* splicing defect in SCDHs and liver tissue via reverse-transcription PCR assay. We found incomplete penetrance of the *CYP2D6*41* allele in liver tissue and variable penetrance in SCDHs.

Conclusion This pharmacogenetic data on CYPs (and other polymorphic ADME genes) will be critical for predictive drug metabolism/toxicity studies utilizing the WiCell® lines as a target cell source.

2.2 Introduction

Pharmacogenetic variability can influence an individual's susceptibility to drug toxicity, contributing to observed adverse drug reactions (ADRs) [109]. Drug-drug interactions are a major concern of pharmaceutical companies, particularly with respect to ADRs, a leading cause of preventable death in the United States [109]. Because of this, preclinical screening of metabolite spectra and toxicity is a necessary and important part of the drug development process. Primary human hepatocytes are the most physiologically relevant *in vitro* preclinical screening system used to evaluate drug metabolism in the liver [110]. This is due to their high-expression of phase I and II drug-metabolizing enzymes, as well as phase III transporters. However, primary human hepatocytes i.) are source limited, ii.) have high donor variability, iii.) only survive short term in culture, and iv.) exhibit a rapid loss of hepatic phenotypes and function in culture [81, 110, 111]. To overcome the limitations associated with primary human hepatocytes, we and others are investigating the potential of pluripotent stem cells as a source for generating hepatocytes for *in vitro* screening of new chemical entities. Pluripotent stem cells offer advantages over traditional hepatocyte sources because stem cells have high self-renewal abilities and provide an unlimited source from which to generate hepatocytes when needed [81, 112]. Stem cell derived hepatocytes (SCDHs) may also provide an improved system for evaluating genotype-phenotype relationships, e.g. cytochrome P450 (CYP) gene polymorphisms and their impact on drug metabolism and toxicity, and in particular drug-induced liver injury.

To demonstrate the utility of SCDHs in pharmacogenetic predictive screening, the aim of this study was to genetically profile the commonly used WiCell® hESC lines H1, H7, H9, H13 and H14 using the Affymetrix DMET™ Plus chip array. This array covers approximately 2000 polymorphisms in Absorption, Distribution, Metabolism and Excretion (ADME) relevant genes.

We focused on CYP2D6 in our analysis in utilizing SCDHs for genotype-phenotype predictions, given its highly polymorphic nature and role in metabolizing about 20% of marketed drugs [113, 114]. In terms of testing genotype-phenotype relationships for CYP2D6 in SCDHs, we assessed the penetrance of *CYP2D6*41*, a splicing defect which results in a CYP2D6 splice product lacking exon 6, through use of a reverse-transcription PCR assay.

2.3 Materials and Methods

2.3.1 Cell Lines

The hESC lines H1 (WA01), H7 (WA07), H9 (WA09), H13 (WA13), and H14 (WA14) were obtained from WiCell® Research Institute (Madison, WI, http://www.wicell.org) and propagated at the University of Washington (UW) Institute for Stem Cell and Regenerative Medicine. All studies were conducted under approval of the University of Washington Embryonic Stem Cell Research Oversight Committee. Two lots of cryopreserved hepatocytes, HUM4012 and HUM4034 phenotyped as a CYP2D6 poor metabolizer and extensive metabolizer, respectively, were obtained from Triangle Research Labs (Research Triangle Park, NC).

2.3.2 DNA Isolation and Genotyping

Genomic DNA was isolated from the WiCell® hESC lines using the Qiagen (Valencia, California) DNeasy blood and tissue kit according to the manufacturer's recommendations. DNA was quantified on a BioRad SmartSpec Plus (Hercules, CA) spectrophotometer, measuring absorbance and 260/280 nm ratio. Genotyping of hESC lines H1, H7, H9, H13, and H14 was conducted using the Affymetrix DMET™ Plus Array according to manufacturer's

recommendations (Santa Clara, CA, http://www.affymetrix.com). Analysis was performed using Affymetrix's DMET™ Console Analysis Software.

2.3.3 RT-PCR and CYP2D6 Copy Number Assay

RNA was isolated using TRIzol Reagent from Invitrogen (Carlsbad, CA) following manufacturer's recommendations. Complementary DNA was synthesized using 1 μg total RNA and the Taqman® Reverse Transcription Reagents in 10 μL total volume (Invitrogen). qRT-PCR for Albumin (ALB), α-feto protein (AFP), CYP2D6, CYP3A4, hepatocyte nuclear factor 4α (HNF4α), Nanog and OCT4 was carried out using Taqman® Gene Expression Assays from Applied Biosystems (Foster City, California) with GUSB as the housekeeping gene. CYP2D6 copy number was assessed using a TaqMan® Copy Number assay from Applied Biosystems (Hs00010001_cn) with RNAseP as a single copy gene calibrator, according to the manufacturer's recommendations, using their SDS 2.3 and Copy Caller v1.0 programs. One copy and more than two copy positive controls were identified in the UW School of Pharmacy Human Liver Bank (Seattle, WA) through sequencing analysis as previously described [115].

2.3.4 Hepatocyte Differentiation

The hESC lines H1 and H9 were cultured on mouse embryonic fibroblasts (MEFs) before being transferred to Matrigel™ (BD Biosciences, San Diego, CA)-coated plates using TeSR2 media (Stem Cell Technologies, Vancouver, Canada). Hepatocyte differentiation was induced in three stages, as published by Hay et al. [84]. Briefly, differentiation was initiated at 60-70% confluence by replacing the TeSR2 media with RPMI 1640 priming medium containing B27 (Invitrogen), 100 ng/mL Activin A (PeproTech, Rocky Hill, NJ), and 50 ng/mL Wnt3a (R&D

Systems, Minneapolis, MN). After 72 hours, with daily media changes, the cells were switched to differentiation medium: Knockout-DMEM containing 20% serum replacer, 1 mM glutamine, 1% nonessential amino acids, 0.1 mM β–mercaptoethanol (Invitrogen), and 1% dimethyl sulfoxide (DMSO) (Sigma, St Louis, MO) for a further 5 days. Lastly, the cells were switched to maturation media: Hepatozyme containing 10 μM hydrocortisone 21-hemisuccinate, 2 mM glutamine, 10 ng/mL hepatocyte growth factor and 20 ng/mL oncostatin M (R&D Systems) [86]. The media was changed every other day during maturation until the end of differentiation at day 17.

2.3.5 Immunocytochemistry

Cells were fixed with ice-cold methanol for 10-15 minutes, washed with PBS, and permeabilized with 0.5% Triton X-100 for 2 minutes. Following a PBS wash, cells were blocked with 2% normal goat serum for 1 hour at room temperature. Cells were then washed with PBS again and incubated overnight at 4 °C with the following primary antibodies: anti-AFP at 1:600 (Dako, Carpinteria, CA); anti-Albumin at 1:1000 (a gift from Dr. Jean Campbell, Department of Pathology, University of Washington); anti-HNF4α at 1:100 (Santa Cruz Biotechnology, Dallas, TX); and anti-CYP3A at 1:100 (Santa Cruz Biotechnology). After washing with PBS, cells were incubated with Alexa Fluor® 488 secondary antibodies at 1:1000 for 1 hour at room temperature (Invitrogen). Finally, cells were mounted with SlowFade® Gold Antifade Mountant with DAPI (Invitrogen).

2.3.6 *CYP2D6*41* reverse-transcription PCR Assay

Total RNA was isolated using Tri Reagent Solution (Invitrogen), following manufacturer's recommendations, and quantified on a BioRad SmartSpec Plus (Hercules, CA) spectrophotometer, measuring absorbance and 260/280 nm ratio. cDNA was synthesized using the TaqMan Reverse Transcription kit (Invitrogen) from 1 μg of total RNA. To detect the presence of exon 6 in CYP2D6, a 579-bp PCR fragment spanning a region from exon 5 to exon 8 was amplified with primers Exon5/8For3 (5'-TCCCCGTCCTCCTGCATA-3') and Exon5/8Rev3 (5'-GTGTTCGGGGTGGAAGCG-3') (IDT, Coralville, Iowa). If exon 6 is skipped due to the presence of *CYP2D6*41*, a smaller PCR fragment of 438-bp is expected. PCR was run under the following conditions, 95^{0}C 5 minutes, 92^{0}C 20 seconds, 59.6^{0}C 30 seconds, 72^{0}C 2 minutes, 72^{0}C 10 minutes, 4^{0}C hold, repeating steps 2-4 for 40 cycles. PCR products were run on 1.5% agarose gels and visualized by staining with 0.5 μg/mL ethidium bromide (BioRad). Human liver samples used for this study were obtained from the liver bank [115]. Genotyping for *CYP2D6*41* was done using an existing TaqMan® assay (C_34816116) (Applied Biosystems).

2.4 Results and Discussion

The University of Wisconsin has made WiCell® lines available to researchers for well over a decade [116]. This has made them some of the most widely used hESC lines in research, and in particular the most commonly used hESC lines in SCDH research, specifically the H1 and H9 lines [82, 84, 85, 88-90, 92, 93, 95-97, 106, 117-125]. To be useful in preclinical drug metabolism and toxicity screening, SCDHs must demonstrate consistent and reproducible activity of drug metabolism proteins, in particular the oxidative CYP enzymes. In addition, it would be ideal if SCDHs demonstrate metabolic activities comparable to human primary

hepatocytes. When evaluating CYP activity versus primary hepatocytes, it's important to take pharmacogenetic variability into account. To demonstrate the utility of SCDHs in pharmacogenetic predictive screening, the aim of this study was to genetically profile the commonly used WiCell® hESC lines.

2.4.1 Genotyping

Select genotyping results for *CYP2D6* can be found in Table 2.1. Analysis of *CYP2D6* copy number found H1 to have 1 copy, with all other lines having 2 copies of *CYP2D6*. No *CYP2D6* duplications were found, indicating there is no representative of a *CYP2D6* ultra-rapid metabolizer within these cell lines (Table 2.1). Lines H7 and H14 were both found to have one copy of the *CYP2D6*4* null allele, with no other polymorphisms associated with aberrant function detected. With regard to the *CYP2D6*41* allele, line H9 was found to be heterozygous for this allele, and the single gene copy of *CYP2D6* in line H1 also contains the *CYP2D6*41* allele. Taking the copy number and genotyping data together, we have made predictions regarding CYP2D6 phenotype in these cell lines, as found in Table 2.1. To summarize, we predict line H1 to be a CYP2D6 poor-intermediate metabolizer, lines H7 and H14 to be intermediate metabolizers, line H9 to be an intermediate-extensive metabolizer, depending on activity from the *CYP2D6*41* allele, and line H13 to be an extensive metabolizer. Select genotyping results for other CYP enzymes can be found in Table 2.2. Notably, all 5 hESC lines were found to be homozygous for *CYP3A5*3*, a null allele, meaning they are all CYP3A5 non-expressors. In addition, the H14 line is homozygous for *CYP2C9*2* and H1 is heterozygous for *CYP2C9*3*; both of these alleles result in decreased CYP2C9 activity and have documented effects on *in vitro* and *in vivo* pharmacokinetics and clinical drug response, e.g. warfarin [30].

Genotyping results for Phase II/III enzymes can be found in Table 2.3. Lines H7, H13, and H14 are heterozygous for the *UGT1A1*28* allele, which results in reduced activity of UGT1A1 [126]. Clinically, reduced activity of the *UGT1A1*28* allele is associated with development of toxicity following administration of the chemotherapeutic irinotecan (The Pharmacogenomics Knowledge Base: https://www.pharmgkb.org) [127]. Additionally, lines H1, H7, and H14 are heterozygous for the *NAT2*5* allele and H13 is homozygous for this allele, likely resulting in slow acetylator status for these cell lines. The Affymetrix DMET™ array genotyping results in their entirety can be accessed from Gene Expression Omnibus (GEO): (www.ncbi.nlm.nig.gov/geo; accession number: to be added, reviewer link: http://www.ncbi.nlm.nih.gov/geo/query/acc.cgi?token=abctqwayxjuljgh&acc=GSE53889).

For use in preclinical drug metabolism screening assays, vendors commonly offer pooled donor lots of hepatocytes to mitigate the effects of interindividual variability. With this in mind, the H1 line has one copy of *CYP2D6*, making it a predicted poor metabolizer in human hepatocytes, meaning SCDHs generated from hESC line H1 may not metabolize CYP2D6 probe drugs at a level comparable to primary hepatocytes. In this case it would be important to ensure that a lot of single donor human primary hepatocytes used for comparison with H1-derived SCDHs have been characterized as a CYP2D6 poor metabolizer. Regarding other CYP isozymes, a commonly used activity test in SCDHs is an ethoxyresorufin-O-deethylase (EROD) assay for CYP1A activity and inducibility [83, 84, 87, 106]. Our genotyping results show the H1 line to be homozygous and H9 to be heterozygous for *CYP1A2*1F*, an allele which has been shown to influence the magnitude of inducibility of CYP1A2 [30, 128].

The genotyping data presented here is important to better understand the activity of metabolizing enzymes and transporters when evaluating metabolism of probe substrates in

SCDHs, particularly when being used as a marker to evaluate the efficiency of differentiation of SCDHs. The Affymetrix DMET™ array used for genotyping in this study provides a thorough evaluation of the major known polymorphisms in ADME-related genes. However, there are examples when calls were not made (e.g. *CYP2B6*6*), such that if evaluating activity of these proteins, individual genotyping for these alleles may be necessary. This study only reports results for the five commonly used WiCell® lines, however this approach to genotyping should be considered for all hESC and human induced pluripotent stem cell (iPSC) lines used as a target cell source for models of drug metabolism and toxicity. In particular, if a bank of hESC or iPSCs is to be established then the use of a genotyping array, such as the Affymetrix DMET™ array, should be implemented with results readily available to researchers. As the cost of whole genome sequencing continues to decrease, it will become an attractive alternative to targeted arrays such as what we employed, with the caveat that mining these large data sets for specific ADME-related polymorphisms is currently challenging.

To further demonstrate the use of SCDHs in pharmacogenetic screening we evaluated the functional capacity of CYP2D6 with regards to xenobiotic metabolism in comparison to two lots of cryopreserved hepatocytes phenotyped as CYP2D6 poor and extensive metabolizers. A commonly used assay to examine CYP activity in SCDHs includes the Promega P450-Glo™ assays. Using the P450-Glo™ CYP2D6 assay we were unable to detect activity in our SCDHs, and activity levels of the two lots of cryopreserved hepatocytes while detectable, were unexpectedly not different. This could be due to the fact that the P450-Glo™ CYP2D6 assay is not recommended for use as a cell-based assay and the substrate provided for CYP2D6 also interacts with CYP1A and CYP2B6, this lack of specificity makes it ill-suited for phenotype discrimination. Using a LC-MS based incubation cocktail assay containing the CYP2D6 probe

dextromethorphan we could detect a difference in activity between the cryopreserved hepatocyte lots, with the poor metabolizers displaying activity just above the limit of detection [129]. However, we again could not detect activity in our SCDHs above the limit of detection. Based on these metabolic assays, we conclude that SCDHs lack detectable activity for CYP2D6 under the hepatocyte differentiation conditions performed. With respect to mRNA production, qRT-PCR results support the hypothesis that H1 cells have less CYP2D6 transcript than H9 cells, as expected based on their genetic makeup (Figure 2.1C). To definitively show a difference in metabolic activity will require improved differentiation efficiencies for SCDHs. For instance, incorporating the use of small molecule maturation compounds, viral transduction with HNF4α or 3D culture conditions and biomaterials to enhance differentiation efficiency of SCDHs [89, 90, 99, 130].

2.4.2 *CYP2D6*41* reverse-transcription PCR Assay

Aberrant splicing resulting from the *CYP2D6*41* polymorphism was assessed *ex vivo* with human liver tissue and *in vitro* using SCDHs. Total RNA was isolated from liver tissue from the UW School of Pharmacy Liver Bank and from SCDHs obtained via differentiation of WiCell® lines H1 and H9. The differentiation protocol yielded SCDHs which morphologically resembled hepatocytes (Figure 2.1A) and were immunocytochemically positive for AFP, albumin, HNF4α and CYP3A (Figure 2.1B). Positive immunocytochemical staining was uniform across the wells with the exception of colonies of cells that failed to differentiate. Typical differentiation efficiency is around 90%, however, we have not conducted quantitative morphometry. Immunocytochemical staining was corroborated by qRT-PCR analyses, which showed that SCDHs express AFP, as well as albumin, HNF4α and CYP3A4 (Figure 2.1C).

While expression of HNF4α in SCDHs is comparable to that seen in cryopreserved hepatocytes, expression levels of albumin and CYP3A4 were lower than that of cryopreserved hepatocytes (Figure 2.1C). Conversely, expression of AFP in SCDHs is higher than that expressed in cryopreserved hepatocytes, suggesting a retention of a fetal phenotype in the SCDHs (Figure 2.1C). Evaluating expression of two pluripotency markers, Nanog and OCT4, SCDHs demonstrate expression that is comparable to that in cryopreserved hepatocytes, and importantly, has decreased from expression in the undifferentiated hESC lines (Figure 2.1C). In the case of CYP2D6, expression levels were detectable in H9 SCDHs, though again below expression in cryopreserved hepatocytes, but H1 SCDHs were below the limit of quantitation (Figure 2.1C). This differential expression is in line with the genotyping results for these two cell lines.

Earlier identification and characterization of the 2988G>A SNP, now referred to as *CYP2D6*41* (Human CYP Allele nomenclature website: http://www.imm.ki.se/), revealed it to cause a splicing defect, resulting in exon 6 being skipped, and a predictor of CYP2D6 intermediate metabolizer phenotype [131-133]. Toscano et al. identified the splice variant lacking exon 6 in liver samples genotyped for *CYP2D6*41* (2988G>A) and found that 2988G>A causes favorable formation of a splice product that lacks exon 6, with up to 7-fold increased levels of the splice variant [132]. We wanted to further elucidate the penetrance of *CYP2D6*41* aberrant splicing and, in addition, we wanted to demonstrate the potential utility of SCDHs to evaluate genotype-phenotype relationships for CYP2D6. Results from PCR amplification using primers Exon5/8For3 and Exon5/8Rev3 are shown in Figure 2.1E. The expected amplicons for samples homozygous for *CYP2D6*41* are 438-bp, for heterozygous samples both 438-bp and 579-bp, and for non-carriers of *CYP2D6*41* 579-bp. As shown in Figure 2.1E, certain samples (lanes 1 and 2) homozygous for **41* have a 579-bp amplicon as well as the expected 438-bp

alternatively spliced band, indicating the unexpected presence of exon 6, and demonstrating incomplete penetrance of this splicing defect. In addition, one sample (lane 7) heterozygous for **41* only displays the 579-bp amplicon, indicating presence of exon 6 in all mRNA produced (or suppression of expression of the **41* allele). It should be noted that the aberrantly spliced band may be present, but simply was below the limit of detection in our RT-PCR assay. The H1 SCDH sample, with one copy of *CYP2D6* containing **41* displays the expected exon 6 spliced band at 438-bp, as seen in Figure 2.1E, lane 13. No properly spliced band was detected, as expected. Our SCDH *CYP2D6*41* heterozygous cell, line H9 (lane 14) also displays a band indicating aberrant exon 6 splicing, but only a weak band for the properly spliced transcript fragment. Again, bands may be present, but simply were below the limit of detection in our RT-PCR assay; based on observations from the qRT-PCR that CYP2D6 expression in H1 SCDHs is below the limit of quantitation and in H9 SCDHs is 16 fold lower than that of cryopreserved hepatocytes based on $\Delta\Delta C_T$ calculations. We are able to show similar results for *CYP2D6*41* splicing in our SCDHs as seen in the liver tissue samples. Overall, our results corroborate the findings of Toscano et al. and provide further evidence that *CYP2D6*41* displays incomplete penetrance.

2.5 Conclusion

Stem cell derived hepatocytes may provide an improved *in vitro* system for evaluating genotype-phenotype relationships of the CYP enzymes and their impact on drug metabolism and toxicity. This is the first published report of genotyping in the WiCell® hESC lines with regards to ADME-relevant polymorphisms**.** In addition, we are able to demonstrate the *CYPP2D6*41* splicing defect displays incomplete penetrance, with similar results observed in SCDHs and liver

tissue. The pharmacogenetic data provided here is vital to understanding metabolism profiles when these hESC lines are used as a target tissue source for models of drug metabolism and toxicity.

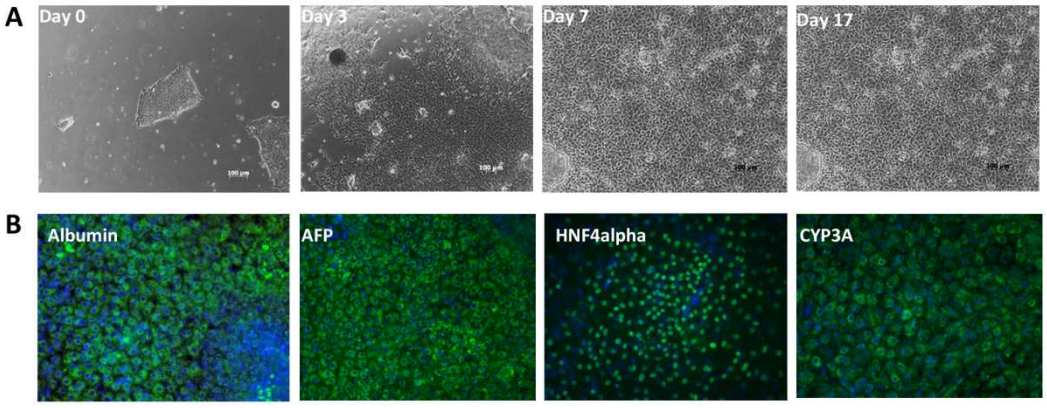
A
Day 0
Day 3
Day 7
Day 17
B
Albumin
AFP
HNF4alpha
CYP3A

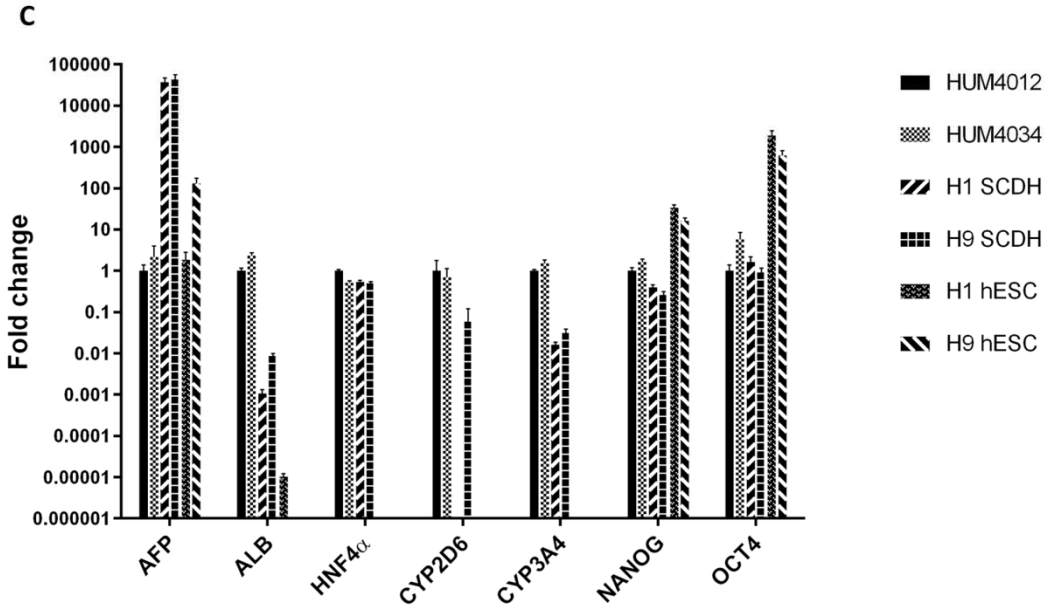
C
Fold change
100000
10000
1000
100
10
1
0.1
0.01
0.001
0.0001
0.00001
0.000001
AFP
ALB
HNF4α
CYP2D6
CYP3A4
NANOG
OCT4
HUM4012
HUM4034
H1 SCDH
H9 SCDH
H1 hESC
H9 hESC

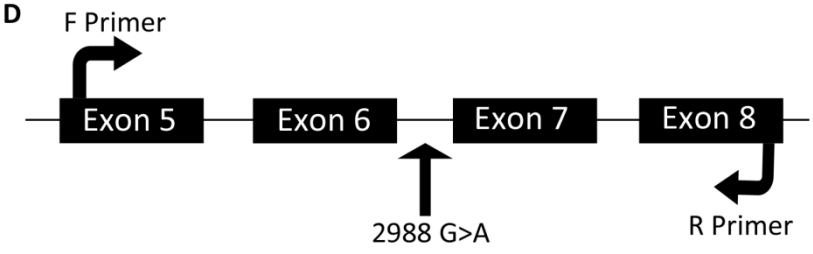
D
F Primer
Exon 5
Exon 6
Exon 7
Exon 8
2988 G>A
R Primer


CYP2D6*41
Exon 5
Exon 7
Exon 8

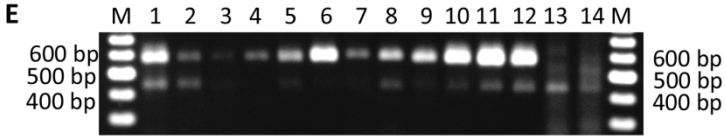
E
M 1 2 3 4 5 6 7 8 9 10 11 12 13 14 M
600 bp
500 bp
400 bp
600 bp
500 bp
400 bp

Figure 2.1 Stem Cell Derived Hepatocyte Characterization and *CYP2D6*41* Reverse Transcription PCR Assay. (A): Phase contrast microscopy depicting human embryonic stem cells (Day 0) and hESCs throughout hepatocyte differentiation (Day 3, 7 and 17). (B): Immunocytochemistry results for albumin, α-feto protein (AFP), HNF4α and CYP3A on Day 17. Positive staining is indicated in green, DAPI was used to stain nuclei, shown in blue. (C): Gene expression results shown as fold change compared to cryopreserved hepatocyte lot HUM4012, which was set to 1. HUM4012 and HUM4034 represent cryopreserved hepatocyte lots; H1 SCDH and H9 SCDH represent Day 17 SCDHs; H1 hESC and H9 hESC represent undifferentiated hESC lines H1 and H9, respectively. The following samples were found to be below the limit of quantitation (BLQ): H1 SCDH – *CYP2D6*; H1 hESC – *HNF4α*, *CYP2D6*, and *CYP3A4*; H9 hESC – *ALB*, *HNF4α*, *CYP2D6*, and *CYP3A4*. (D): Schematic representation of the *CYP2D6* gene. The polymorphism of interest is 2988G>A located between exons 6 and 7, and results in exon 6 skipping. To detect the presence of exon 6 in *CYP2D6*, a 579-bp PCR fragment spanning a region from exon 5 to exon 8 was amplified with primers Exon5/8For3 (F Primer) and Exon5/8Rev3 (R Primer). If exon 6 is skipped due to the presence of *CYP2D6*41*, a smaller PCR fragment of 438-bp is expected. (E): Agarose electrophoretic analysis of reverse transcription PCR products of the *CYP2D6* region indicated in (D) from human liver tissue samples and Day 17 SCDHs generated from WiCell® lines H1 and H9. Lane M, 100 bp maker; lane 1 **41/*41*; lane 2 **41/*41*; lane 3 **1A/*1A*; lane 4 **1A/*1A*; lane 5 **2A/*2A*; lane 6 **1A/*1A*; lane 7 **1A/*41*; lane 8 **4A/*41*; lane 9 **1A/*41*; lane 10 **2A/*41*; lane 11 **2A/*41*; lane 12 **9A/*41*; lane 13 H1 **41*; lane 14 H9 **41* carrier.

Table 2.1 ***CYP2D6*** **genotyping results**. A summary of the *CYP2D6* copy number and genotyping results for WiCell® hESC lines H1, H7, H9, H13, and H14. Based on genotyping results a prediction for expected CYP2D6 phenotype of each cell line was made. PM = poor metabolizer, IM = intermediate metabolizer, EM = extensive metabolizer.

Common Name	Probe Set ID	H1	H7	H9	H13	H14
Copy Number		1	2	2	2	2
CYP2D6*2 **2850C>T**	AM_12261	T	C/T	C/T	T/T	C/T
CYP2D6*3 **2549delA**	AM_12267	A	A/A	A/A	A/A	A/A
CYP2D6*4 **1846G>A**	AM_12274	G	G/A	G/G	G/G	G/A
CYP2D6*6 **1707delT**	AM_12276	T	T/T	T/T	T/T	T/T
CYP2D6*9 **2613_2615delAGA**	AM_12264	AGA	AGA/AGA	AGA/AGA	AGA/AGA	AGA/AGA
CYP2D6*10 **100C>T**	AM_12285	C	C/T	C/T	C/C	C/T
CYP2D6*17 **1023C>T**	AM_12280	C	C/C	C/C	C/C	C/C
CYP2D6*29 **3183G>A**	AM_12255	G	G/G	G/G	G/G	G/G
CYP2D6*35 **4180G>C**	AM_12247	C	C/C	C/C	C/C	C/C
CYP2D6*41 **2988G>A**	AM_12257	A	G/G	G/A	G/G	G/G
Predicted Phenotype		PM-IM	IM	IM-EM	EM	IM

Table 2.2 CYP genotyping results. A summary of the CYP genotyping results for WiCell® hESC lines H1, H7, H9, H13, and H14.

Common Name	Probe Set ID	H1	H7	H9	H13	H14
CYP1A2*1F **-163C>A**	AM_10785	A/A	C/C	A/C	C/C	A/C
CYP2A6 **Deletion**	CN_CYP2A6	One or more	One or more	One or more	One or more	One or more
CYP2B6*5 **25505C>T**	AM_11426	C/C	C/T	C/C	C/T	C/T
CYP2B6*6 **15631G>T**	AM_11411	G/G	No Call	No Call	G/G	G/T
CYP2C9*2 **3608C>T**	AM_10100	C/C	C/C	C/C	C/C	T/T
CYP2C9*3 **42614A>C**	AM_10113	A/C	A/A	A/A	A/A	A/A
CYP2C19*2 **19154G>A**	AM_10070	G/G	G/G	G/G	G/G	G/G
CYP2C19*3 **17948G>A**	AM_10068	G/G	G/G	G/G	G/G	G/G
CYP2C19*17 **-806C>T**	AM_10053	C/T	C/C	C/T	C/C	C/C
CYP2E1*2 **1132G>A**	AM_10249	G/G	G/G	G/G	G/G	G/G
CYP3A5*3 **6986A>G**	AM_14759	G/G	G/G	G/G	G/G	G/G
CYP3A5*6 **14690G>A**	AM_14748	G/G	G/G	G/G	G/G	G/G
CYP3A7*1C **-232A>C**	AM_14791	A/A	A/A	A/A	A/A	A/A
CYP3A7*1C **-284T>A**	AM_14796	T/T	T/T	T/T	T/T	T/T
CYP3A7*2 **26041C>G**	AM_14781	C/C	C/C	C/C	C/C	C/C

Table 2.3 PhaseII/III Genotyping Results. A summary of the genotyping results for phase II and III enzymes for WiCell® hESC lines H1, H7, H9, H13, and H14.

Common Name	Probe Set ID	H1	H7	H9	H13	H14
ALDH2 **1510G>A**	AM_10586	G/G	G/G	G/G	G/G	G/G
GSTM1 **Deletion**	CN_GSTM1	One or more	0	One or more	0	0
GSTT1 **Deletion**	CN_GSTT1	One or more	One or more	One or more	One or more	One or more
NAT1*14 **560G>A**	AM_14978	A/G	G/G	G/G	G/G	G/G
NAT2*5 **341T>C**	AM_15001	C/T	C/T	T/T	C/C	C/T
SULT1A1*2 **638G>A**	AM_11005	A/G	A/G	A/G	G/G	A/G
TPMT*2 **238G>C**	AM_13986	G/G	G/G	G/G	G/G	G/G
TPMT*3B **460G>A**	AM_13980	G/G	G/G	G/G	G/G	G/G
TPMT*3C **719A>G**	AM_13973	A/A	A/A	A/A	A/A	A/A
TPMT*4 **626-1G>A**	AM_13977	G/G	G/G	G/G	G/G	G/G
UGT1A1*28 **TATA-box**	AM_13024	(TA)5or6/ (TA)5or6	(TA)5or6/ (TA)7or8	(TA)5or6/ (TA)5or6	(TA)5or6/ (TA)7or8	(TA)5or6/ (TA)7or8
UGT2B7*2 **802C>T**	AM_13465	T/T	T/T	T/T	C/T	T/T
ABCB1 **1236C>T**	AM_14612	C/T	C/T	C/T	C/T	C/T
ABCB1 **2677G>T>A**	AM_14592	G/T	G/T	G/T	G/T	G/T
ABCB1 **3435C>T**	AM_14581	C/T	C/T	C/T	C/T	C/T
ABCG2 **421C>A**	AM_13688	C/C	C/C	C/C	C/C	C/C
SLCO1A2 **404A>T**	AM_10533	A/A	A/A	A/A	A/A	A/A
SLCO1A2 **516A>C**	AM_10531	A/A	A/A	A/A	A/A	A/A
SLCO1B1*1B **388A>G**	AM_10496	A/G	A/A	A/G	A/A	A/A
SLCO1B1*4 **463C>A**	AM_10498	C/C	C/C	A/C	C/C	C/C
SLCO1B3 **334G>T**	AM_10481	G/G	G/G	G/G	G/G	G/G
SLCO1B3 **699A>G**	AM_10482	A/A	A/A	A/A	A/A	A/A

Chapter 3

Gene Expression Profiling and Metabolic Activity of Human Stem Cell Derived Hepatocytes

3.1 Abstract

Background Primary human hepatocytes are commonly used to evaluate liver drug metabolism and toxicity. Pluripotent stem cell derived hepatocytes (SCDHs) have the potential to overcome access and function-related limitations associated with primary hepatocytes. However, in order for SCDHs to become routinely used in preclinical drug metabolism and toxicity screening, they must demonstrate reproducible activity of drug metabolism proteins, particularly the oxidative CYP enzymes, and at a level comparable to that of primary human hepatocytes. We characterized the differentiation status of SCDHs, with emphasis on the expression and functional capacity of drug-metabolizing enzymes.

Methods Gene expression profiling of pluripotency markers, hepatocyte markers, transcription factors, drug-metabolizing enzymes and transporters was done for SCDHs, fetal liver tissue, adult liver tissue, cryopreserved hepatocytes and the liver cell line HepaRG. To evaluate the functional capacity of CYP enzymes in SCDHs, metabolite formation was assessed using a CYP cocktail approach and LC-MS/MS.

Results Based on gene expression profiling, SCDHs most closely resemble fetal hepatocytes, especially with regards to AFP, CYP3A7 and FMO1 expression. An assay of enzymatic function in SCDHs using a CYP cocktail revealed only minimal activity for CYPs 1A and 3A, with both activities well below that observed in primary hepatocytes.

Conclusion Gene expression profiling and functional assays of CYP activity indicate SCDHs behave largely as immature hepatocytes, lacking CYP expression and activity for most isoforms. More work needs to be done to enhance the maturity through terminal differentiation of SCDHs. Enhanced expression and function of drug-metabolizing enzymes in SCDHs would make them a

more viable option in the pharmaceutical industry for drug metabolism/liver toxicity screening assays.

3.2 Introduction

Drug metabolism studies are an important element of preclinical drug development, as metabolism is the main way that drugs are inactivated or eliminated from the central compartment space. Moreover, metabolism can facilitate the excretion of drugs from the body, as transformed, more polar metabolites [25]. For some drugs, metabolism can result in a more pharmacologically or toxicologically active product, again affecting drug response. Therefore, preclinical screening and characterization of the metabolic pathways of a new drug is a necessary part of its development and can be used to aid in predicting drug bioavailability, drug efficacy, drug-drug interactions, and drug toxicity. The main family of enzymes responsible for oxidative drug metabolism is the Cytochrome P450s (CYPs), in particular members of just three subfamilies (CYP1, CYP2 and CYP3) that are primarily responsible for the metabolism of most drugs [29]. The drug-metabolizing CYPs are highly expressed in the liver, making it the primary organ to study for the metabolism, detoxification and elimination of drugs, and the focus of drug optimization and safety studies [25, 26]. Hepatocytes are the main cell type within the liver, and are where the drug metabolizing enzymes, such as the CYPs, are found [25]. Therefore, human hepatocytes have become an integral component in studying drug metabolism and toxicity [16]. The CYP3A family is the most important of the hepatic drug metabolizing CYPs in humans. It comprises 25-30% of the total hepatic CYP content [45, 47, 134] and is also responsible for the majority of CYP-mediated drug metabolism, accounting for about 50% of all CYP-mediated reactions [114]. Other important drug-metabolizing CYPs, in decreasing order of contribution to CYP-mediated drug metabolism, are CYPs 2C9, 2D6, 2C19, 1A2, 2B6, and 2E1 [114].

Primary human hepatocytes have certain features that limit their utility in preclinical drug development, including: high donor variability, uncertain availability, short-term survival in

culture, and a rapid loss of hepatic functions in culture [81, 110, 111]. Stem cell derived hepatocytes (SCDHs) may provide an alternative or complementary *in vitro* tool to primary human hepatocytes for evaluating drug metabolism and liver toxicity characteristics. Pluripotent stem cells have high self-renewal abilities, providing a potentially unlimited source of hepatocytes of defined genotype and phenotype [81, 112]. In order for SCDHs to become routinely used in preclinical drug metabolism and toxicity screening, they must demonstrate reproducible activity of drug metabolism proteins, particularly the oxidative CYP enzymes. Additionally, it would be ideal if SCDHs produced metabolic activities comparable to that of primary human hepatocytes.

Many groups have published on differentiating human pluripotent stem cells into hepatocytes, both human embryonic stem cells (hESCs) and induced pluripotent stem cells (iPSCs). Researchers from Geron Corporation were the first group to demonstrate limited success, in 2003 [82]. However, early initial differentiation protocols of SCDHs showed low differentiation efficiencies, based on percentages of cells expressing hepatocyte markers such as albumin. One reason for the low differentiation efficiencies early on was the use of spontaneous differentiation through formation of embryoid bodies [82, 83]. There has been marked improvement in this area, with protocols that now rely on directed differentiation using set combinations of various factors, such as activin A, Wnt3, dimethyl sulfoxide (DMSO), hepatocyte growth factor (HGF), oncostatin M (OSM), and dexamethasone, which all contribute to increased differentiation efficiency [84-88]. Additionally, some groups have reported transduction of transcription factors such as FOXA2 and HNF1α, along with the use of growth factors as an efficient process for generating SCDHs [90-92]. More recently, protocols are moving away from the use of growth factors and have demonstrated that small molecules can be

used to efficiently generate SCDHs [99, 135, 136]. Other groups have also investigated 3D culture of cells, such as spheroids and bioreactors, to enhance hepatocyte differentiation [89, 93, 100, 101].

In order for SCDHs to be used in preclinical drug development they need to express functional drug-metabolizing enzymes, such as the CYPs. Common criteria used to evaluate the function of SCDHs include gene expression profiling, immunocytochemistry, western blotting, indocyanine green transport, glycogen accumulation, and albumin secretion. While becoming more common, few groups have assessed the functional activity of drug-metabolizing enzymes such as the CYPs in SCDHs, and not all use the gold standard of human primary hepatocytes for comparison of activity. Many groups have relied upon resorufin and P450-glo assays to assess activity of one or two CYPs; only a few studies have utilized liquid chromatography-mass spectrometry (LC-MS) to evaluate multiple CYP activities of SCDHs, in comparison to the activities of primary hepatocytes [85, 88, 91, 104]. In a study by Duan et al., activity of four major drug-metabolizing CYPs (CYP1A2, 2C9, 3A4 and 2D6) was assessed using LC-MS. Results from this study demonstrated an activity of CYPs 1A2 and 2D6 that was comparable to what is observed in primary hepatocytes, indicating the SCDHs do express some functional CYP enzymes [88]. Additionally, the metabolic capacity, as well as inductive potential of CYP1A is occasionally characterized using the ethoxyresorufin-O-deethylase (EROD) assay. However, when comparing SCDH CYP activity data using either resorufin assays [82, 83, 106] or LC-MS [88, 91], to primary hepatocytes, SCDHs demonstrate lower activities than primary hepatocytes. In a study by Siller et al. evaluating SCDHs generated using a small molecule protocol compared to SCDHs using a standard growth factor protocol, activity of CYPs 1A2 and 3A4 were evaluated using P450-glo assays [135]. In this study they were able to demonstrate basal and

inductive activity for both CYPs, with activity of CYP1A2 being comparable between the two methods and activity of CYP3A4 being about 2.5 fold higher in the small molecule SCDHs, but there was no comparison of activity to primary hepatocytes or other hepatocyte cell lines [135]. In another study evaluating small molecule based protocols for generating SCDHs by Tasnim et al., CYP1A2 and 3A4 activity was measured through monitoring of metabolite formation on LC-MS [136]. Results of this study showed that while there was metabolite formation indicating some functional activity for CYPs 1A2 and 3A4, the activity as measured by LC-MS was only 8-10% of that in primary human hepatocytes [136].

Overall, published studies demonstrate that SCDHs do express CYPs and other drug-metabolizing enzymes, however they seem to be at levels below those in primary human hepatocytes. In addition, the majority of studies have also reported SCDHs as still expressing α feto-protein (AFP), which is highly expressed in fetal livers and not typically expressed in healthy adult livers, indicating the cells may still be in an immature state. Despite the advances made in generating SCDHs, the biggest limitation in the field to date is the inability to reproducibly and consistently generate mature hepatocytes with high levels of functional drug metabolizing enzymes. It should be noted that the lack of maturity is not unique to SCDHs, a lack of functional maturity has been observed in other stem cell derived cell types, most notably stem cell derived cardiomyocytes [103]. In order for SCDHs to be successfully used as an *in vitro* assay platform for metabolite profiling, this is something that must be overcome.

Pluripotent stem cells have a high self-renewal capability and can differentiate into any cell type in the body, making them an attractive tool for researchers in drug discovery and development. SCDHs offer a promising new tool for use in hepatic drug metabolism and toxicity screens, adding to available human derived cell models. There has been extensive

research on SCDHs for this purpose, and while there is evidence SCDHs express drug-metabolizing enzymes, they remain in a de-differentiated state. This indicates there is a significant need for improvement on generating and characterizing SCDHs, particularly with regards to their metabolic capacity as it compares to primary hepatocytes. We sought to further investigate the state of SCDHs as they compare to cryopreserved hepatocytes, with emphasis on the expression and functional capacity of drug-metabolizing enzymes. This was done in part through gene expression profiling of pluripotency markers, hepatocyte markers, drug-metabolizing enzymes and transporters. To evaluate the functional capacity of CYP enzymes in SCDHs, metabolite formation was assessed using a CYP cocktail approach and LC-MS/MS.

3.3 Materials and Methods

3.3.1 Cell culture and hepatocyte differentiation

Cryopreserve hepatocyte lots HU8110 and HU8114 were purchased from Invitrogen (Carlsbad, CA) and cultured according to manufacturer's instructions. Briefly, cells were thawed in CHRM® media and plated in Williams Medium E supplemented with Hepatocyte Plating Supplement Pack from Invitrogen on 24-well plates coated with rat Collagen I. Following a 6-hour incubation period to allow for cell attachment, the media was changed to Williams Medium E supplemented with Hepatocyte Maintenance Supplement Pack from Invitrogen. Cells were maintained in this hepatocyte maintenance media for 4 days with daily fluid changes. Cells were then collected in TRIzol Reagent (Invitrogen) for RNA extraction.

Cryopreserved hepatocyte lots HUM4012 and HUM4034 were purchased from Triangle Research Labs (TRL, Research Triangle Park, NC) and cultured according to manufacturer's instructions. Briefly, cells were thawed in Animal Thawing and Plating Medium from TRL and

plated in Human Hepatocyte Plating Medium from TRL supplemented with the plating supplement on 24-well plates coated with rat Collagen I. Following a 6-hour incubation period to allow for cell attachment, the media was changed to Hepatocyte Maintenance Medium supplemented with the maintenance supplement from TRL. Cells were maintained in this hepatocyte maintenance media for 3 days with daily fluid changes. Cells were then incubated with the CYP cocktail assay. In addition, plated human primary hepatocytes were kindly gifted from Dr. David Eaton's lab at the University of Washington for incubation with the CYP cocktail assay.

Undifferentiated HepaRG cells were obtained from Biopredic International (Saint-Gregoire, France). Undifferentiated HepaRG cells were cultured in Williams Medium E (Invitrogen) supplemented with growth supplement (Biopredic) for 2 weeks with fluid changes every 2-3 days. After 2 weeks in culture, HepaRG cells were differentiated using a 50:50 mix of media supplemented with growth supplement and Williams Medium E supplemented with differentiation supplement (Biopredic). After 2 days in culture, cells were switched to 100% media with differentiation supplement. Cells were maintained in media with differentiation supplement for 2 weeks, with fluid changes every 2-3 days. After 2 weeks of differentiation cells were collected in TRIzol reagent (Invitrogen) for RNA extraction.

The hESC lines H1 (WA01), H7 (WA07) and H9 (WA09) were obtained from WiCell® Research Institute (Madison, WI) and propagated at the University of Washington Institute for Stem Cell and Regenerative Medicine. All studies were conducted under approval of the University of Washington Embryonic Stem Cell Research Oversight Committee. hESCs were cultured on mouse embryonic fibroblasts (MEFs) before being transferred to Matrigel™ (BD Biosciences, San Diego, CA)-coated plates using mTeSR™1 media (Stem Cell Technologies,

Vancouver, Canada). Hepatocyte differentiation was induced in three stages, as published by Hay et al. [84, 86]. Briefly, differentiation was initiated at 60-70% confluence by replacing the mTeSR™1 media with priming medium: RPMI 1640 containing 1xB27 (Invitrogen), 100 ng/mL Activin A (PeproTech, Rocky Hill, NJ), and 50 ng/mL Wnt3a (R&D Systems, Minneapolis, MN). After 72 hours, with daily media changes, the cells were switched to differentiation medium: Knockout-DMEM containing 20% Knockout Serum Replacement, 1 mM glutamine, 1% nonessential amino acids, 0.1 mM β-mercaptoethanol (Invitrogen), and 1% dimethyl sulfoxide (DMSO) (Sigma, St Louis, MO) for a further 5 days. Lastly, the cells were switched to maturation media: Hepatozyme containing 10 μM hydrocortisone 21-hemisuccinate, 2 mM glutamine, 10 ng/mL hepatocyte growth factor and 20 ng/mL oncostatin M (R&D Systems). The media was changed every other day during maturation until day 17. Cells from multiple differentiation experiments were collected in TRIzol reagent at the end of differentiation on Day 17 for RNA extraction. SCDHs used for the CYP cocktail assay were differentiated using a single cell starting method. hESCs were cultured on Matrigel™ plates using mTeSR™1 media as above. Prior to the start of differentiation, cells were passaged with 0.05% Trypsin-EDTA (Invitrogen) to single cells and 1 x 10^5 cells per well were plated on fresh Matrigel™ coated 24-well plates in mTeSR™1 media containing 10 μM Y-27632 (ROCK inhibitor) (Selleck Chemicals, Houston, TX). Cells were cultured in these conditions for 24 hours and then differentiation was initiated with priming medium as described above. To investigate the inductive capacity of CYP enzymes, cells were cultured in the presence of 10 μM rifampicin (Sigma), 2 μM 3-methylcholanthrene (Sigma), 1 mM phenobarbital (Sigma), or 0.1% DMSO as a vehicle control for 72 hours before the end of differentiation on Day 17. Additionally, some cells were cultured with the addition of a small molecule, FPH1, previously shown to enhance

SCDH maturity and referred to as a "maturin", a kind gift from Dr. Sangeeta Bhatia's lab, MIT [99]. FPH1 was added one time at a final concentration of 10 μM on Day 10 of culture.

3.3.2 Fetal and adult liver tissue

Six human fetal liver tissue samples were obtained from the Birth Defects Research Laboratory at the University of Washington, courtesy of Dr. Qingcheng Mao. Fetal liver tissues were obtained with Use of Non-Identifiable Biological Specimens/Data approval. Two human liver tissue samples were obtained from the University of Washington School of Pharmacy Human Liver Bank (Seattle, WA).

3.3.3 Quantitative real-time PCR (qRT-PCR)

RNA was isolated using TRIzol Reagent from Invitrogen (Carlsbad, CA) following manufacturer's recommendations. Complementary DNA (cDNA) was synthesized using 3 μg total RNA and the Taqman® Reverse Transcription Reagents in 30 μL total volume (Invitrogen). Following synthesis, cDNA was diluted to 5 ng/μL and 20 ng was used for qRT-PCR analysis. qRT-PCR for CYPs 3A4, 3A7, 1A2, 1B1, 2A6, 2B6, 2C9, 2C19, 2C8, 2D6, 2E1, FMO1, FMO3, UGT1A1, UGT1A6, UGT2B4, UGT2B7, GSTT1, GSTM1, GSTP1, OATP1B1, OATP1B3, MRP2, ABCB1, ABCG2, ATP7B, NANOG, SOX2, OCT4, ALB, AFP, HNF4α, CAR, PXR, AHR, and POR was carried out using Taqman® Gene Expression Assays from Applied Biosystems (Foster City, California) with GUSB as the housekeeping gene.

3.3.4 CYP cocktail assay and LC-MS/MS

Two CYP cocktail assays developed in Dr. Jashvant Unadkat's lab at the University of Washington were used to assess functional CYP activity [129]. Cocktail A assesses CYPs 3A, 2C9, 1A, 2D6, 2A6, and cocktail B assesses CYPs 2B6, 2C8, and 2E1. Acetaminophen, amodiaquine dihydrochloride dihydrate, bupropion, chlorzoxazone, coumarin, phenacetin, and tolbutamide were purchased from Sigma. Dextromethorphan, d5-diazepam, dextrorphan, testosterone, n-desethylamodiaquine, hydroxy-bupropion, 4-hydroxytolbutamide, 6-hydroxychlorzoxazone, and 6-β-hydroxytestosterone were purchased from Cerilliant (Round Rock, TX). 7-hydroxycoumarin was a kind gift from Dr. Unadkat's lab. A set of metabolite standards was made for nine calibration points and a separate set of three quality control (QC) points was made. The calibrator concentrations ranged as follows: acetaminophen, 0.031-8 μM; OH-bupropion, 0.002-0.5 μM; 4-OH-tolbutamide, 0.013-3.3 μM; 6-OH-testosterone, 0.31-80 μM; 6-OH-chlorzoxazone, 0.0625-16 μM; 7-OH-coumarin, 0.0042-1.08 μM; n-desethylamodiaquine, 0.0083-2.12 μM; dextrorphan, 0.0017-0.44 μM. The QC concentrations ranged as follows: acetaminophen, 0.125-4 μM; OH-bupropion, 0.0078-0.25 μM; 4-OH-tolbutamide, 0.052-1.66 μM; 6-OH-testosterone, 1.25-40 μM; 6-OH-chlorzoxazone, 0.25-8 μM; 7-OH-coumarin, 0.017-0.54 μM; n-desethylamodiaquine, 0.033-1.06 μM; dextrorphan, 0.0068-0.22 μM. All calibrator and QC points were made in hepatozyme maturation media, an equal volume of calibrator or QC was then added to an equal volume of acetonitrile containing 0.06 ng/μL of internal standard d5-diazepam and centrifuged at 13,000 rpm for 10 minutes. The supernatant was removed and stored at 4 °C until analysis.

CYP assay incubations were performed on Day 17 SCDHs and cryopreserved hepatocytes lots HUM4012 and HUM4034. Incubations were performed as described by Liu et al., with some modifications [129]. Briefly, standard stock mixtures of cocktail A and B were

prepared and diluted in hepatozyme maturation media for cell incubations to the following final concentrations: Cocktail A, tolbutamide, 75 μM, testosterone, 100 μM, dextromethorphan, 5 μM, coumarin, 0.5 μM, phenacetin, 50 μM; Cocktail B, bupropion, 100 μM, amodiaquine, 4 μM, chlorzoxazone, 25 μM. The final concentration of organic solvent in cell incubations was 1%. Cocktail incubations with SCDHs were performed for 2 hours at 37 °C, at the end of the incubation period the media was collected and added to an equal volume of acetonitrile containing 0.06 ng/μL d5-diazepam. Cocktail incubations with cryopreserved hepatocytes were performed for 30 minutes or 1 hour at 37 °C, with media collected at the end of the incubation and added to an equal volume of acetonitrile containing d5-diazepam. All incubation samples were then centrifuged at 13,000 rpm for 10 minutes, supernatant was removed and stored at 4 °C until analysis.

The CYP assay metabolites were analyzed using an Agilent 6460 triple quadrupole mass spectrometer (Agilent Technologies, Santa Clara, CA) in the University of Washington Mass Spectrometry center as described by Liu et al., with minor modifications [129]. Briefly, HPLC separation was achieved using an Agilent XDB C18 2.1 x 150 mm, 5 μm column. Compounds were eluted with 0.25 mL/min of 0.1% formic acid in water (solvent A) and 0.1% formic acid in acetonitrile (solvent B) with the following gradient. For the first 1.5 minutes, 99% solvent A, then a linear decrease to 70% solvent A until 4 minutes. The gradient was maintained at 70% solvent A until 6 minutes, then a linear decrease to 25% solvent A until 9 minutes. The gradient was held at 25% solvent A until 13 minutes to wash and then cycled back to initial conditions and the column was allowed to re-equilibrate for 4 minutes before the next sample was injected.

3.4 Results and Discussion

3.4.1 Hepatocyte differentiation and gene expression

hESC lines H1 and H9 were utilized for hepatocyte differentiation. Hepatocyte differentiation was performed using a published protocol [84, 86]. Briefly, this protocol is broken into three stages to induce hepatocyte differentiation: the first stage referred to as the priming stage, is to prime the cells to the definitive endoderm lineage [84, 85, 137], the second stage referred to as the differentiation stage, induces hepatocyte differentiation, and the final stage referred to as the maturation stage, allows for final differentiation and maturation of the resulting hepatocytes. This differentiation protocol yields SCDHs which morphologically resemble hepatocytes, displaying the cuboidal morphology associated with hepatocytes and exhibiting bi-nucleated cells (Figure 3.1A,B,C). For comparison, a representative photomicrograph of cryopreserved hepatocytes is shown in Figure 3.1D.

In order to evaluate the maturity level of SCDHs and gain a better understanding of their potential utility in preclinical drug metabolism screens, gene expression profiling of select pluripotency markers, hepatocytes markers, transcription factors, drug-metabolizing enzymes and transporters was done. This expression profiling was performed for SCDHs at each stage of differentiation, hESCs, cryopreserved hepatocytes, HepaRG cells, human fetal liver tissue and human adult liver tissue. HepaRG cells are a cell line derived from a human adult hepatocarcinoma patient, which resemble the bi-potential hepatoblast cell [138-140]. These cells can be cultured in their hepatoblast, or undifferentiated state, and then undergo a differentiation process to form both biliary epithelial cells and hepatocytes [138-140]. HepaRG cells express many of the drug-metabolizing enzymes and more closely resemble primary hepatocytes than the commonly used HepG2 cells [140].

To determine if SCDHs retain stem cell characteristics, the pluripotency markers NANOG, OCT4 and SOX2 were evaluated. All results are reported as fold change compared to differentiated HepaRG cells, with GUSB as the housekeeping gene. From the gene expression profiling, expression of the pluripotency markers NANOG, OCT4, and SOX2 drops as differentiation progresses from stem cell to SCDHs (Figure 3.2). This demonstrates the cells are undergoing a differentiation process and are not retaining their pluripotency. Notably, expression of NANOG and OCT4 in SCDHs is similar to expression in differentiated HepaRG cells, which is below the level of expression in fetal liver tissue (Figure 3.2). SOX2 expression in SCDHs is more variable between the different cell lines, and ranges from 0.4- to 15-fold compared to differentiated HepaRG cells, based on $\Delta\Delta C_T$ calculations, while SOX2 expression in fetal liver tissue ranges from 0.4- to 7-fold compared to HepaRG cells. Expression of all three pluripotency markers is low in the adult human liver tissues evaluated. With regard to the hepatocyte markers, AFP, ALB and HNF4α, the same expression pattern is observed for all three, with expression increasing from stem cells through differentiation to SCDHs (Figure 3.2). For ALB, expression in SCDHs is still below expression in differentiated HepaRG cells, fetal and adult liver tissues. For HNF4α, expression in SCDHs is comparable to expression observed in fetal and adult liver tissues, though lower than differentiated HepaRG cells (Figure 3.2). With regard to AFP, SCDHs express AFP to a much greater extent than differentiated HepaRG cells, ranging from 2800- to 13000-fold higher than HepaRG cells based on $\Delta\Delta C_T$ calculations (Figure 3.2). Expression of AFP in fetal liver tissue ranges from 3600- to 30000-fold higher than HepaRG cells, indicating SCDHs express AFP at levels similar to or slightly below that in fetal liver tissue. As expected, AFP expression was below the limit of quantitation (BLQ) for one adult liver tissue tested, and minimally expressed in the second adult liver tissue. The persistent

expression of AFP in SCDHs is in accordance with published reports indicating a high retention of AFP expression in SCDHs. Overall, SCDHs appear to express the hepatocyte markers AFP, ALB, and HNF4α at levels comparable to fetal liver tissue, indicating a close resemblance to a fetal state hepatocyte.

In order to assess the utility of SCDHs in preclinical drug metabolism tests, expression of drug-metabolizing enzymes, transporters, and select transcription factors that regulate them were evaluated. The transcription factors constitutive androstane receptor (CAR), pregnane X receptor (PXR) and aryl hydrocarbon receptor (AhR) were selected because they regulate many of the hepatic phase I and II drug-metabolizing enzymes and transporters [141, 142]. For all three transcription factors, expression in SCDHs was minimal. Expression of PXR was only detected in iPSC SCDHs at 0.01-fold the expression found in HepaRG differentiated cells; expression of AhR was 0.1-fold the expression in HepaRG cells for all SCDH samples; and expression of CAR was also around 0.1-fold the level in HepaRG cells; all comparisons based on $\Delta\Delta C_T$ calculations (Figure 3.2). The expression of AhR in SCDHs was similar to or slightly higher than that in fetal liver tissues, which ranged from 0.01- to 0.1-fold of the expression in HepaRG cells, while the expression of CAR and PXR in SCDHs was lower than that in fetal liver tissues.

To examine expression of phase I drug-metabolizing enzymes, CYPs and flavin containing monooxygenases (FMO) were evaluated. With regard to FMOs, FMO1 is normally expressed to a greater extent in the fetal liver, and so can be used as another marker to evaluate how fetal-like SCDHs are. Indeed, from gene expression profiling FMO1 was highly expressed in fetal liver tissue, at levels 20- to 50-fold higher than that in differentiated HepaRG cells, while FMO1 expression was undetected in adult liver tissues (Figure 3.2). FMO1 expression in

SCDHs increases through differentiation, being 7 to 13 fold higher than differentiated HepaRG cells (Figure 3.2). While SCDHs do retain high expression of FMO1, it is lower than that in fetal liver tissue. This indicates SCDHs may be slightly more mature than fetal liver hepatocytes. Expression of FMO3 was only minimally detected in the iPSC SCDHs (Figure 3.2). The CYP enzymes CYP3A4 and CYP3A7 also exhibit differential expression between fetal and adult liver, with CYP3A7 being the predominant isoform in fetal liver and CYP3A4 being predominant in the adult liver. Based on gene expression profiling, this pattern was observed between fetal and adult liver tissue, with CYP3A7 being highly expressed in fetal liver tissue, and CYP3A4 highly expressed in adult tissue compared to fetal liver tissue. CYP3A4 was detected in only one SCDH sample, with expression well below that observed in HepaRG cells, being 0.0003-fold lower than HepaRG cells (Figure 3.2). In addition, CYP3A4 expression in the SCDH sample was below that observed in adult liver tissue, which was 0.006- to 0.016-fold lower than that in HepaRG cells. CYP3A7 was detected in two SCDH samples, at 4.5- and 11.8-fold higher than HepaRG cells. CYP3A7 expression in SCDHs was still below expression levels in fetal liver tissue, which ranged from 32- to 1100-fold higher than HepaRG cells, based on $\Delta\Delta C_T$ calculations (Figure 3.2). From this data, SCDHs do retain expression of CYP3A7, a fetal enzyme, though its expression was lower than fetal liver tissue, indicating an overall lack of CYP3A expression in SCDHs. CYPs 1A2, 2C19 and 2D6 were undetectable in SCDHs. CYP2A6 was expressed in SCDHs, at levels slightly above adult liver tissue, though below those observed in fetal liver tissue. CYP2B6 was undetectable in fetal liver tissue samples, but was expressed in SCDHs, though at levels below adult liver tissue. Expression of CYPs 2C8, 2C9 and 2E1 were detectable in SCDHs, but at levels much lower than expression in adult liver tissue, while comparable to expression in fetal liver tissue.

Overall, there was minimal expression of the hepatic CYP enzymes in SCDHs, with the exception of the fetal CYP3A7 enzyme. This low expression of CYP enzymes in SCDHs would result in low functional activity. This observed low expression of CYP enzymes is interesting, given that HNF4α is expressed in SCDHs at a level comparable to that in fetal and adult liver tissue. HNF4α is known to have a role in supporting the constitutive expression of CYP enzymes in human hepatocytes [143]. Given the relative expression of HNF4α and its role in promoting CYP expression, we might expect higher CYP expression in the SCDHs. The expression of P450 oxidoreductase (POR) was also evaluated. POR is essential for normal function of the CYP enzymes - it is needed for electron transfer from NADPH to the CYP [144, 145]. POR expression in SCDHs was below that expressed in HepaRG differentiated cells, ranging from 0.07- to 0.56-fold compared to HepaRG cells (Figure 3.2). This expression was also well below that found in fetal and adult liver tissues, which ranged from 0.7- to 6.5-fold the expression of POR in HepaRG cells (Figure 3.2). The low expression of POR in SCDHs may contribute to the observed low functional activity for the drug-metabolizing CYP enzymes. Interestingly, 3 of the 4 hESC samples and the iPSC sample exhibited higher POR expression than SCDHs. A potential reason for the higher expression of POR in stem cells could be its use in supporting other CYP enzymes. For example, CYP26 plays an important role in embryonic stem cells to promote cell differentiation through retinoid signaling [146, 147].

To examine expression of phase II drug-metabolizing enzymes, UDP-glucuronosyltransferases (UGT) and glutathione-S-transferases (GST) were evaluated. Expression of UGT1A1 in SCDHs was below expression in HepaRG cells, but similar to expression levels in both fetal and adult liver tissue (Figure 3.2). UGT1A6 expression was undetectable in fetal liver tissue, and expression in SCDHs was similar to that in adult liver

tissue. In contrast, expression of UGT2B4 in SCDHs was below that of both fetal and adult liver tissue and UGT2B7 in SCDHs was comparable to fetal liver tissue (Figure 3.2). For GSTT1, GSTM1 and GSTP1 there was largely no difference in expression between stem cells and SCDHs (Figure 3.2). GSTT1 expression in SCDHs was below that in differentiated HepaRG cells and in between expression in fetal and adult liver, based on $\Delta\Delta C_T$ calculations. GSTM1 and GSTP1 are both expressed at levels higher than that in differentiated HepaRG cells, being 4- to 7-fold higher than HepaRG cells for GSTP1 and 12- to 15-fold higher for GSTM1 (Figure 3.2). GSTM1 and GSTP1 expression in SCDHs was also higher than that observed in fetal liver tissue, which was 0.3- to 3-fold higher than HepaRG cells for GSTP1 and was 3- to 9-fold higher for GSTM1. For the H1 and H9 cell lines evaluated in the gene expression profiling, no polymorphisms for the GSTs were detected in the DMET genotyping analysis. The gene expression data for phase II drug-metabolizing enzymes indicates a mix of expression patterns, some more comparable to adult liver tissue, for example UGT1A1 and UGT1A6, while UGT2B7 and GSTs M1 and P1 are more comparable to fetal liver tissue.

To examine the expression of drug transporters in SCDHs, P-gp, BCRP, MRP2, OATP1B1, OATP1B3, and ATP7B mRNA levels were measured. ATP7B is a copper transporting ATPase expressed in the liver, and is responsible for transporting copper from hepatocytes into the bile [148]. Mutations in ATP7B are associated with Wilson's disease, a disorder in copper metabolism with manifestations in the liver and the brain [148]. Expression of ATP7B was up-regulated in SCDHs, compared to stem cells, with expression in SCDHs being slightly above that in differentiated HepaRG cells, fetal and adult liver tissue (Figure 3.2). The transporter P-gp was expressed in SCDHs, at levels similar to that in fetal liver tissue and below HepaRG differentiated cells and adult liver tissue (Figure 3.2). Expression of OATP1B1 and

OATP1B3 was minimal in SCDHs, and well below that in fetal and adult liver tissue. BCRP expression was higher in SCDHs compared to HepaRG cells, fetal and adult liver tissue (Figure 3.2). Expression of BCRP in fetal liver tissue ranged from 0.3- to 3.6-fold higher than HepaRG cells, while BCRP expression in SCDHs was 5- to 18-fold higher than HepaRG cells, based on $\Delta\Delta C_T$ calculations. Lastly, while MRP2 mRNA was detected in SCDHs, it was below the expression levels in HepaRG cells, fetal and adult liver tissue (Figure 3.2). Similar to the other results obtained for gene expression, some transporters are minimally expressed (OATP1B1, OATP1B3, MRP2), while some are similar to that in fetal liver tissue (P-gp and ATP7B), with the exception of BCRP which is highly expressed in SCDHs, comparatively.

Separate differentiation and gene expression experiments demonstrated similar results with regards to the expression of pluripotency markers NANOG, OCT4, and SOX2, in that expression was lower in SCDHs compared to hESCs (Figure 3.3). This again indicates the cells are undergoing a differentiation process and moving away from being pluripotent stem cells. SCDHs were incubated with the canonical inducers rifampicin, 3-MC, and phenobarbital and effects on CYP3A4, CYP3A7, CAR and PXR expression were evaluated. Results are reported as fold change compared to SCDHs incubated with a DMSO vehicle control. In this instance, basal expression of CYPs 3A4 and 3A7 were both detected in SCDHs (Figure 3.3). CYP3A4 expression exhibited an inductive response to rifampicin and phenobarbital, with the phenobarbital induced SCDHs expressing CYP3A4 at levels comparable to a fetal liver tissue sample (Figure 3.3). An inductive response for CYP3A7 to phenobarbital is also observed (Figure 3.3). A similar response to phenobarbital for CAR was observed, bringing expression levels of CAR to within 10-fold of the expression in fetal and adult liver tissue (Figure 3.3). Lastly, a minor inductive response was observed for PXR in response to rifampicin and

phenobarbital, though expression of PXR remained below fetal and adult liver tissue levels. The gene expression results reported here indicate SCDHs are capable of responding to the inducers rifampicin and phenobarbital. Overall, gene expression profiling of SCDHs indicates they are largely immature hepatocytes, especially with regard to the CYP enzymes. If SCDHs are to be used in conjunction with, or as an alternative to, cryopreserved hepatocytes a differentiation protocol that generates more mature hepatocytes is needed.

3.4.2 CYP cocktail assay

To assess the metabolic function of the CYP enzymes in SCDHs, a CYP cocktail assay was utilized and metabolite formation was measured using LC-MS/MS. The CYP cocktail was broken into two assays, each incubated separately with Day 17 SCDHs or cryopreserved hepatocytes for comparison. Cocktail A uses the probe substrates tolbutamide, testosterone, dextromethorphan, coumarin, and phenacetin to measure CYPs 2C9, 3A, 2D6, 2A6, and 1A, respectively. Cocktail B uses the probe substrates bupropion, amodiaquine, and chlorzoxazone to measure CYPs 2B6, 2C8, and 2E1, respectively. In addition, a set of SCDHs was dosed with a maturin compound at Day 10 of differentiation, to see if it would enhance the function of drug-metabolizing enzymes [99].

For SCDHs, the following metabolites were below the limit of quantitation: n-desethylamodiaquine, OH-bupropion, 6-OH-chlorzoxazone, dextrorphan, 7-OH-coumarin, and 4-OH-tolbutamide, indicating no functional metabolic activity for CYPs 2C8, 2B6, 2E1, 2D6, 2A6, and 2C9, respectively. Acetaminophen and 6-OH-testosterone were detectable at levels right at or slightly above the lower limit of quantitation for each compound, indicating some measurable activity for CYPs 1A and 3A, respectively. Acetaminophen was detectable for both

H1 and H9 SCDHs, with concentrations measuring around 0.1-0.13 μM, with the lower limit of quantitation for acetaminophen being 0.125 μM. In contrast, acetaminophen concentrations in cryopreserved and primary hepatocyte samples ranged from 0.7 – 2 μM. 6-OH-testosterone was also detectable for both H1 and H9 SCDHs, with concentrations ranging from 0.356-0.88 μM. The lower limit of quantitation for 6-OH-testosterone was 0.312 μM. In contrast, 6-OH-testosterone concentrations in cryopreserved and primary hepatocytes ranged from 2 – 13 μM. Representative chromatograms for metabolites generated by SCDHs are shown in Figure 3.4C. Incubation of SCDHs with the inducers rifampicin and 3-MC had no effect on metabolite formation. In addition, there was no difference in metabolite formation for SCDHs with and without the maturin compound. Positive control primary and cryopreserved hepatocytes generated measurable metabolites for all compounds tested, indicating the incubation assay and LC-MS/MS method was working. Representative chromatograms for each metabolite generated from primary hepatocytes is shown in Figure 3.4B. This metabolite data demonstrates there was minimal detectable CYP activity for SCDHs, which is expected based on gene expression profiling. Metabolites indicating activity for CYPs 1A and 3A were detected, however, they were right at the lower limit of quantitation and well below the activity seen in cryopreserved and primary hepatocytes. Overall, these results demonstrate an absence of functional drug-metabolizing enzyme activity in SCDHs, corroborating what has largely been reported for SCDHs to date; that they are immature compared to cryopreserved hepatocytes, especially with regards to drug-metabolizing enzyme functions.

3.5 Conclusion

In conclusion, gene expression profiling and functional assays of CYP activity indicate SCDHs are largely immature hepatocytes, lacking significant CYP expression and activity. Based on gene expression profiling, SCDHs most closely resemble fetal hepatocytes, especially with regards to AFP, CYP3A7 and FMO1 expression. Functional assay of enzyme activity in SCDHs using a CYP cocktail revealed only minor activity for CYPs 1A and 3A, with this activity being below that observed in primary hepatocytes. This data demonstrates that more work needs to be done to promote the maturity of SCDHs. Enhanced expression and function of drug-metabolizing enzymes in SCDHs would make them a more viable option to supplant primary hepatocytes in the pharmaceutical industry for drug metabolism/liver toxicity assays.

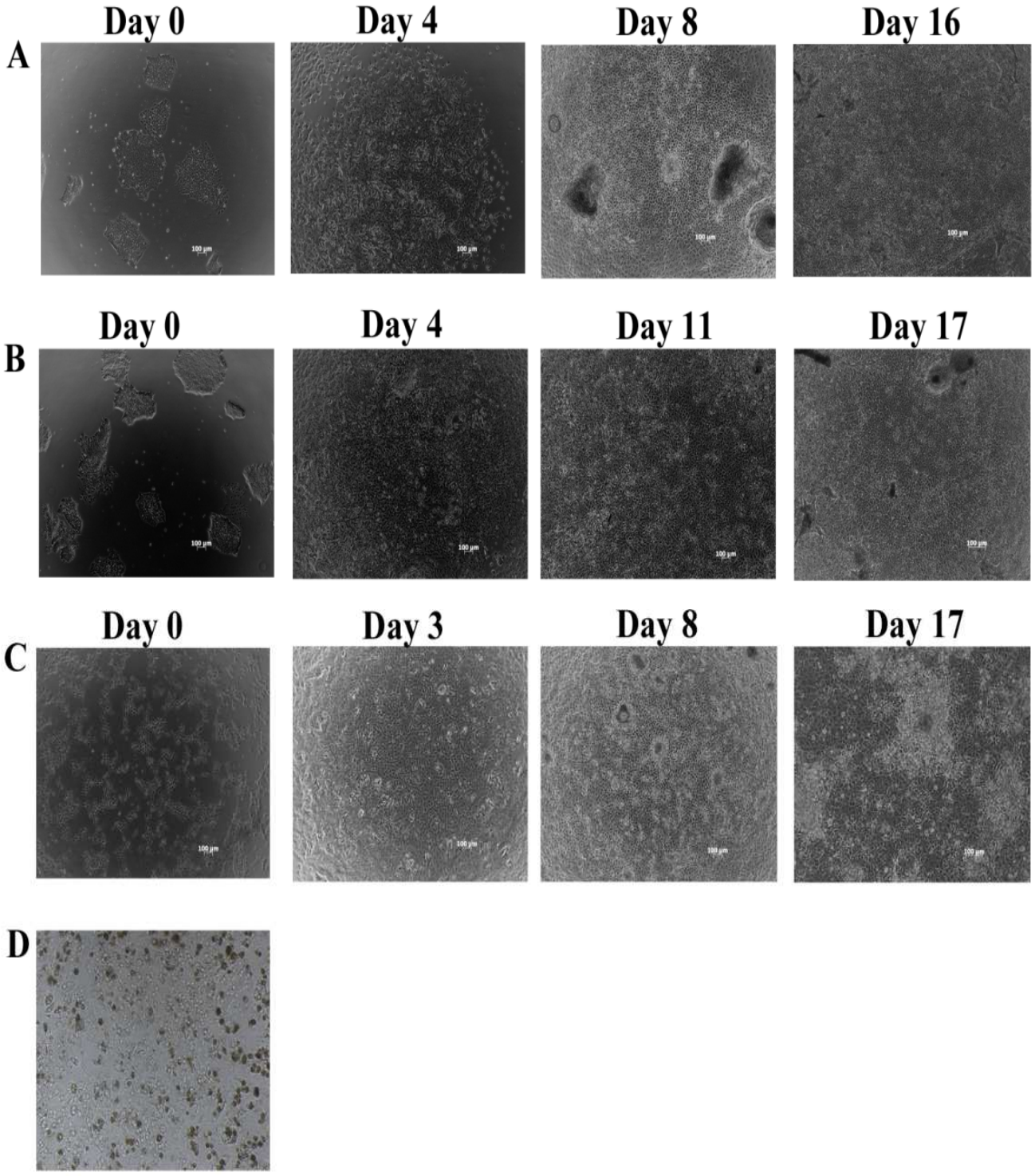
A
Day 0
Day 4
Day 8
Day 16
B
Day 0
Day 4
Day 11
Day 17
C
Day 0
Day 3
Day 8
Day 17
D

Figure 3.1 SCDH photomicrographs. (A) Photomicrographs depicting H1 SCDHs at days 0, 4, 8 and 16 of differentiation. **(B)** Photomicrographs depicting H9 SCDHs at days 0, 4, 11 and 17 of differentiation. **(C)** Photomicrographs depicting H9 SCDHs at days 0, 3, 8 and 17 of differentiation. This set of photomicrographs represents differentiation with hESCs which were Trypsin passaged, resulting in single hESCs as opposed to the colony formation seen in **(A)** and **(B)**. **(D)** Representative photomicrograph of Hu8114 cryopreserved hepatocytes at day 4 of culture.

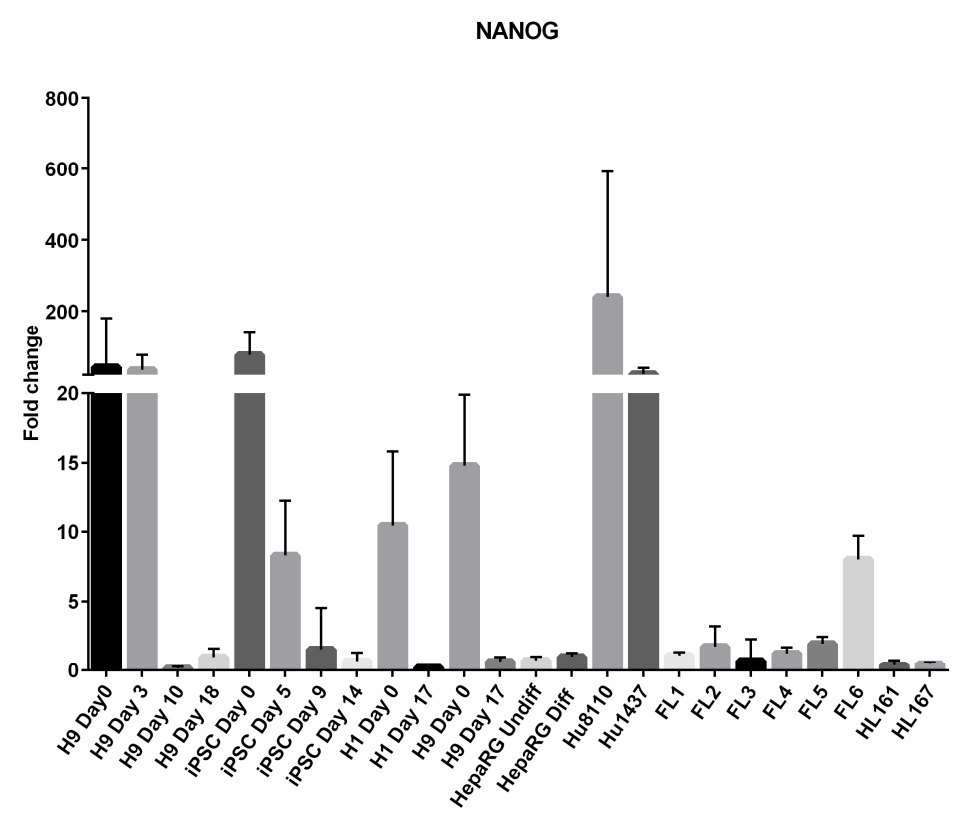
NANOG
Fold change
800
600
400
200
20
15
10
5
0
H9 Day0
H9 Day 3
H9 Day 10
H9 Day 18
iPSC Day 0
iPSC Day 5
iPSC Day 9
iPSC Day 14
H1 Day 0
H1 Day 17
H9 Day 0
H9 Day 17
HepaRG Undiff
HepaRG Diff
Hu8110
Hu1437
FL1
FL2
FL3
FL4
FL5
FL6
HL161
HL167

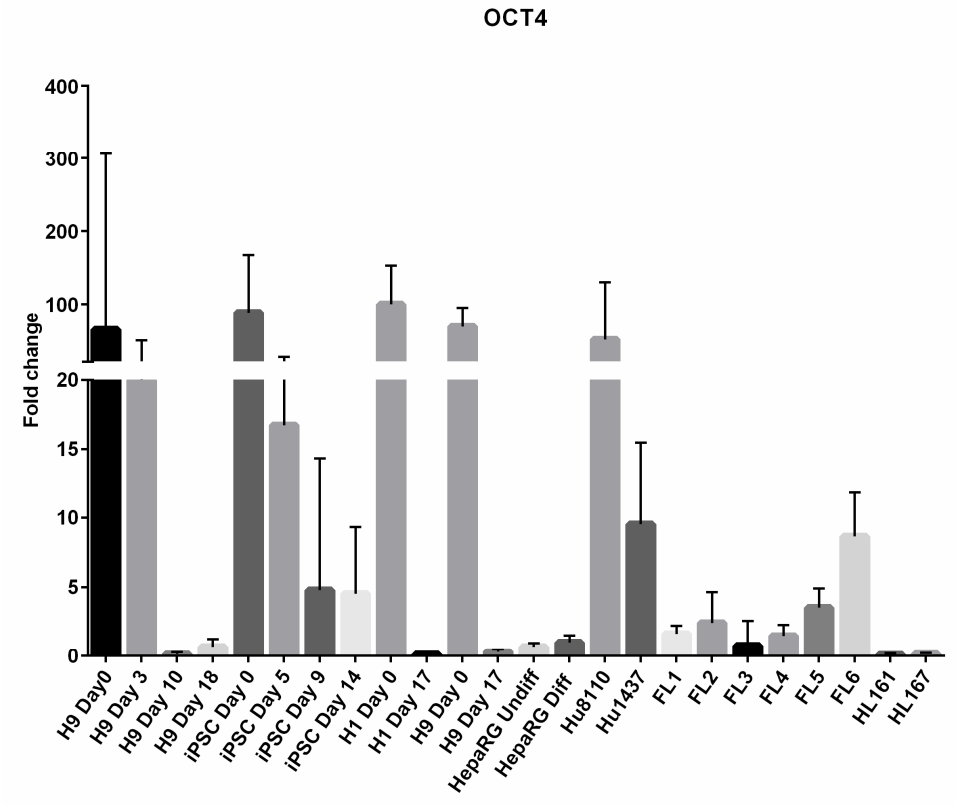
OCT4
Fold change
400
300
200
100
20
15
10
5
0
H9 Day0
H9 Day 3
H9 Day 10
H9 Day 18
iPSC Day 0
iPSC Day 5
iPSC Day 9
iPSC Day 14
H1 Day 0
H1 Day 17
H9 Day 0
H9 Day 17
HepaRG Undiff
HepaRG Diff
Hu8110
Hu1437
FL1
FL2
FL3
FL4
FL5
FL6
HL161
HL167

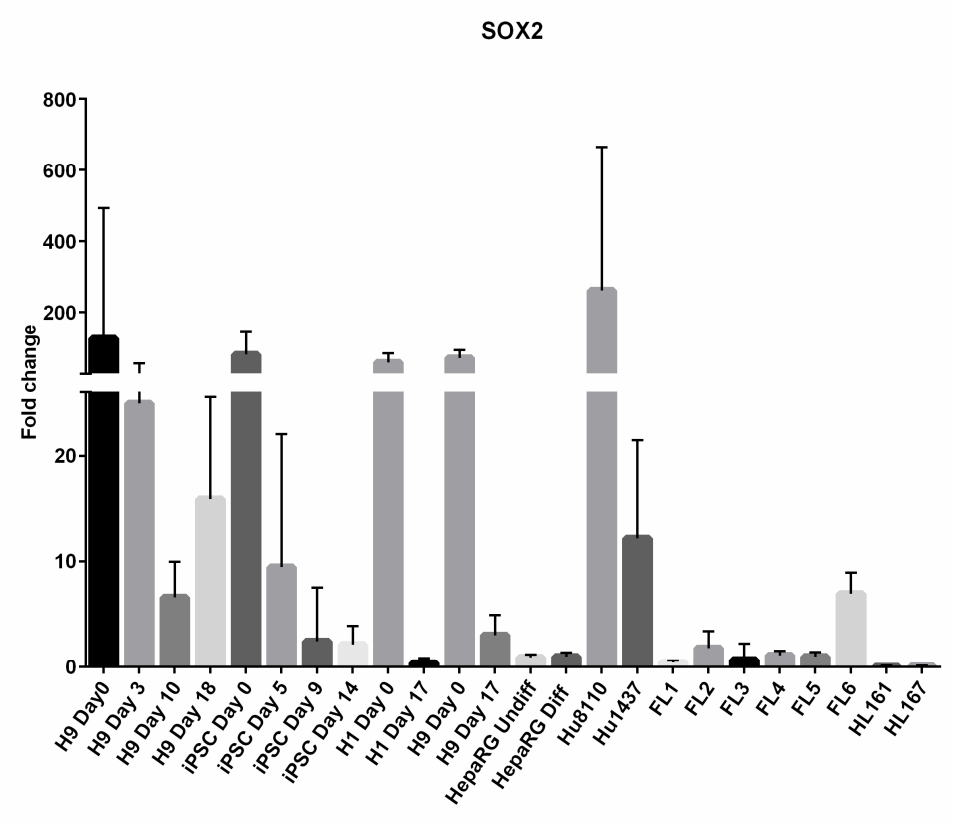
SOX2
Fold change
800
600
400
200
20
10
0
H9 Day0
H9 Day 3
H9 Day 10
H9 Day 18
iPSC Day 0
iPSC Day 5
iPSC Day 9
iPSC Day 14
H1 Day 0
H1 Day 17
H9 Day 0
H9 Day 17
HepaRG Undiff
HepaRG Diff
Hu8110
Hu1437
FL1
FL2
FL3
FL4
FL5
FL6
HL161
HL167

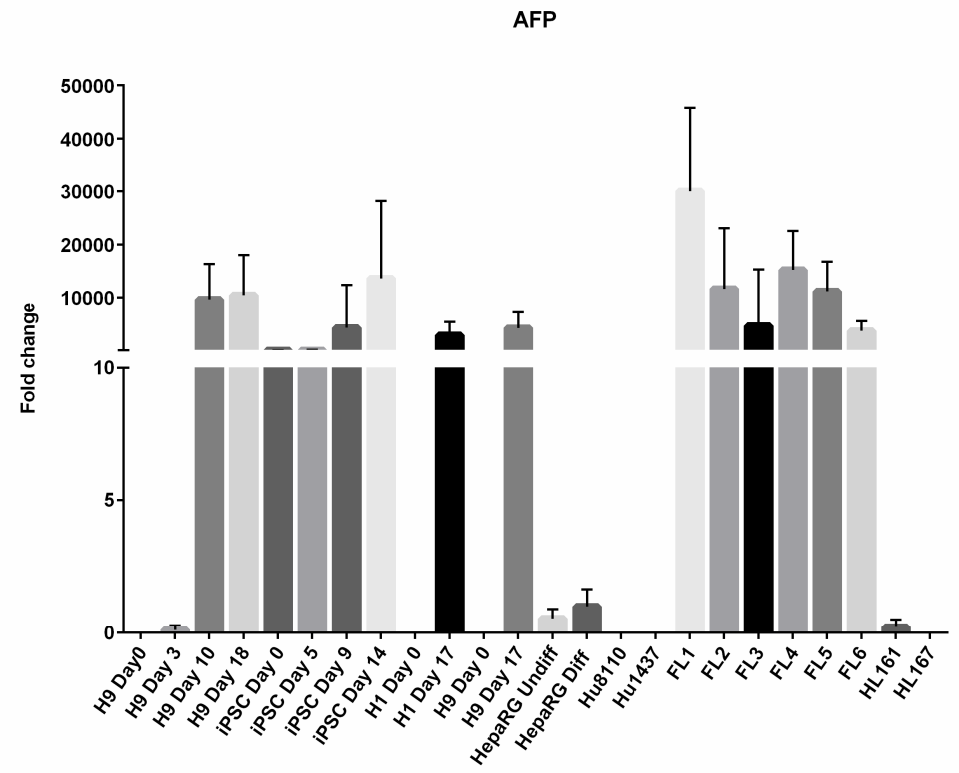
AFP
Fold change
50000
40000
30000
20000
10000
10
5
0
H9 Day0
H9 Day 3
H9 Day 10
H9 Day 18
iPSC Day 0
iPSC Day 5
iPSC Day 9
iPSC Day 14
H1 Day 0
H1 Day 17
H9 Day 0
H9 Day 17
HepaRG Undiff
HepaRG Diff
Hu8110
Hu1437
FL1
FL2
FL3
FL4
FL5
FL6
HL161
HL167

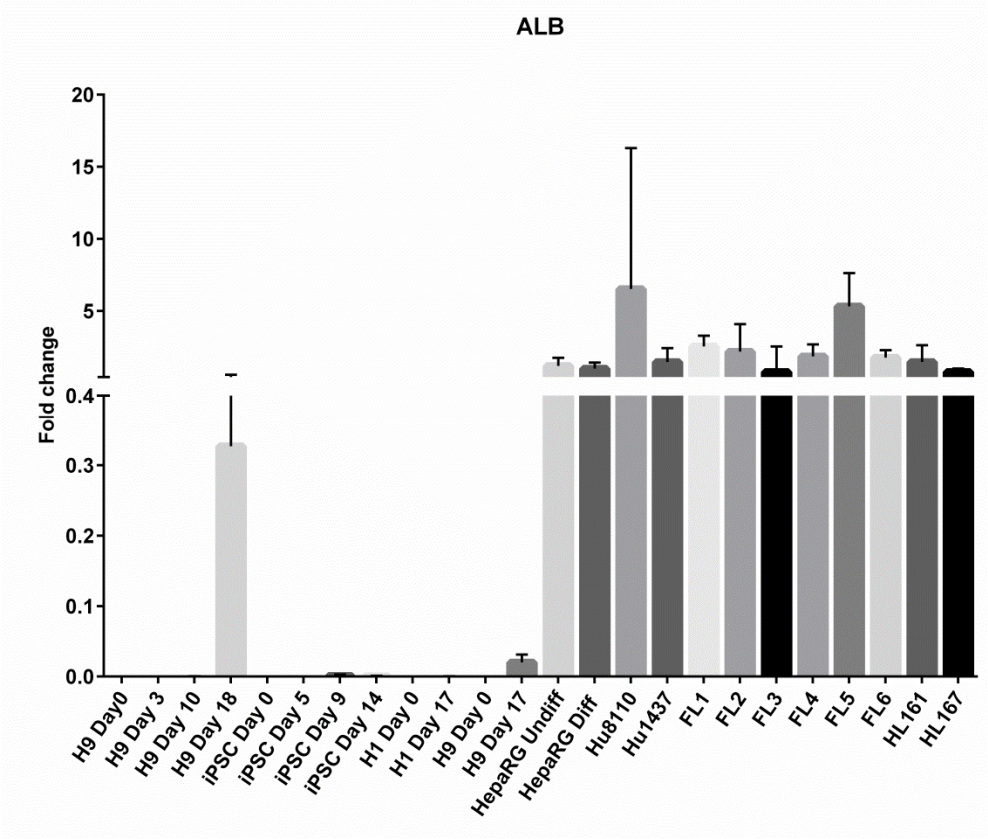
ALB
Fold change
20
15
10
5
0.4
0.3
0.2
0.1
0.0
H9 Day0
H9 Day 3
H9 Day 10
H9 Day 18
iPSC Day 0
iPSC Day 5
iPSC Day 9
iPSC Day 14
H1 Day 0
H1 Day 17
H9 Day 0
H9 Day 17
HepaRG Undiff
HepaRG Diff
Hu8110
Hu1437
FL1
FL2
FL3
FL4
FL5
FL6
HL161
HL167

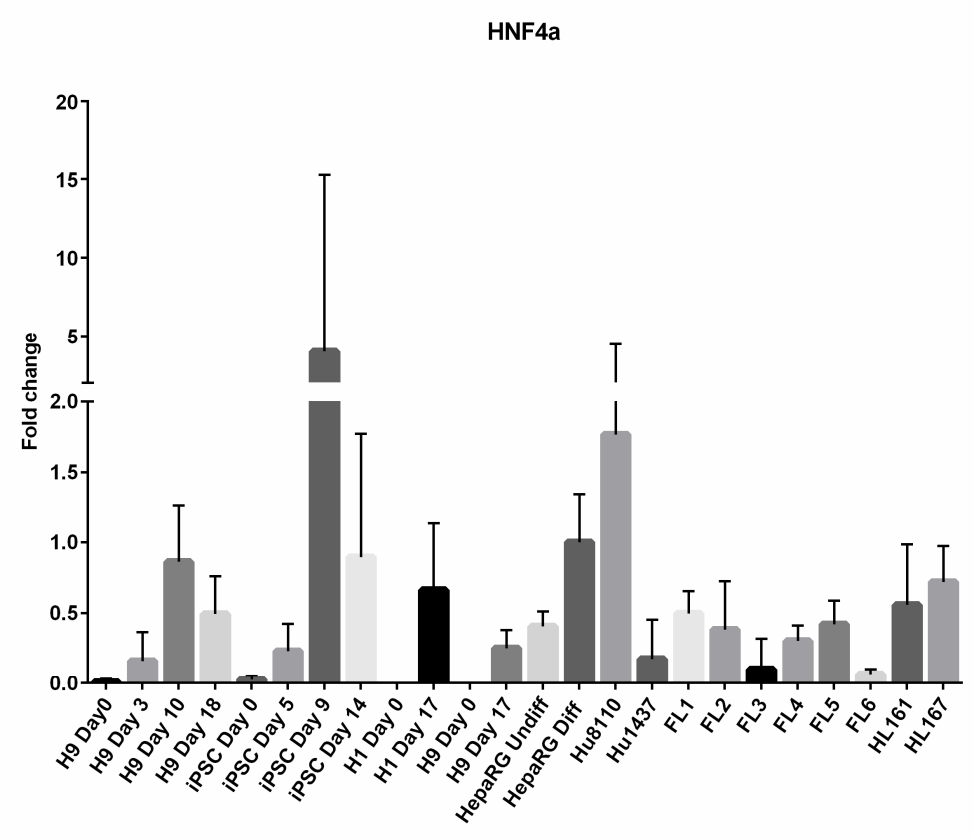
HNF4a
Fold change
20
15
10
5
2.0
1.5
1.0
0.5
0.0
H9 Day0
H9 Day 3
H9 Day 10
H9 Day 18
iPSC Day 0
iPSC Day 5
iPSC Day 9
iPSC Day 14
H1 Day 0
H1 Day 17
H9 Day 0
H9 Day 17
HepaRG Undiff
HepaRG Diff
Hu8110
Hu1437
FL1
FL2
FL3
FL4
FL5
FL6
HL161
HL167

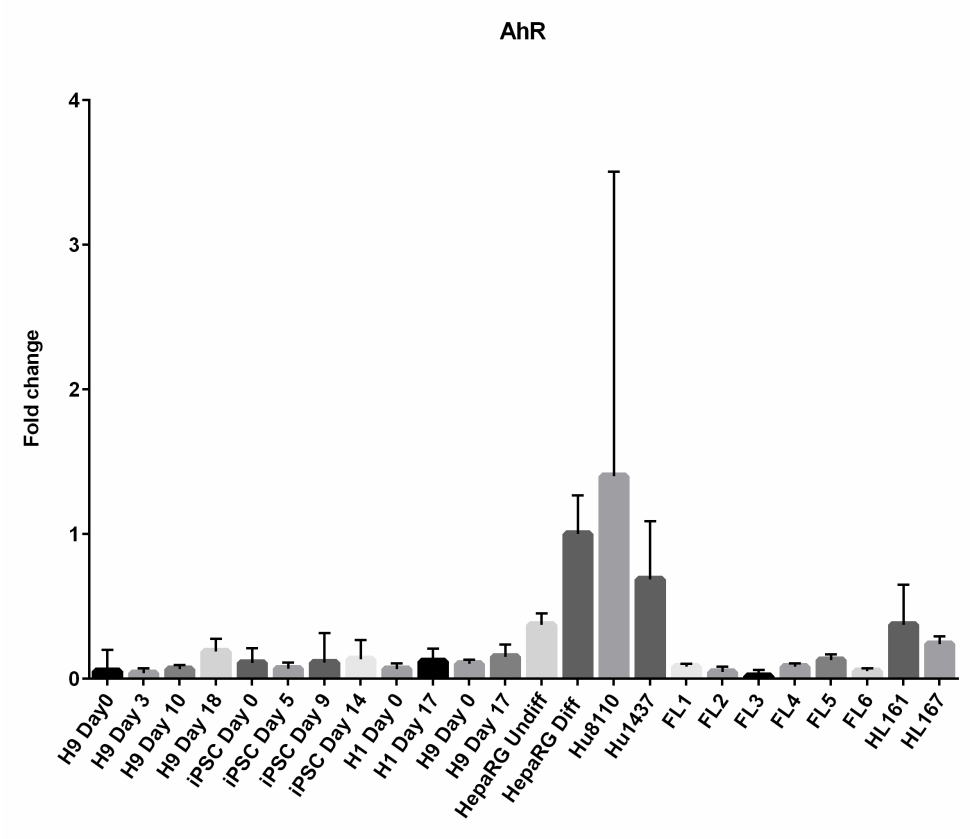
AhR
Fold change
4
3
2
1
0
H9 Day0
H9 Day 3
H9 Day 10
H9 Day 18
iPSC Day 0
iPSC Day 5
iPSC Day 9
iPSC Day 14
H1 Day 0
H1 Day 17
H9 Day 0
H9 Day 17
HepaRG Undiff
HepaRG Diff
Hu8110
Hu1437
FL1
FL2
FL3
FL4
FL5
FL6
HL161
HL167

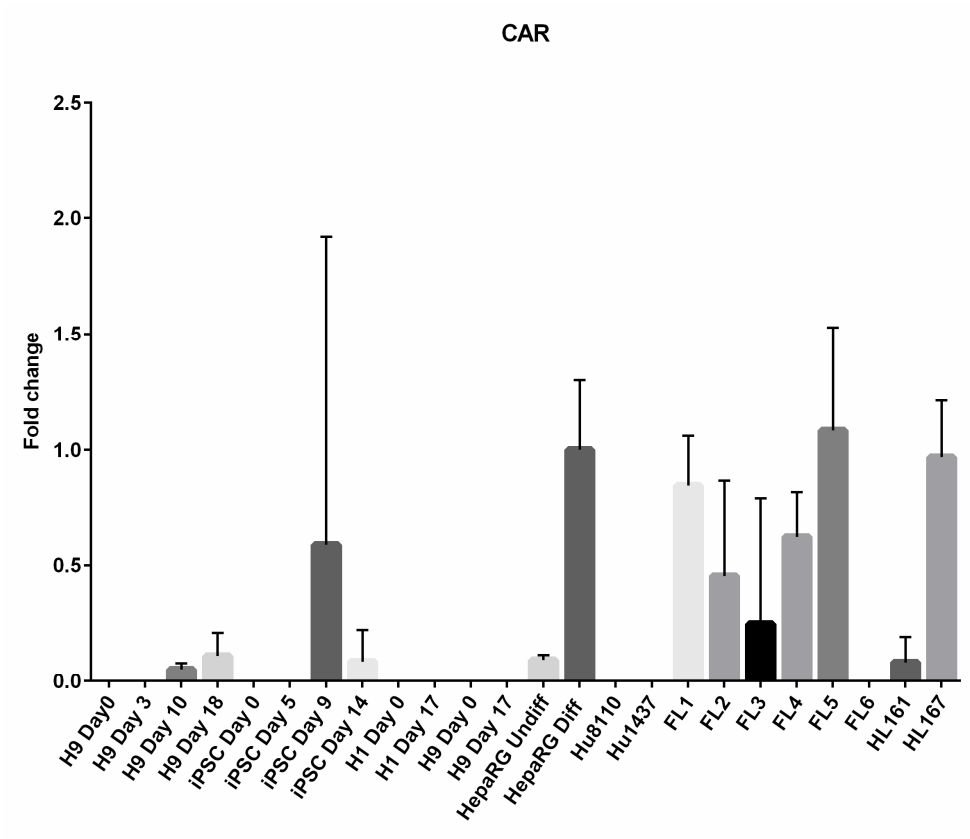
CAR
Fold change
2.5
2.0
1.5
1.0
0.5
0.0
H9 Day0
H9 Day 3
H9 Day 10
H9 Day 18
iPSC Day 0
iPSC Day 5
iPSC Day 9
iPSC Day 14
H1 Day 0
H1 Day 17
H9 Day 0
H9 Day 17
HepaRG Undiff
HepaRG Diff
Hu8110
Hu1437
FL1
FL2
FL3
FL4
FL5
FL6
HL161
HL167

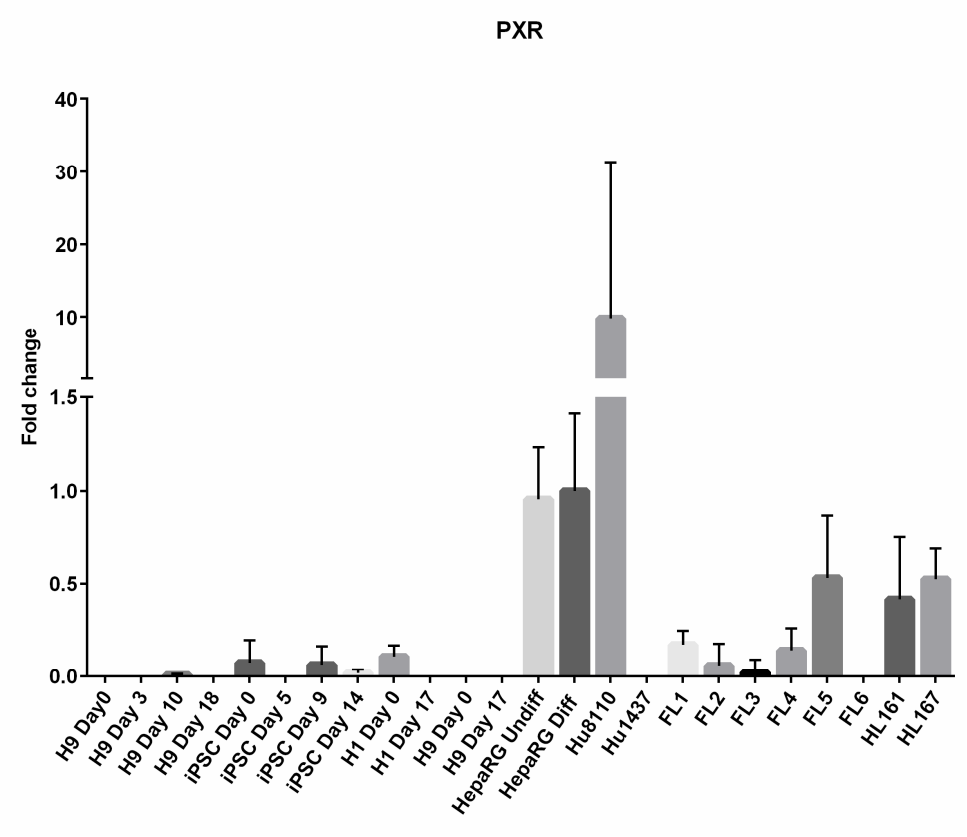
PXR
Fold change
40
30
20
10
1.5
1.0
0.5
0.0
H9 Day0
H9 Day 3
H9 Day 10
H9 Day 18
iPSC Day 0
iPSC Day 5
iPSC Day 9
iPSC Day 14
H1 Day 0
H1 Day 17
H9 Day 0
H9 Day 17
HepaRG Undiff
HepaRG Diff
Hu8110
Hu1437
FL1
FL2
FL3
FL4
FL5
FL6
HL161
HL167

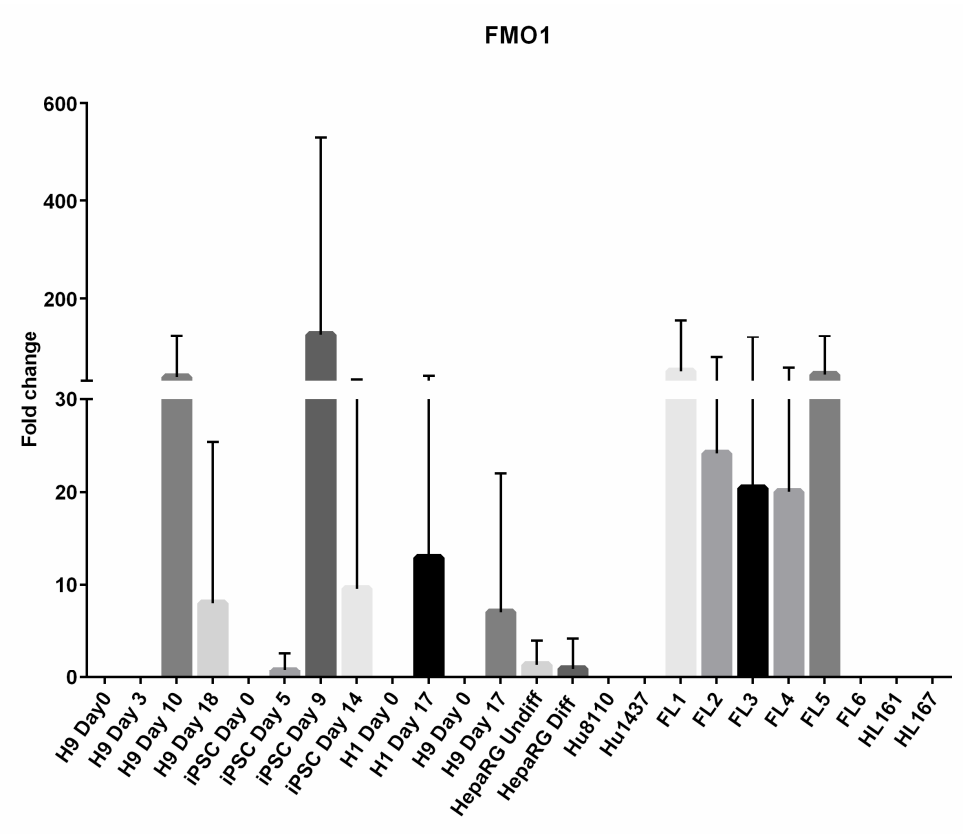
FMO1
Fold change
600
400
200
30
20
10
0
H9 Day0
H9 Day 3
H9 Day 10
H9 Day 18
iPSC Day 0
iPSC Day 5
iPSC Day 9
iPSC Day 14
H1 Day 0
H1 Day 17
H9 Day 0
H9 Day 17
HepaRG Undiff
HepaRG Diff
Hu8110
Hu1437
FL1
FL2
FL3
FL4
FL5
FL6
HL161
HL167

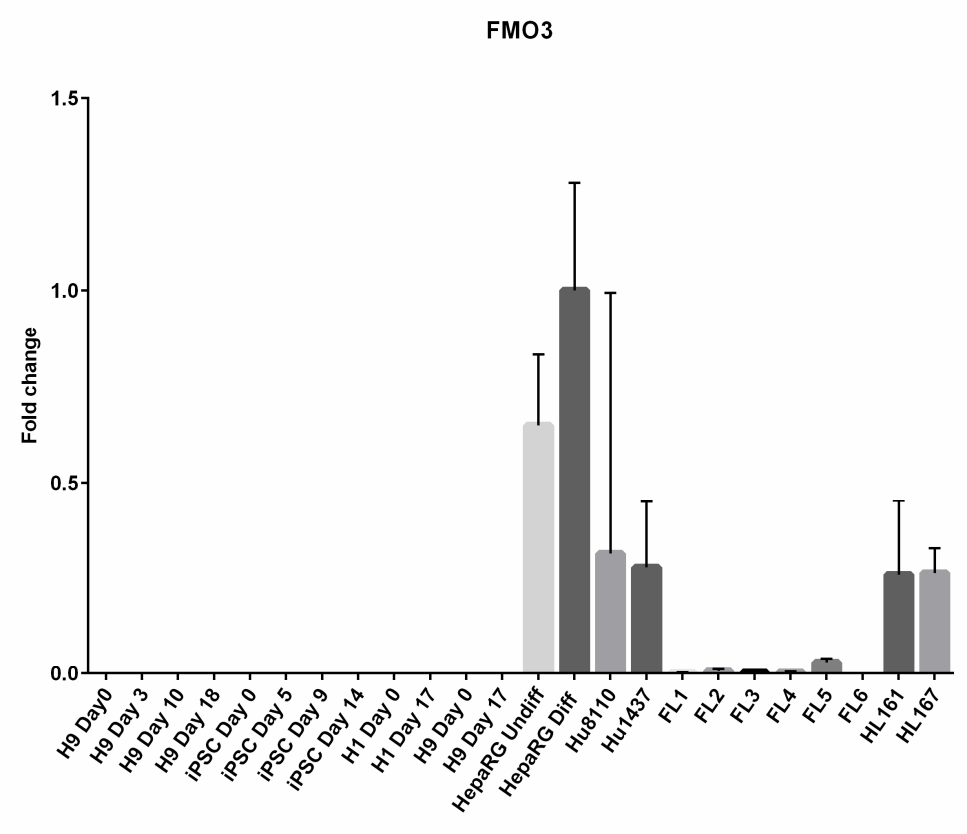
FMO3
Fold change
1.5
1.0
0.5
0.0
H9 Day0
H9 Day 3
H9 Day 10
H9 Day 18
iPSC Day 0
iPSC Day 5
iPSC Day 9
iPSC Day 14
H1 Day 0
H1 Day 17
H9 Day 0
H9 Day 17
HepaRG Undiff
HepaRG Diff
Hu8110
Hu1437
FL1
FL2
FL3
FL4
FL5
FL6
HL161
HL167

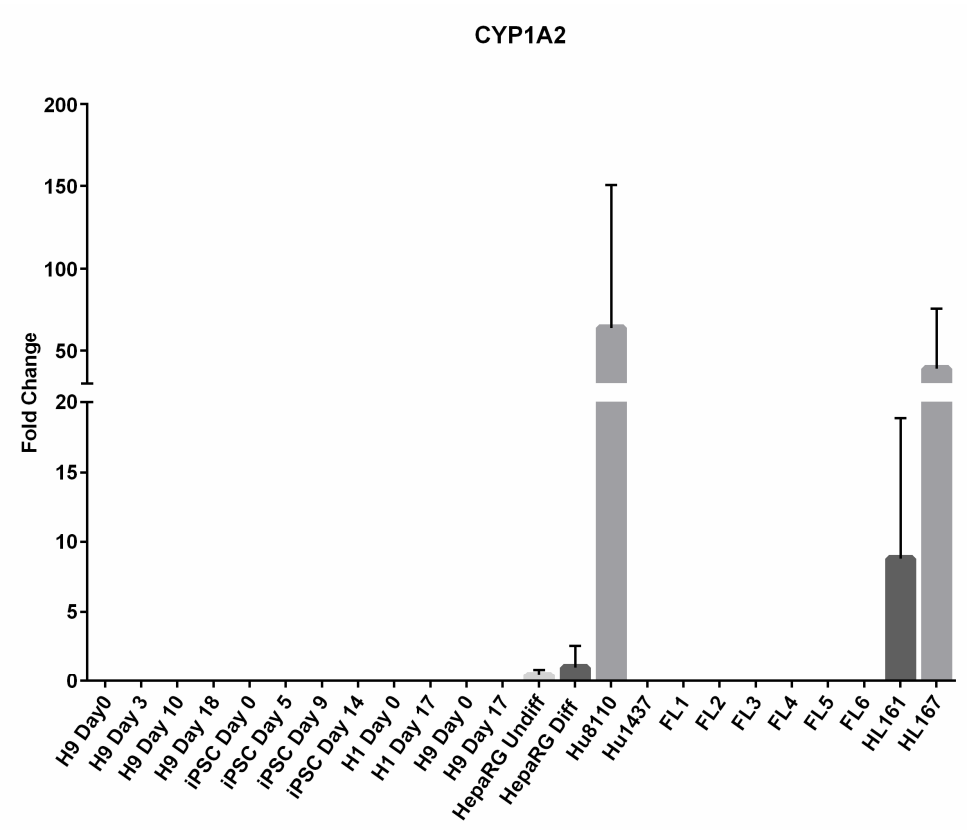
CYP1A2
Fold Change
200
150
100
50
20
15
10
5
0
H9 Day0
H9 Day 3
H9 Day 10
H9 Day 18
iPSC Day 0
iPSC Day 5
iPSC Day 9
iPSC Day 14
H1 Day 0
H1 Day 17
H9 Day 0
H9 Day 17
HepaRG Undiff
HepaRG Diff
Hu8110
Hu1437
FL1
FL2
FL3
FL4
FL5
FL6
HL161
HL167

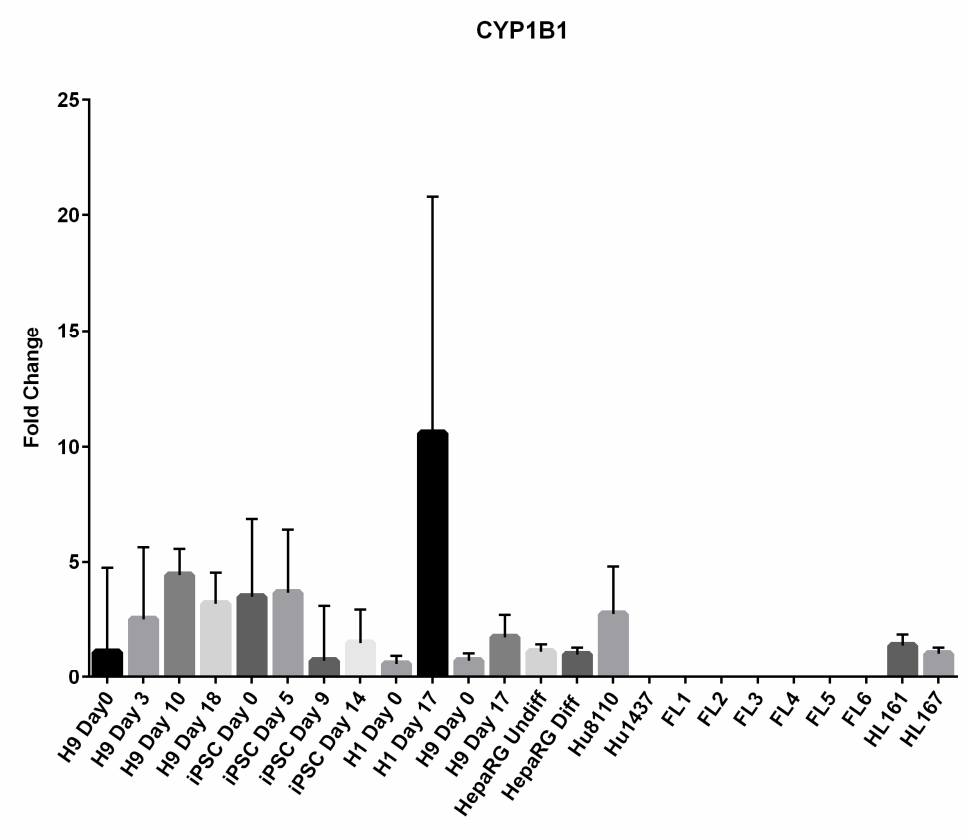
CYP1B1
Fold Change
25
20
15
10
5
0
H9 Day0
H9 Day 3
H9 Day 10
H9 Day 18
iPSC Day 0
iPSC Day 5
iPSC Day 9
iPSC Day 14
H1 Day 0
H1 Day 17
H9 Day 0
H9 Day 17
HepaRG Undiff
HepaRG Diff
Hu8110
Hu1437
FL1
FL2
FL3
FL4
FL5
FL6
HL161
HL167

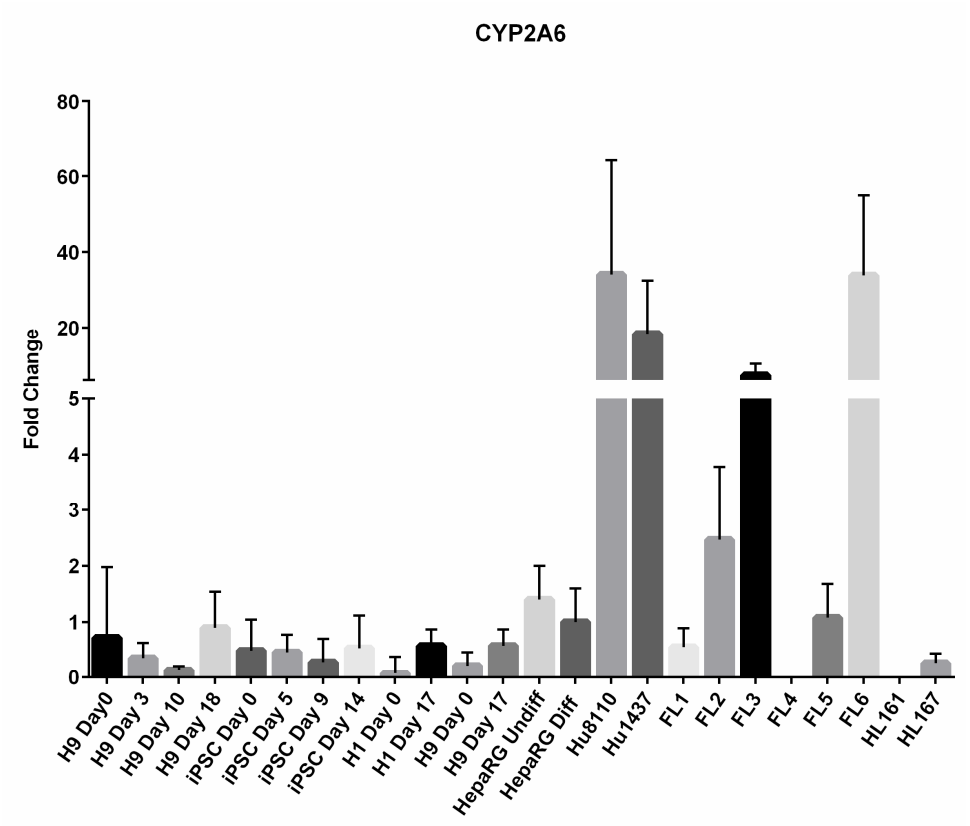
CYP2A6
Fold Change
80
60
40
20
5
4
3
2
1
0
H9 Day0
H9 Day 3
H9 Day 10
H9 Day 18
iPSC Day 0
iPSC Day 5
iPSC Day 9
iPSC Day 14
H1 Day 0
H1 Day 17
H9 Day 0
H9 Day 17
HepaRG Undiff
HepaRG Diff
Hu8110
Hu1437
FL1
FL2
FL3
FL4
FL5
FL6
HL161
HL167

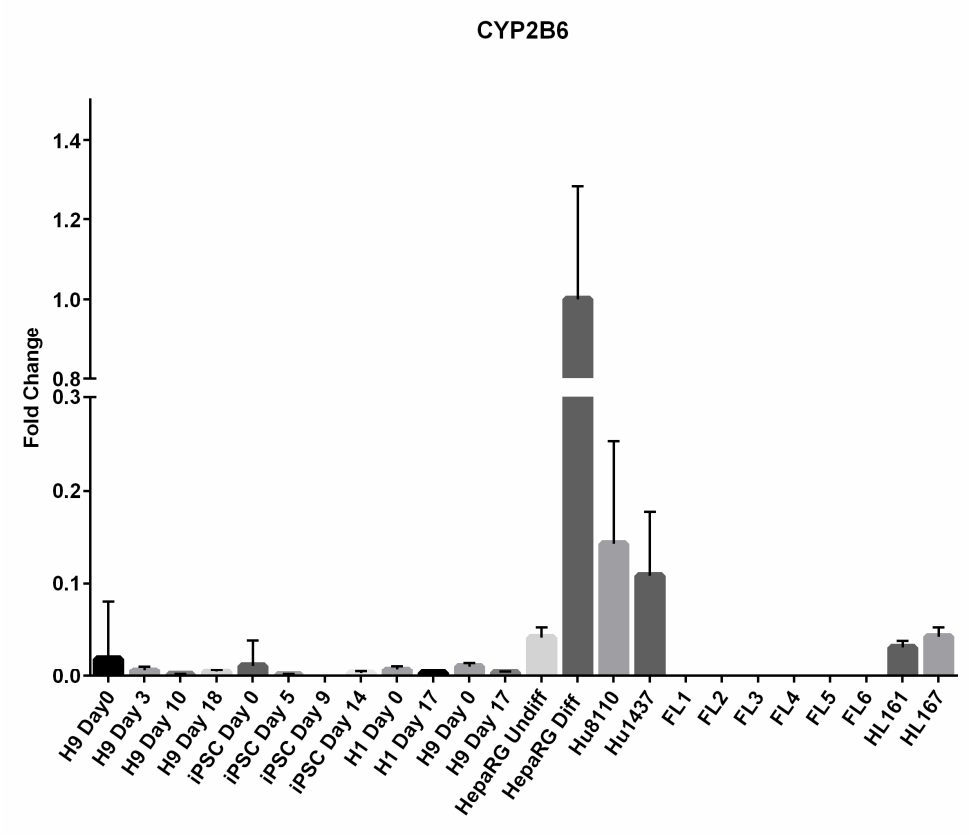
CYP2B6
Fold Change
1.4
1.2
1.0
0.8
0.3
0.2
0.1
0.0
H9 Day0
H9 Day 3
H9 Day 10
H9 Day 18
iPSC Day 0
iPSC Day 5
iPSC Day 9
iPSC Day 14
H1 Day 0
H1 Day 17
H9 Day 0
H9 Day 17
HepaRG Undiff
HepaRG Diff
Hu8110
Hu1437
FL1
FL2
FL3
FL4
FL5
FL6
HL161
HL167

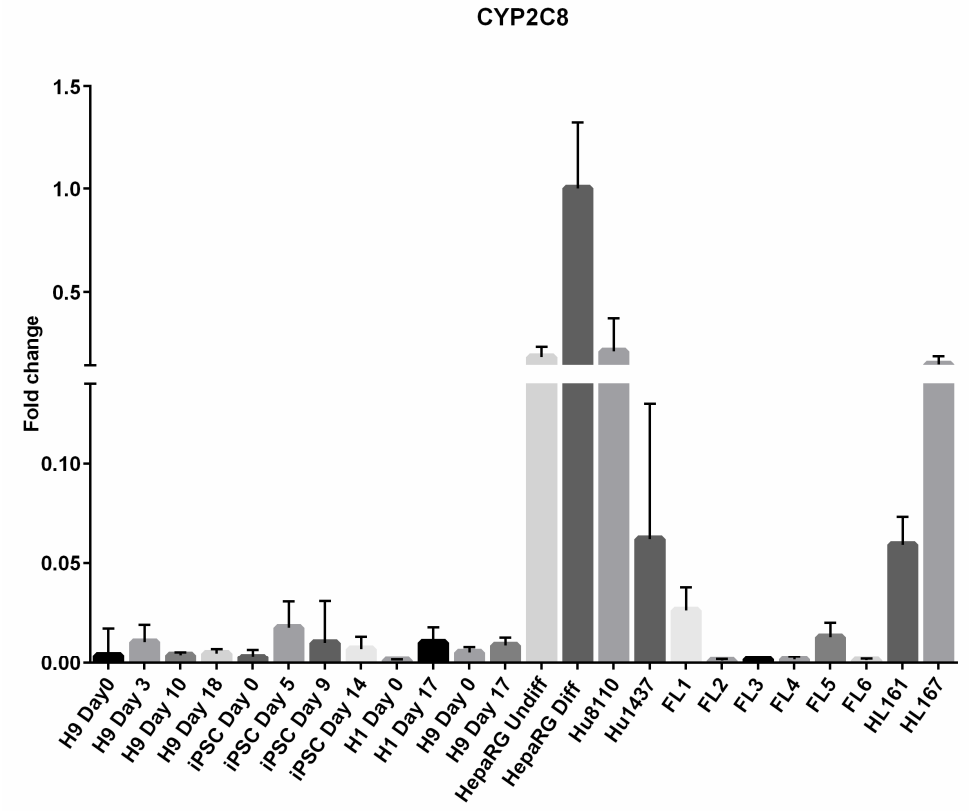
CYP2C8
Fold change
1.5
1.0
0.5
0.10
0.05
0.00
H9 Day0
H9 Day 3
H9 Day 10
H9 Day 18
iPSC Day 0
iPSC Day 5
iPSC Day 9
iPSC Day 14
H1 Day 0
H1 Day 17
H9 Day 0
H9 Day 17
HepaRG Undiff
HepaRG Diff
Hu8110
Hu1437
FL1
FL2
FL3
FL4
FL5
FL6
HL161
HL167

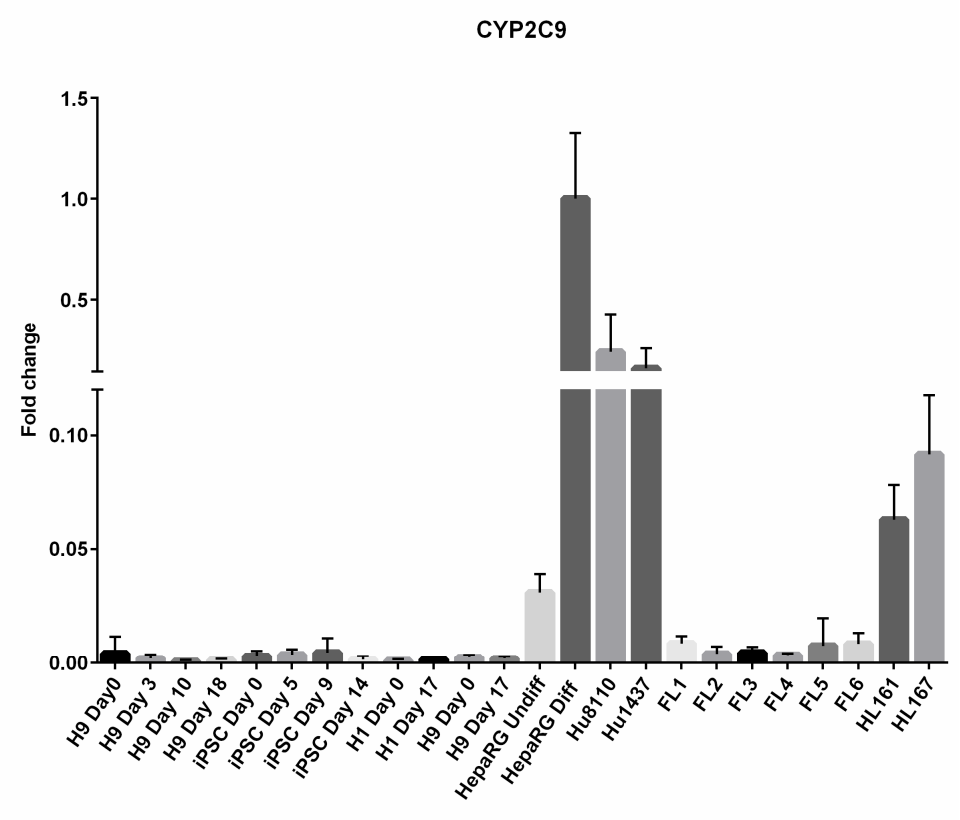
CYP2C9
Fold change
1.5
1.0
0.5
0.10
0.05
0.00
H9 Day0
H9 Day 3
H9 Day 10
H9 Day 18
iPSC Day 0
iPSC Day 5
iPSC Day 9
iPSC Day 14
H1 Day 0
H1 Day 17
H9 Day 0
H9 Day 17
HepaRG Undiff
HepaRG Diff
Hu8110
Hu1437
FL1
FL2
FL3
FL4
FL5
FL6
HL161
HL167

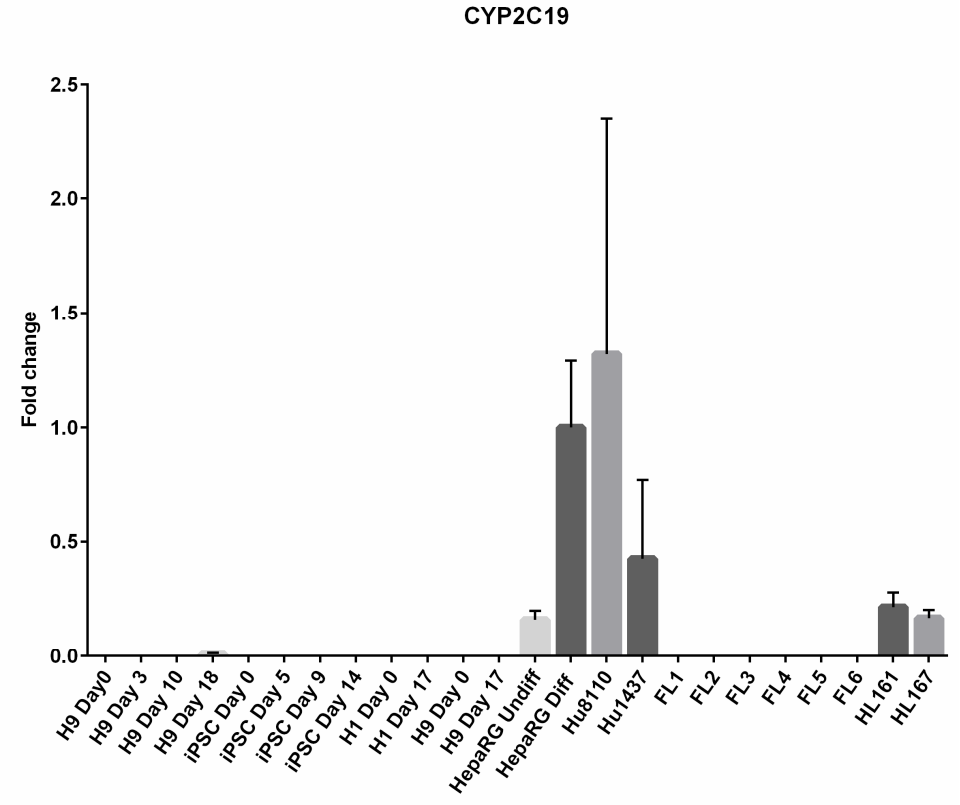
CYP2C19
Fold change
2.5
2.0
1.5
1.0
0.5
0.0
H9 Day0
H9 Day 3
H9 Day 10
H9 Day 18
iPSC Day 0
iPSC Day 5
iPSC Day 9
iPSC Day 14
H1 Day 0
H1 Day 17
H9 Day 0
H9 Day 17
HepaRG Undiff
HepaRG Diff
Hu8110
Hu1437
FL1
FL2
FL3
FL4
FL5
FL6
HL161
HL167

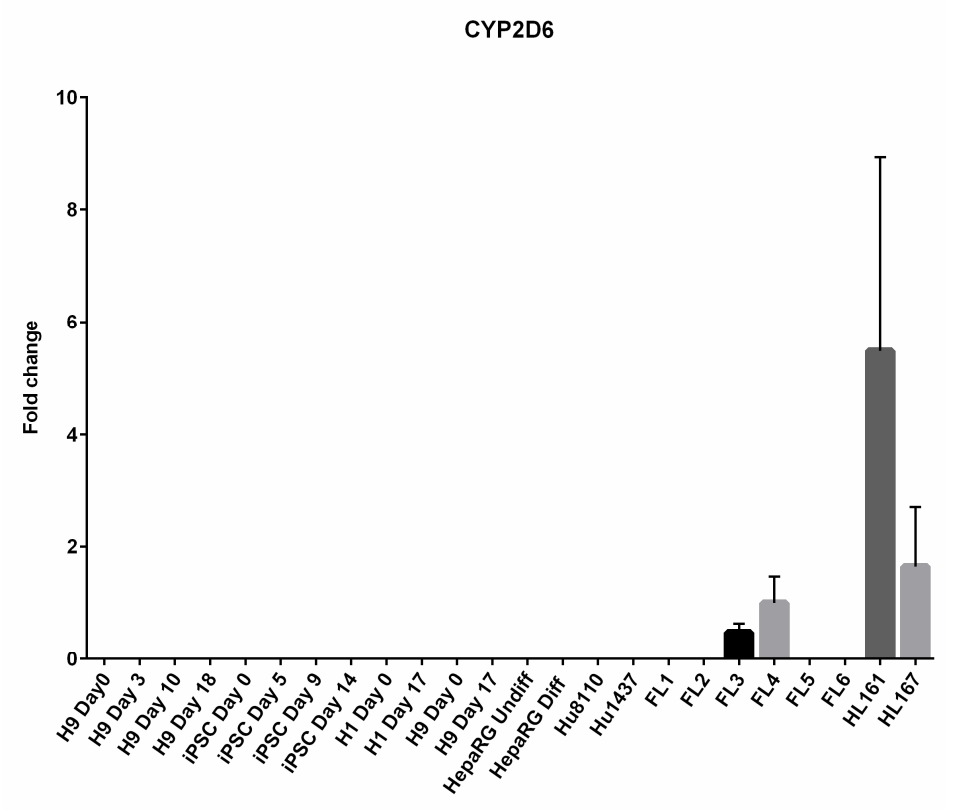
CYP2D6
Fold change
10
8
6
4
2
0
H9 Day0
H9 Day 3
H9 Day 10
H9 Day 18
iPSC Day 0
iPSC Day 5
iPSC Day 9
iPSC Day 14
H1 Day 0
H1 Day 17
H9 Day 0
H9 Day 17
HepaRG Undiff
HepaRG Diff
Hu8110
Hu1437
FL1
FL2
FL3
FL4
FL5
FL6
HL161
HL167

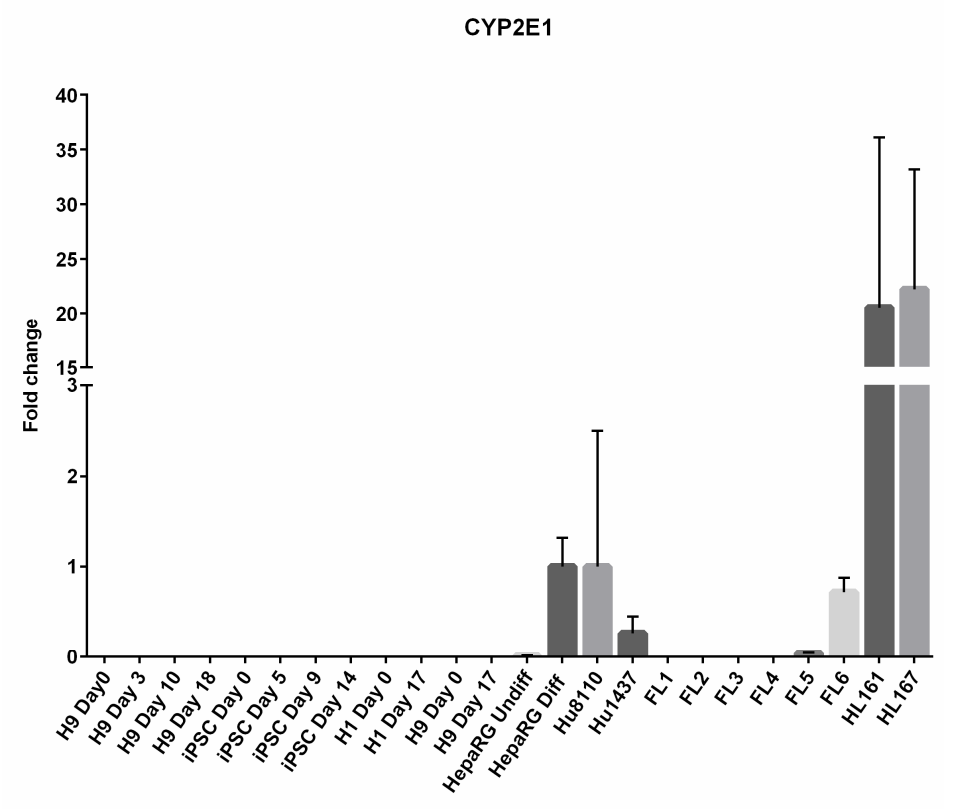
CYP2E1
Fold change
40
35
30
25
20
15
3
2
1
0
H9 Day0
H9 Day 3
H9 Day 10
H9 Day 18
iPSC Day 0
iPSC Day 5
iPSC Day 9
iPSC Day 14
H1 Day 0
H1 Day 17
H9 Day 0
H9 Day 17
HepaRG Undiff
HepaRG Diff
Hu8110
Hu1437
FL1
FL2
FL3
FL4
FL5
FL6
HL161
HL167

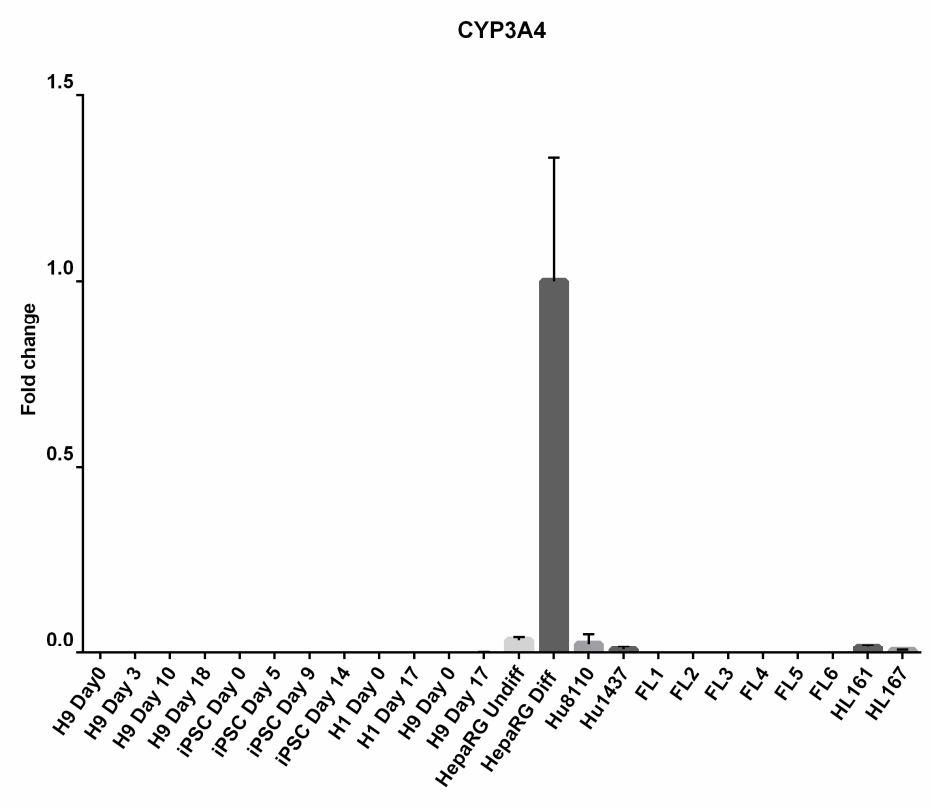
CYP3A4
Fold change
1.5
1.0
0.5
0.0
H9 Day0
H9 Day 3
H9 Day 10
H9 Day 18
iPSC Day 0
iPSC Day 5
iPSC Day 9
iPSC Day 14
H1 Day 0
H1 Day 17
H9 Day 0
H9 Day 17
HepaRG Undiff
HepaRG Diff
Hu8110
Hu1437
FL1
FL2
FL3
FL4
FL5
FL6
HL161
HL167

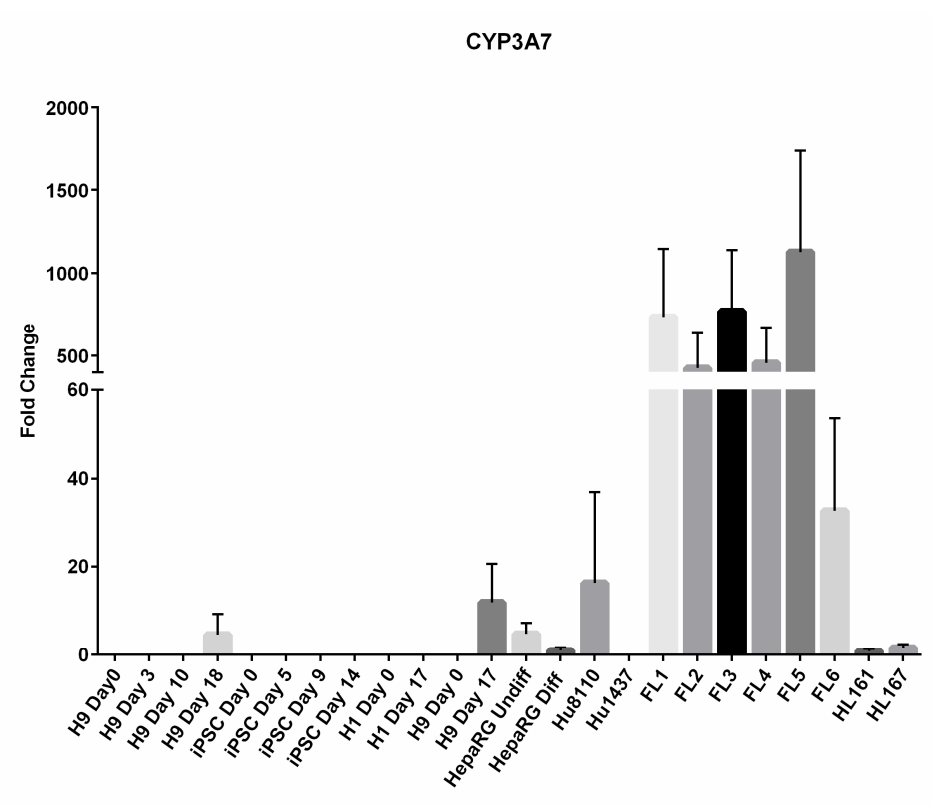
CYP3A7
Fold Change
2000
1500
1000
500
60
40
20
0
H9 Day0
H9 Day 3
H9 Day 10
H9 Day 18
iPSC Day 0
iPSC Day 5
iPSC Day 9
iPSC Day 14
H1 Day 0
H1 Day 17
H9 Day 0
H9 Day 17
HepaRG Undiff
HepaRG Diff
Hu8110
Hu1437
FL1
FL2
FL3
FL4
FL5
FL6
HL161
HL167

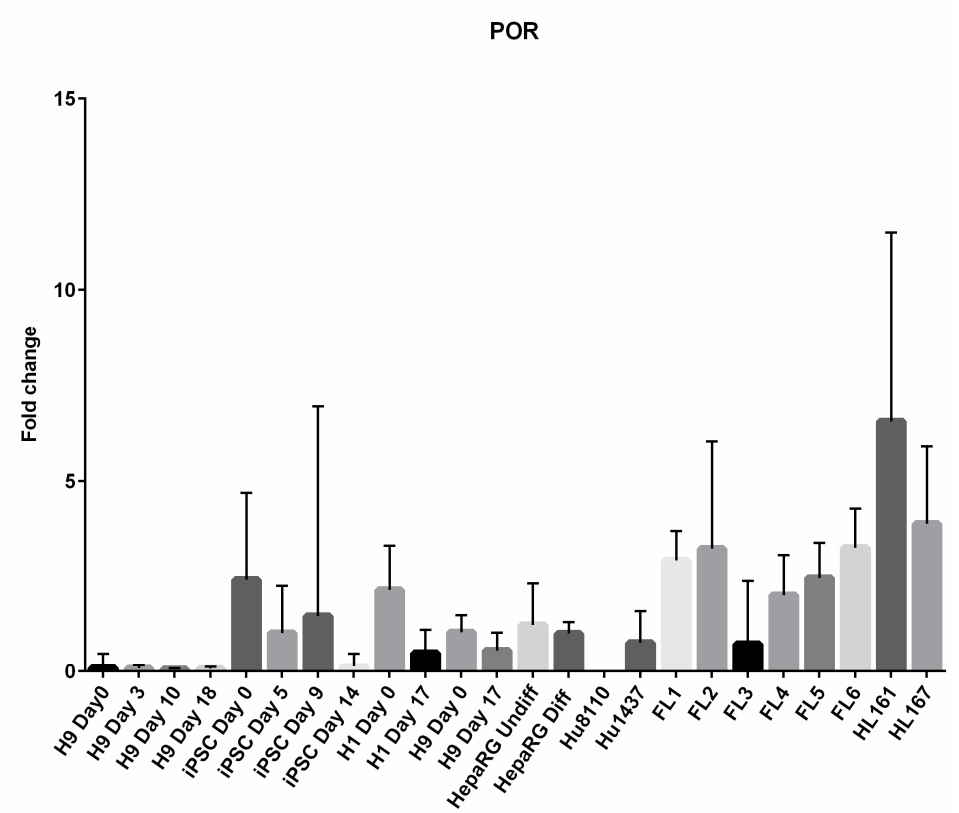
POR
Fold change
15
10
5
0
H9 Day0
H9 Day 3
H9 Day 10
H9 Day 18
iPSC Day 0
iPSC Day 5
iPSC Day 9
iPSC Day 14
H1 Day 0
H1 Day 17
H9 Day 0
H9 Day 17
HepaRG Undiff
HepaRG Diff
Hu8110
Hu1437
FL1
FL2
FL3
FL4
FL5
FL6
HL161
HL167

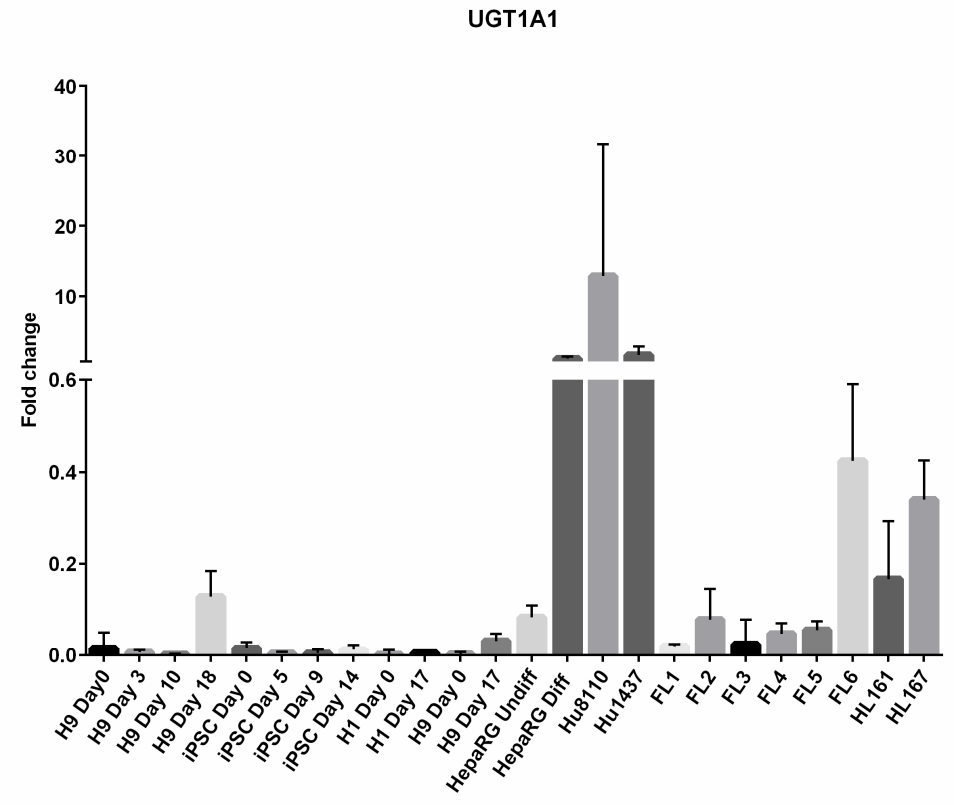
UGT1A1
Fold change
40
30
20
10
0.6
0.4
0.2
0.0
H9 Day0
H9 Day 3
H9 Day 10
H9 Day 18
iPSC Day 0
iPSC Day 5
iPSC Day 9
iPSC Day 14
H1 Day 0
H1 Day 17
H9 Day 0
H9 Day 17
HepaRG Undiff
HepaRG Diff
Hu8110
Hu1437
FL1
FL2
FL3
FL4
FL5
FL6
HL161
HL167

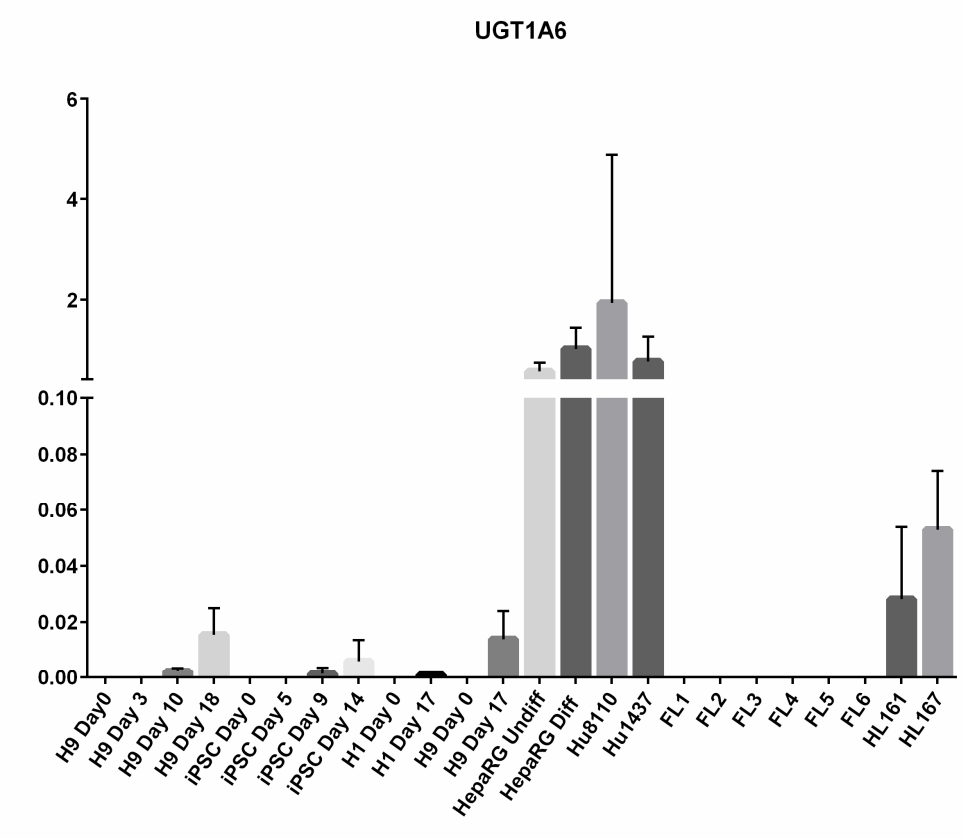
UGT1A6
6
4
2
0.10
0.08
0.06
0.04
0.02
0.00
H9 Day0
H9 Day 3
H9 Day 10
H9 Day 18
iPSC Day 0
iPSC Day 5
iPSC Day 9
iPSC Day 14
H1 Day 0
H1 Day 17
H9 Day 0
H9 Day 17
HepaRG Undiff
HepaRG Diff
Hu8110
Hu1437
FL1
FL2
FL3
FL4
FL5
FL6
HL161
HL167

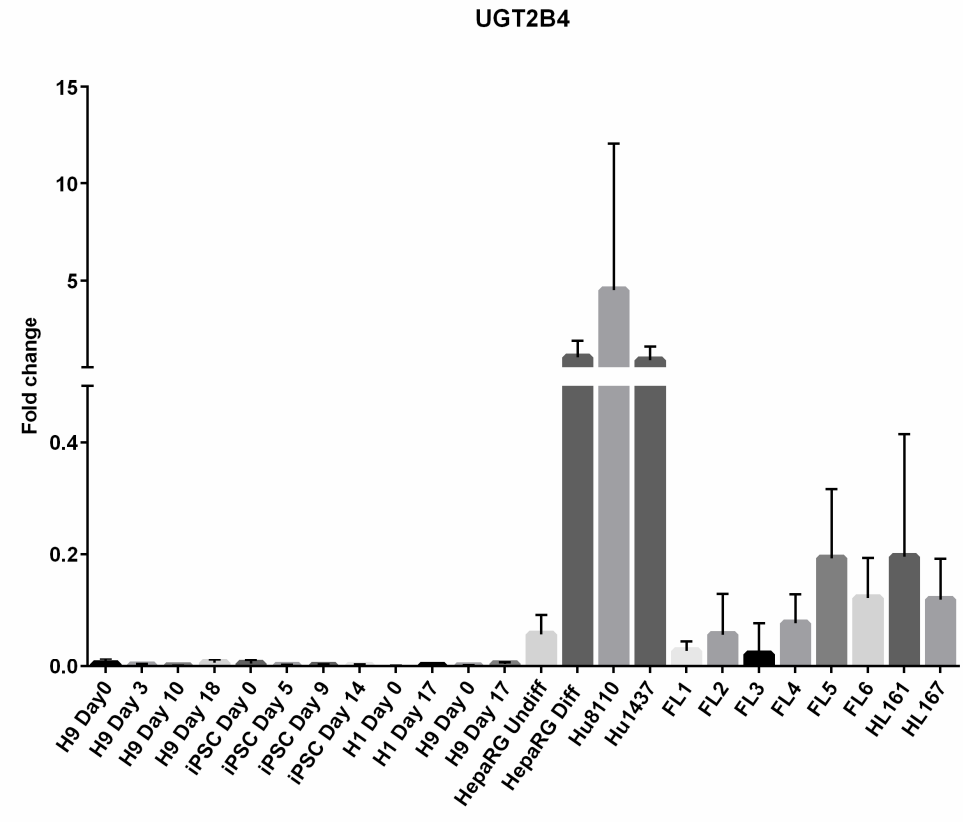
UGT2B4
Fold change
15
10
5
0.4
0.2
0.0
H9 Day0
H9 Day 3
H9 Day 10
H9 Day 18
iPSC Day 0
iPSC Day 5
iPSC Day 9
iPSC Day 14
H1 Day 0
H1 Day 17
H9 Day 0
H9 Day 17
HepaRG Undiff
HepaRG Diff
Hu8110
Hu1437
FL1
FL2
FL3
FL4
FL5
FL6
HL161
HL167

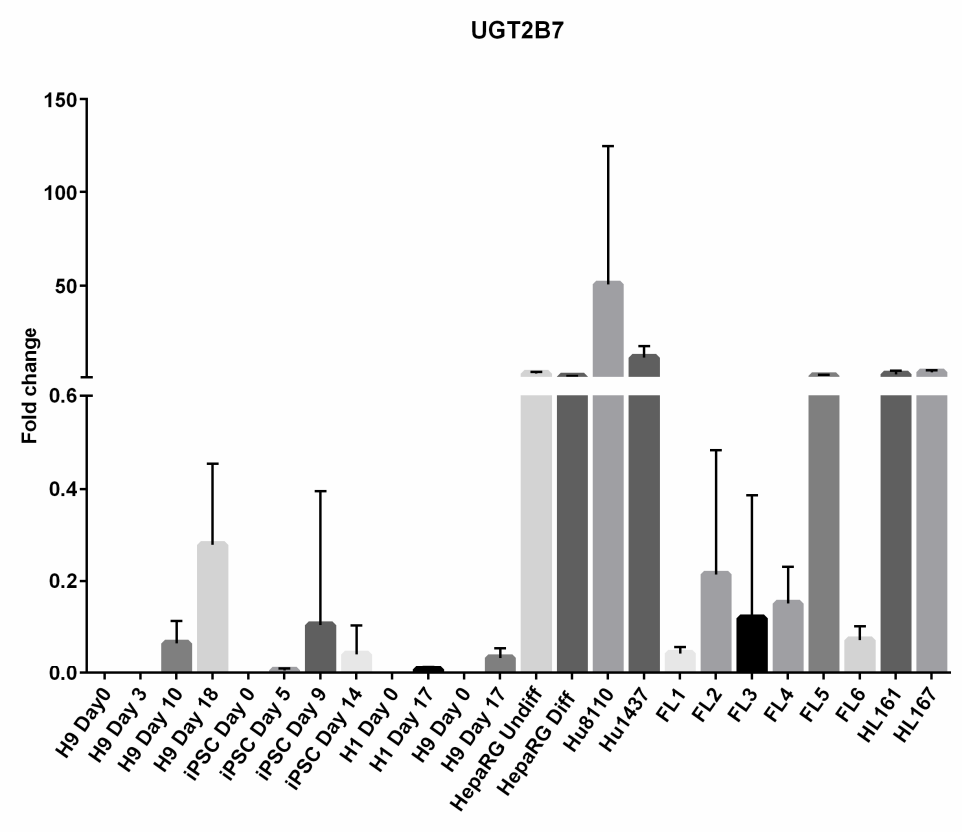
UGT2B7
Fold change
150
100
50
0.6
0.4
0.2
0.0
H9 Day0
H9 Day 3
H9 Day 10
H9 Day 18
iPSC Day 0
iPSC Day 5
iPSC Day 9
iPSC Day 14
H1 Day 0
H1 Day 17
H9 Day 0
H9 Day 17
HepaRG Undiff
HepaRG Diff
Hu8110
Hu1437
FL1
FL2
FL3
FL4
FL5
FL6
HL161
HL167

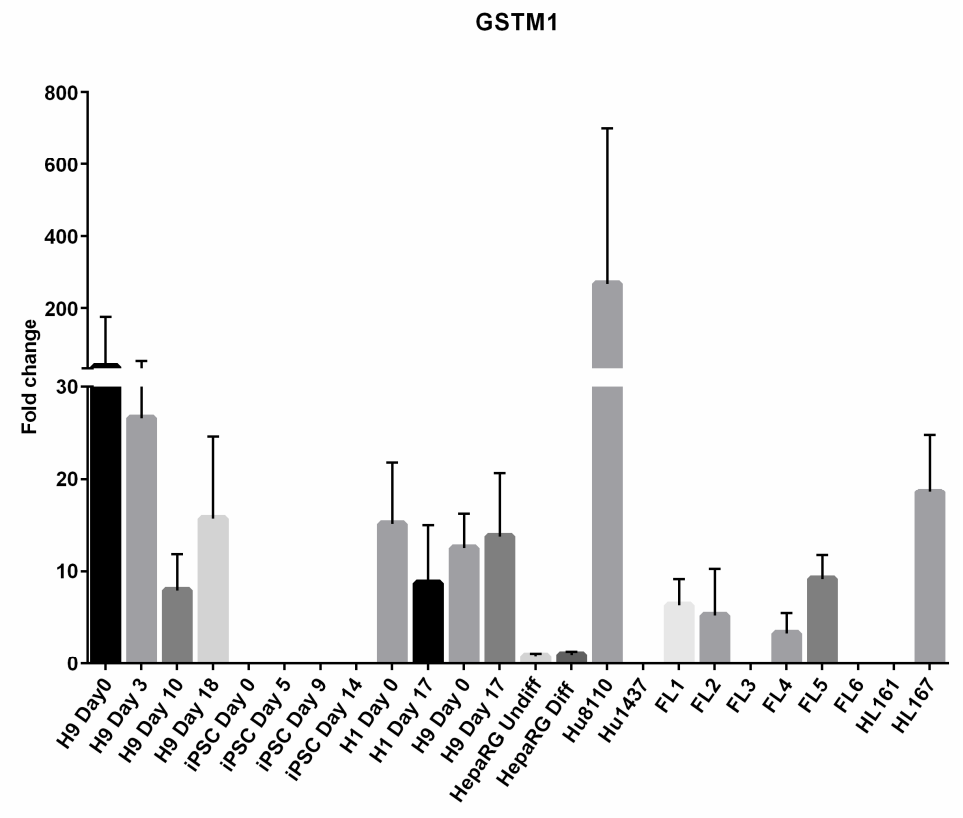
GSTM1
Fold change
800
600
400
200
30
20
10
0
H9 Day0
H9 Day 3
H9 Day 10
H9 Day 18
iPSC Day 0
iPSC Day 5
iPSC Day 9
iPSC Day 14
H1 Day 0
H1 Day 17
H9 Day 0
H9 Day 17
HepaRG Undiff
HepaRG Diff
Hu8110
Hu1437
FL1
FL2
FL3
FL4
FL5
FL6
HL161
HL167

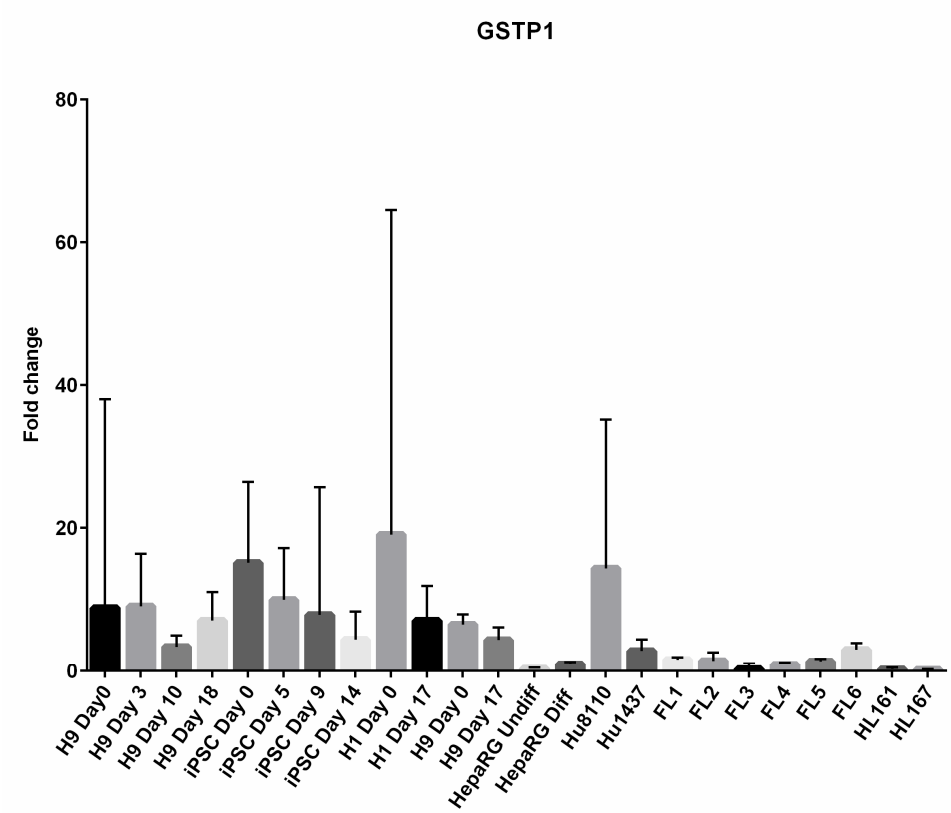
GSTP1
Fold change
80
60
40
20
0
H9 Day0
H9 Day 3
H9 Day 10
H9 Day 18
iPSC Day 0
iPSC Day 5
iPSC Day 9
iPSC Day 14
H1 Day 0
H1 Day 17
H9 Day 0
H9 Day 17
HepaRG Undiff
HepaRG Diff
Hu8110
Hu1437
FL1
FL2
FL3
FL4
FL5
FL6
HL161
HL167

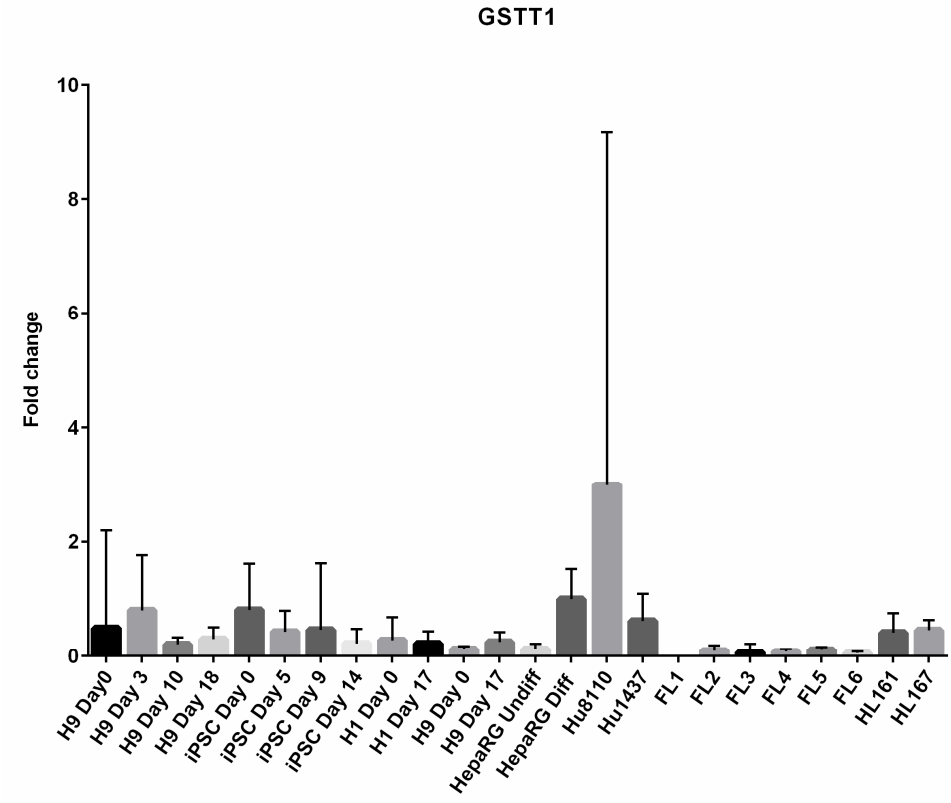
GSTT1
Fold change
10
8
6
4
2
0
H9 Day0
H9 Day 3
H9 Day 10
H9 Day 18
iPSC Day 0
iPSC Day 5
iPSC Day 9
iPSC Day 14
H1 Day 0
H1 Day 17
H9 Day 0
H9 Day 17
HepaRG Undiff
HepaRG Diff
Hu8110
Hu1437
FL1
FL2
FL3
FL4
FL5
FL6
HL161
HL167

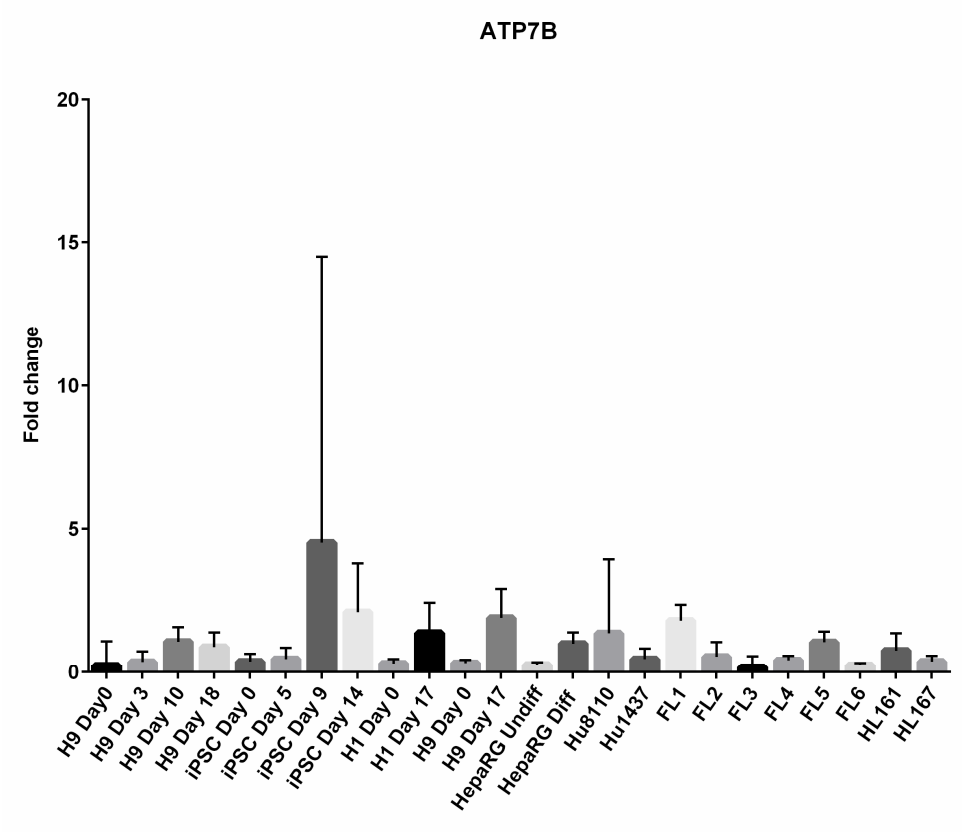
ATP7B
Fold change
20
15
10
5
0
H9 Day0
H9 Day 3
H9 Day 10
H9 Day 18
iPSC Day 0
iPSC Day 5
iPSC Day 9
iPSC Day 14
H1 Day 0
H1 Day 17
H9 Day 0
H9 Day 17
HepaRG Undiff
HepaRG Diff
Hu8110
Hu1437
FL1
FL2
FL3
FL4
FL5
FL6
HL161
HL167

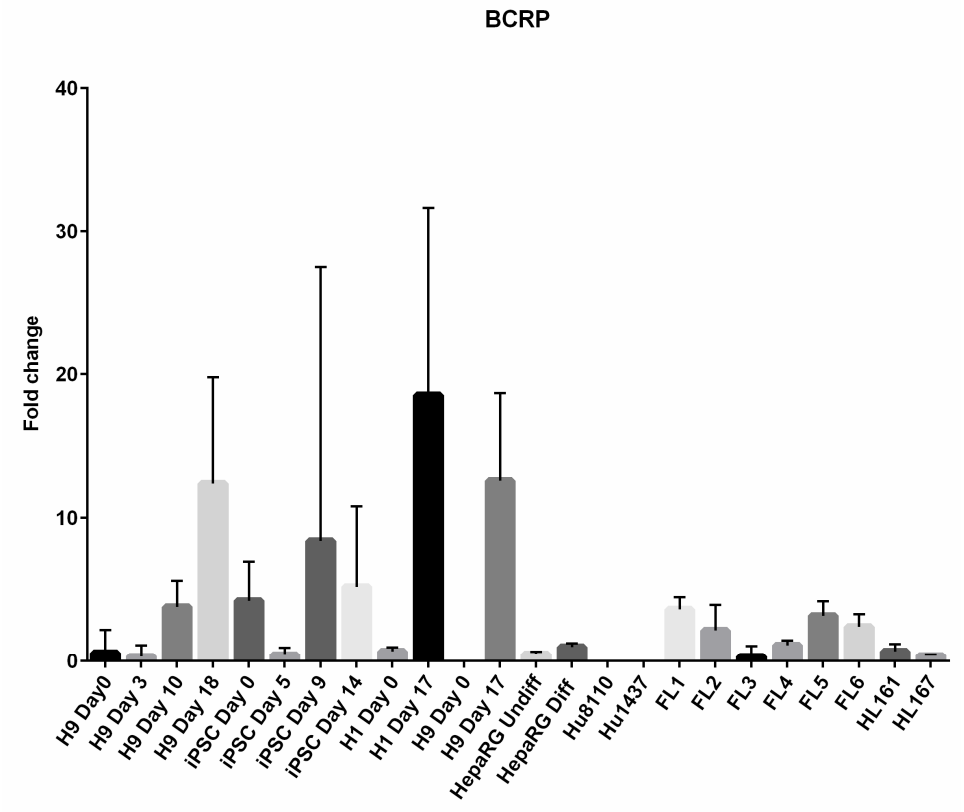
BCRP
Fold change
40
30
20
10
0
H9 Day0
H9 Day 3
H9 Day 10
H9 Day 18
iPSC Day 0
iPSC Day 5
iPSC Day 9
iPSC Day 14
H1 Day 0
H1 Day 17
H9 Day 0
H9 Day 17
HepaRG Undiff
HepaRG Diff
Hu8110
Hu1437
FL1
FL2
FL3
FL4
FL5
FL6
HL161
HL167

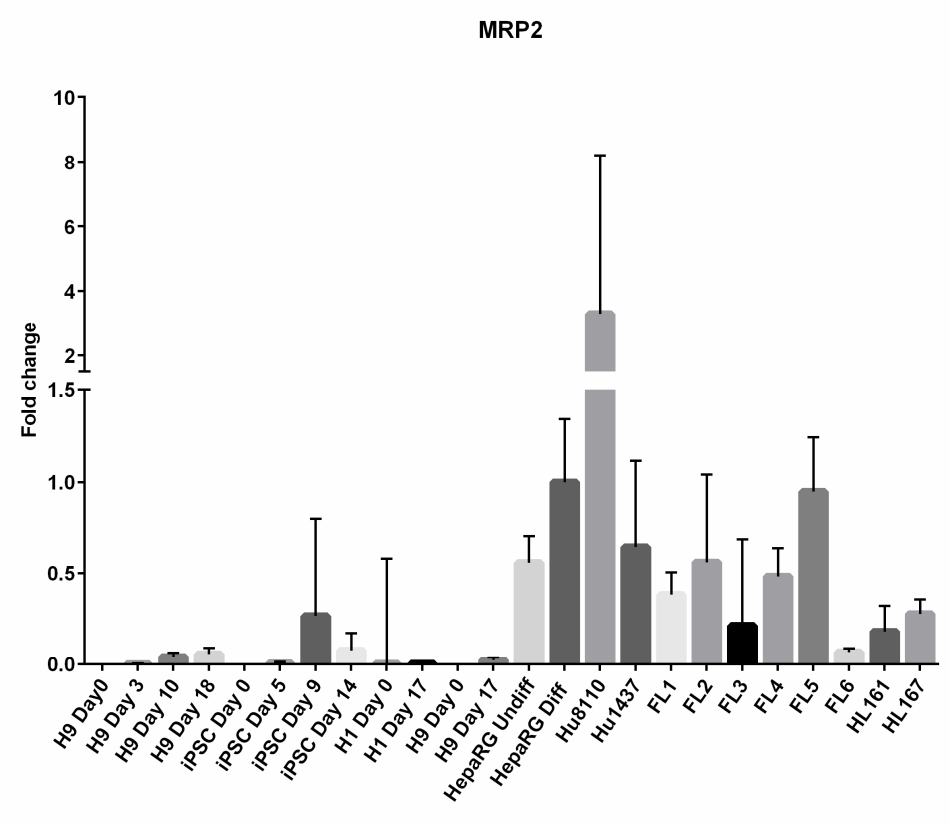
MRP2
Fold change
10
8
6
4
2
1.5
1.0
0.5
0.0
H9 Day0
H9 Day 3
H9 Day 10
H9 Day 18
iPSC Day 0
iPSC Day 5
iPSC Day 9
iPSC Day 14
H1 Day 0
H1 Day 17
H9 Day 0
H9 Day 17
HepaRG Undiff
HepaRG Diff
Hu8110
Hu1437
FL1
FL2
FL3
FL4
FL5
FL6
HL161
HL167

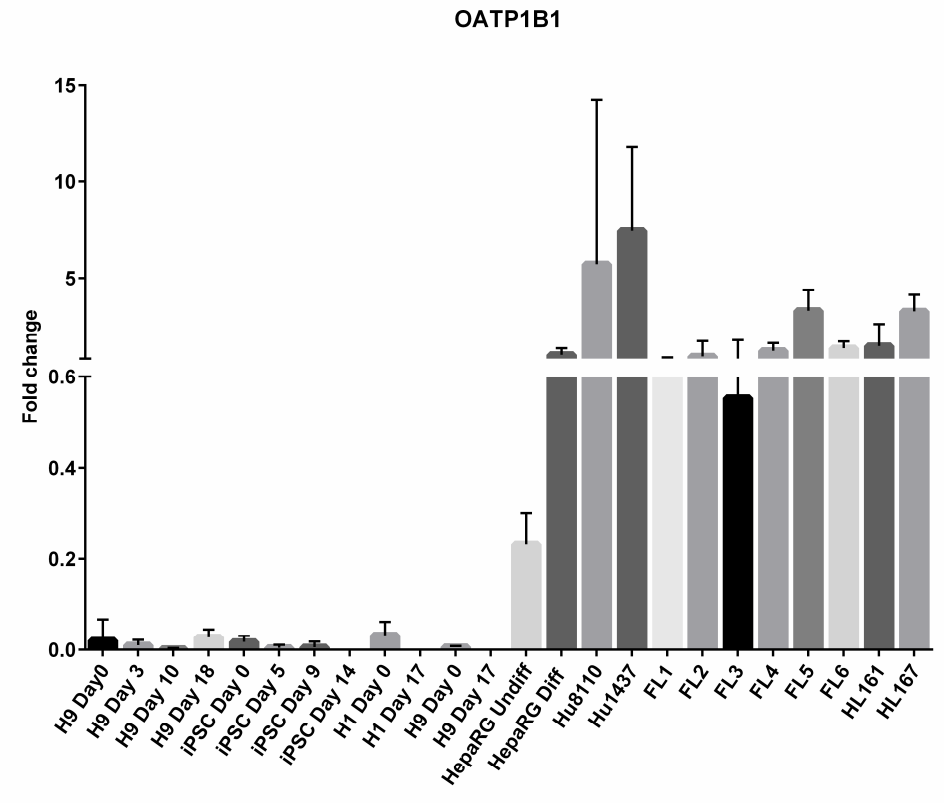
OATP1B1
Fold change
15
10
5
0.6
0.4
0.2
0.0
H9 Day0
H9 Day 3
H9 Day 10
H9 Day 18
iPSC Day 0
iPSC Day 5
iPSC Day 9
iPSC Day 14
H1 Day 0
H1 Day 17
H9 Day 0
H9 Day 17
HepaRG Undiff
HepaRG Diff
Hu8110
Hu1437
FL1
FL2
FL3
FL4
FL5
FL6
HL161
HL167

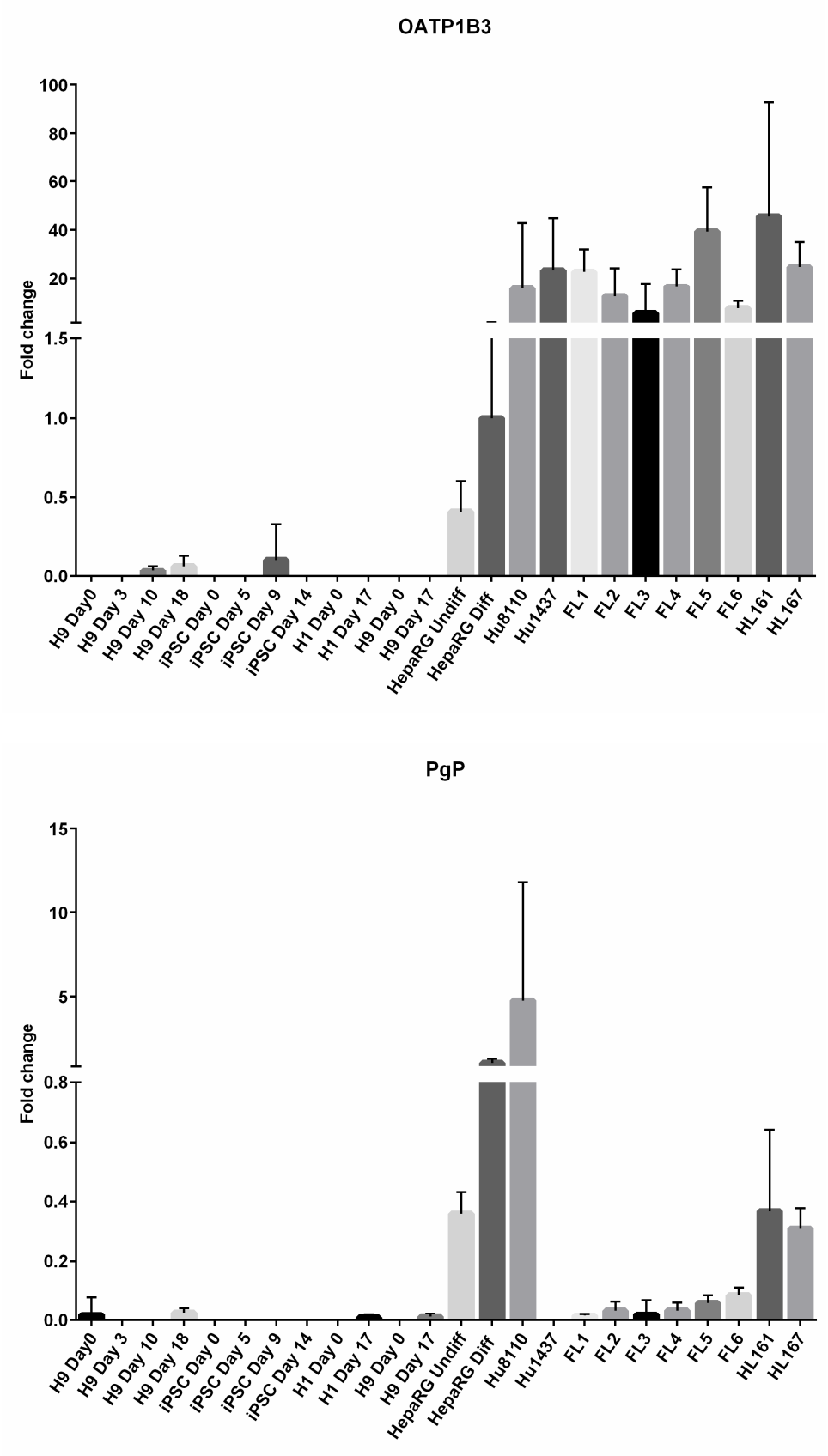
OATP1B3
Fold change
100
80
60
40
20
1.5
1.0
0.5
0.0
H9 Day0
H9 Day 3
H9 Day 10
H9 Day 18
iPSC Day 0
iPSC Day 5
iPSC Day 9
iPSC Day 14
H1 Day 0
H1 Day 17
H9 Day 0
H9 Day 17
HepaRG Undiff
HepaRG Diff
Hu8110
Hu1437
FL1
FL2
FL3
FL4
FL5
FL6
HL161
HL167
PgP
Fold change
15
10
5
0.8
0.6
0.4
0.2
0.0
H9 Day0
H9 Day 3
H9 Day 10
H9 Day 18
iPSC Day 0
iPSC Day 5
iPSC Day 9
iPSC Day 14
H1 Day 0
H1 Day 17
H9 Day 0
H9 Day 17
HepaRG Undiff
HepaRG Diff
Hu8110
Hu1437
FL1
FL2
FL3
FL4
FL5
FL6
HL161
HL167

Figure 3.2 SCDH gene expression characterization. qRT-PCR results shown as fold change compared to differentiated HepaRG cells, which was set to 1. GUS-B was used as a housekeeping gene. For all stem cell and SCDH samples, error bars represent a pool of triplicate biological replicates and triplicate technical replicates. For all other samples, error bars represent triplicate technical replicates. HepaRG Undiff represents undifferentiated HepaRG cells; HepaRG Diff represents differentiated HepaRG cells; FL1, FL2, FL3, FL4, FL5, FL6 represents fetal liver tissue 1, 2, 3, 4, 5, 6, respectively; HL161 and HL167 represent human liver bank samples 161 and 167, respectively.

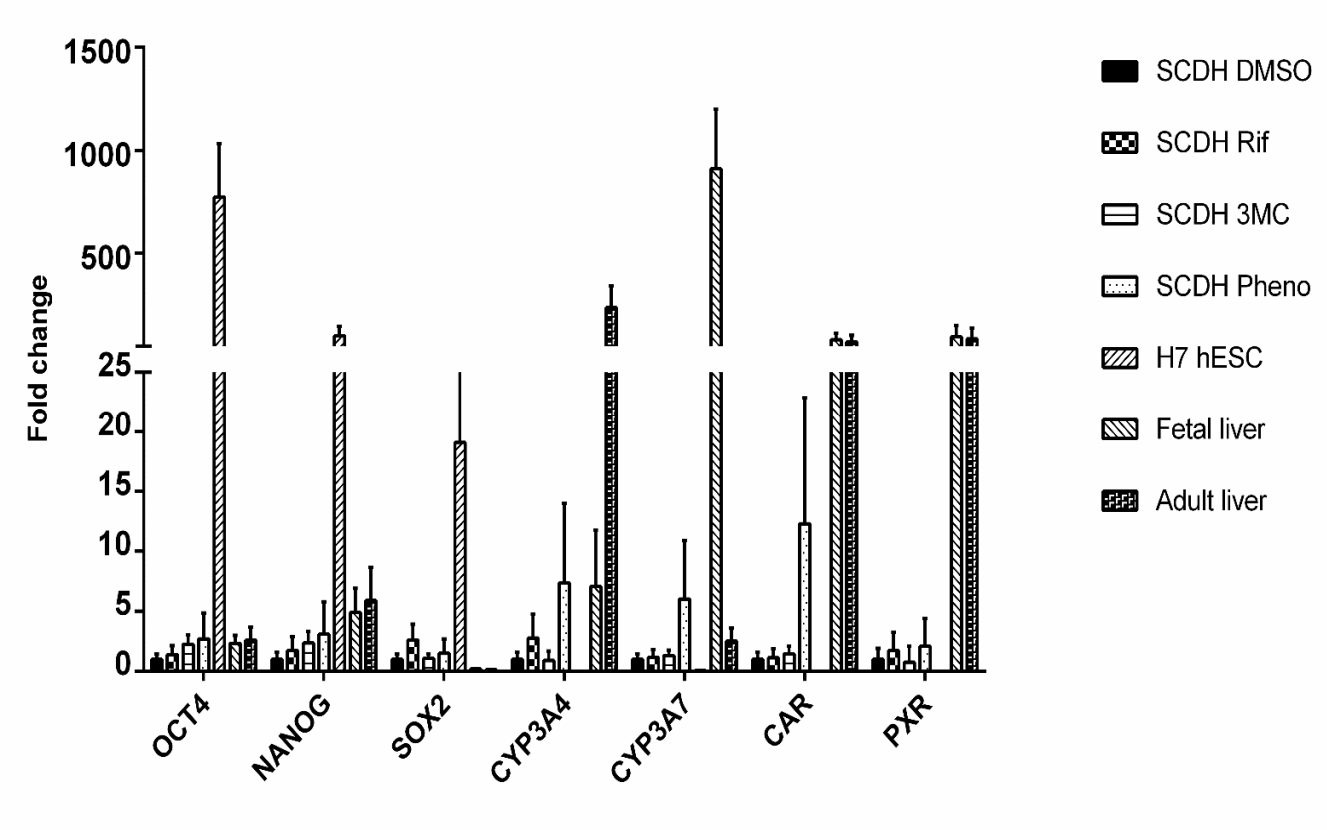

Figure 3.3 qRT-PCR results. qRT-PCR results for SCDHs incubated with the inducers rifampicin, 3-methylcholanthrene, and phenobarbital, shown as fold change compared to SCDHs incubated with DMSO, which was set to 1. GUS-B was used as a housekeeping gene. SCDH Rif represents SCDHs incubated with rifampicin; SCDH 3MC represents SCDHs incubated with 3-methylcholanthrene; SCDH Pheno represents SCDHs incubated with phenobarbital.

A

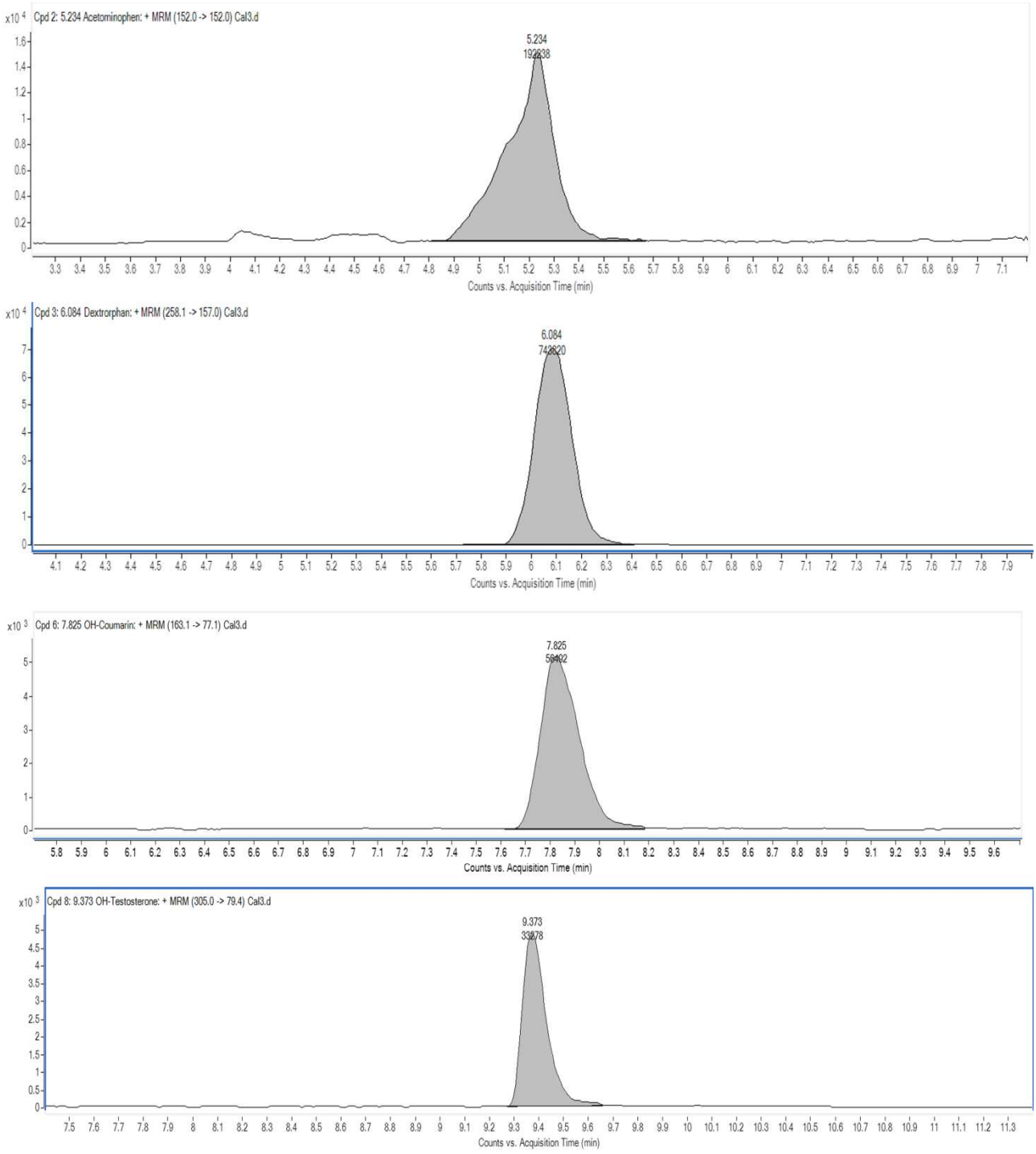
x10 4 Cpd 2: 5.234 Acetominophen: + MRM (152.0 -> 152.0) Cal3.d
5.234
192838
Counts vs. Acquisition Time (min)
x10 4 Cpd 3: 6.084 Dextrorphan: + MRM (258.1 -> 157.0) Cal3.d
6.084
743820
Counts vs. Acquisition Time (min)
x10 3 Cpd 6: 7.825 OH-Coumarin: + MRM (163.1 -> 77.1) Cal3.d
7.825
58492
Counts vs. Acquisition Time (min)
x10 3 Cpd 8: 9.373 OH-Testosterone: + MRM (305.0 -> 79.4) Cal3.d
9.373
33278
Counts vs. Acquisition Time (min)

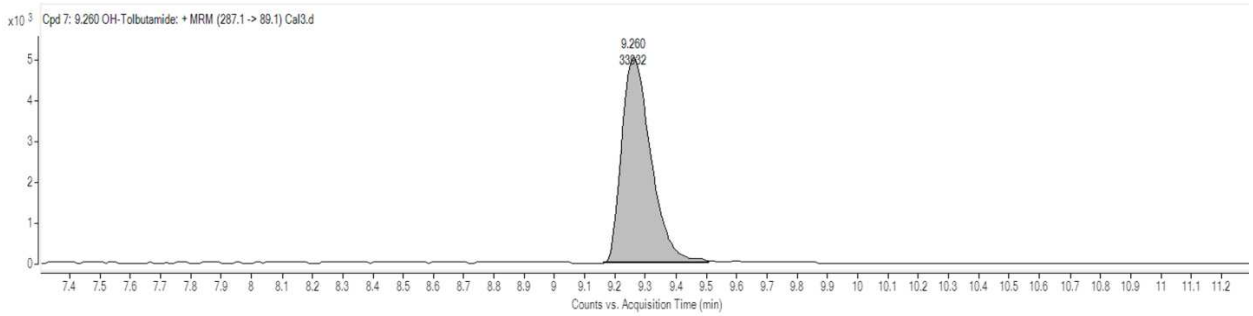
x10 3
Cpd 7: 9.260 OH-Tolbutamide: + MRM (287.1 -> 89.1) Cal3.d
9.260
33832
Counts vs. Acquisition Time (min)

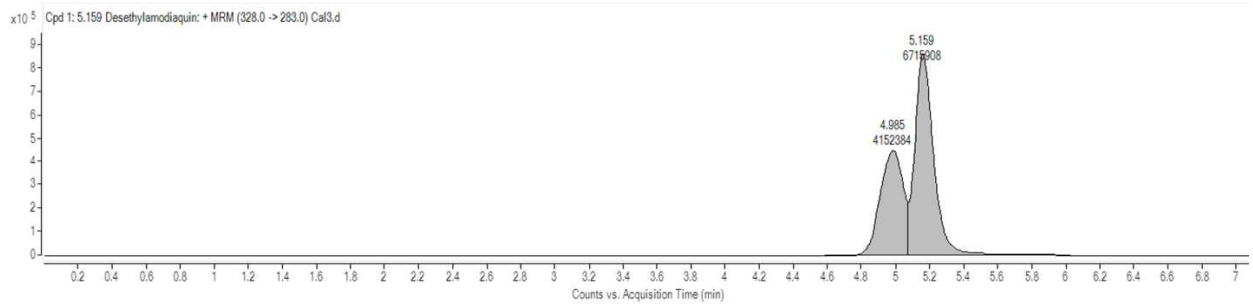
x10 5
Cpd 1: 5.159 Desethylamodiaquin: + MRM (328.0 -> 283.0) Cal3.d
5.159
6715908
4.985
4152384
Counts vs. Acquisition Time (min)

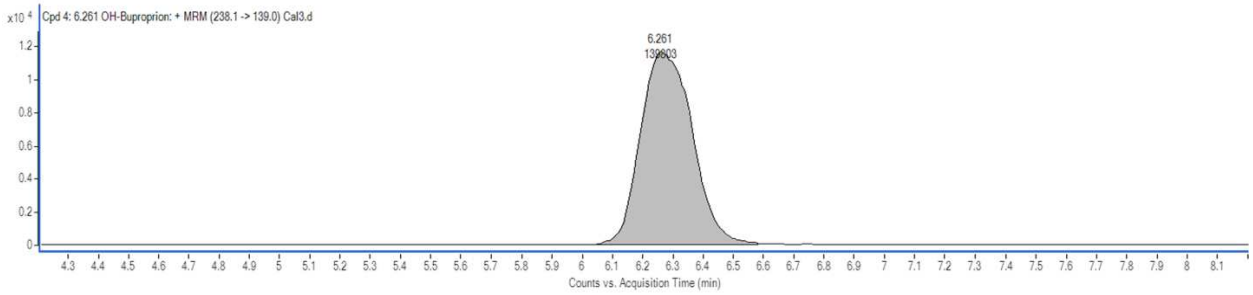
x10 4
Cpd 4: 6.261 OH-Bupropion: + MRM (238.1 -> 139.0) Cal3.d
6.261
139603
Counts vs. Acquisition Time (min)

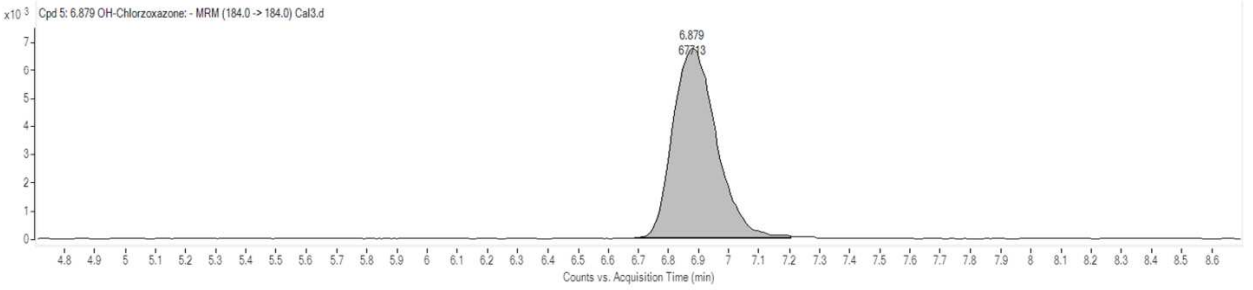
x10 3
Cpd 5: 6.879 OH-Chlorzoxazone: - MRM (184.0 -> 184.0) Cal3.d
6.879
67713
Counts vs. Acquisition Time (min)

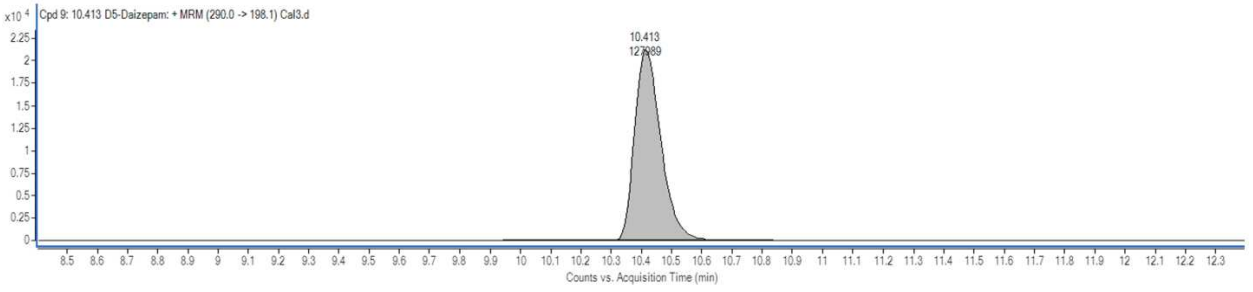
x10 4
Cpd 9: 10.413 D5-Daizepam: + MRM (290.0 -> 198.1) Cal3.d
10.413
127089
Counts vs. Acquisition Time (min)

B

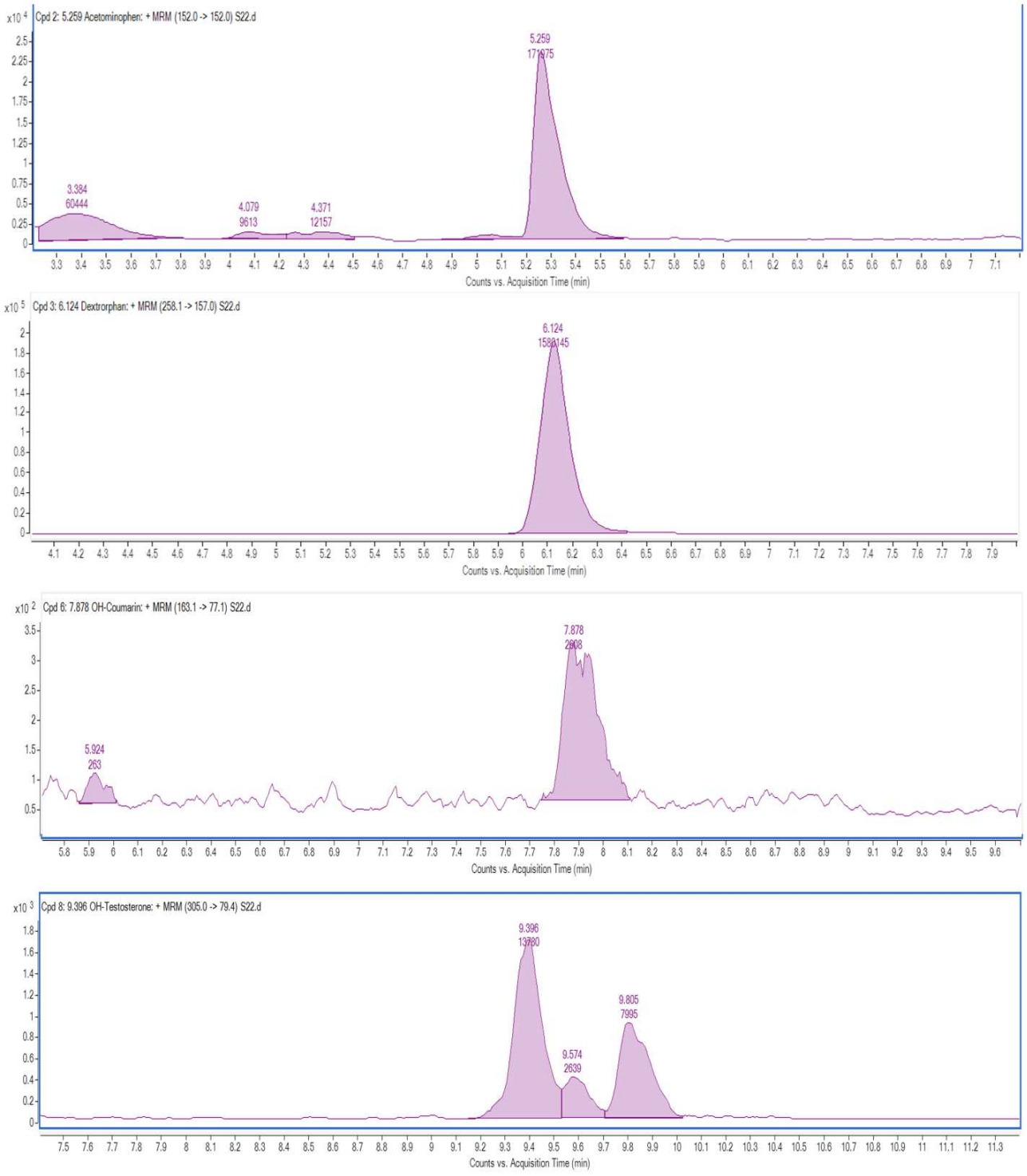
x10 4 Cpd 2: 5.259 Acetominophen: + MRM (152.0 -> 152.0) S22.d
5.259
171975
3.384
60444
4.079
9613
4.371
12157
Counts vs. Acquisition Time (min)
x10 5 Cpd 3: 6.124 Dextrorphan: + MRM (258.1 -> 157.0) S22.d
6.124
1586145
Counts vs. Acquisition Time (min)
x10 2 Cpd 6: 7.878 OH-Coumarin: + MRM (163.1 -> 77.1) S22.d
7.878
2608
5.924
263
Counts vs. Acquisition Time (min)
x10 3 Cpd 8: 9.396 OH-Testosterone: + MRM (305.0 -> 79.4) S22.d
9.396
13780
9.805
7995
9.574
2639
Counts vs. Acquisition Time (min)

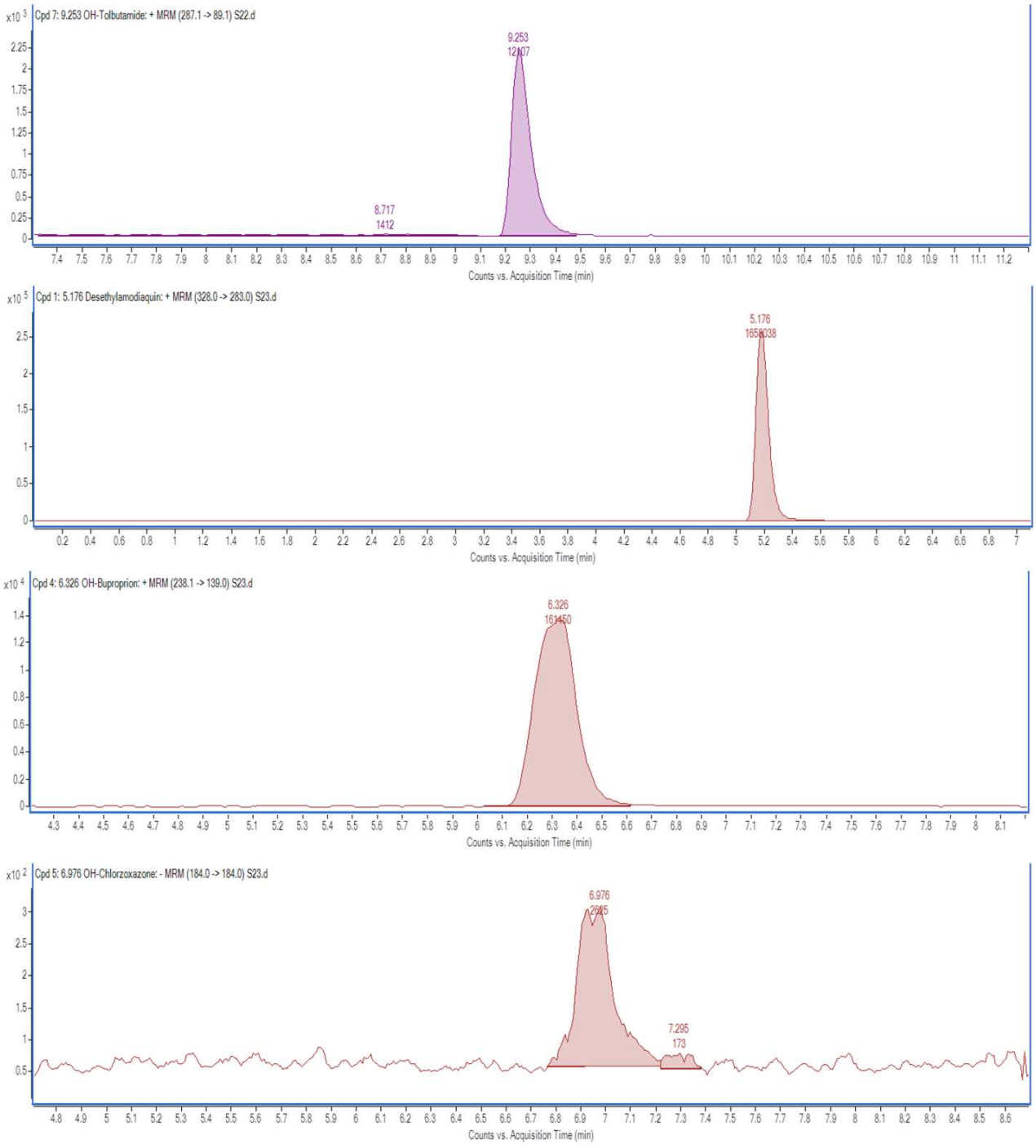
x10 3 Cpd 7: 9.253 OH-Tolbutamide: + MRM (287.1 -> 89.1) S22.d
9.253
12107
8.717
1412
Counts vs. Acquisition Time (min)
x10 5 Cpd 1: 5.176 Desethylamodiaquin: + MRM (328.0 -> 283.0) S23.d
5.176
1656038
Counts vs. Acquisition Time (min)
x10 4 Cpd 4: 6.326 OH-Bupropion: + MRM (238.1 -> 139.0) S23.d
6.326
16150
Counts vs. Acquisition Time (min)
x10 2 Cpd 5: 6.976 OH-Chlorzoxazone: - MRM (184.0 -> 184.0) S23.d
6.976
2965
7.295
173
Counts vs. Acquisition Time (min)

C

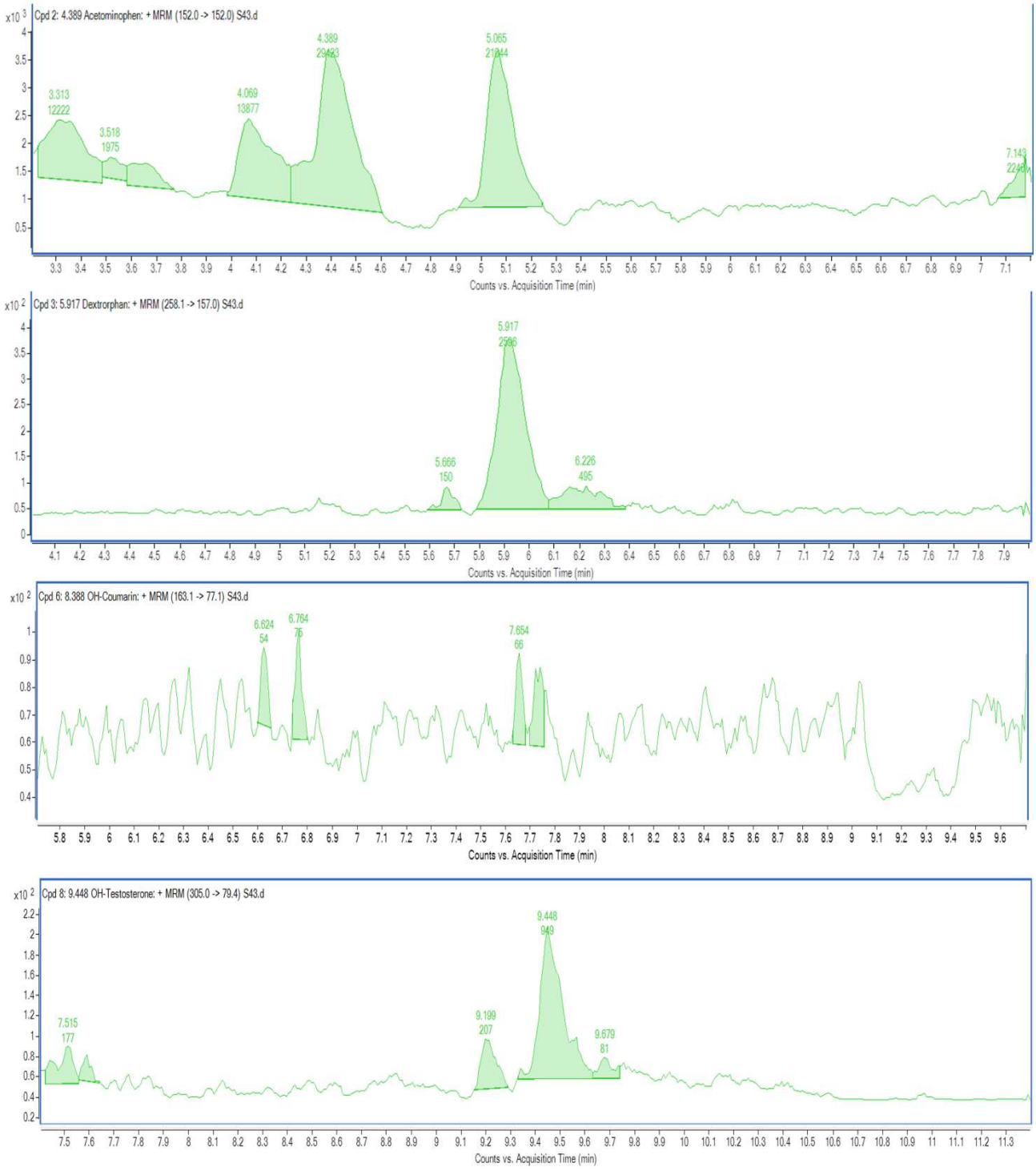
Cpd 2: 4.389 Acetominophen: + MRM (152.0 -> 152.0) S43.d
3.313 12222
3.518 1975
4.069 13877
4.389 29423
5.065 21944
7.143 2249
Counts vs. Acquisition Time (min)
Cpd 3: 5.917 Dextrorphan: + MRM (258.1 -> 157.0) S43.d
5.666 150
5.917 2586
6.226 495
Counts vs. Acquisition Time (min)
Cpd 6: 8.388 OH-Coumarin: + MRM (163.1 -> 77.1) S43.d
6.624 54
6.764 76
7.654 66
Counts vs. Acquisition Time (min)
Cpd 8: 9.448 OH-Testosterone: + MRM (305.0 -> 79.4) S43.d
7.515 177
9.199 207
9.448 949
9.679 81
Counts vs. Acquisition Time (min)

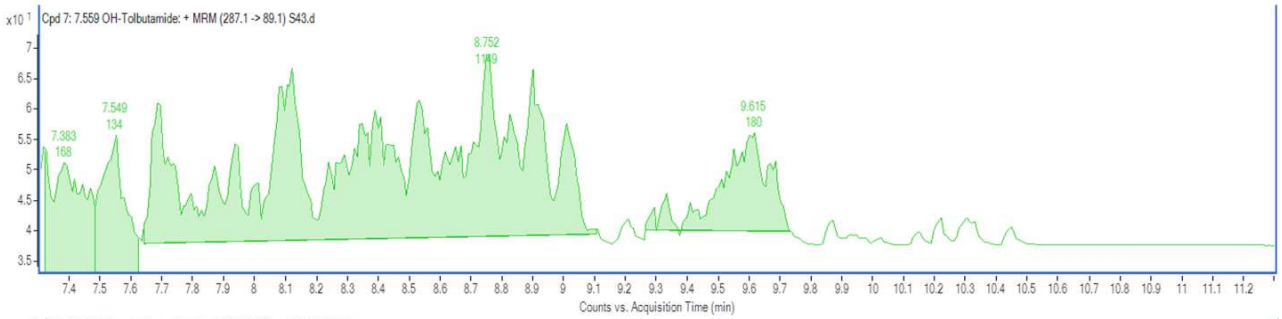
x10 1
Cpd 7: 7.559 OH-Tolbutamide: + MRM (287.1 -> 89.1) S43.d
8.752
1149
7.549
134
7.383
168
9.615
180
Counts vs. Acquisition Time (min)

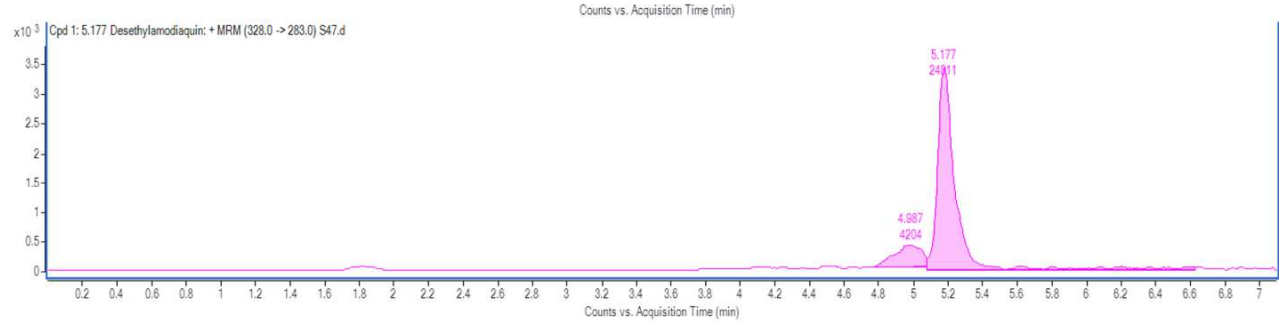
x10 3
Cpd 1: 5.177 Desethylamodiaquin: + MRM (328.0 -> 283.0) S47.d
5.177
24911
4.987
4204
Counts vs. Acquisition Time (min)

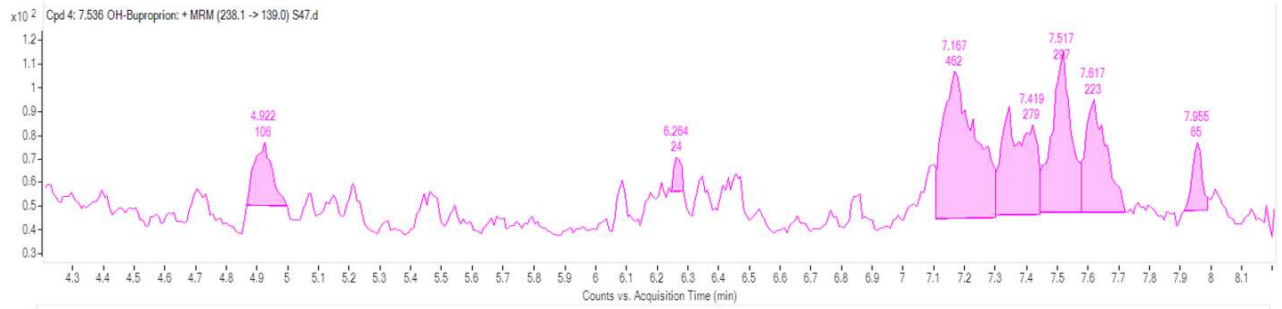
x10 2
Cpd 4: 7.536 OH-Bupropion: + MRM (238.1 -> 139.0) S47.d
7.167
462
7.517
297
7.617
223
7.419
279
4.922
106
6.264
24
7.955
65
Counts vs. Acquisition Time (min)

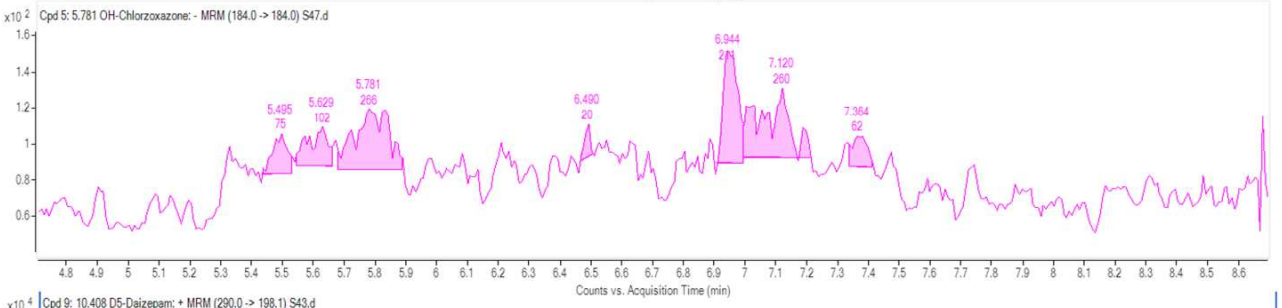
x10 2
Cpd 5: 5.781 OH-Chlorzoxazone: - MRM (184.0 -> 184.0) S47.d
6.944
7.120
260
5.781
266
5.495
75
5.629
102
6.490
20
7.364
62
Counts vs. Acquisition Time (min)

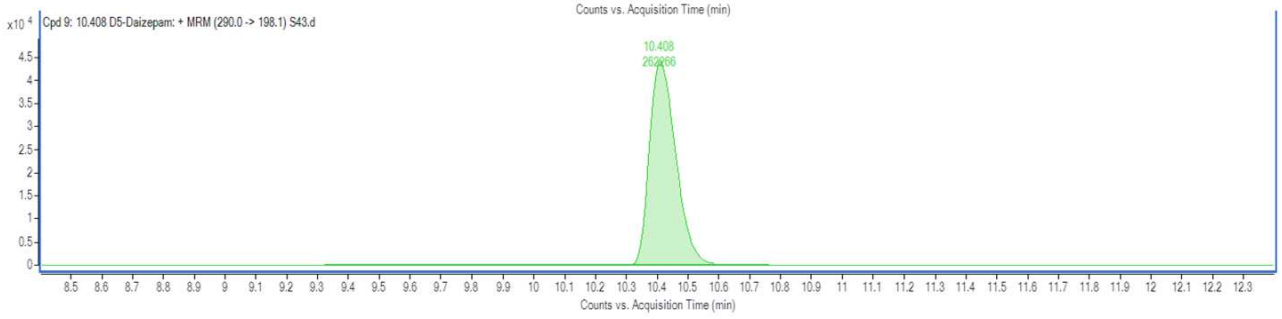
x10 4
Cpd 9: 10.408 D5-Daizepam: + MRM (290.0 -> 198.1) S43.d
10.408
Counts vs. Acquisition Time (min)

Figure 3.4 LC-MS/MS Chromatograms. Representative chromatograms for each metabolite assayed using LC-MS/MS. **(A)** Standard curve chromatograms. **(B)** Primary hepatocyte sample chromatograms. **(C)** H1 SCDH sample chromatograms.

Chapter 4

Characterization of miRNAs in Human Pluripotent Stem Cells and Liver in Relation to Hepatocyte Differentiation and Maturation

4.1 Abstract

Background microRNAs (miRNAs) regulate many genes, making them similar to transcription factors, and therefore potential regulators of cellular process such as differentiation. Since miRNAs have been shown to be expressed in a tissue and developmental stage-specific manner, with liver specific miRNAs such as miR-122 identified, we postulated that miRNA profiling of our human embryonic stem cells (hESCs) throughout the differentiation process may provide insight into the lack of maturity observed in our hESC-derived hepatocytes. This set of microarrays will provide information on the potential role of miRNAs in liver differentiation and maturation, and specifically provide insight on miRNAs that could be manipulated during *in vitro* hepatocyte differentiation to enhance maturation of the cells.

Methods miRNA microarray analyses utilizing the Affymetrix GeneChip® miRNA array were performed on hESCs and induced pluripotent stem cells (iPSCs), stem cell derived hepatocytes at each stage of differentiation, cryopreserved hepatocytes, and human livers from the University of Washington liver bank.

Results One of the highest expressed miRNAs in stem cell derived hepatocytes is the liver specific miR-122. Based on the microarray results, and further qRT-PCR analysis, miR-122 appears to be expressed at sufficient levels in stem cell derived hepatocytes, compared to cryopreserved hepatocytes. Patterns of miRNA expression show that the let-7 family is down-regulated in stem cell derived hepatocytes compared to cryopreserved hepatocytes and human liver tissue. Another prominent pattern is the high overall expression and up-regulation compared to cryopreserved hepatocytes and human liver tissue of members in the miR-17-92, 302-367 and 371-373 clusters, normally expressed in pluripotent stem cells. The top toxicological pathways identified among the miRNAs with large differences in expression

between stem cell derived hepatocytes and undifferentiated stem cells are liver-related - liver steatosis, liver damage, hepatocellular carcinoma, and liver inflammation/hepatitis.

Conclusion This work is largely hypothesis-generating, but nonethelss informative. The miRNA expression patterns in stem cell derived hepatocytes compared to other cell sources indicate global changes associated with immaturity in stem cell derived hepatocytes. The data suggests that the let-7 family of miRNAs and/or the miR-17-92, miR-302-367, and miR-371-373 clusters may be viable targets for manipulation within the currently used differentiation protocol to enhance the maturation and function of stem cell derived hepatocytes.

4.2 Introduction

4.2.1 MicroRNAs

MicroRNAs (miRNAs) are small, single-stranded, noncoding RNAs responsible for posttranscriptional gene regulation [149]. They modify gene expression by binding to complementary regions of target messenger RNAs (mRNAs), resulting in translational repression or mRNA degradation [150]. miRNAs are evolutionarily conserved, and are encoded in the genomes of plants, invertebrates, and vertebrates [151-155]. There are currently about 2,000 human miRNAs identified, with more than half of the known miRNAs conserved across vertebrates [149, 156]. Mature miRNAs are usually 21-23 nucleotides long and are excised from 60 to 80 nucleotide long double-stranded RNA (dsRNA) hairpins [151]. The biogenesis of miRNA from transcripts that form these distinctive hairpin structures is in part what makes them unique from other small RNAs such as small interfering RNAs (siRNAs) [157, 158]. Biogenesis of miRNA begins with transcription of the miRNA gene by RNA polymerase II to the primary transcript (pri-miRNA), which is typically over 1 kb in length [156, 158]. The pri-miRNA is then trimmed by Drosha RNAse III to an about 70 nucleotide miRNA precursor hairpin (pre-miRNA) within the nucleus [151, 159]. The pre-miRNA is then exported to the cytoplasm and Dicer RNase III cuts the double-stranded portion of the pre-miRNA, forming a miRNA:miRNA* duplex [151, 160]. The mature miRNA strand of this duplex, also referred to as the guide strand, is then loaded into the RNA-induced silencing complex (RISC) with an Argonaute effector protein, and the miRNA* (or passenger) strand is peeled away and usually degraded, though it may also remain an active miRNA [159-161]. Mature miRNA within the RISC then acts through primarily two mechanisms to regulate gene expression, varying between plants and animals [160-162]. In plants, for the most part, miRNAs bind with target mRNA by precise or

nearly precise complementarity, resulting in direct cleavage and degradation of the mRNA [162]. In contrast, miRNAs in animals tend to bind to target mRNA with imprecise complementarity, resulting instead in translational repression – they inhibit protein synthesis while maintaining the stability of the mRNA [162]. Within the mature miRNA, only nucleotides 2-7 at the 5' end are necessary for binding to the target mRNA, this region is known as the seed sequence [157, 159]. This small sequence, coupled with imprecise base pairing between animal miRNAs and target mRNAs, suggests that any one miRNA can target multiple mRNAs, thus possessing a large regulatory potential [162]. Indeed, miRNAs are predicted to regulate more than 60% of all protein-coding genes in mammals [163, 164]. Though miRNAs are mainly translational repressors, there is evidence that they can also act as translational activators [159, 165-168]. For example, it has been demonstrated that select miRNAs switch to act as translational activators under growth-arrest conditions in cells, while acting as translational repressors in proliferating cells [165]. Another interesting example where a miRNA acts as an activator involves the liver-specific miRNA, miR-122 and its interaction with the Hepatitis C virus (HCV); miR-122 has been found to upregulate HCV by binding to the 5'-UTR region of HCV RNA and stimulating replication [166, 168, 169]. In these cases, it appears binding of the miRNA to the 3'-UTR of the target mRNA results in translational repression while binding to the 5'-UTR has a stimulatory effect [166, 168]. Additionally, many miRNAs seem to have specific expression patterns. For example, paralogs and orthologs of the *C. elegans lin-4* and *let-7* RNAs have similar stage-specific expression in development [160]. Others seem to be expressed in a tissue specific manner, such as miR-1 in the heart, miR-122 in the liver, and the mir-290-mir-295 cluster in mouse embryonic stem cells [154, 160, 170, 171]. Such distinct expression profiles suggest a potential role of miRNAs in regulating the transcriptome [160].

The discovery of miRNAs occurred in the early 1990's when a group from Harvard found that *lin-4*, a gene that is known to control the timing of larval development in *C. elegans*, actually did not code for a protein, but rather produced two small RNAs – one 22 nucleotides in length and the other 61 nucleotides [160, 172]. The longer RNA was predicted to fold into a stem loop precursor of the shorter RNA [160, 172]. They then found that these small RNAs had antisense complementarity to a repeated sequence element in the 3'-untranslated region (UTR) of the *lin-14* gene, and that they reduced the amount of LIN-14 protein without affecting the levels of *lin-14* mRNA [160, 172, 173]. Taken together, their discovery suggested that the small RNA produced by *lin-4* binds to the 3'-UTR of *lin-14* resulting in translational repression of *lin-14* as part of the regulatory pathway triggering the transition from the first larval stage to the second in *C. elegans* [160, 172, 173]. It was not until seven years later, in 2000, when a second small, 21 nucleotide long regulatory RNA encoded by *let-7* was discovered in *C. elegans* [160, 174, 175]. In this case, the *let-7* RNA acted to promote the transition from the late-larval to adult cell fates in the nematode by negatively regulating *lin-41*, similar to how *lin-4* acts in the earlier developmental stages [160, 174, 175]. Since both the *lin-4* and the *let-7* RNAs controlled the timing of developmental transitions, they were named small temporal RNAs (stRNAs) [160, 176]. Shortly after the discovery of let-7, three separate labs cloned small RNAs from flies, worms, and human cells, totaling over one hundred genes for small, noncoding RNAs resembling the *lin-4* and *let-7* stRNAs [152-154, 160]. However, unlike the *lin-4* and *let-7* RNAs, most of the newly identified small RNAs were not expressed in distinct stages of development, but rather were expressed in specific cell types. Therefore, the new term microRNA was developed to refer to the original stRNAs and all other small RNAs with similar features [152-154, 160]. Based on the functions associated with the earliest known miRNAs,

such as *lin-4* and *let-7*, they seem to play an important role in animal development and physiology [162].

The nomenclature of a miRNA follows some basic guidelines; they are named in a numeric style, such as hsa-miR-122, where the first three letters designate the genus and species of origin – "hsa" for homo sapiens. In most of the literature, the mature miRNA is designated by miR-122, and the miRNA gene and precursor hairpin is designated by mir-122 [177, 178]. Orthologous miRNAs are given the same numerical identifier, such as hsa-miR-22 in humans and mmu-miR-22 in mouse [149, 178]. Mature miRNA sequences that differ only by one or two positions, also called sister miRNAs, are given lettered suffixes, for example, miR-10a and miR-10b [149, 156, 178]. While these paralogues differ by one or two bases, they often retain identical seed sequences at the 5' end of the miRNA [158]. Identical mature miRNAs that are derived from distinct hairpin loci are given numbered suffixes, for example, miR-281-1 and miR-281-2 [149, 178]. Usually, one strand of the precursor miRNA forms the more prevalent and biologically active mature miRNA while the opposite arm of the precursor forms the passenger strand and is given a * designation [156]. In cases when it is unknown which strand is the more predominant one formed, then they are named for the arm they are derived from, such as miR-17-5p from the 5' arm of the hairpin precursor and miR-17-3p from the 3' arm of the hairpin precursor [156, 178]. There are a few exceptions to the numbering scheme, namely *let-7* and *lin-4*, which have retained the original designations they were given for historical reasons.

4.2.2 Role of miRNAs in cancer

Expression profiling studies of miRNAs indicate they are controlled by developmental and tissue specific signaling [158]. Control of miRNA expression is important to maintain

normal cellular functions, indeed dysregulation of miRNA has been associated with diseases such as cancer [149, 158]. There is evidence that miRNAs can act both as tumor suppressors and as oncogenes, depending on the target mRNA [179-181]. The first study to show a relationship between miRNAs and cancer found that a region of chromosome 13q14 containing *mir-15a* and *mir-16-1* was deleted in the majority of B cell chronic lymphocytic leukemia cases evaluated [182, 183]. The same group went on to map 186 known miRNAs to show that most are located at genomic regions associated with cancer, for example, fragile sites (for just over half of the miRNAs evaluated) and common breakpoint regions [182, 184]. Several studies have further shown that aberrant miRNA expression is associated with tumor formation, miRNA expression profiles vary across tumor types, and they reflect the differentiation state of the tumor [182, 185, 186]. For example, the *mir-17-92* cluster has been shown to be upregulated in B-cell lymphomas, and overexpression of the *mir-17-92* cluster was found to interact with c-*myc* and accelerate tumor formation in a mouse lymphoma model, implicating the *mir-17-92* cluster as an oncogene [187, 188]. Other examples of tumors with altered miRNA expression profiles include miR-143 and miR-145 in colorectal cancer, miR-155 in Burkitt lymphoma, miRs-221, 128, 181 in glioblastoma, let-7 in lung cancer, and miR-21 in a variety of hematological malignancies and solid tumors [185, 188-193]. It seems clear that miRNAs are associated with cancer etiology, however, it is still unclear whether altered miRNA expression is a cause or consequence of tumor formation [182].

There are a few mechanisms that may be responsible for miRNA dysregulation in cancers, including genomic abnormalities, epigenetic regulation, and transcriptional control [194]. Transcriptional control is a major regulator of miRNA biogenesis. Some miRNAs have been shown to be under the control of tumor-suppressive and oncogenic transcription factors,

such as p53 and c-Myc [158]. p53 is a well-known tumor suppressor that is frequently inactivated in cancer, and select miRNAs have been shown to be under control of p53 [194]. For example, genes encoding the miRs-34a-b-c (or collectively the miR-34s) have been shown to be direct transcriptional targets of p53 [195-197]. The miR-34s are induced by p53, and in certain tumors and cancer cell lines deficient in p53, the miR-34s were also down-regulated [194, 195]. The miR-34s have proapoptotic effects and have been implicated as tumor suppressor genes in pancreatic, colon and breast cancers [193, 196, 197]. C-Myc is an oncogene, and is known to either trans-activate or repress miRNAs involved in the cell cycle and apoptosis [158, 198]. c-Myc is involved in angiogenesis in tumors, it has been shown to activate the *mir-17-92* cluster which targets, and represses, the antiangiogenic factor *Tsp-1* [194, 199]. Another contributor to miRNA gene regulation is epigenetic status, for example, the miR-203 promoter is frequently found to undergo DNA methylation in T-cell lymphoma, but not in normal T lymphocytes [158, 200]. Another example includes the silencing of miR-127 by promoter hypermethylation in prostate and bladder cancers [193, 201].

The dysregulation of miRNAs in cancer makes them a potentially useful biomarker for cancer diagnostics, or a target for treatment [180]. There are some cases where altered expression of miRNAs have proven useful as a prognostic marker [180]. For example, a few studies have identified reduced let-7 expression in lung cancer patients, as well as high expression of miR-155, which both correlated with poor survival [191, 192, 202]. This identification of unique miRNA profiles in lung tumors implicates a relationship between miRNA expression and patient survival; therefore, monitoring miRNA expression profiles in cancer patients may have prognostic value [182, 192, 202]. Interestingly, one study which analyzed a few hundred normal and cancerous tissue samples found that the miRNA expression

profiles, or miRNome, was better at predicting the cancer type and stage than the mRNA expression profile, indicating the potential of the miRNome as a tool in cancer diagnosis and prognosis [186, 194]. Additionally, circulating miRNAs have been detected in the blood and serum, opening another avenue of use as a biomarker in cancer diagnosis [180, 203]. One of the first reports to evaluate serum levels of miRNA showed that miR-155 and miR-21 levels were higher in patient serum than control, and high levels of miR-21 were associated with relapse-free survival in patients with diffuse large B-cell lymphoma [180, 203]. This is not limited to the blood cancers - in prostate cancer patients, serum levels of miR-141 were found to distinguish them from healthy subjects [180, 204]. Another example of miRNA profiles that can be used as a cancer diagnostic is miR-196a and miR-217 in pancreatic ductal adenocarcinoma (PDAC) [194]. miR-196a has high expression in PDAC and low expression in normal tissues and chronic pancreatitis, while miR-217 exhibits an opposite pattern [194, 205]. Therefore, the ratio of miR-196a to miR-217 can be used to diagnose PDAC [194, 205]. Serum miRNAs have also been shown to be stable, resisting RNase digestion and degradation by freeze/thaw cycles, low/high pH, and boiling [206]. In addition, miRNAs have been found in other body fluids, most notably the urine [206]. This demonstrates the potential utility of miRNAs as biomarkers for diagnosis of cancer or other diseases [206].

miRNAs can function as either oncogenes or tumor suppressors, depending on the mRNAs they target [180]. This makes them targets for cancer therapy through either antisense-mediated inhibition of miRNAs acting as oncogenes or replacement of down-regulated miRNAs acting as tumor suppressors with miRNA mimetics [180]. Although, the evidence to date shows that the majority of miRNAs are down-regulated in tumor tissues, indicating that most miRNAs associated with cancer act as tumor suppressors [180, 186, 194]. This general downregulation of

miRNAs probably contributes to tumor formation by allowing for increased expression of oncogenic proteins [198]. A role for miRNA repression in cancers was further corroborated when a global depletion of miRNAs by knockdown of the miRNA-processing machinery was shown to stimulate tumorigenesis *in vivo* [194, 207]. This suggests that miRNA dysregulation is not simply a consequence of tumor formation, but that it may play an active role in cancer development [194, 207]. Since miRNAs may have multiple targets involved in various oncogenic pathways, targeting a single miRNA for treatment could affect multiple pathways [193]. Manipulation of miRNAs through overexpression or inhibition can be achieved in several ways. For overexpression, synthetic miRNA mimics can be made such as siRNA-like oligonucleotide duplexes and chemically modified oligoribonucleotides [194]. For inhibition, one can use modified antisense oligonucleotides such as 2'-*O*-methyl antisense oligonucleotides, locked nucleic acids, and antagomirs [180, 194]. Additionally, for miRNAs altered by epigenetic changes, the use of chromatin-modifying drugs may be a novel strategy for anticancer therapy [201]. Indeed, there are a few biotechnology companies focused on developing miRNA therapeutics, such as Regululs Therapeutics and Mirna Therapeutics. At Mirna Therapeutics they are focused on developing miRNA mimics for the treatment of cancer, with one product named MRX34 (a mimic of miR-34) in Phase I clinical trials for treatment of hepatocellular carcinoma and other solid tumors, as well as lymphoma and multiple myeloma (www.mirnarx.com). In pre-clinical development at Mirna Therapeutics are also miRNA mimics of miR-101, miR-215, miR-16, and let-7 (www.mirnarx.com). Regulus Therapeutics currently has two anti-miRNA therapeutics in clinical trials, one is an anti-miR-122 for HCV treatment in phase II clinical trial, and the other is an anti-miR-21 for treatment of Alport Syndrome, a type of kidney disease, in phase I clinical trial (www.regulusrx.com). Regulus also

has some anti-miRNA products in pre-clinical development, such as anti-miR-21 and anti-miR-221 for hepatocellular carcinoma, and anti-miR-103/107 for non-alcoholic steatohepatitis (NASH) in patients with type 2 diabetes (www.regulusrx.com).

4.2.3 Role of miRNAs in development and differentiation

miRNAs are now known to play an important role in posttranscriptional gene regulation of fundamental cellular processes, as well as pathological and physiological processes; this includes cell differentiation, organogenesis, cell signaling, disease development, carcinogenesis, immune response, and drug response [149, 182]. let-7, one of the first miRNAs discovered, is also probably one of the more well studied miRNAs, and is known to play an important role in development. In *C. elegans*, let-7 is required for the terminal differentiation of seam cells from the last larval stage to the adult stage [174, 191]. Seam cells are the lateral epidermal cells in *C. elegans*, and are well-studied because they mimic the self-renewal patterns stem cells go through [208]. In *C. elegans*, seam cells both proliferate to self-renew and divide to produce differentiated neural and epidermal cells, with the last of the seam cells terminally differentiating at the end of the last larval stage [208]. When let-7 is mutated, the seam cells fail to terminally differentiate and instead continue to divide, also a hallmark of cancer [174, 191]. In addition, let-7 exhibits very low expression in embryonic tissues and high expression in most all differentiated tissues [194]. Specifically, during differentiation, double-negative feedback control is often used by specific miRNAs as a genetic switch [158]. For example, the conserved loop between let-7 and LIN28 (a protein expressed in embryonic stem cells) – let-7 suppresses LIN28 protein synthesis and LIN28 in turn blocks *let-7* maturation [158, 209, 210]. LIN28 interferes with *let-7* maturation by binding to the loop structure of the *let-7* primary transcript

and blocking Drosha processing to the mature miRNA [209, 211, 212]. Additionally, LIN28 has been shown to induce uridylation of the pre-let-7, blocking Dicer processing to the mature miRNA [210]. Therefore, in embryonic stem cells (ESCs), LIN28 blocks generation of mature let-7 and helps maintain ES cells [213]. Upon differentiation, LIN28 is down-regulated allowing for an increase in mature let-7, which in turn further represses LIN28 [214]. Also, a double-negative feedback loop exists with the miR-200 family and the transcriptional repressors ZEB1 and ZEB2 in epithelial to mesenchymal transition (EMT) [158, 215]. Specifically, the miR-200 family and miR-205 are important in specifying the epithelial phenotype through inhibition of ZEB1 and ZEB2 [215, 216]. In EMT, epithelial cells are converted to mesenchymal cells; this process occurs during embryonic development and allows for tissue remodeling [215, 216]. EMT is also thought to be an important early step in tumor metastasis [215, 216].

A role for miRNAs in the development of animals, as well as plants, is suggested by the phenotypes of mutations in Dicer and Argonaute family genes [155]. For example, in *C. elegans*, reduced function mutations in *dcr-1* (Dicer) and *alg-1/alg-2* (Argonaute-like gene) result in improper processing of miRNA precursors and reduced mature miRNA expression [155, 217]. This results in developmental timing defects, causing the animals to continue stem cell like divisions and delay the switch to later-stage development [155, 217]. Additionally, use of RNAi to knockdown *dcr-1* results in a mixed phenotype, including embryonic lethality and the observed developmental timing defects [187, 217]. The role of miRNAs in development has been investigated in the fruitfly, zebrafish and mammals as well. For example, in a model of *D. melanogaster* mutants lacking *dcr-1* in germline stem cells, the miRNA pathway is shown to be important for stem cell division and to bypass the normal G1/S phase checkpoint (allowing the stem cells to continue dividing rather than stopping the cell cycle) [182, 218]. In the mouse,

homozygous *Dicer1* null mutants die at an early developmental stage, with the mutant embryos having defects in axis formation and gastrulation, as well as lacking OCT4-positive stem cells [182, 187, 219]. Additionally, conditional inactivation of *Dicer1* in mouse embryonic stem cell lines results in proliferation defects and severe defects in differentiation, both *in vitro* and *in vivo* [182, 220, 221]. Of course, the effects seen in *Dicer* mutants may not be solely due to the loss of miRNA processing, as *Dicer* has other roles as well, but does imply a role of miRNAs in normal development processes [187]. To elucidate the specific role of miRNA in these developmental defects, knockdown of miRNAs to perform loss-of-function analysis has been done in the fruitfly, *D. melanogaster*, with antisense oligonucleotides [187, 222]. In this study, antisense oligonucleotides were injected into *D. melanogaster* embryos complementary to the 46 miRNAs known to be expressed in the first half of embryogenesis [187, 222]. They observed that knocking down 25 of the 46 embryonically expressed miRNAs resulted in abnormal defects, including defects in blastoderm cellularization and patterning, morphogenesis, cell survival, and an increase in programmed cell death, demonstrating that miRNAs are specific and essential regulators of a wide range of developmental processes [187, 222].

In ESCs, miRNAs play an important role in maintaining pluripotency, proliferation, cell differentiation, and lineage specification [213, 214, 223, 224]. In fact, the expression of miRNAs seems to be regulated in a temporal manner in differentiating human ESCs (hESCs), with miRNAs regulating lineage specification for the three germ layers – ectoderm, mesoderm, and endoderm [214, 223, 224]. In order to maintain pluripotency in ESCs, differentiation and developmental genes must be silenced, but also ready to be swiftly activated upon the appropriate signals [214]. Conversely, once the appropriate signals for differentiation are received, pluripotency genes need to be rapidly silenced while the differentiation genes are

activated [214]. miRNAs can act to support this fluid environment by suppressing genes involved in the pluripotency and differentiation processes [214]. One of the first studies to examine miRNA profiles in undifferentiated and differentiated mouse ESCs identified a set of miRNAs that seemed to be specific to undifferentiated ESCs, including miR-290, miR-291-as, miR-292-as, miR-293, miR-294, and miR-295, collectively part of the miR-290-295 cluster [171]. To investigate the role of miRNAs in ESC proliferation, one group utilized mouse *Dgcr8* knockout ESCs (a model in which cells lack normal Drosha activity and mature miRNA expression, resulting in slow cell proliferation and cell accumulation in the G1 phase of the cell cycle) and transfected them with miRNA mimics, where they found a set of miRNAs that could rescue the defect in proliferation, calling them ES cell specific cell cycle (ESCC)-regulating miRNAs [214, 225]. Some of the miRNAs identified as ESCC-regulating miRNAs include miRNAs in the miR-302/367 cluster and the miR-290-295 cluster [214, 225]. The miR-302/367 cluster contains at least five mature miRNAs, and is highly expressed in mouse and human ESCs, while being downregulated during differentiation [214, 226-228]. In addition, the transcription factors OCT4, SOX2 and Nanog (known as pluripotency markers) bind to the promoter region of the miR-302/367 cluster, suggesting they are activated to help maintain pluripotency in ESCs [214, 229]. Specifically, miR-302a represses cyclin D1, a G1 phase regulator, contributing to miRNA regulation of the cell cycle in ESCs, allowing for a shortened G1 phase and proliferation [229]. Moreover, ectopic expression of the miR-302/367 cluster in combination with valproic acid was found to be sufficient to reprogram mouse and human somatic cells to iPSCs [214, 230]. The miR-290-295 cluster produces at least 14 mature miRNAs, and is expressed in mice but not in humans [214]. As discussed earlier, this cluster accounts for the majority of miRNAs expressed in mESCs, and is downregulated during

differentiation [171, 214, 231]. As with the miR-302/367 cluster, the transcription factors OCT4, SOX2, and Nanog, have also been shown to bind to the promoter region of the miR-290-295 cluster [213, 231]. The miR-371-373 cluster is the human homolog of the mouse miR-290-295 cluster; it produces three mature miRNAs that are highly expressed in hESCs and are downregulated during differentiation [214]. Another miRNA cluster found to be enriched in hESCs and iPSCs is the miR-17-92 cluster, which is also a pro-tumorigenic miRNA cluster activated by c-myc [213, 232, 233].

From this work it is now clear that ESCs express a distinct set of miRNAs that may be important regulators in the maintenance of pluripotency and in mammalian embryonic development [171, 227]. Numerous studies have further identified miRNAs expressed in undifferentiated ESCs compared to differentiated cells. The most predominant miRNAs found in undifferentiated hESCs include the clusters mentioned above, the miR-302/367 cluster, the miR-371-373 cluster, and the miR-17-92 cluster, and are known as ESC-enriched miRNAs [214, 225-229, 233-237]. Other analyses of undifferentiated hESCs compared to differentiated cells have also identified the miR-106a, miR-450 clusters and members of the miR-515 and miR-506 families as being predominant in undifferentiated cells [235, 236]. Sequencing analyses have also identified some miRNAs outside of the main families in undifferentiated ESCs compared to differentiated cells, including miRs-200c, -368, -154*, -301, -101, -141, -148a, -374, -135a, -187, -324-3p, -766, -21, -29a, -29c, -143, -222, -296, -494, -25, -184, -221, -320, -340, -423, -594, -744 [226-228, 234, 236]. These may represent other miRNAs apart from the main clusters involved in maintaining pluripotency in hESCs [226].

In addition to miRNAs that maintain and regulate pluripotency, there are miRNAs that assist in cell differentiation. Among the first miRNAs identified as being significantly

upregulated following induction of differentiation are miR-21 and miR-22, suggesting a role in cell differentiation [171, 236, 238]. Other miRNAs expressed in differentiated cells include miRs-134, -296, and -470 [238-241]. This set of miRNAs have been found to target and suppress the pluripotency factors OCT4, SOX2, and Nanog, thereby promoting differentiation [238-241]. There is also evidence that miR-134 specifically enhances differentiation toward ectodermal lineages in mESCs [241]. miR-34 is another miRNA that has been shown to target SOX2 and Nanog, as well as n-myc, contributing to cell differentiation [214, 242]. Additionally, miR-145 acts to induce differentiation by suppressing pluripotency factors OCT4, SOX2, and KLF4, and in another feedback loop, OCT4 represses miR-145 expression in hESCs [213, 236, 239, 243]. miR-125 and miR-9 are also up-regulated during differentiation of hESCs [214]. miR-125 is the homolog of lin-4, ectopic expression of miR-125 in mESCs results in a loss of pluripotency factors [214, 244]. miR-9 has also been reported to target the pluripotency marker LIN28 [214, 245]. Also, as discussed above, let-7 is highly expressed in most differentiated tissues and plays an important role in cell differentiation, through targeting of LIN28 [158, 194, 209, 214]. In summary, miRNAs regulate differentiation, with some miRNAs maintaining pluripotency and others driving cell fate decisions [214].

4.2.3.1 miRNAs in cardiac development

Many miRNAs appear to be tissue specific – this strongly implicates miRNAs as a potential important factor to influence *in vitro* differentiation [179]. As with pluripotency in embryonic stem cells and early cell differentiation of the embryonic germ layers, miRNAs have also been shown to influence cell fates in later stages of development [213, 214, 227, 234]. Some miRNAs appear to be very tissue specific in their expression, suggesting a role in tissue

specification and cell lineage decisions [170]. Indeed, one study found that in tissues such as the heart, liver, and brain, a single, tissue-specific miRNA dominates the miRNA pool [170]. In this study examining tissue specific miRNA expression in the mouse, miR-1 was found to be the predominant miRNA in the heart, accounting for 45% of all miRNAs expressed in the heart [154, 170]. miRNAs have been shown to have an important role in cardiac differentiation and maintenance of muscle gene expression *in vivo* in species as diverse as *D. melanogaster* and mice [224, 246-248]. In a study examining mesoderm formation in both mouse and human ESCs, miR-1 and miR-133 were found to promote mesoderm formation, but then had opposing functions in further differentiation to cardiac muscle progenitor cells, with miR-1 promoting differentiation of both cardiac and skeletal progenitors, while miR-133 did not enhance further differentiation [224]. During differentiation, miR-1 and miR-133 both acted as potent repressors of non-muscle gene expression and cell fate [224]. miR-1 has been shown to promote differentiation of cardiac progenitor cells, while miR-133 has been shown to inhibit differentiation of skeletal myoblasts maintaining them in a proliferative state [224, 246-249]. Additionally, ectopic expression of either miR-1 or miR-133 caused enhanced expression of mesoderm genes in embryoid bodies, while suppressing ectoderm and endoderm lineages [224]. Ivey et al. also identified the Notch ligand *Delta-like 1* (DIL-1) as a target of miR-1 in mouse and human ESCs, with miR-1 promoting differentiation to cardiac and skeletal muscle fates [224]. Additionally, in *Drosophila*, miR-1 was shown to target the Notch ligand *delta* [246]. Notch signaling promotes neural differentiation while inhibiting muscle differentiation, therefore knockdown of Notch signaling by miR-1 may promote muscle development *in vivo* [224, 246, 250, 251]. miR-1 has also been found to target histone deacetylase 4 (HDAC4), which in turn up-regulates myocyte enhancer factor 2C (MEF2C), an important muscle-related transcription

factor that promotes myogenesis [238, 249]. Anderson et al. identified miR-1 and miR-206, which is expressed specifically in skeletal muscle, as promoters of myogenesis through targeting of connexin 43 (CX43), which is essential for normal skeletal muscle differentiation [238, 252, 253]. Another miRNA involved in skeletal muscle differentiation is miR-26a [238, 254, 255]. miR-26a works indirectly by targeting the histone methyltransferase enhancer of zeste homologue 2 (EZH2), which normally suppresses skeletal muscle differentiation [238, 254, 255]. Overall, miR-1 has a role in fine-tuning cardiac regulatory proteins to balance differentiation and proliferation during cardiogenesis [246, 247].

4.2.3.2 miRNAs in neuronal development

In the work done by Lagos-Quintana et al., discussed above, the authors examined tissue specific expression of miRNAs in the mouse, including cortex, cerebellum, and midbrain to try and understand miRNA distribution in neural tissue [170]. The authors identified miR-124 as the dominant miRNA in brain tissue, accounting for 25% of all miRNAs expressed in the midbrain, 44% of all miRNAs expressed in the cortex, and 48% of all miRNAs expressed in the cerebellum [170]. They also identified miRs-101, -127, -128, -131, and -132 as being predominantly expressed in brain tissues [170]. To further understand expression patterns of miRNAs in brain development, Krichevsky et al. utilized an oligonucleotide array to examine expression of miRNAs in mouse and rat cortical neurons during development [256]. From this study they identified some distinct expression patterns during cortical neurogenesis, including postnatal expression of miR-128, prenatal expression of miR-19b, increasing expression during embryonic development followed by stable expression postnatal of miR-124a and miR-266, and peak expression at embryonic day (E) 21 for miR-9, -125b, -131, and -178 [256]. Furthermore,

the authors examined these miRNAs in presenilin-1 null mice, a model for severe brain developmental defects, and found that expression of miR-9 and miR-131 was significantly reduced in the forebrains of these knockout mice compared to their heterozygous littermates, indicating their potential role in regulating normal brain development [256]. Further studies of neuronal stem cells, neurons and astrocytes have identified miR-124 and miR-128 as being specifically expressed in neurons, miR-23 specific to astrocytes, miR-26 and miR-29 preferentially expressed in astrocytes, and miR-9 and miR-125 being evenly expressed in both neurons and astrocytes [238, 257]. Additionally, overexpression of miR-124 and miR-9 in neural progenitor cells enhanced neurogenesis [238, 258]. miR-124 has been shown to target the small carboxy-terminal domain phosphatase 1 (SCP1), which normally prevents expression of neural genes in non-neural tissues, therefore, inhibition of SCP1 by miR-124 allows for expression of neural genes and induces neurogenesis [238, 259, 260]. Conversely to the tissue specific miRNAs, there are some miRNAs that have been found to be fairly ubiquitous in their expression. For example, the let-7 family of miRNAs are expressed in most all somatic tissues, as well as miR-16, -26a, -27a, and -143a [151]. Interestingly, miR-21 is also fairly ubiquitous in its expression, with the exception of neuronal tissue [151]. Expression of the brain-specific miR-124 in combination with the absence of miR-21 may determine neuronal cell specification [151].

4.2.4 Hepatocyte development and miRNAs

In the Lagos-Quintana study examining tissue specific expression of miRNAs in the mouse, miR-122 was found to be the predominant miRNA in the liver, accounting for 72% of all miRNAs expressed, and was undetectable in all the other tissues analyzed [170]. Hepatocytes are derived from the endoderm lineage; a study examining miRNAs in hESCs differentiated to

definitive endoderm cells identified a distinct miRNA profile for definitive endoderm [223]. In this study, Hinton et al. utilized 2 hESC lines and identified a set of 17 miRNAs that were up-regulated in definitive endoderm cells compared to hESCs and 37 miRNAs that were down-regulated [223]. Specifically, the 17 miRNAs that are up-regulated may have a role in commitment to endoderm-derived cell lineages, such as hepatocytes [223]. The miRNA that was the most highly up-regulated in definitive endoderm cells was miR-375, with miRs-708, -653, -373, -372, and -371-5p accounting for other highly expressed miRNAs [223]. While the miR-371-373 cluster is highly expressed in hESCs, it did maintain expression in definitive endoderm cells, and this seems to be unique to the endoderm cells as it was found to decrease in ectodermal cells [223]. Other studies examining miRNA profiles in definitive endoderm cells have identified miR-375, miR-122, miR-24, miR-10a, and members of the let-7 family as being up-regulated in endoderm cells [235, 261]. A study by Kim et al. identified 13 miRNAs that were down-regulated in definitive endoderm cells compared to hESCs, and 56 miRNAs that were up-regulated [262]. miRNAs upregulated in definitive endoderm cells compared to hESCs include miRs-326, -181a, -30a*, -532-3p, -23b, -125a-5p, -218, 27b, and -30a, with miR-9*, miR-205 and miR-375 as being highly enriched in definitive endoderm cells [262]. Kim et al. also observed expression of members of the miR-371-373 and miR-302/367 clusters in definitive endoderm cells, that were down-regulated upon further differentiation to hepatocytes [262]. As discussed above, miR-205 is known to regulate EMT through inhibition of ZEB1/2 [215, 216]. Since EMT is an important part of embryonic development, enrichment of miR-205 in definitive endoderm cells indicates EMT may play an important role in endoderm formation and hepatocyte differentiation [158, 215, 216, 262]. In the study by Kim et al., they identified 30 miRNAs down-regulated in hepatocytes compared to definitive endoderm and 92 miRNAs up-

regulated in hepatocytes [262]. Among the miRNAs up-regulated in hepatocytes, miR-122, miR-10a, miR-21, and miR-214 were found to be enriched in hepatocytes [262]. Other miRNAs found to be highly expressed in stem cell derived hepatocytes include miRs-21, -214, -216a, -137, -143, -152, -24-1, -10b, and members of the miR-30 family [262]. Chen et al. examined miRNA profiles during differentiation of rat liver-derived progenitor cells (LDPCs) to mature hepatocytes and found a large degree of overlap in miRNA expression between the two cell types, including two miRNAs expressed in human fetal livers, miR-21 and miR-26a, indicating that these LDPCs are already committed toward a hepatocyte fate [263, 264]. Some miRNAs Chen et al. found to be higher in LDPCs include miRs-23a, -23b, -130b, -690, -691, and -467a/b, while miRNAs found to be higher in differentiated hepatocytes include miRs-122, -101, -142-5p, 146a/b, -125b, -352, and let-7c/d [263]. Further work examining miRNA profiles in human embryonic (gestational age 7-10 weeks) and adult liver tissues also identified a unique miRNA expression profile between these stages of development [265]. In this set of livers, the authors identified miRs-122, -192, and -194 as being highly expressed in both embryonic and adult livers [265]. They also identified a set of miRNAs with higher expression in embryonic liver compared to adult, the top 15% of these miRNAs included miRs-18a, -409-3p, -451, -483-3p, and -92a – which overlap with another study of miRNAs expressed in fetal liver [264, 265]. Additionally, the investigators identified a set of miRNAs with higher expression in adult liver compared to embryonic liver, whose top 15% included miRs-125b, -192, -22, -23b, -99a and let-7a/b/c [265]. However, in this set, miRs-125b and -22 were identified as being expressed in a separate study examining fetal liver, indicating that they may be expressed at a later stage of fetal development than what was examined in this study or they may be expressed in both fetal and adult liver, similar to miR-122 [264, 265]. While each of these studies displays differences in

the miRNA profiles identified in each cell type, there are select miRNAs that repeatedly show up, such as miR-375 and the 371/373 cluster in definitive endoderm cells and miR-122, 23b, 125b and the let-7 family in differentiated rat hepatocytes, human SCDHs, and liver tissue [170, 223, 235, 261-265]. Overall, these studies further support the notion that select miRNAs function in a lineage-specific manner during differentiation, and there may be a set of miRNAs specific for hepatocyte differentiation [262].

miR-122 is known to be a liver-specific miRNA. It is reasonable to assume that expression of miR-122 in hESCs may induce differentiation towards liver lineages, such as hepatocytes, or may help in maturation of stem cell derived hepatocytes. In one study by Tzur et al., lentiviral transduction was used to express miR-122 in a hESC line, which was then allowed to spontaneously differentiate [261]. In these miR-122 transduced hESCs, expression of miR-122 did not drive the cells towards an endodermal or hepatic fate, rather it slowed differentiation and induced pluripotency markers such as OCT4, SOX2 and NANOG compared to control cells [261]. Some possible explanations for this result put forward by Tzur et al. are that some important targets of miR-122 may not yet be expressed in hESCs; the expression level of miR-122 in hESC may not reflect physiologic levels; or miR-122 requires additional miRNAs or proteins in concert to promote differentiation [261]. This study also indicates that perhaps timing of miR-122 expression during differentiation is important, i.e. once the cells have committed towards endodermal pathways, which would coincide with their explanation that certain targets of miR-122 are not expressed in hESCs. A second group utilizing miR-122 transfection of human fetal liver stem/progenitor cells was able to enhance expression of hepatocyte genes and liver-enriched transcription factors [266]. In this study, Doddapaneni et al. examined expression of hepatocyte markers AFP, ALB, HNF4α, and C/EBPα and saw an

increase in all four markers in hepatic cells differentiated from fetal liver progenitor cells transfected with miR-122 compared to control [266]. Specifically, at day 21 post transfection they observed a 20-fold increase in AFP expression, 31-fold increase in ALB expression, 6.9-fold increase in HNF4α expression, and a 5.5-fold increase in C/EBPα expression compared to control cells [266]. In the Doddapaneni et al. study the protocol used cells that were already committed towards a hepatic fate as opposed to hESCs as in the Tzur et al. study; this may be why they see a positive effect on select hepatocyte markers with miR-122 transfection.

A now well-studied activity of miR-122 is to aid in viral replication of Hepatitis C – an RNA virus that replicates primarily in the liver [168, 169]. miR-122 interacts with Hepatitis C by binding to the 5'-UTR of the viral genome, stimulating viral translation [168, 169]. When miR-122 is inactivated, HCV translation is strongly reduced, with levels of viral replicon reduced as much as 80% [168, 169]. Conversely, when miR-122 is introduced to liver and non-liver cell lines, HCV translation is stimulated [168]. The binding site for miR-122 is highly conserved among all six HCV genotypes [169]. Targeting miR-122 for inactivation may provide a therapeutic option that would combat all HCV genotypes [169]. Because of this, the first miRNA therapeutic to reach clinical trial was developed to target miR-122 for treatment of HCV [267]. This therapeutic is named Miravirsen (SPC3649) under development by Santaris Pharma, in late 2014 Santaris Pharma was acquired by Roche [267, 268]. Miravirsen is a mixed locked nucleic acid (LNA)/DNA phosphorothioated sequence complementary to miR-122 [268]. The LNA technology allows for high affinity to the target miRNA and provides resistance to nuclease degradation, allowing for greater stability. Miravirsen has a terminal half-life of about 20 days [269]. The first *in vivo* studies of miR-122 inhibition were conducted in mice. One study utilized cholesterol-conjugated 2'-*O*-methylated antisense oligonucleotides, which they termed

'antagomirs' [267, 270]. In this study Krutzfeldt et al. administered single 80 mg/kg doses of miR-122 antagomir (for 1, 2, or 4 days) intravenously to mice and observed a marked decrease in endogenous miR-122 levels, along with upregulation of predicted miR-122 target genes, such as aldolase-A (*Aldoa*), IQ-motif-containing GTPase-activating protein 1 (*Iqgap1*), and a number of genes involved in cholesterol biosynthesis [267, 270]. Shortly after, a second study was published in which Esau et al. used a 2'-*O*-methoxyethyl phosphorothioate antisense oligonucelotide, and reported similar results of miR-122 knockdown [267, 271]. In this study mice were dosed with a miR-122 antisense oligonucleotide ranging from 12.5 to 75 mg/kg intraperitoneally twice a week for four weeks [271]. There were no overt toxic effects on the mice, with the exception of a mild increase in plasma ALT and AST levels at the 75 mg/kg dose [271]. Based on these preliminary studies, five target mRNAs (GYS1, ALDOA, CCNG1, P4HA1, SLC7A1) of miR-122 were selected for monitoring, with four of the five target mRNAs increasing in expression following miR-122 knockdown, and miR-122 levels were reduced up to 10-fold at the highest dose [271]. In addition to the aforementioned effects, there was also a 26-28% reduction in plasma levels of total cholesterol across all doses of miR-122 antisense oligonucleotide tested [271].

Preclinical studies in African green monkeys utilizing SPC3649 also demonstrated the cholesterol lowering effect of miR-122 knockdown [267, 272]. In this study three I.V. injections ranging from 1 to 10 mg/kg were administered over 5 days, resulting in a 30-40% reduction in total cholesterol, which was dose-dependent and prolonged, slowly returning to baseline over three months, making plasma cholesterol a potential biomarker for miR-122 knockdown when evaluating SPC3649 in HCV infected patients [267, 272]. No acute or sub-chronic toxicities were observed, as determined by normal measurements for all clinical chemistries monitored, no

change in blood coagulation profiles, and normal histopathology on liver biopsies [272]. However, the reduction in cholesterol does affect both LDL and HDL levels, and in the animal models has a more pronounced lowering of HDL – the 'good' cholesterol - at higher dosages [267]. Studies of SPC3649 in chimpanzees chronically infected with HCV showed a maximal decrease of 2.6 orders of magnitude in serum HCV RNA levels and 2.3 orders of magnitude in liver HCV RNA levels at the high dose - 5 mg/kg once a week over 12 weeks [267, 269]. In the chimpanzee model there was also a 30-40% reduction of total cholesterol, and no adverse side effects [267, 269]. In a phase 2a clinical study, Miravirsen was found to reduce HCV RNA levels at all studied doses, with no dose-limiting adverse effects and no escape mutations in the HCV miR-122 binding sites [273]. In this study, 36 patients received a weekly subcutaneous injection at 3, 5, or 7 mg/kg for 5 weeks, or a placebo [273]. HCV RNA levels were reduced by 1.2, 2.9, and 3.0 $\log_{10}$ IU per milliliter from baseline in the 3, 5 and 7 mg/kg dose groups, respectively [273]. In addition, there was a decrease in serum total cholesterol during this study, with no change in the ratio of LDL to HDL [273].

Santaris is not the only pharmaceutical company exploring miR-122 as a therapeutic target. A competitor to Miravirsen is in development by Regulus Therapeutics. Regulus has developed a GalNAC-conjugated anti-miR targeting miR-122 for the treatment of HCV, known as RG-101, currently in phase II clinical trials (www.regulusrx.com). In a phase I study, HCV patients received a single subcutaneous dose of either 2 mg/kg or 4 mg/kg of RG-101, and 29 days following dosing an average of 4.1-log and 4.8-log reduction in patient viral loads was observed for the 2 mg/kg and 4 mg/kg doses, respectively (www.regulusrx.com). Phase I studies of RG-101 revealed no serious adverse events or discontinuations in HCV patients (www.regulusrx.com). While antisense targeting of miR-122 so far seems to be a viable

therapeutic option for treatment of HCV, there are still some concerns, such as the effect on lipid metabolism, including reductions in HDL levels, and risk of developing hepatocellular carcinoma [267].

4.2.4.1 miRNA regulation of ADME genes

miRNAs are expressed in a tissue specific manner and have been shown to regulate most cellular and physiologic processes, and their role may extend to regulation of ADME-related genes [150]. Current knowledge regarding miRNA regulation of drug metabolizing enzymes and other ADME genes is extensively summarized in two related reviews by Yokoi and Nakajima [149, 150]. The first study to demonstrate miRNAs could regulate CYP enzymes was reported for human CYP1B1 in 2006 [150, 274]. In this study, miR-27b was found to regulate CYP1B1 in a breast cancer cell line, MCF-7 [150, 274]. When further examining tissue from a small group of breast cancer patients, miR-27b was found to be decreased and CYP1B1 protein levels increased in cancerous tissue compared to noncancerous tissue [149, 274]. The most abundant hepatic CYP, CYP3A4, has been found to be indirectly regulated by miRNAs through PXR - miR-148a has been shown to regulate PXR, which in turn regulates CYP3A4 mRNA [149, 150, 275]. There is some evidence indicating CYP3A4 may also be directly regulated by miR-27b [149, 276]. miR-27b is also reported to regulate PPARα, PPARγ, and RXRα [149, 179, 277-280]. miR-27b seems to regulate a number of transcription factors as well as CYP1B1, indicating it may be a particularly important miRNA in terms of drug response and toxicity [150]. Additionally, PPARα has been shown to be regulated by miR-21, HNF4α by miR-24 and miR-34a, CYP2E1 by miR-378, and CYP2C19 by miR-29a-3p [149, 277, 281-284]. In a study by Rieger et al. on select miRNAs with predicted binding sites in ADME genes, they identified a

number of correlations between miRNAs and CYP gene expression utilizing a liver bank [179]. This included a negative effect on protein or activity level for CYP1A1 by miRs-132, -142-3p, -21; CYP2A6 by miR-142-3p and miR-21; CYP2C19 by miRs-130b, -185, -34a; and CYP2E1 by miR-10a, miR-200c and let-7g [179].

Some studies evaluating the role of miRNAs in toxicology, or utility as biomarkers for toxicological response, have been conducted. One such study observed a change in miRNA expression profiles in the liver of rats given a single toxic dose of acetaminophen or carbon tetrachloride [150, 285]. In this study a microRNA microarray was utilized to assess changes in miRNA expression, but focused on miR-298 and miR-370 because these specific miRNAs are predicted to bind to target genes involved in oxidative stress [285]. Notably in this study, the down regulation of miR-298 and miR-370 occurred as early as 6 hours post-administration, correlating with early phase toxicity [150, 285]. While only a few animals were utilized in the experiment, it provides some evidence that miRNAs may be involved in toxicological outcomes, and also that monitoring of miRNAs may be a useful biomarker for toxicity [285]. For example, a separate study in which mice were dosed with acetaminophen to induce liver injury showed a number of miRNAs that were up-regulated in plasma, particularly liver-enriched miRNAs miR-122 and miR-192 [286]. Additionally, miR-122 and miR-192 levels in the plasma exhibited dose and exposure dependent changes in expression that paralleled serum aminotransferase changes and histopathological changes, but were detected significantly earlier [150, 286]. An additional study also corroborated the finding that miR-122 levels in the plasma increased in patients and mice with hepatic disease, and the change occurred earlier than changes in aminotransferase levels [149, 287]. These changes in miRNA profiles that can be monitored in plasma provide a potential biomarker for drug-induced liver injury, and may be superior to current biomarkers

such as the serum aminotransferases, ALT and AST [149, 286, 287]. Conversely, it's been shown that 2,3,7,8-tetrachlorodibenzo-*p*-dioxin (TCDD) administration to rats and mice does not cause any significant change in hepatic miRNA profiles, indicating miRNAs are unlikely to play a role in TCDD toxicity in rodent liver [150, 288]. This demonstrates the potential role of miRNAs in toxicity outcomes may be substrate dependent. Overall, there is evidence that miRNAs may play an important role in regulating drug-metabolizing enzymes and other ADME genes, but more work is needed in this area to understand potential contributions of miRNA to drug response and pharmacokinetics.

As noted above, miRNAs regulate many genes, similar to transcription factors, and therefore are potential modifiers of cellular process such as differentiation [224, 289]. Since miRNAs have been shown to be expressed in a tissue and developmental stage specific manner, with liver specific miRNAs such as miR-122 identified, we postulate that miRNA profiling of our hESCs throughout the differentiation process may provide insight into the lack of functional maturity observed in our hESC-derived hepatocytes [170, 171, 227]. To test this hypothesis, we performed miRNA microarray analyses on hESCs and iPSCs, SCDHs at each stage of our differentiation protocol, cryopreserved hepatocytes, and a set of human livers from the University of Washington liver bank. This set of microarray results provided information on the potential role of miRNAs in liver differentiation and maturation, and the specific miRNAs that could be manipulated during *in vitro* hepatocyte differentiation to enhance maturation of the cells.

4.3 Materials and Methods

4.3.1 Cell culture and hepatocyte differentiation

Cryopreserve hepatocyte lots HU8110 and HU8114 were purchased from Invitrogen (Carlsbad, CA) and cultured according to manufacturer's instructions. Briefly, cells were thawed in CHRM® media and plated in Williams Medium E supplemented with Hepatocyte Plating Supplement Pack from Invitrogen on 24-well plates coated with Collagen I. Following a 6-hour incubation period to allow for cell attachment, the media was changed to Williams Medium E supplemented with Hepatocyte Maintenance Supplement Pack from Invitrogen. Cells were maintained in this hepatocyte maintenance media for 4 days with daily fluid changes. Cells were then collected in TRIzol Reagent (Invitrogen) and sent to the University of Washington Center for Ecogenetics and Environmental Health (CEEH) Functional Genomics and Proteomics Facility Core for RNA extraction and processing. A set of hepatocytes from lot HU8114 were cultured in a sandwich configuration – following cell attachment in hepatocyte plating media, the media was changed to ice cold hepatocyte maintenance media containing 0.35 mg/mL Geltrex® LDEV-Free Reduced Growth Factor Basement Membrane (Invitrogen). The following day, Day 1, hepatocytes were incubated in hepatocyte maintenance media containing 10% of one of the following serum conditions obtained from Dr. Catherine Yeung (University of Washington, Department of Pharmacy and Kidney Research Institute): control human serum, control ultrafiltrate, uremic serum, or uremic ultrafiltrate. Cells were incubated in these conditions for 72 hours, with daily fluid changes and on Day 4 were collected in TRIzol Reagent and sent to the University of Washington CEEH for RNA extraction and processing.

The hESC lines H1 (WA01) and H9 (WA09) were obtained from WiCell® Research Institute (Madison, WI) and propagated at the University of Washington Institute for Stem Cell and Regenerative Medicine. All studies were conducted under approval of the University of

Washington Embryonic Stem Cell Research Oversight Committee. hESC lines H1 and H9 were cultured on mouse embryonic fibroblasts (MEFs) before being transferred to Matrigel™ (BD Biosciences, San Diego, CA)-coated plates using mTeSR™1 media (Stem Cell Technologies, Vancouver, Canada). Hepatocyte differentiation was induced in three stages, as published by Hay et al. [84, 86]. Briefly, differentiation was initiated at 60-70% confluence by replacing the mTeSR™1 media with priming medium: RPMI 1640 containing 1xB27 (Invitrogen), 100 ng/mL Activin A (PeproTech, Rocky Hill, NJ), and 50 ng/mL Wnt3a (R&D Systems, Minneapolis, MN). After 72 hours, with daily media changes, the cells were switched to differentiation medium: Knockout-DMEM containing 20% Knockout Serum Replacement, 1 mM glutamine, 1% nonessential amino acids, 0.1 mM β-mercaptoethanol (Invitrogen), and 1% dimethyl sulfoxide (DMSO) (Sigma, St Louis, MO) for a further 5 days. Lastly, the cells were switched to maturation media: Hepatozyme (Invitrogen) containing 10 μM hydrocortisone 21-hemisuccinate, 2 mM glutamine, 10 ng/mL hepatocyte growth factor and 20 ng/mL oncostatin M (R&D Systems). The media was changed every other day during maturation until day 17. Cells were collected in TRIzol reagent prior to differentiation (Day 0) and at the end of differentiation on Day 17 and sent to the University of Washington CEEH for RNA extraction and processing. In addition, samples from hESC line H9 and an induced pluripotent stem cell (iPSC) line undergoing the same differentiation conditions were obtained from Dr. David Hay's lab (MRC Centre for Regenerative Medicine, University of Edinburgh). They provided samples at each stage of differentiation -- Days 0, 3, 10, and 18 for hESC line H9 and Days 0, 5, 9, and 14 for iPSCs in TRIzol reagent, also sent to the University of Washington CEEH for RNA extraction and processing.

4.3.2 microRNA microarray

TRIzol samples from cryopreserved hepatocyte lots HU8110 and HU8114, along with hESC, iPSC, and human liver tissue samples from the University of Washington School of Pharmacy Human Liver Bank (Seattle, WA) were processed by the University of Washington CEEH to collect miRNA. A subset of the liver bank was selected based on tissue availability and was composed of tissue samples from 59 individuals, including male donors and female donors with an age range of 7 – 70 years. Liver bank samples were analyzed using the Affymetrix GeneChip® miRNA 2.0 array according to manufacturer's recommendations. Cryopreserved hepatocyte lots HU8110 and HU8114 along with hESC and iPSC samples were analyzed using the Affymetrix GeneChip® miRNA 3.0 array according to manufacturer's recommendations. Only human miRNAs were used for data analyses.

4.3.3 Real-time quantitative polymerase chain reaction (qRT-PCR)

Taqman® microRNA assays (Invitrogen) were used to quantify expression of miR-122, let-7i, and let-7c according to the manufacturer's instructions. Complementary DNA (cDNA) was synthesized using 5 ng of total RNA and the Taqman® microRNA Reverse Transcription kit in 15 μL total volume (Invitrogen). Real-time quantitative polymerase chain reaction (qRT-PCR) was then carried out using the Taqman® microRNA assays (Invitrogen) with 18S as a housekeeping gene. Relative quantification was calculated using the $\Delta\Delta C_T$ method with 18S as the endogenous control.

4.3.4 Let-7 transfections

Viral transduction of H9 stem cell derived hepatocytes was conducted at day 7 of differentiation. Cells were transduced with either pLKO-let7i or pLKO-dsred (gifts from Dr. Hannele Ruohola-Baker, University of Washington) as a fluorescent control using 4 μg/mL polybrene. Briefly, a 0.5 mL mix of virus, polybrene and differentiation media was added to appropriate wells of cells on a 24-well plate. Plates were then centrifuged at 3000 rpm for 1 hour at 37 °C. Following the spin, an additional 0.5 mL of differentiation media was added to each well and plates were placed in the incubator for overnight. The following day, viral media was removed and replaced with regular maturation media. On day 13 of differentiation (day 6 following transduction), transduced cells were collected in TRIzol reagent for RNA extraction.

Transfection of H9 stem cell derived hepatocytes was conducted at day 8 of differentiation. Cells were transfected with a let-7c mimic (miRIDIAN microRNA Human has-let-7c-5p mimic) or a control mimic (mimic transfection control with Dy547) (Dharmacon, Lafayette, CO). For transfection, dilutions of Lipofectamine® RNAiMAX (Invitrogen) in Opti-MEM® media (Invitrogen), let-7c mimic in Opti-MEM® media, and control mimic in Opti-MEM® media were made. The Lipofectamine® mix was then mixed with either the let-7c mix or the control mimic mix at a 1:1 ratio and incubated at room temperature for 20 minutes. The let-7c mimic and control mimic solutions were then diluted 10x with differentiation media and 0.5 mL was aliquoted to appropriate wells on 24-well plates and incubated for 5 hours or overnight. Following incubation, transfection media is aspirated and replaced with differentiation media or maturation media. On day 12 of differentiation (day 4 following transfection), cells were collected in TRIzol reagent for RNA extraction.

4.3.5 Statistical analysis

All statistical analyses were performed using R software (www.r-project.org) and Bioconductor (www.bioconductor.org) by the University of Washington CEEH. To be included in analysis, each miRNA was required to have a $\log_2$ expression value > 7 in at least 3 samples. A weighted analysis of variance model (ANOVA) was then fit to the data and empirical Bayes adjusted contrasts were calculated for comparisons with replicates for at least one sample type. For comparisons between samples with no replicates, the miRNAs were required to have an absolute fold change ≥ 2, and the requirement that one of the two samples had to have a $\log_2$ expression value > 7. For comparisons where multiple samples were grouped together, i.e. all the differentiated cells versus all cryopreserved cells, the model was re-parameterized to combine the groups, and then the comparison was made. For comparisons, probesets (miRNAs) were selected at a false discovery rate (FDR) adjusted *p*-value < 0.05 and an absolute fold change ≥ 2, except for comparisons between samples with no replicates, in which case just the absolute fold change ≥ 2 criterion was used.

Liver bank samples were analyzed using the Affymetrix GeneChip® miRNA 2.0 array, while all other samples were analyzed using the miRNA 3.0 array. In order to make comparisons with the liver bank samples, each set of arrays was processed separately and then only the human miRNAs found on each array were combined. Data was then normalized by subtracting the median expression value from each sample. Probesets with a $\log_2$ expression value < 6 in fewer than 5 samples were filtered out. An ANOVA model was then fit to the data and empirical Bayes adjusted contrasts were computed. Probesets were then selected at an FDR adjusted *p*-value < 0.05 and an absolute fold change ≥ 2. Liver bank sample HL-159 was determined to be an outlier, and removed from further analyses. To further analyze the miRNAs identified from statistical analysis as being significantly different between comparators,

Ingenuity Pathway Analysis (IPA) was used (http://www.ingenuity.com). It should be noted that for confidence in the identification of mRNA targets, the filter was set to only include those with experimentally observed evidence.

4.4 Results

4.4.1 Expression of miRNAs in human liver tissue

The overall most abundantly expressed miRNA in our liver bank was the liver-specific miR-122, as shown in Figure 4.1a. This is in accordance with what has been demonstrated by others [170, 179, 290]. Microarray analysis revealed a total of 121 miRNAs with an average $\log_2$ expression value > 6, the cut-off value used to delineate miRNAs that are not expressed at a significant level. The top 25 miRNAs expressed in the liver bank are shown in Figure 4.1a. Of the remaining 25 most highly expressed miRNAs in the liver bank, miRs-23b, -194, -22, -192, -125b, and let-7a/b/c have been identified in other studies examining miRNA expression in the liver [179, 262, 265]. Also in the top 25 miRNAs is miR-24, which has been described to regulate HNF4α [149, 179, 282]. Other miRNAs expressed in the liver bank, outside of the top 25, found to regulate ADME-related genes include miR-27b, described as a regulator of CYP1B1 [150, 274], CYP3A4 [276], VDR [276], PPARα, PPARγ and RXRα [277-280]; miR-148a, described as a regulator of PXR [275]; miR-21, described as a regulator of PPARα [277]; miR-34a, described as a regulator of HNF4α [281]; miR-378 described as a regulator of CYP2E1 [283]. A study from 2013 by Rieger et al. examined the expression of 56 miRNAs that were selected based on predictive binding sites to ADME-related genes and liver expression [179]. This set of 56 miRNAs included 6 miRNAs solely because of their high liver expression, despite having low predictions for ADME gene regulation; our liver bank expression profile includes 5

of these 6 miRNAs, miRs-106a, -106b, -122, -19b, -21 [179]. Of the remaining 50 miRNAs with high predictions for ADME gene regulation from the Rieger et al. study, 32 were expressed in our liver bank. These are: miRs -16, -17, -125b, -130a, -130b, -143, -146a, -148a, -150, -152, -15a, -185, -18a, -214, -22, -221, -24, -26a, -27a, -27b, -28-3p, -28-5p, -29a, -34a, -455-3p, and let-7a/b/c/d/e/f/g [179]. In the Rieger et al. study they also identified select miRNAs that negatively affected protein or activity levels of CYP enzymes. The following miRNAs with this attribute that were identified in our liver bank are listed with the CYPs they were found to affect: miR-21 and CYP1A1, miR-21 and CYP2A6, miRs-130b, -185, -34a and CYP2C19, let-7g and CYP2E1 [179].

4.4.2 Expression of miRNAs in SCDHs compared to cryopreserved hepatocytes

miR-122 is one of the highest expressed miRNAs in the SCDH samples, and is the top miRNA expressed in cryopreserved hepatocytes, much like the liver bank samples (Figure 4.1b,c). Among the top 25 miRNAs expressed in SCDHs and cryopreserved hepatocytes, 19 of them are the same between the two groups (Figure 4.1b,c). Comparisons were made between the set of end-stage (Day 17) SCDHs and cryopreserved hepatocytes. The expression level of miRNAs was compared between SCDHs and cryopreserved hepatocytes. miRNAs were deemed as significantly different based on a greater than two-fold change and an FDR adjusted p-value < 0.05. There were a large number of miRNAs that had differing expression levels between the two groups - a total of 211. To limit the number of miRNAs used for further analyses we decided to focus on those with an absolute log fold change value greater than 4 (or 16 on normal scale). This was intended to limit the miRNAs analyzed to those with truly large differences between our comparison groups, with the assumption that those miRNAs with larger fold

changes may have a more significant impact on hepatocyte differentiation. Using this additional filtering criteria, the 211 miRNAs identified when comparing SCDHs to cryopreserved hepatocytes was lowered to 51, consisting of 38 miRNAs that were up-regulated in SCDHs compared to cryopreserved hepatocytes and 13 miRNAs that were down-regulated; these are listed in Table 4.1. Notably, of the 13 miRNAs down-regulated in SCDHs compared to cryopreserved hepatocytes, 7 of them are members of the let-7 family. This data set of up- and down-regulated miRNAs was then analyzed using IPA software to identify genes and biological processes regulated by these miRNAs. Analysis with IPA software revealed toxicological pathways that these miRNAs may influence, as shown in Figure 4.2a. Of the top toxicological pathways identified among the miRNAs with large differences in expression between SCDHs and cryopreserved hepatocytes are liver damage, liver inflammation/hepatitis, liver cirrhosis, and liver hyperplasia/hyperproliferation. Other pathways identified include renal inflammation, renal nephritis, and cardiac fibrosis. These other organ-related pathways show the diversity of miRNAs and their targets, and emphasize the fact that one single miRNA may target many mRNAs and thus have multiple functions. Of the biological functions and diseases pathways identified the top two are cancer and organismal injury and abnormalities (Figure 4.2b-g). Other pathways identified include cellular development, cellular growth and proliferation, hepatic system development and function, and hepatic system disease. There are many biological functions and disease pathways implicated from this set of miRNAs, again indicating the many processes and functions miRNAs can regulate.

4.4.3 Expression of miRNAs in SCDHs compared to human liver tissue

Among the top 25 miRNAs expressed in SCDHs and the liver bank, 12 of them overlap between the two groups while 13 are different (Figure 4.1a,c). Of the top 25 miRNAs in SCDHs that are also in the top 25 of the liver bank are the liver specific miR-122; miR-23b, previously identified as being expressed in liver tissue; and miR-24 which has been shown to target HNF4α [179, 262, 265, 282]. Further comparing SCDHs and the liver bank, 95 miRNAs were identified with differing expression levels. To limit the number of miRNAs used for further analyses we focused on those with an absolute log fold change value greater than 4. Using this filtering criteria the 95 miRNAs identified were lowered to 40, consisting of 26 miRNAs that were up-regulated in SCDHs compared to the liver bank and 14 that were down-regulated in SCDHs; these are listed in Table 4.2. Notably, of the 14 miRNAs down-regulated in SCDHs compared to the liver bank, 7 of them are members of the let-7 family. This is qualitatively very similar to the comparison observed between SCDHs and cryopreserved hepatocytes. This data set of up- and down-regulated miRNAs was then analyzed using IPA software to identify genes and biological processes regulated by these miRNAs. Analysis with IPA software identified the toxicological pathways these miRNAs may influence, as depicted in Figure 4.3a. Of the toxicological pathways identified among the miRNAs with large differences in expression between SCDHs and the liver bank are liver damage, liver inflammation/hepatitis, and liver cirrhosis; the same pathways identified from the set of miRNAs from SCDHs and cryopreserved hepatocytes. Similar to the pathways identified for SCDHs compared to cryopreserved hepatocytes, renal inflammation and renal nephritis are the top two identified by the SCDH-liver bank comparison. Again, for the biological functions and diseases pathways identified, the top two are identical to the ones identified for SCDHs compared to cryopreserved hepatocytes – cancer and organismal injury and abnormalities (Figure 4.3b-g). Overall, the set of miRNAs with large differences in

expression between SCDHs and the liver bank, and SCDHs and cryopreserved hepatocytes, seem to influence the same toxicological and biological function pathways. This is expected, as the majority of the set of miRNAs with a large fold change between SCDHs and the liver bank are also in the set of miRNAs with a large fold change between SCDHs and cryopreserved hepatocytes.

4.4.4 Expression of miRNAs in SCDHs compared to undifferentiated stem cells

Of the top 25 miRNAs expressed for all undifferentiated stem cells, 18 of them are the same as the top 25 miRNAs expressed in SCDHs (Figure 4.1c, d). This includes 3 members of the miR-17-92 cluster, found to be enriched in hESCs and iPSCs (REF 196, 215, 216). For comparison, of the top 25 miRNAs expressed in undifferentiated stem cells, only 5 of them are also found in the top 25 miRNAs expressed in the liver bank (Figure 4.1a, d). Comparing H1 SCDHs to H1 hESCs, 278 miRNAs were identified with differing expression levels. Using the filtering criteria to focus on the larger fold changes, 278 were reduced to 35, consisting of 19 miRNAs that were up-regulated in H1 SCDHs compared to H1 hESCs and 16 miRNAs that were down-regulated, listed in Table 4.3. Notably, the liver-specific miR-122 was up-regulated in H1 Differentiated cells at a log fold change of 12.82, with a *p*-value of 5.26E-23. Comparing H9 SCDHs to H9 hESCs, 226 miRNAs were identified with differing expression levels. Upon further filtering, 226 were reduced to 32, consisting of 20 miRNAs that were up-regulated in H9 SCDHs compared to H9 hESCs and 12 miRNAs that were down-regulated, listed in Table 4.4. Similar to the results in H1 cells, miR-122 was up-regulated in H9 SCDHs at a log fold change of about 12, with a p-value of 5.09E-24. Comparing iPSC SCDHs to iPSC, 131 miRNAs were identified with differing expression levels. Upon further filtering, the 131 miRNAs were

reduced to 10, consisting of 7 miRNAs that were up-regulated in iPSC SCDHs compared to iPSCs and 3 miRNAs that were down-regulated, listed in Table 4.5. Again, miR-122 was up-regulated in iPSC SCDHs compared to iPSCs, at a log fold change of 5.18. Among the miRNAs up-regulated in H1 and H9 SCDHs compared to H1 and H9 hESCs, 5 of them are within the top 25 miRNAs expressed in the liver bank, these are miRs-122, -145, -194, -192, and -22. miRs-122, -194, and -22 are also within the top 25 miRNAs in cryopreserved hepatocytes. This indicates an increase in expression of some liver-related miRNAs upon differentiation. Also, of the miRNAs down-regulated in H1 and H9 SCDHs compared to H1 and H9 hESCs, half of them are members of the miR-371-372 and miR-302/367 clusters, which are clusters predominantly associated with undifferentiated cells. This indicates the SCDHs are removed from hESCs. While the iPSCs do have some differences in miRNA expression patterns compared to the hESCs, among the miRNAs up-regulated in iPSC SCDHs compared to iPSCs are also miRs-122, -194, and -192, indicating an increase in expression of liver-related miRNAs and comparable responses to the differentiation protocol.

The data sets of up- and down-regulated miRNAs were then analyzed using IPA software to identify genes and biological processes regulated by these miRNAs. Of the toxicological pathways identified among the miRNAs with large differences in expression between H1/H9 SCDHs and H1/H9 hESCs, the top three pathways are liver steatosis, liver damage and liver inflammation/hepatitis (Figures 4.4a and 4.5a). Similar results were obtained for the toxicological pathways among the miRNAs with large differences in expression between iPSC SCDHs and iPSCs, being the liver-related pathways liver steatosis, hepatocellular carcinoma, and liver hyperplasia/hyperproliferation (Figure 4.6a). Of the biological functions and diseases pathways identified, for all three stem cell lines, the top two are cancer and organismal injury

and abnormalities, as seen in the comparisons with liver bank and cryopreserved hepatocytes (Figures 4b-g, 5b-g, and 6b-e). Again, with all the comparisons evaluated the sets of miRNAs seem to influence the same or very similar toxicological and biological functions. Importantly, among the top pathways identified are liver-related functions and development-related functions such as cellular development, and cellular growth and proliferation. This indicates the miRNAs with large fold differences between groups are associated with liver-related functions, and could have an influence on hepatocyte differentiation and functional maturation.

4.4.5 Expression of miRNAs in hESCs and iPSCs during differentiation into hepatocytes

Stem cells were analyzed at each stage of differentiation, being differentiated stem cells at the end of stage 1 of the differentiation protocol, which we have termed definitive endoderm for reference (Day 3 for hESCs and Day 5 for iPSCs), and differentiated stem cells at the end of stage 2 of the differentiation protocol, which we have termed hepatoblast for reference (Day 10 for hESCs and Day 9 for iPSCs). Of the top 25 miRNAs expressed in definitive endoderm cells, almost all of them (23) are the same as the top 25 miRNAs expressed in undifferentiated stem cells (Figure 4.1d, e). Of the top 25 miRNAs expressed in hepatoblast cells, 18 of them are the same as the top 25 miRNAs expressed in undifferentiated cells (Figure 4.1d, f). This is the same as the number of miRNAs (18) over-lapping in the top 25 of SCDHs and undifferentiated stem cells. Comparing SCDHs and hepatoblast cells, 24 of the top 25 miRNAs are the same between the two groups. This indicates that stem cells at the end of stage 2 in the differentiation process are very similar to the end-stage SCDHs, and perhaps the cells do not mature much past stage 2, based on these miRNA profiles.

4.4.6 miR-122 qRT-PCR

To validate the microarray results, qRT-PCR was performed for miR-122. As seen in Figure 4.7, for both hESC lines and the iPSC line evaluated, miR-122 expression is minimal or below the limit of quantitation at Day 0 and at the definitive endoderm stage, but increases at the hepatoblast stage and in end-stage SCDHs. Furthermore, based on $\Delta\Delta C_T$ calculations, miR-122 expression in the iPSC SCDHs is at the same level as that in the cryopreserved hepatocyte lot tested and H1 SCDH expression is 80% of that in cryopreserved hepatocytes. miR-122 expression in the H9 SCDHs reaches 60% and 30% of that in cryopreserved hepatocytes, as shown in Figure 4.7. All SCDH samples and cryopreserved hepatocytes demonstrate lower miR-122 expression than select liver bank sample. The observed variability in miR-122 expression, both between cell lines and different batches of differentiation using the same cell line, demonstrates the variability in differentiation efficiency. These results and the expression pattern of miR-122 mirror the data obtained from the miRNA microarray.

4.4.7 Let-7 transfection

Based on the well-known role of let-7 in development and differentiation [160, 174, 175, 191, 194], we identified let-7 as a candidate for manipulation in culture of SCDHs to enhance maturation. From the microarray results we observed that let-7 expression is much lower in SCDHs compared to cryopreserved hepatocytes and human liver tissue, with the let-7 family accounting for the majority of down-regulated miRNAs with a greater than 4 fold change in SCDHs compared to either cryopreserved hepatocytes or the liver bank (Tables 4.1 and 4.2). Due to this observation and the work of Dr. Ruohola-Baker's lab at the University of

Washington Institute for Stem Cell and Regenerative Medicine on the role of let-7 in the maturation of stem cell derived cardiomyocytes, we induced let-7 expression in SCDHs during the differentiation process [291]. For this, H9 SCDHs were virally transduced at day 7 of differentiation with either pLKO-let7i or pLKO-dsred, a fluorescent control, both gifts from Dr. Ruohola-Baker's lab. At 6 days post-transduction, or day 13 of the differentiation process, transduced and control cells were collected for RNA extraction and qRT-PCR analysis. Fluorescence in SCDHs transduced with the pLKO-dsred control was monitored, however a fluorescent signal was not detectable. qRT-PCR analysis revealed no change in let-7i expression in let-7i transduced cells compared to ds-red control cells indicating the transduction was unsuccessful, see Figure 4.8a.

Since transduction with let-7i using conditions established for stem cell derived cardiomyocytes did not produce positive results in SCDHs, transfection with a commercially available let-7c mimic was done. H9 SCDHs were transfected at day 8 of differentiation with either a let-7c mimic or a fluorescent control mimic for 5 hours or overnight. At day 4 post-transfection, or day 12 of the differentiation process, transfected and control cells were collected for RNA extraction and qRT-PCR analysis. qRT-PCR analysis revealed let-7c expression to be about 880 fold higher in let-7c 5 hour transfected samples compared to control, and about 1800 fold higher in let-7c overnight transfected samples compared to control based on $\Delta\Delta C_T$ calculations (Figure 4.8b). Let-7c expression was undetectable in no reverse transcriptase controls for all let-7c and control transfected samples, indicating the observed higher expression of let-7c was not due to remnants from the mimic itself (Figure 4.8b). Additional qRT-PCR analysis of let-7c expression in transfected samples compared to no transfection controls and mimic controls yielded similar results. There was no observed effect on let-7c expression in

cells transfected with the mimic control compared to no transfection controls, and a marked increase in let-7c expression in both 5 hour and overnight transfected samples (Figure 4.8c). To investigate if let-7c transfection had any effect on the SCDHs, expression of three genes related to hepatocyte maturity (AFP, ALB, HNF4α) and two target genes of let-7c (HMGA2 and LIN28B) were evaluated. Notably, based on $\Delta\Delta C_T$ calculations, both the 5 hour and overnight let-7c transfection had no discernable effect on expression of hepatocyte genes AFP, ALB and HNF4α (Figure 4.8d). This data represents only one attempt at transfection with only one time point post-transfection being monitored. Further work is needed to determine if let-7c transfection will affect the maturity of SCDHs.

4.5 Discussion

Among the miRNAs identified as down-regulated in SCDHs compared to cryopreserved hepatocytes, as well as SCDHs compared to the liver bank, the majority of them belong to the let-7 family. Let-7 is known to play an important role in development, and specifically exhibits low expression in embryonic tissue and high expression in most all differentiated tissues [174, 191, 194]. This indicates that let-7 expression may be at an insufficient level in the SCDHs, possibly contributing to the observed lack of maturity.

Of the miRNAs highly up-regulated in SCDHs compared to cryopreserved hepatocytes, 8 of them belong to either the miR-302/367 cluster or the miR-371-373 cluster. These results are also similar to those obtained comparing SCDHs to the liver bank, in which 7 of the highly up-regulated miRNAs belong to the miR-302/367 and miR-371-373 clusters. These two miRNA clusters are highly expressed in undifferentiated stem cells, and are implicated in maintaining cell pluripotency [214, 225-229, 233-237]. However, these two clusters have also been found to

still be expressed in definitive endoderm cells, though were indeed down-regulated upon further differentiation to hepatocytes [223, 262]. This suggests that the SCDHs are maintaining expression of miRNAs involved in maintaining cell pluripotency, and could be another contributing factor to the lack of maturity observed in SCDHs. In contrast, the miRNA that was most up-regulated in SCDHs compared to cryopreserved hepatocytes is miR-145, this miRNA has been found to induce differentiation by suppressing the pluripotency factors OCT4, SOX2 and KLF4 [213, 236, 239, 243]. The higher miR-145 expression in SCDHs compared to cryopreserved hepatocytes could be a result of the fact that cryopreserved hepatocytes are essentially dying cells, most likely going through a de-differentiation process themselves, as the difference in miR-145 expression was not detected between SCDHs and the liver bank.

To visualize miRNAs with both a large fold change and high statistical significance, a volcano plot comparing cryopreserved hepatocytes to SCDHs was generated (Figure 4.9). When combining both log fold change and high statistical significance, one miRNA is identified, miR-205, shown as a red dot in Figure 4.9. Note for this comparison SCDHs are in the denominator, meaning miR-205 shows as a negative fold-change in Figure 4.9. miR-205 is also the miRNA with the highest log fold change in up-regulation comparing SCDHs to the liver bank. miR-205 is described as regulating EMT (an important part of embryonic development) [215, 216], and was also identified as being enriched in definitive endoderm cells by Kim et al. [262]. In EMT, miR-205 specifically is important in specifying the epithelial phenotype of cells by inhibiting ZEB1 and ZEB2 [215, 216]. During normal embryonic development epithelial cells are converted to mesenchymal cells [215, 216], therefore, the observed high expression of miR-205 in SCDHs compared to cryopreserved hepatocytes and liver tissue could be a contributing reason for the lack of maturity in SCDHs. Additional miRNAs identified in our study as up-regulated in

SCDHs compared to cryopreserved hepatocytes and/or the liver bank that have been found in other studies as enriched in definitive endoderm cells are miRs -125a-5p, -708, -10a [223, 262]. Taken together, these results indicate a mix of miRNAs from pluripotent and definitive endoderm type cells that are expressed in our SCDHs at a higher level than in cryopreserved hepatocytes, as well as the liver bank. To visualize miRNA expression as it compares to the liver bank, a heatmap was generated. In this heatmap the average miRNA expression in the liver bank was used as the comparator, each column shows the log fold change between the given sample and the liver bank (Figure 4.10). From this heatmap, cryopreserved hepatocytes have the closest expression profile to the liver bank, as indicated by the number of miRNAs shown in white, meaning no change in expression. Overall, the miRNA expression profiles in undifferentiated stem cells, definitive endoderm cells, hepatoblast cells and SCDHs group together as compared to the liver bank, in that generally the same sets of miRNAs are up-regulated (red) or down-regulated (blue) in these cells compared to the liver bank, see Figure 4.10. This indicates that SCDHs do exhibit a number of miRNAs with differing expression levels compared to the liver bank. It should be noted that the liver bank samples were processed in a different batch, and run on a different array (2.0 vs. 3.0 array), from the rest of the samples. Therefore, differences between the liver bank and other samples may be due to a batch effect rather than a true biological effect. However, we have only considered miRNAs found on both array versions and for IPA analyses and discussion we have focused on miRNAs with very high expression differences (absolute value of log fold change >4), with the assumption that large differences may represent true biological differences, in excess of any batch effect.

Among the top 25 miRNAs in SCDHs and undifferentiated hESCs and iPSCs, are 3 members of the miR-17-92 cluster and miR-93, a member of the closely related miR-106b-25

cluster [292]. The miR-17-92 cluster is reported to be enriched in hESCs and iPSCs, and is also a pro-tumorigenic cluster activated by c-myc [213, 232, 233]. The tumorigenic activity of the miR-17-92 cluster has resulted in its designation as "OncomiR-1", with over-expression of this cluster reported in hepatocellular carcinoma [292]. A study by Fu et al. examining miRNA expression in human fetal liver tissue identified miR-17 and miR-93 as being expressed in the fetal liver [264]. Other fetal liver miRNAs identified in the Fu et al. study found in the top 25 miRNAs in SCDHs include miR-122, miR-24, and miR-26a [264]. This indicates the SCDHs are expressing some miRNAs associated with fetal liver tissue. The present study has produced similar results to a study by Kim et al. evaluating expression profiles of miRNAs in hESCs during hepatocyte differentiation. In the study by Kim et al., among the top 10 miRNAs identified as down-regulated in SCDHs compared to hESCs are the same members of the miR-302-367 and miR-371-373 clusters identified in our set of down-regulated miRNAs [262]. Also, among the top 10 miRNAs identified as up-regulated in SCDHs compared to hESCs in the Kim et al study, miRs-122, -214, -143, and -152 are in our set of up-regulated miRNAs [262]. The data from this study in combination with the Kim et al. study indicates there may be a distinct miRNA profile for differentiation of hepatocytes from hESCs. Differences in miRNA profiles between different studies may be due to differing differentiation conditions and the exact state/stage the cells are in. Additionally, there may be varying degrees of still undifferentiated cells in the culture influencing results.

An initial hypothesis we had regarding miRNAs that may influence the maturity of SCDHs centered on miR-122, because it has been established as a liver-specific miRNA. Based on the microarray results, and further qRT-PCR analysis, miR-122 appears to be expressed at sufficient levels in SCDHs, compared to cryopreserved hepatocytes (Figure 4.7). Therefore, we

predict that targeting or over-expressing miR-122 in the current differentiation protocol will have minimal effects to increase the maturity or functionality of SCDHs, as compared to cryopreserved hepatocytes. Evaluating the global changes in miRNAs between SCDHs and cryopreserved hepatocytes and human liver tissue, some top candidates of miRNAs warranting further evaluation in the differentiation process include the let-7 family, the miR-17-92, miR-302-367, and miR-371-373 clusters, and miR-205. Preliminary experiments investigating the influence of let-7c transfection on SCDHs have shown that let-7c expression can be induced through transfection. Further work is needed to determine if induced let-7c expression will enhance the maturity of SCDHs.

4.6 Conclusion

This work was largely hypothesis-generating, but nonetheless informative. The miRNA expression patterns in SCDHs compared to undifferentiated stem cells, cryopreserved hepatocytes and human liver tissue indicate global changes associated with immaturity in SCDHs. One such pattern is the down-regulation of the let-7 family in SCDHs compared to cryopreserved hepatocytes and human liver tissue, a family normally expressed in mature tissue. Another prominent pattern is the high overall expression and up-regulation compared to cryopreserved hepatocytes and human liver tissue of members in the miR-17-92, 302-367 and 371-373 clusters, normally expressed in pluripotent stem cells. This data suggests that the let-7 family of miRNAs and/or the miR-17-92, miR-302-367, and miR-371-373 clusters may be viable targets for manipulation within the currently used differentiation protocol to enhance the maturation and function of SCDHs.

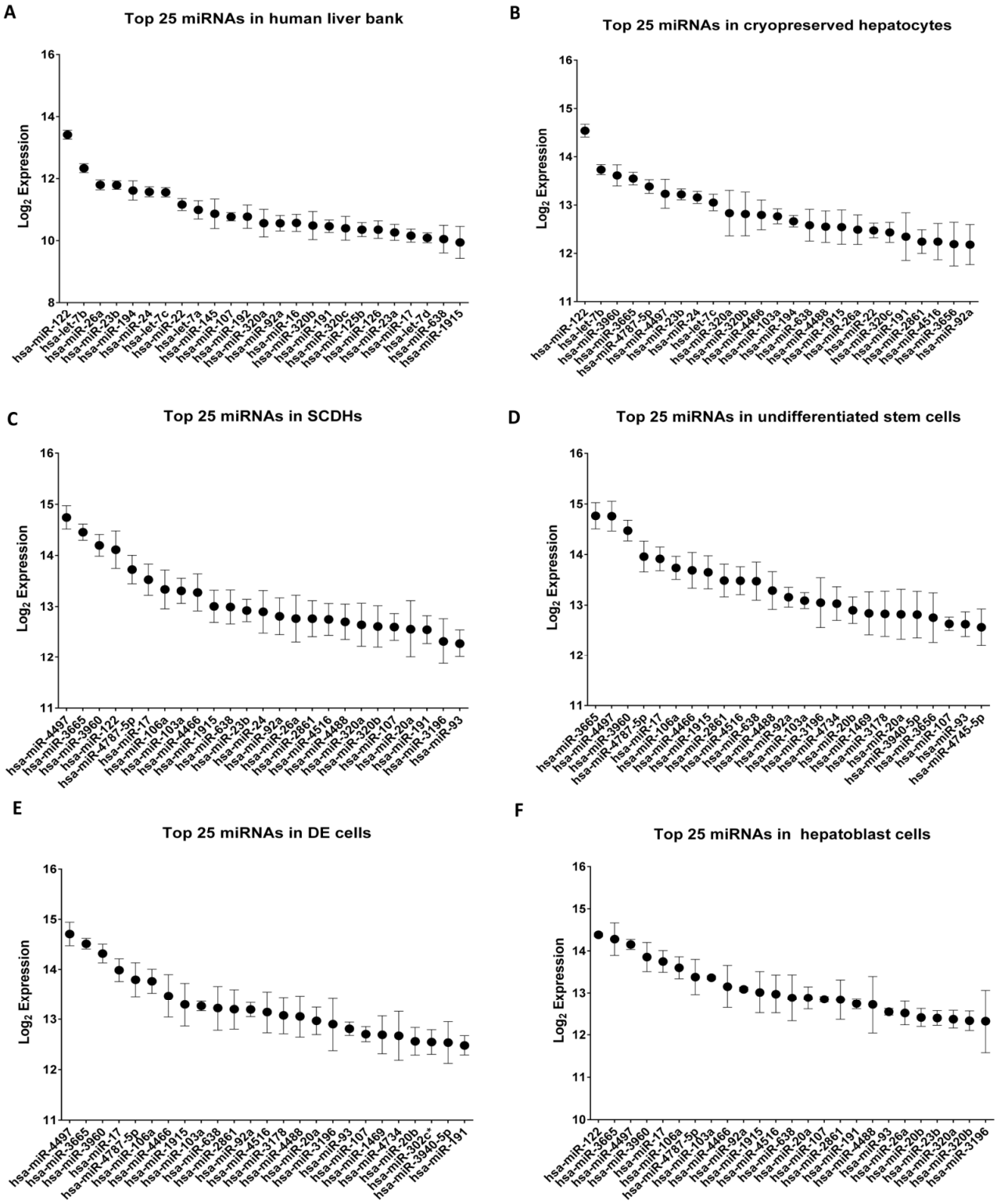
A
Top 25 miRNAs in human liver bank
Log2 Expression
hsa-miR-122
hsa-let-7b
hsa-miR-26a
hsa-miR-23b
hsa-miR-194
hsa-miR-24
hsa-let-7c
hsa-miR-22
hsa-let-7a
hsa-miR-145
hsa-miR-107
hsa-miR-192
hsa-miR-320a
hsa-miR-92a
hsa-miR-16
hsa-miR-320b
hsa-miR-191
hsa-miR-320c
hsa-miR-125b
hsa-miR-126
hsa-miR-23a
hsa-miR-17
hsa-let-7d
hsa-miR-638
hsa-miR-1915
B
Top 25 miRNAs in cryopreserved hepatocytes
Log2 Expression
hsa-miR-122
hsa-let-7b
hsa-miR-3960
hsa-miR-3665
hsa-miR-4787-5p
hsa-miR-4497
hsa-miR-23b
hsa-miR-24
hsa-let-7c
hsa-miR-320a
hsa-miR-320b
hsa-miR-4466
hsa-miR-103a
hsa-miR-194
hsa-miR-638
hsa-miR-4488
hsa-miR-1915
hsa-miR-26a
hsa-miR-22
hsa-miR-320c
hsa-miR-191
hsa-miR-2861
hsa-miR-4516
hsa-miR-3656
hsa-miR-92a
C
Top 25 miRNAs in SCDHs
Log2 Expression
hsa-miR-4497
hsa-miR-3665
hsa-miR-3960
hsa-miR-122
hsa-miR-4787-5p
hsa-miR-17
hsa-miR-106a
hsa-miR-103a
hsa-miR-4466
hsa-miR-1915
hsa-miR-638
hsa-miR-23b
hsa-miR-24
hsa-miR-92a
hsa-miR-26a
hsa-miR-2861
hsa-miR-4516
hsa-miR-4488
hsa-miR-320a
hsa-miR-320b
hsa-miR-107
hsa-miR-20a
hsa-miR-191
hsa-miR-3196
hsa-miR-93
D
Top 25 miRNAs in undifferentiated stem cells
Log2 Expression
hsa-miR-3665
hsa-miR-4497
hsa-miR-3960
hsa-miR-4787-5p
hsa-miR-17
hsa-miR-106a
hsa-miR-4466
hsa-miR-1915
hsa-miR-2861
hsa-miR-4516
hsa-miR-638
hsa-miR-4488
hsa-miR-92a
hsa-miR-103a
hsa-miR-3196
hsa-miR-4734
hsa-miR-20b
hsa-miR-1469
hsa-miR-3178
hsa-miR-20a
hsa-miR-3940-5p
hsa-miR-3656
hsa-miR-107
hsa-miR-93
hsa-miR-4745-5p
E
Top 25 miRNAs in DE cells
Log2 Expression
hsa-miR-4497
hsa-miR-3665
hsa-miR-3960
hsa-miR-17
hsa-miR-4787-5p
hsa-miR-106a
hsa-miR-4466
hsa-miR-1915
hsa-miR-103a
hsa-miR-638
hsa-miR-2861
hsa-miR-92a
hsa-miR-4516
hsa-miR-3178
hsa-miR-4488
hsa-miR-20a
hsa-miR-3196
hsa-miR-93
hsa-miR-107
hsa-miR-1469
hsa-miR-4734
hsa-miR-20b
hsa-miR-302c*
hsa-miR-3940-5p
hsa-miR-191
F
Top 25 miRNAs in hepatoblast cells
Log2 Expression
hsa-miR-122
hsa-miR-3665
hsa-miR-4497
hsa-miR-3960
hsa-miR-17
hsa-miR-106a
hsa-miR-4787-5p
hsa-miR-103a
hsa-miR-4466
hsa-miR-92a
hsa-miR-1915
hsa-miR-4516
hsa-miR-638
hsa-miR-20a
hsa-miR-107
hsa-miR-2861
hsa-miR-191
hsa-miR-4488
hsa-miR-93
hsa-miR-26a
hsa-miR-20b
hsa-miR-23b
hsa-miR-320a
hsa-miR-320b
hsa-miR-3196

Figure 4.1. Top 25 miRNAs. The top 25 miRNAs expressed in (A) liver bank, (B) cryopreserved hepatocytes, (C) SCDHs, (D) undifferentiated stem cells, (E) DE cells, (F) hepatoblast cells reported as the average $\log_2$ expression with standard deviation.

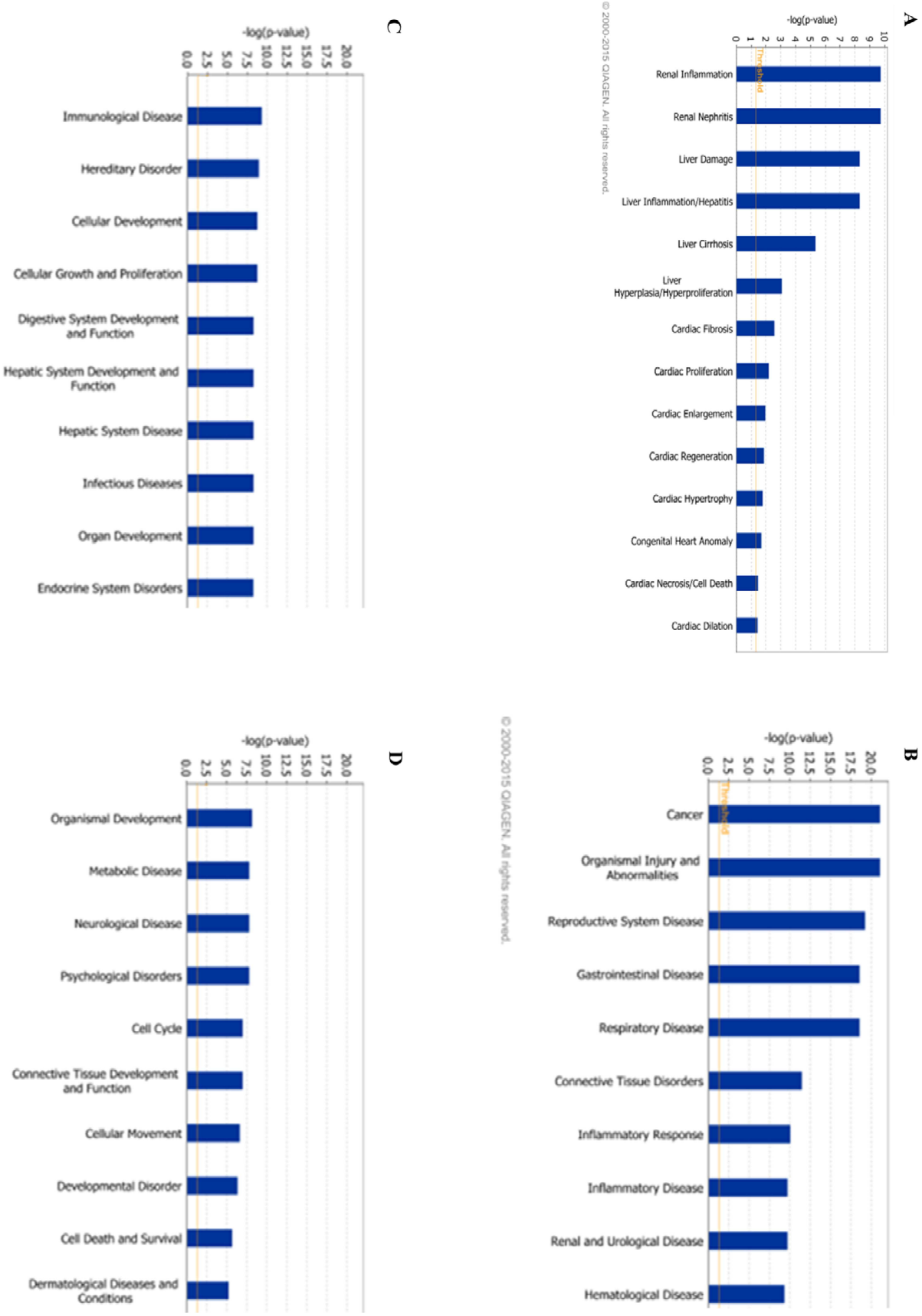
A
-log(p-value)
0 1 2 3 4 5 6 7 8 9 10
Threshold
Renal Inflammation
Renal Nephritis
Liver Damage
Liver Inflammation/Hepatitis
Liver Cirrhosis
Liver Hyperplasia/Hyperproliferation
Cardiac Fibrosis
Cardiac Proliferation
Cardiac Enlargement
Cardiac Regeneration
Cardiac Hypertrophy
Congenital Heart Anomaly
Cardiac Necrosis/Cell Death
Cardiac Dilation
© 2000-2015 QIAGEN. All rights reserved.
B
-log(p-value)
0.0 2.5 5.0 7.5 10.0 12.5 15.0 17.5 20.0
Threshold
Cancer
Organismal Injury and Abnormalities
Reproductive System Disease
Gastrointestinal Disease
Respiratory Disease
Connective Tissue Disorders
Inflammatory Response
Inflammatory Disease
Renal and Urological Disease
Hematological Disease
© 2000-2015 QIAGEN. All rights reserved.
C
-log(p-value)
0.0 2.5 5.0 7.5 10.0 12.5 15.0 17.5 20.0
Immunological Disease
Hereditary Disorder
Cellular Development
Cellular Growth and Proliferation
Digestive System Development and Function
Hepatic System Development and Function
Hepatic System Disease
Infectious Diseases
Organ Development
Endocrine System Disorders
D
-log(p-value)
0.0 2.5 5.0 7.5 10.0 12.5 15.0 17.5 20.0
Organismal Development
Metabolic Disease
Neurological Disease
Psychological Disorders
Cell Cycle
Connective Tissue Development and Function
Cellular Movement
Developmental Disorder
Cell Death and Survival
Dermatological Diseases and Conditions

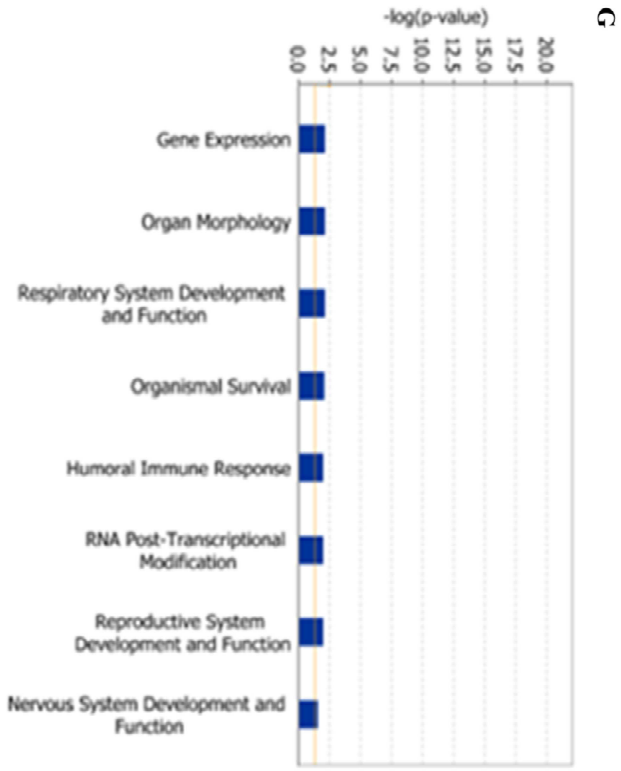
G
-log(p-value)
0.0
2.5
5.0
7.5
10.0
12.5
15.0
17.5
20.0
Gene Expression
Organ Morphology
Respiratory System Development and Function
Organismal Survival
Humoral Immune Response
RNA Post-Transcriptional Modification
Reproductive System Development and Function
Nervous System Development and Function

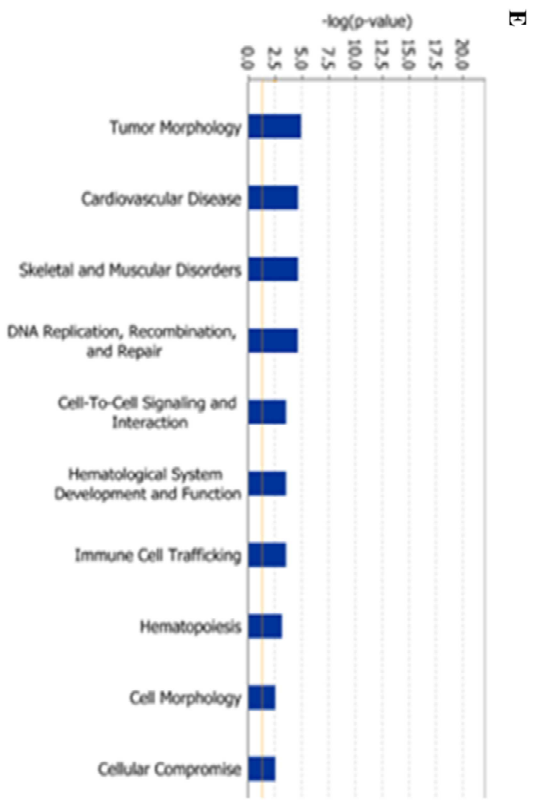
E
-log(p-value)
0.0
2.5
5.0
7.5
10.0
12.5
15.0
17.5
20.0
Tumor Morphology
Cardiovascular Disease
Skeletal and Muscular Disorders
DNA Replication, Recombination, and Repair
Cell-To-Cell Signaling and Interaction
Hematological System Development and Function
Immune Cell Trafficking
Hematopoiesis
Cell Morphology
Cellular Compromise

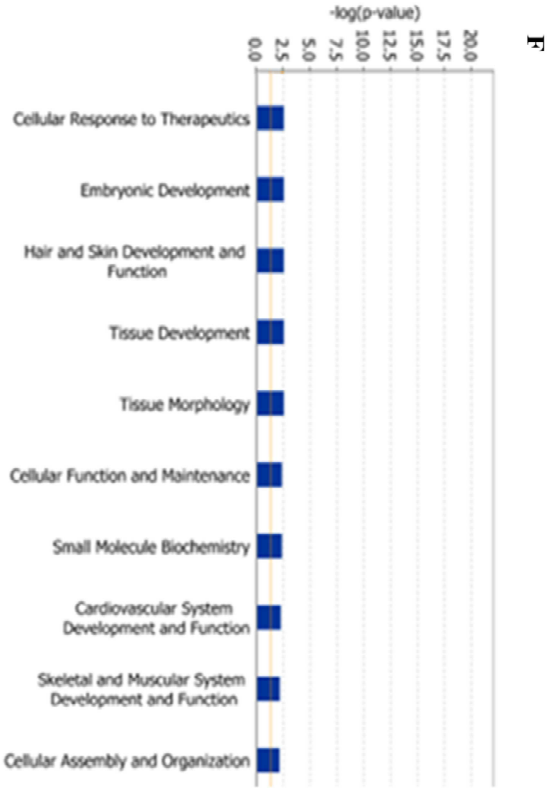
F
-log(p-value)
0.0
2.5
5.0
7.5
10.0
12.5
15.0
17.5
20.0
Cellular Response to Therapeutics
Embryonic Development
Hair and Skin Development and Function
Tissue Development
Tissue Morphology
Cellular Function and Maintenance
Small Molecule Biochemistry
Cardiovascular System Development and Function
Skeletal and Muscular System Development and Function
Cellular Assembly and Organization

Figure 4.2. SCDHs versus cryopreserved hepatocytes IPA analysis. (A) The toxicological functions associated with the set of miRNAs that showed an absolute value log fold change greater than 4 between SCDHs and cryopreserved hepatocytes. (B)-(G) The biological functions and diseases associated with the set of miRNAs that showed an absolute value log fold change greater than 4 between SCDHs and cryopreserved hepatocytes. The functions have been broken into sets of 10, with the highest 10 in (B) and the lowest in (G). The threshold line represents the –log of *p*-value 0.05.

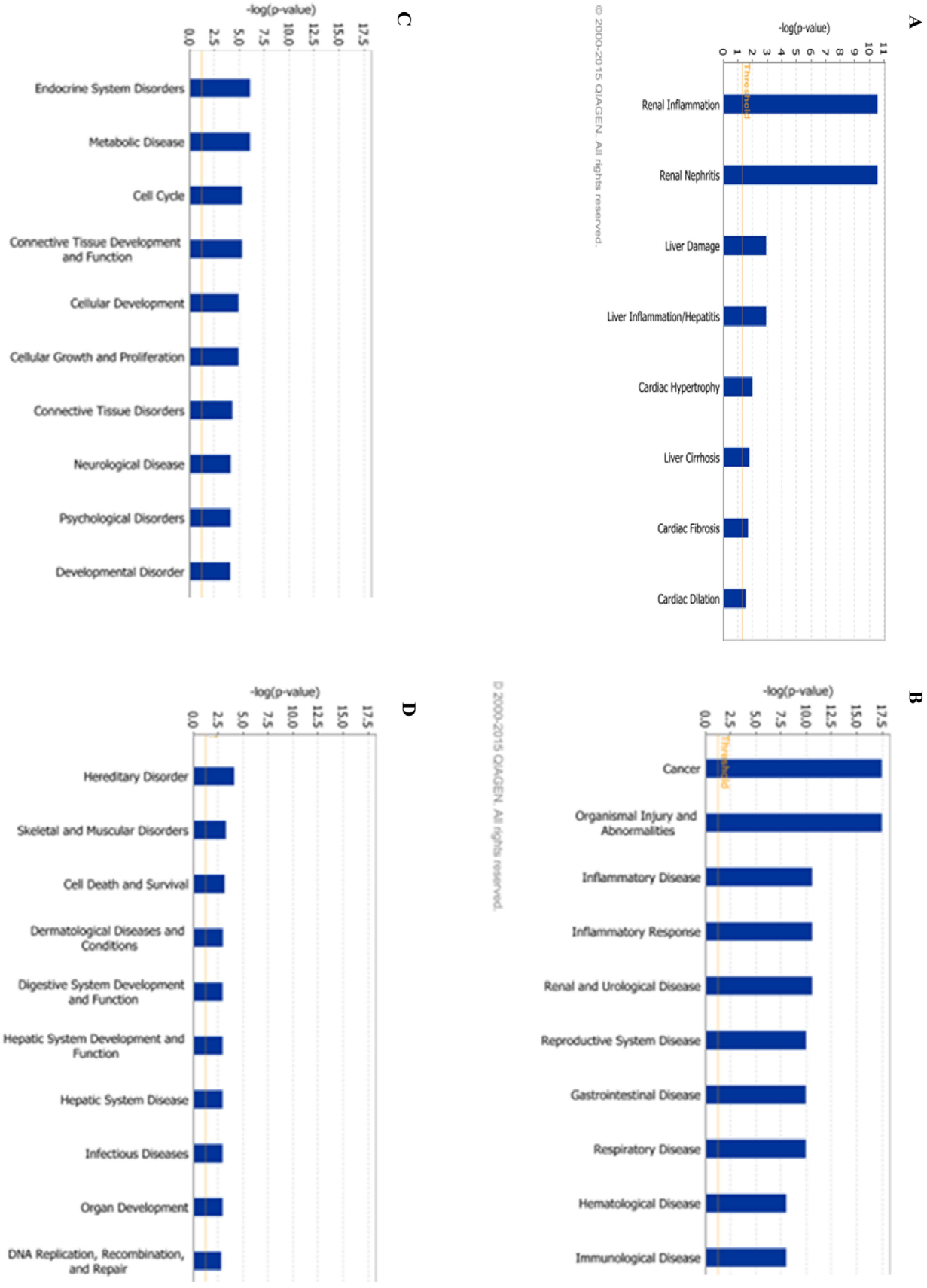
A
-log(p-value)
0
1
2
3
4
5
6
7
8
9
10
11
Threshold
Renal Inflammation
Renal Nephritis
Liver Damage
Liver Inflammation/Hepatitis
Cardiac Hypertrophy
Liver Cirrhosis
Cardiac Fibrosis
Cardiac Dilation
© 2000-2015 QIAGEN. All rights reserved.
B
-log(p-value)
0.0
2.5
5.0
7.5
10.0
12.5
15.0
17.5
Threshold
Cancer
Organismal Injury and Abnormalities
Inflammatory Disease
Inflammatory Response
Renal and Urological Disease
Reproductive System Disease
Gastrointestinal Disease
Respiratory Disease
Hematological Disease
Immunological Disease
© 2000-2015 QIAGEN. All rights reserved.
C
-log(p-value)
0.0
2.5
5.0
7.5
10.0
12.5
15.0
17.5
Endocrine System Disorders
Metabolic Disease
Cell Cycle
Connective Tissue Development and Function
Cellular Development
Cellular Growth and Proliferation
Connective Tissue Disorders
Neurological Disease
Psychological Disorders
Developmental Disorder
D
-log(p-value)
0.0
2.5
5.0
7.5
10.0
12.5
15.0
17.5
Hereditary Disorder
Skeletal and Muscular Disorders
Cell Death and Survival
Dermatological Diseases and Conditions
Digestive System Development and Function
Hepatic System Development and Function
Hepatic System Disease
Infectious Diseases
Organ Development
DNA Replication, Recombination, and Repair

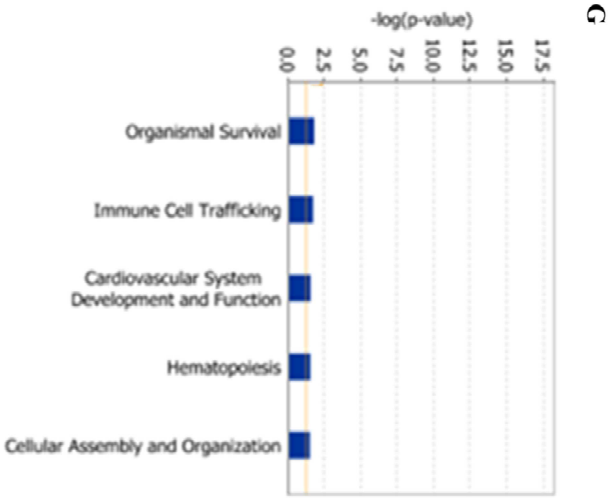
G
-log(p-value)
0.0
2.5
5.0
7.5
10.0
12.5
15.0
17.5
Organismal Survival
Immune Cell Trafficking
Cardiovascular System Development and Function
Hematopoiesis
Cellular Assembly and Organization

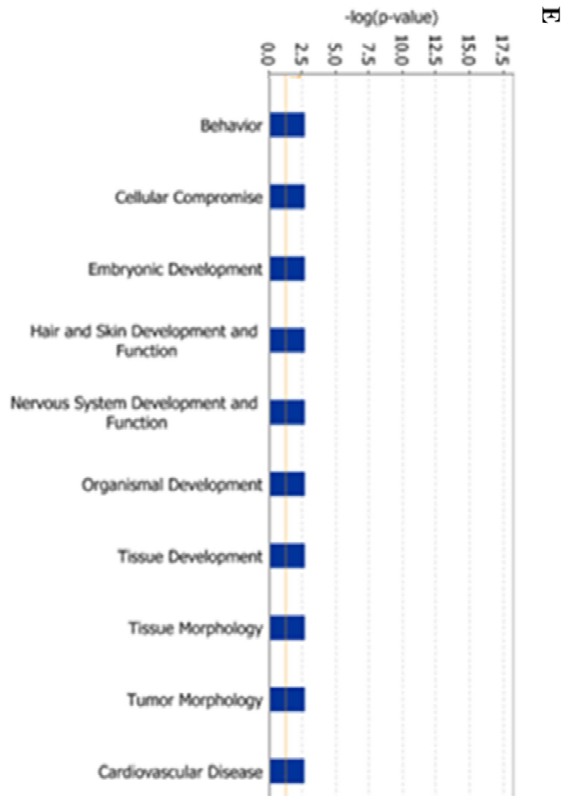
E
-log(p-value)
0.0
2.5
5.0
7.5
10.0
12.5
15.0
17.5
Behavior
Cellular Compromise
Embryonic Development
Hair and Skin Development and Function
Nervous System Development and Function
Organismal Development
Tissue Development
Tissue Morphology
Tumor Morphology
Cardiovascular Disease

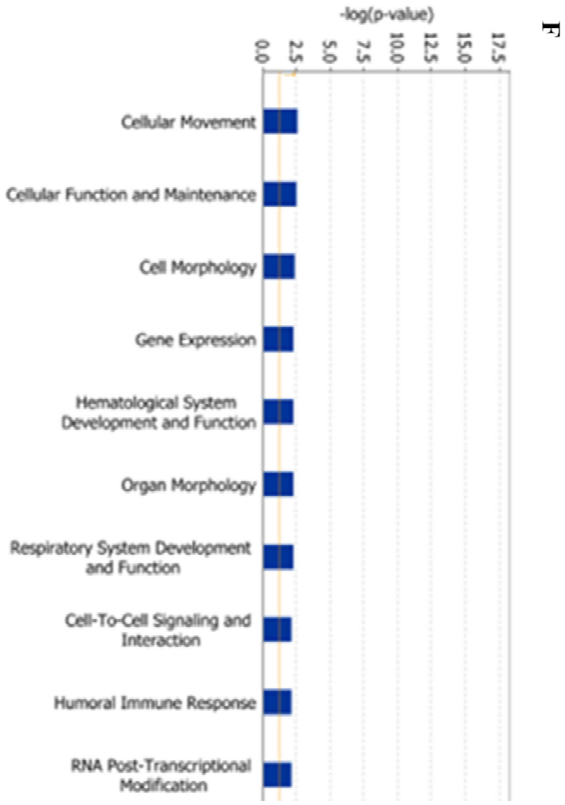
F
-log(p-value)
0.0
2.5
5.0
7.5
10.0
12.5
15.0
17.5
Cellular Movement
Cellular Function and Maintenance
Cell Morphology
Gene Expression
Hematological System Development and Function
Organ Morphology
Respiratory System Development and Function
Cell-To-Cell Signaling and Interaction
Humoral Immune Response
RNA Post-Transcriptional Modification

Figure 4.3. SCDHs versus liver bank IPA analysis. (A) The toxicological functions associated with the set of miRNAs that showed an absolute value log fold change greater than 4 between SCDHs and the liver bank. (B)-(G) The biological functions and diseases associated with the set of miRNAs that showed an absolute value log fold change greater than 4 between SCDHs and the liver bank. The functions have been broken into sets of 10, with the highest 10 in (B) and the lowest in (G). The threshold line represents the –log of *p*-value 0.05.

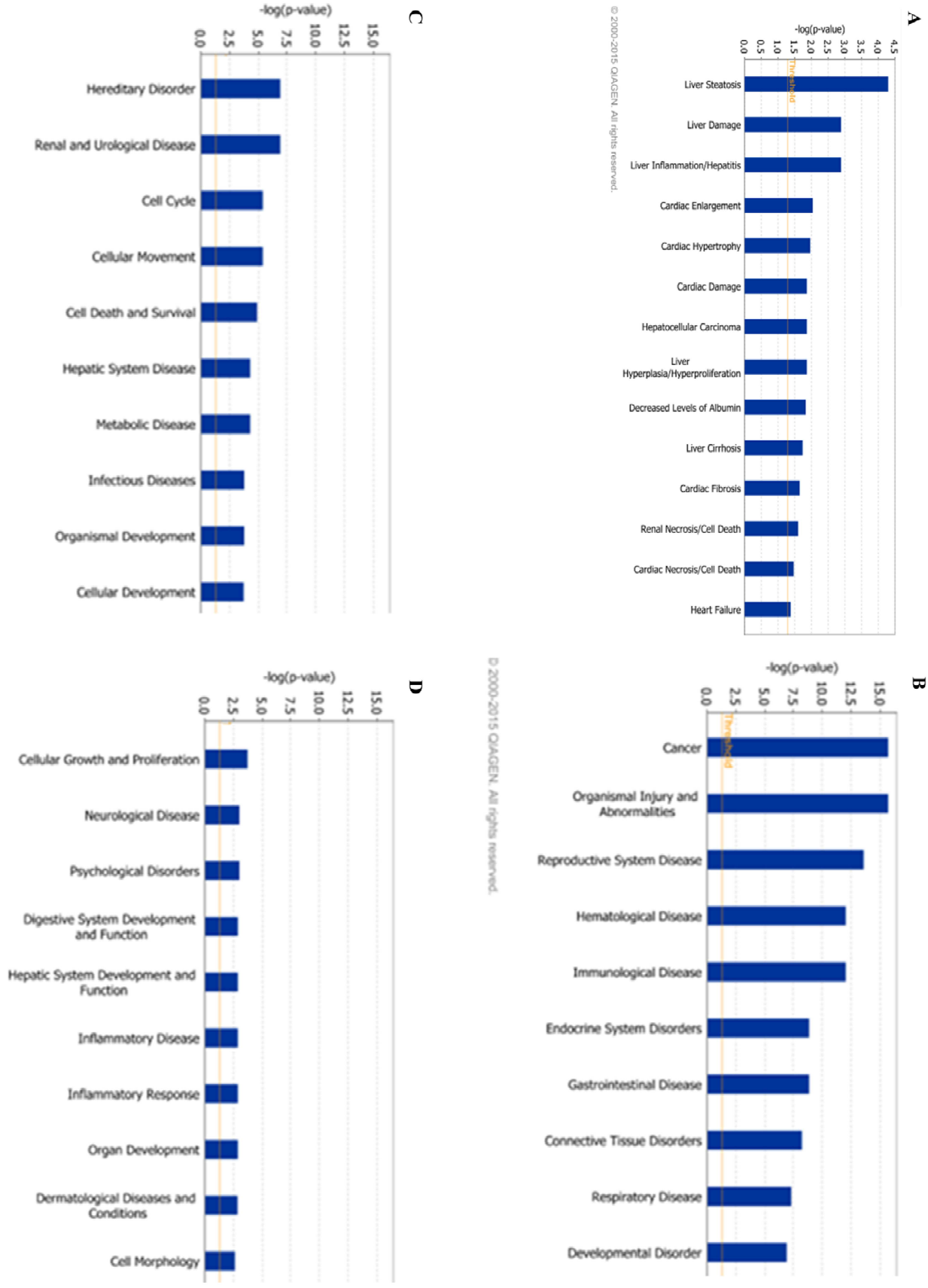
A
-log(p-value)
0.0
0.5
1.0
1.5
2.0
2.5
3.0
3.5
4.0
4.5
Threshold
Liver Steatosis
Liver Damage
Liver Inflammation/Hepatitis
Cardiac Enlargement
Cardiac Hypertrophy
Cardiac Damage
Hepatocellular Carcinoma
Liver Hyperplasia/Hyperproliferation
Decreased Levels of Albumin
Liver Cirrhosis
Cardiac Fibrosis
Renal Necrosis/Cell Death
Cardiac Necrosis/Cell Death
Heart Failure
© 2000-2015 QIAGEN. All rights reserved.
B
-log(p-value)
0.0
2.5
5.0
7.5
10.0
12.5
15.0
Threshold
Cancer
Organismal Injury and Abnormalities
Reproductive System Disease
Hematological Disease
Immunological Disease
Endocrine System Disorders
Gastrointestinal Disease
Connective Tissue Disorders
Respiratory Disease
Developmental Disorder
© 2000-2015 QIAGEN. All rights reserved.
C
-log(p-value)
0.0
2.5
5.0
7.5
10.0
12.5
15.0
Hereditary Disorder
Renal and Urological Disease
Cell Cycle
Cellular Movement
Cell Death and Survival
Hepatic System Disease
Metabolic Disease
Infectious Diseases
Organismal Development
Cellular Development
D
-log(p-value)
0.0
2.5
5.0
7.5
10.0
12.5
15.0
Cellular Growth and Proliferation
Neurological Disease
Psychological Disorders
Digestive System Development and Function
Hepatic System Development and Function
Inflammatory Disease
Inflammatory Response
Organ Development
Dermatological Diseases and Conditions
Cell Morphology

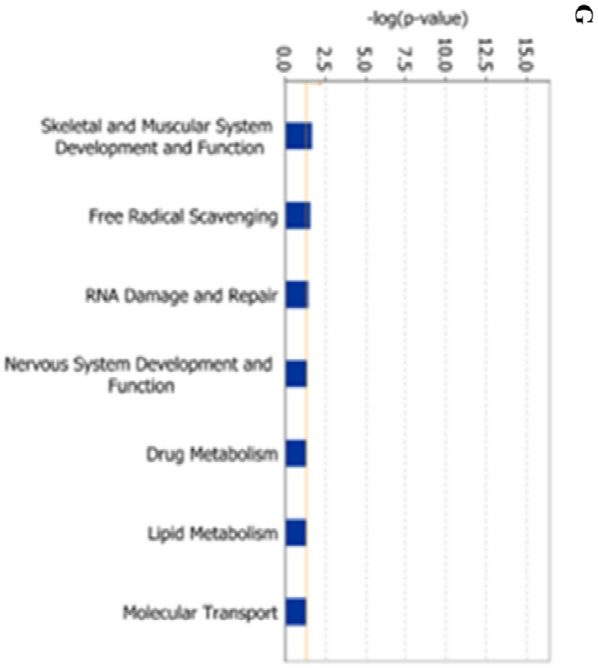
G
-log(p-value)
0.0
2.5
5.0
7.5
10.0
12.5
15.0
Skeletal and Muscular System Development and Function
Free Radical Scavenging
RNA Damage and Repair
Nervous System Development and Function
Drug Metabolism
Lipid Metabolism
Molecular Transport

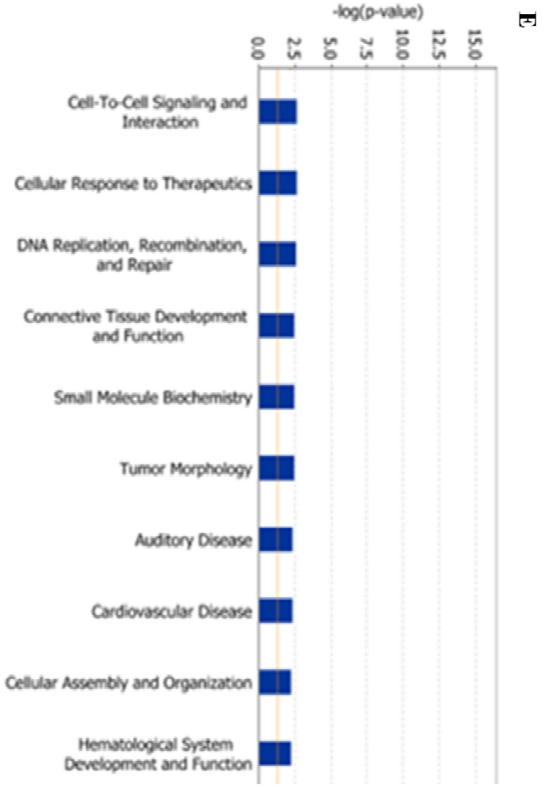
E
-log(p-value)
0.0
2.5
5.0
7.5
10.0
12.5
15.0
Cell-To-Cell Signaling and Interaction
Cellular Response to Therapeutics
DNA Replication, Recombination, and Repair
Connective Tissue Development and Function
Small Molecule Biochemistry
Tumor Morphology
Auditory Disease
Cardiovascular Disease
Cellular Assembly and Organization
Hematological System Development and Function

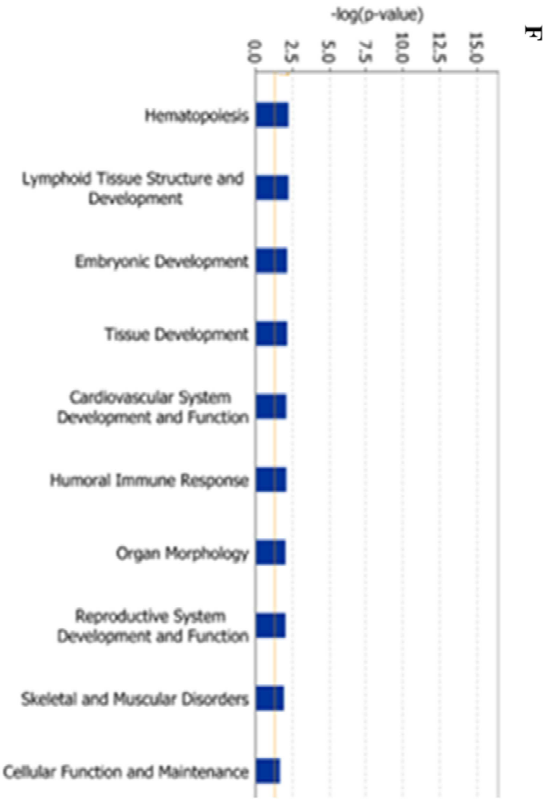
F
-log(p-value)
0.0
2.5
5.0
7.5
10.0
12.5
15.0
Hematopoiesis
Lymphoid Tissue Structure and Development
Embryonic Development
Tissue Development
Cardiovascular System Development and Function
Humoral Immune Response
Organ Morphology
Reproductive System Development and Function
Skeletal and Muscular Disorders
Cellular Function and Maintenance

Figure 4.4. H1 SCDHs versus H1 hESCs IPA analysis. (A) The toxicological functions associated with the set of miRNAs that showed an absolute value log fold change greater than 4 between H1 SCDHs and H1 hESCs. (B)-(G) The biological functions and diseases associated with the set of miRNAs that showed an absolute value log fold change greater than 4 between H1 SCDHs and H1 hESCs. The functions have been broken into sets of 10, with the highest 10 in (B) and the lowest in (G). The threshold line represents the –log of *p*-value 0.05.

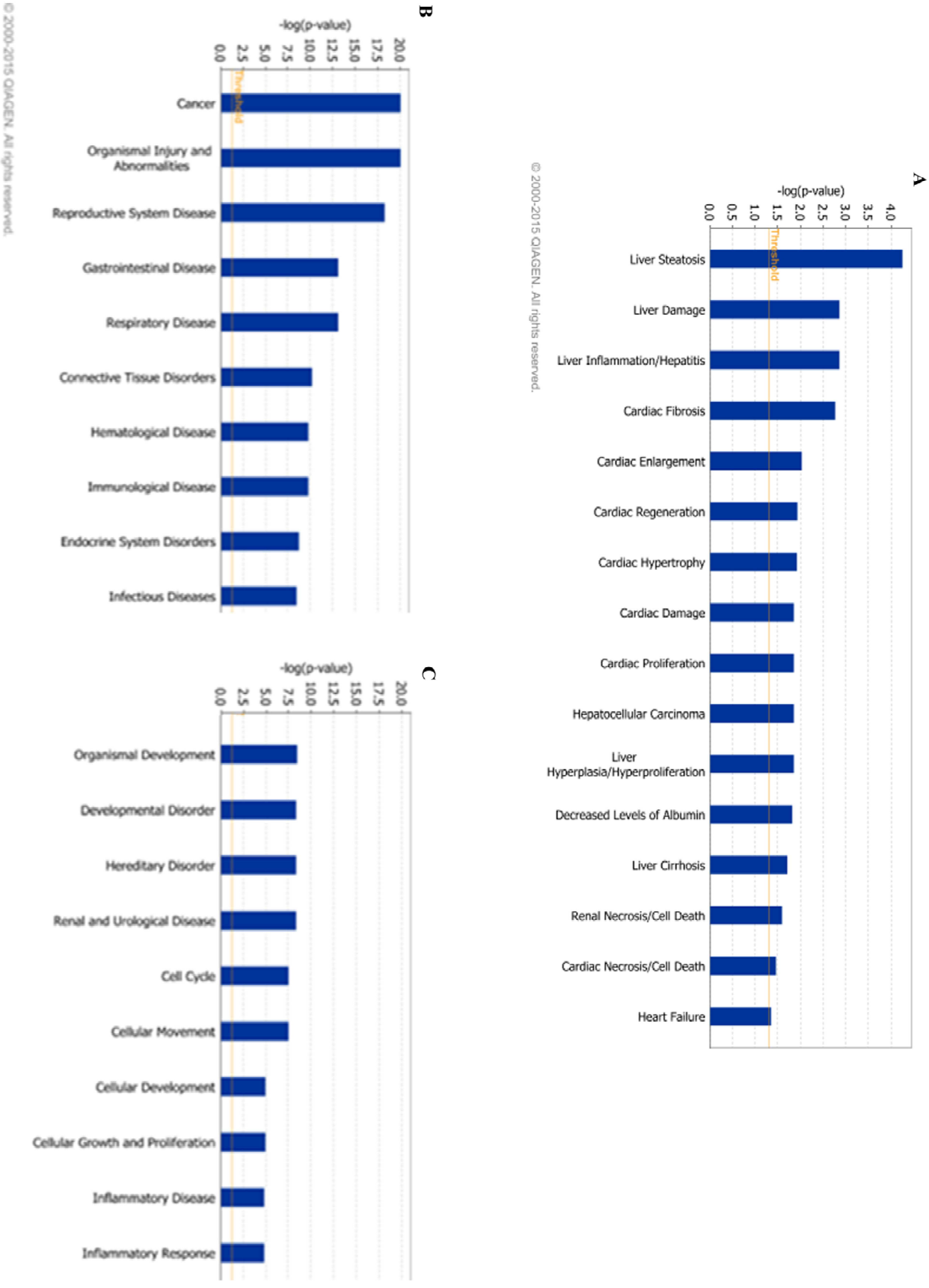
A
-log(p-value)
0.0
0.5
1.0
1.5
2.0
2.5
3.0
3.5
4.0
Threshold
Liver Steatosis
Liver Damage
Liver Inflammation/Hepatitis
Cardiac Fibrosis
Cardiac Enlargement
Cardiac Regeneration
Cardiac Hypertrophy
Cardiac Damage
Cardiac Proliferation
Hepatocellular Carcinoma
Liver Hyperplasia/Hyperproliferation
Decreased Levels of Albumin
Liver Cirrhosis
Renal Necrosis/Cell Death
Cardiac Necrosis/Cell Death
Heart Failure
© 2000-2015 QIAGEN. All rights reserved.
B
-log(p-value)
0.0
2.5
5.0
7.5
10.0
12.5
15.0
17.5
20.0
Threshold
Cancer
Organismal Injury and Abnormalities
Reproductive System Disease
Gastrointestinal Disease
Respiratory Disease
Connective Tissue Disorders
Hematological Disease
Immunological Disease
Endocrine System Disorders
Infectious Diseases
© 2000-2015 QIAGEN. All rights reserved.
C
-log(p-value)
0.0
2.5
5.0
7.5
10.0
12.5
15.0
17.5
20.0
Organismal Development
Developmental Disorder
Hereditary Disorder
Renal and Urological Disease
Cell Cycle
Cellular Movement
Cellular Development
Cellular Growth and Proliferation
Inflammatory Disease
Inflammatory Response

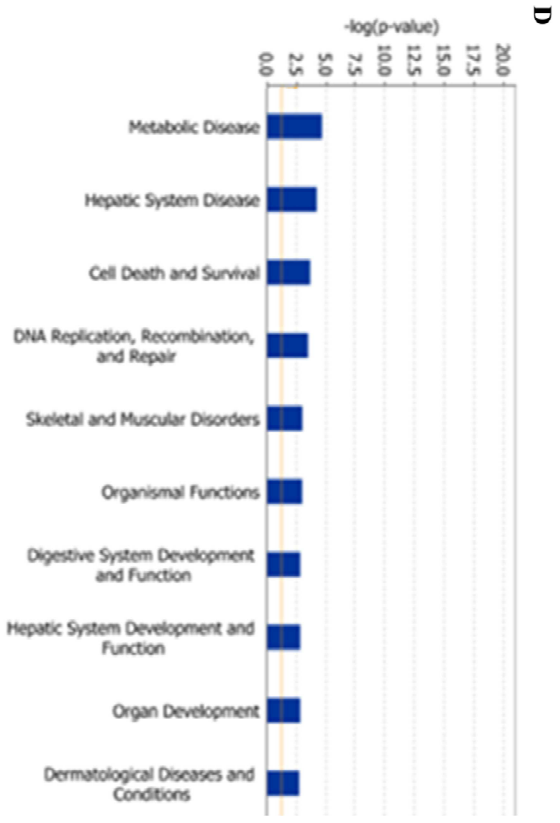
D
-log(p-value)
0.0
2.5
5.0
7.5
10.0
12.5
15.0
17.5
20.0
Metabolic Disease
Hepatic System Disease
Cell Death and Survival
DNA Replication, Recombination, and Repair
Skeletal and Muscular Disorders
Organismal Functions
Digestive System Development and Function
Hepatic System Development and Function
Organ Development
Dermatological Diseases and Conditions

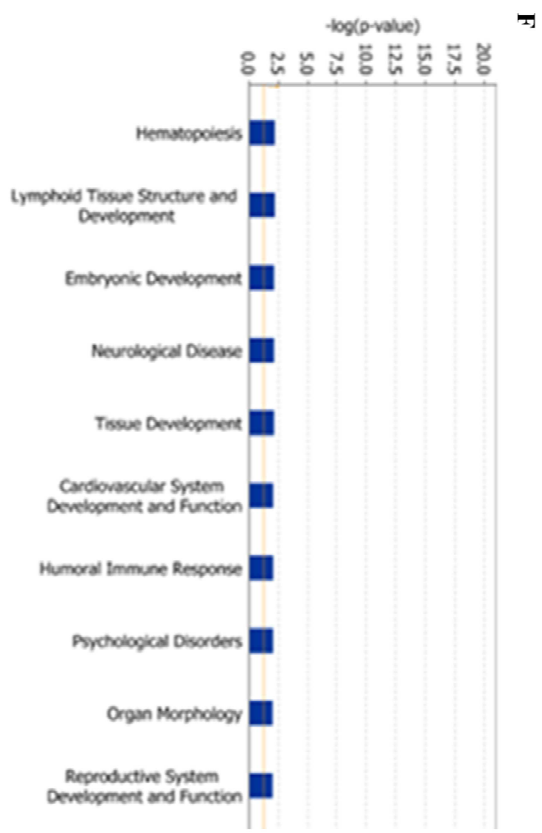
F
-log(p-value)
0.0
2.5
5.0
7.5
10.0
12.5
15.0
17.5
20.0
Hematopoiesis
Lymphoid Tissue Structure and Development
Embryonic Development
Neurological Disease
Tissue Development
Cardiovascular System Development and Function
Humoral Immune Response
Psychological Disorders
Organ Morphology
Reproductive System Development and Function

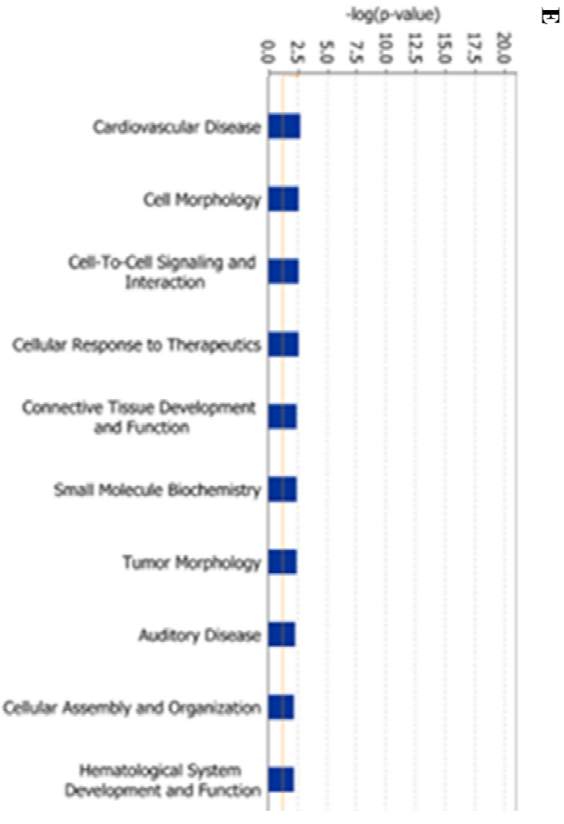
E
-log(p-value)
0.0
2.5
5.0
7.5
10.0
12.5
15.0
17.5
20.0
Cardiovascular Disease
Cell Morphology
Cell-To-Cell Signaling and Interaction
Cellular Response to Therapeutics
Connective Tissue Development and Function
Small Molecule Biochemistry
Tumor Morphology
Auditory Disease
Cellular Assembly and Organization
Hematological System Development and Function

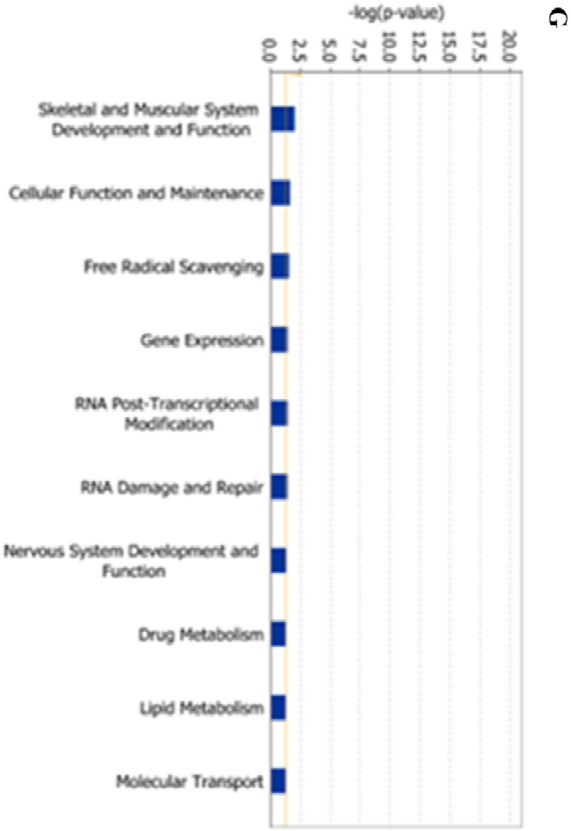
G
-log(p-value)
0.0
2.5
5.0
7.5
10.0
12.5
15.0
17.5
20.0
Skeletal and Muscular System Development and Function
Cellular Function and Maintenance
Free Radical Scavenging
Gene Expression
RNA Post-Transcriptional Modification
RNA Damage and Repair
Nervous System Development and Function
Drug Metabolism
Lipid Metabolism
Molecular Transport

Figure 4.5. H9 SCDHs versus H9 hESCs IPA analysis. (A) The toxicological functions associated with the set of miRNAs that showed an absolute value log fold change greater than 4 between H9 SCDHs and H9 hESCs. (B)-(G) The biological functions and diseases associated with the set of miRNAs that showed an absolute value log fold change greater than 4 between H9 SCDHs and H9 hESCs. The functions have been broken into sets of 10, with the highest 10 in (B) and the lowest in (G). The threshold line represents the –log of *p*-value 0.05.

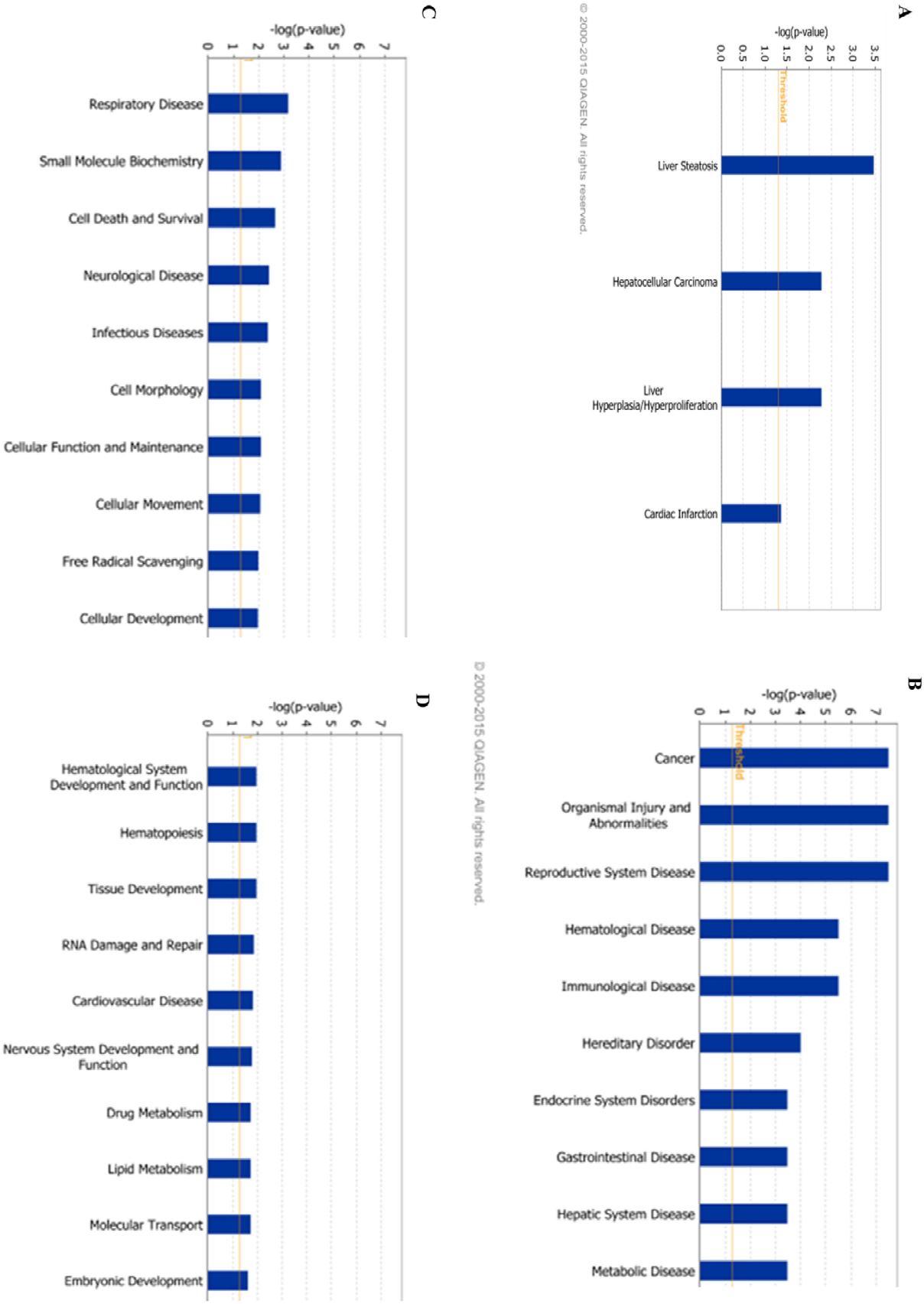
A
-log(p-value)
0.0
0.5
1.0
1.5
2.0
2.5
3.0
3.5
Threshold
Liver Steatosis
Hepatocellular Carcinoma
Liver Hyperplasia/Hyperproliferation
Cardiac Infarction
© 2000-2015 QIAGEN. All rights reserved.
B
-log(p-value)
0
1
2
3
4
5
6
7
Threshold
Cancer
Organismal Injury and Abnormalities
Reproductive System Disease
Hematological Disease
Immunological Disease
Hereditary Disorder
Endocrine System Disorders
Gastrointestinal Disease
Hepatic System Disease
Metabolic Disease
© 2000-2015 QIAGEN. All rights reserved.
C
-log(p-value)
0
1
2
3
4
5
6
7
Respiratory Disease
Small Molecule Biochemistry
Cell Death and Survival
Neurological Disease
Infectious Diseases
Cell Morphology
Cellular Function and Maintenance
Cellular Movement
Free Radical Scavenging
Cellular Development
D
-log(p-value)
0
1
2
3
4
5
6
7
Hematological System Development and Function
Hematopoiesis
Tissue Development
RNA Damage and Repair
Cardiovascular Disease
Nervous System Development and Function
Drug Metabolism
Lipid Metabolism
Molecular Transport
Embryonic Development

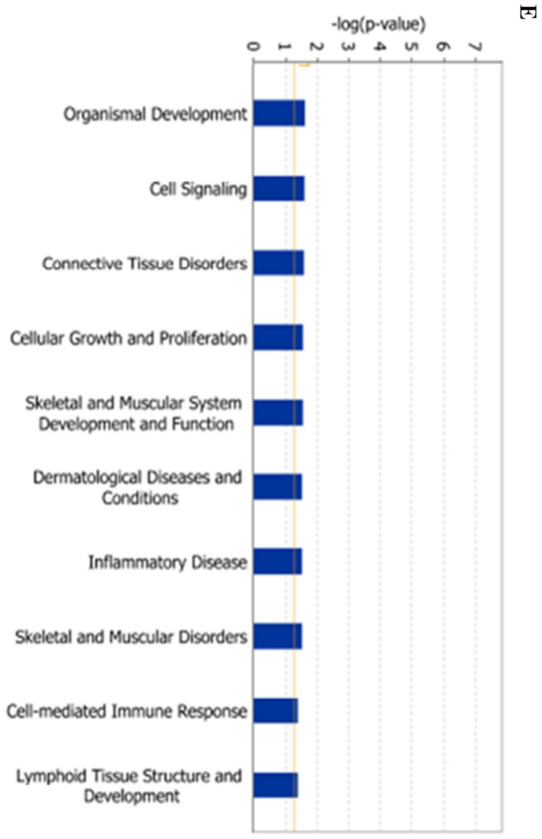
E
-log(p-value)
0
1
2
3
4
5
6
7
Organismal Development
Cell Signaling
Connective Tissue Disorders
Cellular Growth and Proliferation
Skeletal and Muscular System Development and Function
Dermatological Diseases and Conditions
Inflammatory Disease
Skeletal and Muscular Disorders
Cell-mediated Immune Response
Lymphoid Tissue Structure and Development

Figure 4.6. iPSC SCDHs versus iPSCs IPA analysis. (A) The toxicological functions associated with the set of miRNAs that showed an absolute value log fold change greater than 4 between iPSC SCDHs and iPSCs. (B)-(E) The biological functions and diseases associated with the set of miRNAs that showed an absolute value log fold change greater than 4 between iPSC SCDHs and iPSCs. The functions have been broken into sets of 10, with the highest 10 in (B) and the lowest in (E). The threshold line represents the –log of *p*-value 0.05.

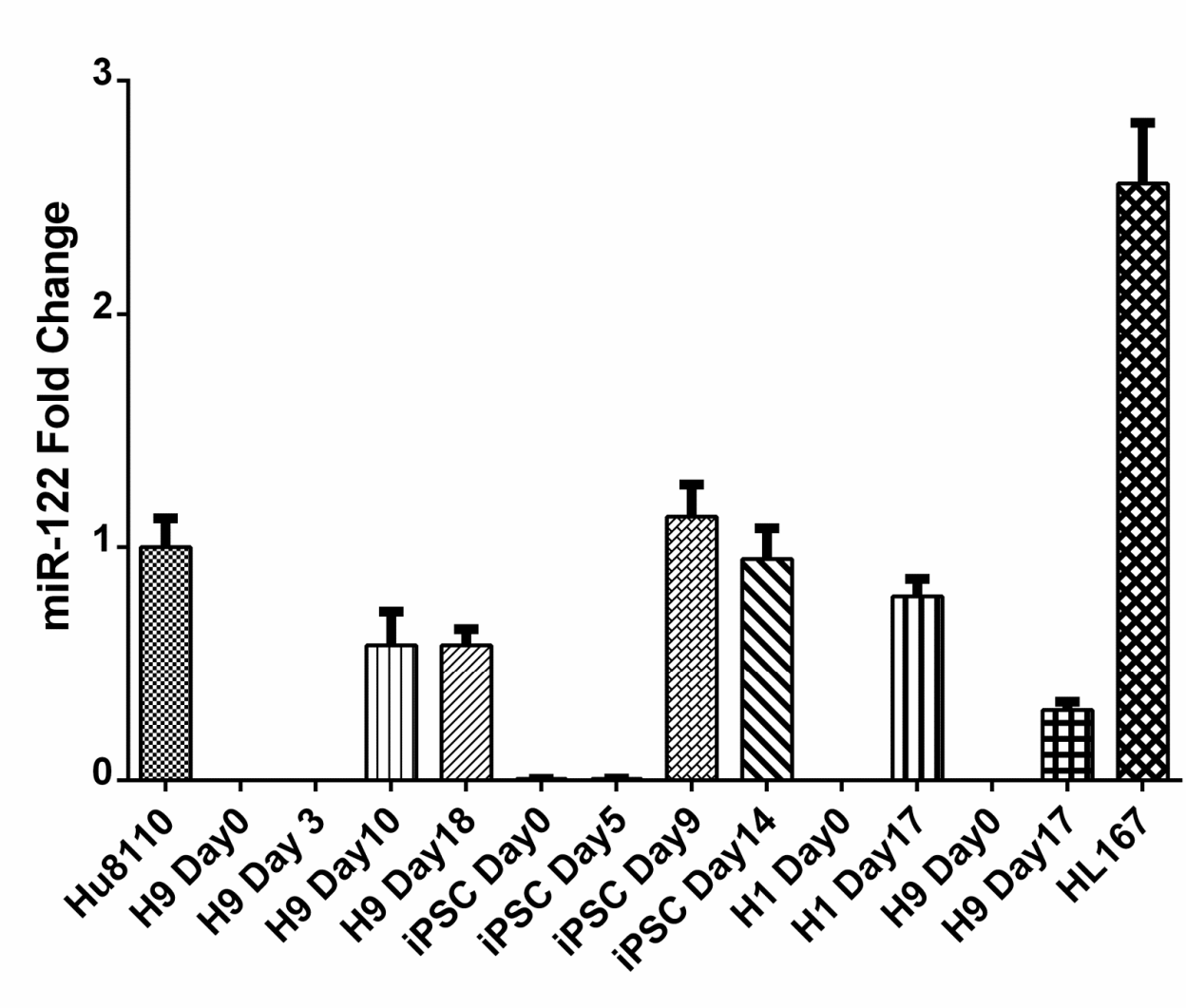

Figure 4.7. miR-122 qRT-PCR. Gene expression results for miR-122 shown as fold change compared to cryopreserved hepatocyte lot Hu8110, which was set to 1. HL167 represents human liver bank sample 167. The following samples were found to be below the limit of quantitation (BLQ): H1 Day 0, H9 Day 0.

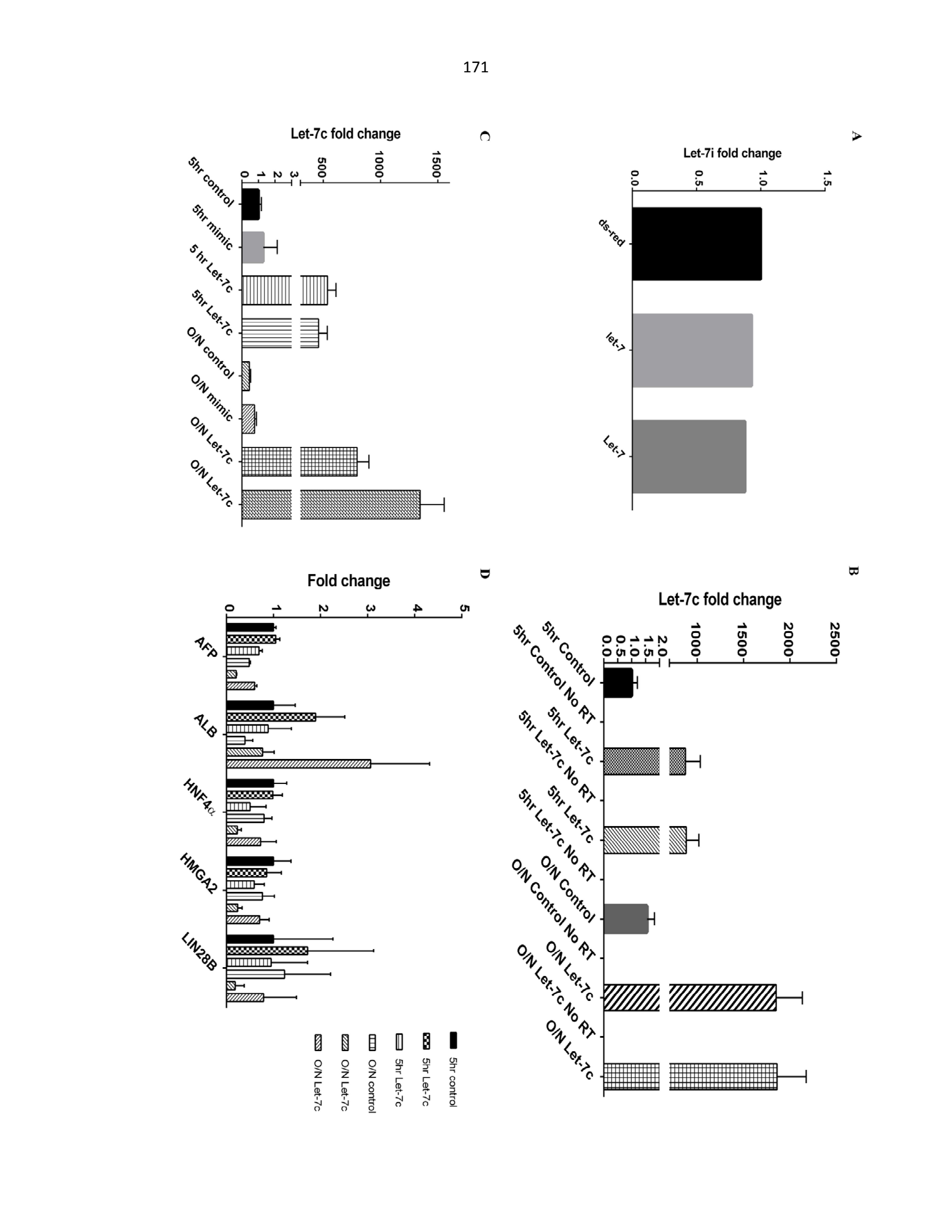
A
Let-7i fold change
0.0
0.5
1.0
1.5
ds-red
let-7
Let-7
B
Let-7c fold change
0.0
0.5
1.0
1.5
2.0
1000
1500
2000
2500
5hr Control
5hr Control No RT
5hr Let-7c
5hr Let-7c No RT
5hr Let-7c
5hr Let-7c No RT
O/N Control
O/N Control No RT
O/N Let-7c
O/N Let-7c No RT
O/N Let-7c
C
Let-7c fold change
0
1
2
3
500
1000
1500
5hr control
5hr mimic
5 hr Let-7c
5hr Let-7c
O/N control
O/N mimic
O/N Let-7c
O/N Let-7c
D
Fold change
0
1
2
3
4
5
AFP
ALB
HNF4α
HMGA2
LIN28B
5hr control
5hr Let-7c
5hr Let-7c
O/N control
O/N Let-7c
O/N Let-7c

Figure 4.8. Let-7 qRT-PCR. (A) Gene expression results for let-7i following transduction with either pLKO-let7i or pLKO-dsred. Results are shown as fold change compared to the ds-red control, which was set to 1. **(B)** Gene expression results for let-7c following transfection with either a let-7c mimic or a control mimic, with or without reverse transcriptase (RT). Results are shown as fold change compared to the 5 hour transfection control, which was set to 1. All no RT samples were found to be below the limit of quantitation (BLQ). **(C)** Gene expression results for let-7c following transfection with let-7 mimic or a control mimic. 5-hour control and O/N control represent no transfection controls. Results are shown as fold change compared to the 5 hour no transfection control, which was set to 1. **(D)** Gene expression results for AFP, ALB, HNF4α, HMGA2, LIN28B following transfection with let-7c mimic or a control mimic. Results are shown as fold change compared to the 5-hour transfection control, which was set to 1. O/N = overnight.

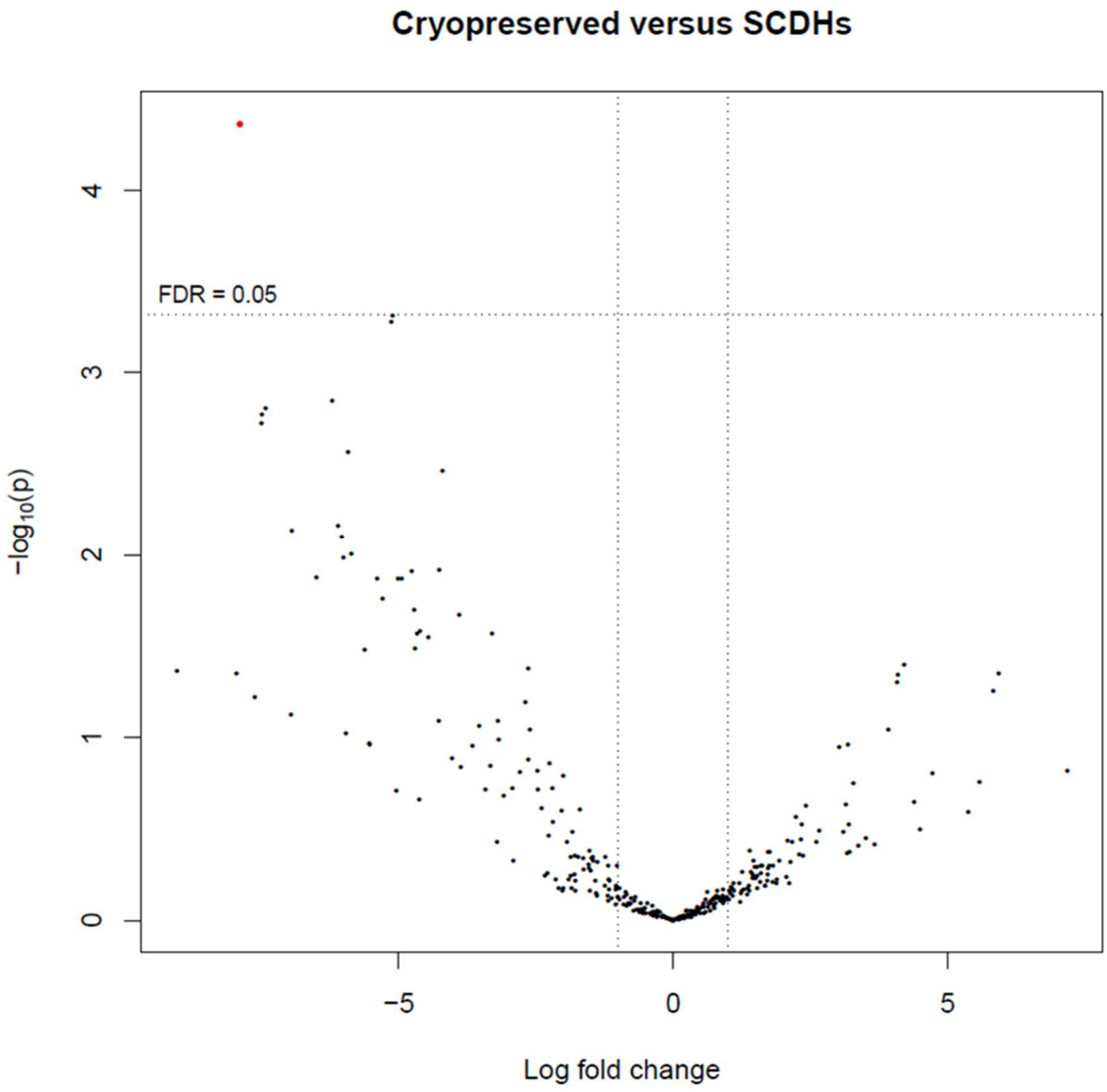

Figure 4.9. Cryopreserved hepatocytes versus SCDHs volcano plot. A volcano plot of miRNA results comparing SCDHs to cryopreserved hepatocytes. The x-axis is the $\log_2$ fold change of miRNAs between the two groups. The y-axis is the –log(*p*-value). The dashed vertical lines represent a 1.5 log fold change, and the dashed horizontal line represents an FDR *p*-value of 0.05. The red dot represents miR-205, found to be significantly different with a large fold change between SCDHs and cryopreserved hepatocytes.

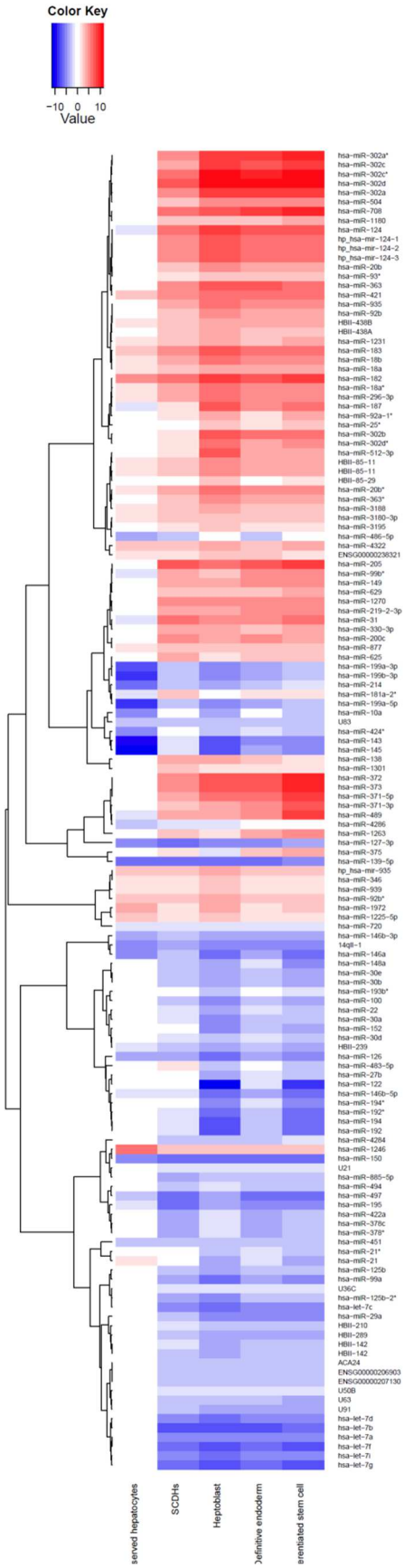
Color Key
−10 0 10
Value
hsa-miR-302a*
hsa-miR-302c
hsa-miR-302c*
hsa-miR-302d
hsa-miR-302a
hsa-miR-504
hsa-miR-708
hsa-miR-1180
hsa-miR-124
hp_hsa-mir-124-1
hp_hsa-mir-124-2
hp_hsa-mir-124-3
hsa-miR-20b
hsa-miR-93*
hsa-miR-363
hsa-miR-421
hsa-miR-935
hsa-miR-92b
HBII-438B
HBII-436A
hsa-miR-1231
hsa-miR-183
hsa-miR-16b
hsa-miR-16a
hsa-miR-182
hsa-miR-18a*
hsa-miR-296-3p
hsa-miR-187
hsa-miR-92a-1*
hsa-miR-25*
hsa-miR-302b
hsa-miR-302d*
hsa-miR-512-3p
HBII-85-11
HBII-85-11
HBII-85-29
hsa-miR-20b*
hsa-miR-363*
hsa-miR-3188
hsa-miR-3180-3p
hsa-miR-3195
hsa-miR-486-5p
hsa-miR-4322
ENSG00000238321
hsa-miR-205
hsa-miR-99b*
hsa-miR-149
hsa-miR-629
hsa-miR-1270
hsa-miR-219-2-3p
hsa-miR-31
hsa-miR-330-3p
hsa-miR-200c
hsa-miR-877
hsa-miR-625
hsa-miR-199a-3p
hsa-miR-199b-3p
hsa-miR-214
hsa-miR-181a-2*
hsa-miR-199a-5p
hsa-miR-10a
U83
hsa-miR-424*
hsa-miR-143
hsa-miR-145
hsa-miR-138
hsa-miR-1301
hsa-miR-372
hsa-miR-373
hsa-miR-371-5p
hsa-miR-371-3p
hsa-miR-489
hsa-miR-4286
hsa-miR-1263
hsa-miR-127-3p
hsa-miR-375
hsa-miR-139-5p
hp_hsa-mir-935
hsa-miR-346
hsa-miR-939
hsa-miR-92b*
hsa-miR-1972
hsa-miR-1225-5p
hsa-miR-720
hsa-miR-146b-3p
14q8-1
hsa-miR-146a
hsa-miR-148a
hsa-miR-30e
hsa-miR-30b
hsa-miR-193b*
hsa-miR-100
hsa-miR-22
hsa-miR-30a
hsa-miR-152
hsa-miR-30d
HBII-239
hsa-miR-126
hsa-miR-483-5p
hsa-miR-27b
hsa-miR-122
hsa-miR-146b-5p
hsa-miR-194*
hsa-miR-192*
hsa-miR-194
hsa-miR-192
hsa-miR-4284
hsa-miR-1246
hsa-miR-150
U21
hsa-miR-885-5p
hsa-miR-494
hsa-miR-497
hsa-miR-195
hsa-miR-422a
hsa-miR-378c
hsa-miR-378*
hsa-miR-451
hsa-miR-21*
hsa-miR-21
hsa-miR-125b
hsa-miR-99a
U36C
hsa-miR-125b-2*
hsa-let-7c
hsa-miR-29a
HBII-210
HBII-289
HBII-142
HBII-142
ACA24
ENSG00000206903
ENSG00000207130
U50B
U63
U91
hsa-let-7d
hsa-let-7b
hsa-let-7a
hsa-let-7f
hsa-let-7i
hsa-let-7g
served hepatocytes
SCDHs
Heptoblast
Definitive endoderm
orentiated stem cell

Figure 4.10. Heatmap. Heatmap representing miRNA expression differences comparing the liver bank, cryopreserved hepatocytes, SCDHs, hepatoblast cells, definitive endoderm cells, and undifferentiated stem cells. The liver bank was used as the reference to generate the heat map. Each column represents the log fold change between the given sample type and the liver bank. Red means the miRNA is up-regulated compared to the liver bank, blue means the miRNA is down-regulated compared to the liver bank, white means no change. The brackets on the left are a dendrogram, showing groups of similar genes that are clustered together.

Table 4.1. Comparison of miRNAs with log fold change greater than 4 between SCDHs and cryopreserved hepatocytes.

Down-regulated		Up-regulated	
miRNA	**Log Fold Change**	**miRNA**	**Log Fold Change**
hsa-let-7b	-7.27	hsa-miR-145	8.95
hsa-let-7f	-6.02	hsa-miR-143	7.86
hsa-let-7g	-5.92	hsa-miR-205	7.79
hsa-let-7d	-5.67	hsa-miR-125a-5p	7.53
hsa-let-7c	-5.47	hsa-miR-124	7.41
hsa-let-7i	-4.81	hsa-miR-31	7.40
hsa-let-7a	-4.59	hsa-miR-708	7.33
hsa-miR-195	-4.48	hsa-miR-99b	6.87
ENSG00000207130	-4.30	hsa-miR-302d	6.85
ACA24	-4.19	hsa-miR-302c*	6.41
ENSG00000206903	-4.17	hsa-miR-99b*	6.11
hsa-miR-378i	-4.16	hp_hsa-mir-124-1	6.01
hsa-miR-125b-2*	-4.01	hp_hsa-mir-124-2	5.94
		hsa-miR-424*	5.91
		hsa-miR-199a-5p	5.86
		hsa-miR-363	5.83
		hp_hsa-mir-124-3	5.77
		hsa-miR-200c	5.53
		hsa-miR-199a-3p	5.44
		hsa-miR-199b-3p	5.44
		hsa-miR-149	5.30
		hsa-miR-302a	5.20
		hsa-miR-138	5.04
		hsa-miR-1270	5.02
		hsa-miR-214	4.95
		hsa-miR-10a	4.92
		hsa-miR-301a	4.86
		hsa-miR-372	4.85
		hsa-miR-489	4.67
		hsa-miR-373	4.63
		hsa-miR-302a*	4.61
		hsa-miR-302c	4.57
		hsa-miR-20b	4.53
		hsa-miR-371-5p	4.52
		hsa-miR-625	4.37
		hsa-miR-92b	4.18
		hsa-miR-935	4.17
		hsa-miR-219-2-3p	4.11

Table 4.2. Comparison of miRNAs with log fold change greater than 4 between SCDHs and liver bank.

Downregulated		Upregulated	
miRNA	**Log Fold Change**	**miRNA**	**Log Fold Change**
hsa-let-7b	-7.36	hsa-miR-205	7.64
hsa-miR-195	-6.47	hsa-miR-302d	7.07
hsa-let-7f	-6.43	hsa-miR-302c*	6.64
hsa-miR-150	-6.42	hsa-miR-182	6.50
hsa-miR-497	-6.20	hsa-miR-708	6.49
hsa-let-7g	-6.18	hsa-miR-124	6.01
hsa-miR-127-3p	-5.78	hsa-miR-31	5.96
hsa-miR-139-5p	-5.73	hsa-miR-363	5.68
hsa-let-7d	-5.45	hsa-miR-200c	5.68
hsa-let-7c	-5.45	hp_hsa-mir-124-1	5.64
hsa-let-7i	-5.41	hp_hsa-mir-124-2	5.39
hsa-let-7a	-5.02	hsa-miR-1270	5.33
14qII-1	-4.45	hp_hsa-mir-124-3	5.24
hsa-miR-99a	-4.00	hsa-miR-302a	5.23
		hsa-miR-421	5.12
		hsa-miR-372	4.88
		hsa-miR-183	4.78
		hsa-miR-373	4.75
		hsa-miR-302a*	4.74
		hsa-miR-149	4.63
		hsa-miR-371-5p	4.56
		hsa-miR-302c	4.54
		hsa-miR-99b*	4.50
		hsa-miR-935	4.31
		hsa-miR-219-2-3p	4.30
		hsa-miR-18b	4.17

Table 4.3. Comparison of miRNAs with log fold change greater than 4 between H1 SCDHs and H1 hESCs.

Downregulated		**Upregulated**	
miRNA	**Log Fold Change**	**miRNA**	**Log Fold Change**
hsa-miR-373	-6.86	hsa-miR-122	12.82
hsa-miR-512-3p	-6.47	hsa-miR-143	7.05
hsa-miR-371-3p	-6.31	hsa-miR-152	6.43
hsa-miR-302b	-6.26	hsa-miR-145	6.36
hsa-miR-372	-5.96	hsa-miR-194	6.32
hsa-miR-517a	-5.65	hsa-miR-192	5.88
hsa-miR-371-5p	-5.24	hsa-miR-375	5.53
hsa-miR-302d*	-4.85	hsa-miR-146b-5p	5.40
hsa-miR-187	-4.80	hsa-miR-199a-5p	5.29
hsa-miR-302a*	-4.70	hsa-miR-194*	5.22
hsa-miR-302a	-4.63	hsa-miR-181a-2*	5.07
hsa-miR-498	-4.50	hsa-miR-214	4.87
hsa-miR-302c	-4.28	hsa-miR-181a	4.46
hp_hsa-mir-124-3	-4.17	hsa-miR-181b	4.29
hsa-miR-92a-2*	-4.13	hsa-miR-574-3p	4.27
hsa-miR-3622a-5p	-4.04	hsa-miR-22	4.18
		hsa-miR-424*	4.13
		hsa-miR-21	4.03
		hsa-miR-21*	4.01

Table 4.4. Comparison of miRNAs with log fold change greater than 4 between H9 SCDHs and H9 hESCs.

Downregulated		**Upregulated**	
miRNA	**Log Fold Change**	**miRNA**	**Log Fold Change**
hsa-miR-302b	-6.14	hsa-miR-122	12.62
hsa-miR-512-3p	-5.31	hsa-miR-143	8.37
hsa-miR-92a-2*	-5.12	hsa-miR-145	7.46
hsa-miR-517a	-5.12	hsa-miR-194	6.17
hsa-miR-302c*	-5.04	hsa-miR-192	6.10
hsa-miR-302a*	-5.03	hsa-miR-199a-5p	6.01
hsa-miR-187	-4.37	hsa-miR-152	5.33
hsa-miR-302c	-4.31	hsa-miR-146b-5p	5.33
hsa-miR-302a	-4.30	hsa-miR-199b-3p	5.17
hsa-miR-302d*	-4.27	hsa-miR-199a-3p	4.96
hsa-miR-363*	-4.26	hsa-miR-483-5p	4.91
hsa-miR-20b*	-4.01	hsa-miR-10a	4.87
		hsa-miR-21	4.86
		hsa-miR-375	4.86
		hsa-miR-424*	4.55
		hsa-miR-675	4.35
		hsa-miR-194*	4.32
		hsa-miR-214	4.26
		hsa-miR-30a*	4.10
		hsa-miR-30a	4.09

Table 4.5. Comparison of miRNAs with log fold change greater than 4 between iPSC SCDHs and iPSCs.

Downregulated		**Upregulated**	
miRNA	**Log Fold Change**	**miRNA**	**Log Fold Change**
hsa-miR-187	-4.28	hsa-miR-10a	5.89
hsa-miR-517a	-4.26	hsa-miR-483-5p	5.41
hsa-miR-512-3p	-4.24	hsa-miR-122	5.18
		hsa-miR-194	4.95
		hsa-miR-192	4.94
		hsa-miR-146b-5p	4.32
		hsa-miR-194*	4.29

Chapter 5

Summary and General Conclusions

The work presented in this dissertation explores the potential of stem cell derived hepatocytes (SCDHs) to be used as an *in vitro* pre-clinical model for drug metabolism studies. Namely, we focus on further identifying how similar SCDHs are to primary human hepatocytes with regard to drug-metabolizing enzymes. Moreover, we performed genotype profiling on the commonly used human embryonic stem cell lines (hESCs) to further identify their utility in pharmacogenetic screening. In addition, we investigated the miRNA expression profile of SCDHs to identify miRNA candidates that could improve the maturity of SCDHs.

In general, we showed that SCDHs are immature compared to primary human hepatocytes in terms of the expression and activity of drug-metabolizing enzymes, notably the CYP enzymes. We found that SCDHs more closely resemble fetal hepatocytes regarding expression of hepatocyte markers, drug-metabolizing enzymes, transporters, and transcription factors. This translated into minimal CYP activity for only CYPs 1A and 3A when examining metabolite formation. In addition, we show that the miRNA expression profile of SCDHs compared to stem cells, cryopreserved hepatocytes and human liver tissue indicates global changes associated with immaturity in SCDHs. Taken together, our findings provide a more thorough characterization of SCDHs with regards to their use in drug metabolism studies, and provide insight into a possible mechanism to enhance the maturity and functionality of SCDHs.

In Chapter 2, we sought to demonstrate the utility of SCDHs in pharmacogenetic screening. SCDHs may provide an improved system for evaluating genotype-phenotype relationships, e.g. cytochrome P450 (CYP) gene polymorphisms and their impact on drug metabolism and toxicity. For this, we genotyped the five commonly used WiCell® hESC lines, H1, H7, H9, H13 and H14 using the Affymetrix DMET™ Plus chip array. This array covers a large number of polymorphisms in Absorption, Distribution, Metabolism and Excretion (ADME)

relevant genes. We focused on CYP2D6 in our analysis in utilizing SCDHs for genotype-phenotype predictions, given its highly polymorphic nature and role in metabolizing about 20% of marketed drugs [113, 114]. Genotyping results for CYP2D6 identified H1 as having only one gene copy which also harbors the CYP2D6*41 splicing defect, predictive of a CYP2D6 poor/intermediate metabolizer. We identified no CYP2D6 gene duplications, indicating no representative ultra-rapid metabolizer. The H7 and H14 lines are heterozygous for the non-functional CYP2D6*4 variant resulting in a predicted intermediate metabolizer phenotype. To further test genotype-phenotype relationships for CYP2D6 in SCDHs, we assessed the penetrance of CYP2D6*41, a splicing defect which results in a CYP2D6 splice product lacking exon 6, through use of a reverse-transcription PCR assay. Through reverse-transcription PCR, we were able to demonstrate the CYPP2D6*41 splicing defect displays incomplete penetrance, with similar results observed in SCDHs and liver tissue. Genotyping results for other CYP enzymes identified all 5 hESC lines to be homozygous for CYP3A5*3, a null allele, meaning they are all CYP3A5 non-expressors. We found the H14 line to be homozygous for CYP2C9*2 and H1 to be heterozygous for CYP2C9*3, which both result in decreased CYP2C9 activity. Regarding Phase II enzymes, we identified hESC lines H7, H13, and H14 as heterozygous for the UGT1A1*28 allele, which results in reduced activity of UGT1A1. And we found hESC lines H1, H7, and H14 to be heterozygous for the NAT2*5 allele and H13 to be homozygous for this allele, likely resulting in slow acetylator status for these cell lines.

Induced pluripotent stem cells (iPSCs) allow for collection of cells from individuals with various ethnic and genetic backgrounds, potentiating establishment of cell banks with defined genetic profiles for conducting pharmacogenetic profiling of drug metabolism. With this in mind, we collected peripheral blood mononuclear cells (PBMCs) from used Pall filters from the

Puget Sound Blood Center to genotype and use in pharmacogenetic screening of the CYP enzymes. We collected cells from a total of 170 Pall filters, numbered as F1 – F170. Genotyping of the major polymorphisms associated with CYPs 2B6, 2C9, 2C19, 2D6 and 3A5 was performed on a portion of the collected samples. The genotyping results for CYP2D6 are shown in Table 5.1, and all other CYPs are in Table 5.2. From this genotyping we have identified four donors (F40, F52, F53 and F61) homozygous for the non-functional CYP2D6*4 allele, indicating they would have no functional CYP2D6 activity and represent CYP2D6 poor metabolizers, Table 5.1. Additionally, we have identified one donor, F9, homozygous for the CYP2D6*41 allele, which causes a splicing defect of variable penetrance. From the donors genotyped, we have identified 7 donors (F13, F15, F17, F22, F29, F43 and F54) heterozygous for the CYP3A5*3 null allele, meaning they would represent CYP3A5 expressors, Table 5.2. We identified a number of donors heterozygous for the CYP2C9*2 allele, with no homozygous donors, and only 3 donors (F47, F58 and F62) heterozygous for the CYP2C9*3 allele, with no homozygous donors, both of these alleles result in decreased CYP2C9 activity. This bank of cells was established with the aim of being used to generate iPSC lines with defined CYP genotype profiles for pharmacogenetic screening.

The pharmacogenetic data presented in Chapter 2 on CYPs, and other polymorphic ADME genes, will be critical for understanding metabolism profiles when these hESC lines are used as a target cell source for models of drug metabolism and toxicity. In addition, the establishment of our bank of cells with defined CYP genotypes may be useful in generating iPSC lines for use in predictive drug metabolism/toxicity studies.

In Chapter 3, we sought to further characterize the differentiation status of SCDHs compared to primary hepatocytes, with emphasis on the expression and functional capacity of

drug-metabolizing enzymes. In order to do this, we performed gene expression profiling of pluripotency markers, hepatocyte markers, transcription factors, drug-metabolizing enzymes and transporters for SCDHs, fetal liver tissue, adult liver tissue, cryopreserved hepatocytes and the liver cell line HepaRG. In addition, to evaluate the functional capacity of CYP enzymes in SCDHs, metabolite formation from probe substrates was assessed using a CYP cocktail approach and LC-MS/MS. Based on gene expression profiling we were able to demonstrate that SCDHs have undergone a differentiation process and no longer express pluripotency markers. Gene expression profiling of hepatocyte markers and drug-metabolizing enzymes revealed that SCDHs most closely resemble fetal hepatocytes, especially with regard to known fetal hepatocyte markers AFP, CYP3A7 and FMO1. However, we were able to demonstrate that SCDHs respond to the inducers rifampicin and phenobarbital as measured by fold-increases in expression of CYPs 3A4 and 3A7. Further, functional assay of enzyme activity in SCDHs using a CYP cocktail revealed only minor activity for CYPs 1A and 3A, with this activity being below that observed in primary hepatocytes. This low CYP activity was not surprising given the low expression of CYP enzymes indicated in the gene expression profiling. Overall, these results indicate that SCDHs are still immature hepatocytes, they do not express typical hepatocyte markers, or drug-metabolizing enzymes to the same extent that mature adult hepatocytes do, and they lack functional CYP activity.

The work in Chapters 2 and 3 further demonstrates the need for improved differentiation protocols to generate more mature and functional SCDHs. Enhanced expression and function of drug-metabolizing enzymes in SCDHs would make them a more viable option in the pharmaceutical industry for drug metabolism assays. To address this issue, we sought to investigate the role of miRNAs in hepatocyte differentiation and maturation, with the goal of

identifying miRNAs that could be manipulated in the culture of SCDHs to enhance their maturity and function. This work is presented in Chapter 4. To do this we utilized microRNA microarrays to profile the miRNA expression profile of SCDHs throughout differentiation and compare them to cryopreserved hepatocytes and human liver tissue. From this microarray profiling we were able to identify a large number of differences in miRNA expression between SCDHs, cryopreserved hepatocytes and human liver tissue. Using IPA analysis, we identified the top toxicological pathways associated with those differences in miRNAs to be liver-related, such as liver steatosis, liver damage, hepatocellular carcinoma, and liver inflammation/hepatitis. Among the most prominent patterns in expression differences were the down-regulation of the let-7 family in SCDHs compared to both cryopreserved hepatocytes and liver tissue, and up-regulation of the miR-17-92, 302-367 and 371-373 clusters in SCDHs compared to cryopreserved hepatocytes and liver tissue. The let-7 family of miRNAs are known to exhibit low expression in embryonic tissue and high expression in most all differentiated tissues, indicating the observed low expression of let-7 in SCDHs may be contributing to the observed lack of maturity. Meanwhile, the miR-17-92, 302-367 and 371-373 clusters are normally expressed in pluripotent stem cells, therefore the high expression of these clusters in SCDHs could be another contributing factor to the lack of maturity observed.

The work presented in Chapter 4 is hypothesis-generating, but informative. From the miRNA microarray profiling, we have identified global changes associated with immaturity in SCDHs. The data suggests that the let-7 family of miRNAs, miR-205, or the miR-17-92, miR-302-367, and miR-371-373 clusters may be viable targets for manipulation within the currently used differentiation protocol to enhance the maturation and function of SCDHs.

In summary, this dissertation presented a series of studies aimed at characterizing SCDHs as they compared to cryopreserved hepatocytes and human liver tissue, with a focus on drug-metabolizing enzymes. SCDHs have potential to be used as an *in vitro* pre-clinical model for drug metabolism studies once fully vetted as comparable to primary hepatocytes in regards to the function of drug-metabolizing enzymes and transporters. We have genotyped the commonly used human embryonic stem cell lines for use in pharmacogenetic screening. We have shown that SCDHs are immature, largely resembling fetal hepatocytes in terms of gene expression with minimal CYP activity. Additionally, we show that the miRNA expression profile of SCDHs compared to stem cells, cryopreserved hepatocytes and human liver tissue indicates global changes associated with immaturity in SCDHs. However, we have identified some candidate miRNAs for manipulation in culture of SCDHs that may enhance their maturity and, therefore, the function of drug-metabolizing enzymes. Taken together, our findings provide a more thorough characterization of SCDHs with regards to their use in drug metabolism studies, and provide insight into a possible mechanism to enhance the maturity and functionality of SCDHs. There is still more work to be done to enhance the maturity and functionality of SCDHs if they are to be used as a pre-clinical cell model of drug metabolism.

Table 5.1 PBMC Genotyping for CYP2D6. Hetero. indicates a heterozygous call, Homo. indicates a homozygous call.

	2D6*3 (A Del)	2D6*4 (G>A)	2D6*6 (T Del)	2D6*9 (AAG Del)	2D6*10 (C>T)	2D6*17 (C>T)	2D6*35 (G>C)	2D6*41 (G>A)
F1	AA	GG	TT	Homo. WT	CC	CC	GC	GG
F2	AA	GG	TT	Homo. WT	CC	CT	GG	GG
F3	AA	GG	TT	Homo. WT	CC	CT	GC	GG
F5	AA	GG	TT	Homo. WT	CC	CT	GG	GG
F6	AA	GG	TT	Homo. WT	CC	CT	GG	GA
F7	AA	GG	TT	Homo. WT	CC	CT	GC	GG
F8	AA	GG	TT	Homo. WT	CC	CC	GC	GA
F9	AA	GG	TT	Homo. WT	CC	CC	GG	AA
F10	AA	GG	TT	Homo. WT	CC	CT	GC	GG
F11	Hetero.	GG	TT	Homo. WT	CT	CT	GG	GA
F12	AA	GG	TT	Homo. WT	CT	CT	GC	GA
F13	AA		TT	Hetero.	CT	CT	GG	GG
F14	AA	GG	TT	Homo. WT	CC	CC	GC	GA
F15	AA	GA	TT	Homo. WT	CT	CC	GG	GA
F16	AA	GA	Hetero.	Homo. WT	CT	CC	GG	GG
F17	AA	GG	TT	Homo. WT	CC	CC	GC	GA
F18	AA	GG	TT	Homo. WT	CT	CC	GC	GG
F19	AA	GG	TT	Homo. WT	CT	CC	GG	GG
F20	AA	GG	TT	Homo. WT	CC	CC	GC	GG
F21	AA	GA	TT	Homo. WT	CT	CC	GC	GG
F22	AA	GG	TT	Homo. WT	CC	CC	GC	GG
F23	AA	GA	TT	Homo. WT	TT	CC	GG	GG
F24		GG	TT				GG	
F25	Homo. Del.	GG	TT	Homo. WT	CC	CC	GG	GG
F26	AA	GG	TT	Homo. WT	CC		GC	
F27	AA	GG	TT	Homo. WT	CC	CC	GC	GG
F28	AA	GA	TT	Homo. WT	CT		GG	
F29	AA	GG	TT	Homo. WT	CC	CC	GG	GG
F30	AA	GG	TT	Homo. WT	CC	CC	GC	GG
F31	AA	GG	TT	Homo. WT	CC	CC	GG	GA
F32	AA	GG	TT	Homo. WT	CC	CC	GG	GG
F33	AA	GG	TT	Homo. WT	CC	CT	GG	GG
F34	AA	GG	TT	Homo. WT	CC	CC	GG	GA
F35	AA	GA	TT	Hetero.	CT	CC	GG	GG
F37	AA	GA	TT	Homo. WT	CT	CT	GG	GG
F38	AA	GG	TT	Homo. WT	CC	CT	CC	GG
F39	Hetero.	GG		Homo. WT	CC	CT	GG	GA
F40		AA	TT	Homo. WT	TT	CC	GG	GG

F42	AA	GG	TT	Homo. WT	CT	CT		GG
F43	Hetero.	GG	TT	Homo. WT	CT	CT	GG	GG
F45			TT	Homo. WT	CC			
F46	AA	GA	TT	Homo. WT	CT	CT	GG	GG
F47	AA	GG	TT	Homo. WT	CC	CC	CC	GG
F48	AA	GA	TT	Homo. WT	CT	CC	GC	GG
F49				Homo. WT				
F50	AA	GA	TT		CT	CC	GC	GA
F51	AA	GG	TT	Homo. WT	CT	CT	GG	GG
F52		AA	TT	Homo. WT	TT			
F53		AA	TT	Homo. WT	TT	CC	GG	
F54		GG		Homo. WT	CC			
F55		GG		Homo. WT	CC	CC	GG	GG
F56		GG		Hetero.	CC	CC	CC	
F57	Hetero.	GG	TT	Homo. WT	CC	CT	GC	GG
F58	AA	GG	TT	Homo. WT	CC	CC	GC	GA
F59	AA	GG	TT	Hetero.	CC	CT	GG	GG
F60	AA	GG	TT	Homo. WT	CC	CC	GC	GA
F61		AA			CT			
F62	Hetero.	GG	TT	Homo. WT	CC	CT	GC	GA
F63	AA	GG	TT	Homo. WT	CT	CC	GC	GA
F64	AA	GG	TT	Homo. WT	CT	CT	GC	GA

Table 5.2 PBMC Genotyping for CYPs 2B6, 2C9, 2C19 and 3A5.

	2B6*5 (C>T)	2B6*6 (G>T)	2C9*2 (C>T)	2C9*3 (A>C)	2C19*2 (G>A)	2C19*3 (G>A)	3A5*3
F1	CC	GT	CT	AA	GG	GG	*3/*3
F2	CT	GG	CT	AA	GA	GG	*3/*3
F3	CT	GT	CT	AA	GG	GG	*3/*3
F5	CT	GG	CC	AA	GG	GG	*3/*3
F6	CT	GT	CC	AA	GA	GG	*3/*3
F7	CT	GG	CT	AA	GG	GG	*3/*3
F8	CC	GG	CC	AA	GG	GG	*3/*3
F9	CT	GG	CC	AA	GA	GG	*3/*3
F10	CC	GT	CC	AA	GA	GG	*3/*3
F11	CT	TT	CC	AA	GG	GG	*3/*3
F12	CC	GT	CC	AA	GA	GG	*3/*3
F13	CC	GG	CT	AA	GG	GG	*1/*3
F14	CC	GG	CC	AA	GG	GG	*3/*3
F15	CC	GT	CT	AA	GG	GG	*1/*3
F16	CC	GG	CT	AA	GG	GG	*3/*3
F17	CC	GT	CC	AA	GG	GG	*1/*3
F18	CC	GG	CT	AA	GG	GG	*3/*3
F19	CC	GG	CC	AA	GG	GG	*3/*3
F20	CT	GG	CC	AA	GG	GG	*3/*3
F21	CT	GT	CC	AA	GA	GG	*3/*3
F22	CT	GG	CC	AA	GG	GG	*1/*3
F23	CT	GG	CT	AA	GG	GG	*3/*3
F24	CC			AA			*3/*3
F25	CC	GG	CC	AA	GG	GG	*3/*3
F26	CC		CC	AA	GG	GG	*3/*3
F27	CT	GG	CC	AA	GG	GG	*3/*3
F28	CC		CC	AA	GG	GG	*3/*3
F29	CC	GG	CT	AA	GG	GG	*1/*3
F30	CT	GT	CC	AA	GG	GG	*3/*3
F31	CT	GG	CC	AA	GG	GG	*3/*3
F32	CT	GG	CC	AA	GG	GG	*3/*3
F33	CT	GT	CC	AA	GG	GG	*3/*3
F34	CC	GG	CT	AA	GA	GG	*3/*3
F35	CT	GG	CT	AA	GA	GG	*3/*3
F37	CT	GT	CT	AA	GG	GG	*3/*3
F38	TT	GG	CT	AA	GG	GG	*3/*3
F39	CT	GG	CC	AA	GG	GG	*3/*3
F40			CC	AA		GG	*3/*3
F42	CC	GG	CC	AA	GA	GG	
F43	CT	GT	CC	AA	GG	GG	*1/*3
F44							*3/*3

F45			CC		GG	GG	*3/*3
F46	CT	GG	CT	AA	GA	GG	*3/*3
F47	CC		CC	AC	GG	GG	*3/*3
F48	CC	TT	CT	AA	GG	GG	*3/*3
F50		GG	CC	AA	GA	GG	*3/*3
F51	CT	GG	CT	AA	GG	GG	*3/*3
F52	CC	GG	CC	AA	GG	GG	*3/*3
F53	CT	GG	CT	AA	GG	GG	*3/*3
F54	CC	GT	CC	AA	GG	GG	*1/*3
F55	CT	GT	CC	AA	GG	GG	*3/*3
F56	CT	GG	CC	AA	GG	GG	*3/*3
F57	CT	GT	CT	AA	GG	GG	*3/*3
F58	CT	GG	CC	AC	GG	GG	*3/*3
F59	CT	GT	CT	AA	GG	GG	*3/*3
F60	CT	TT	CT	AA	GA	GG	*3/*3
F61	CC	TT	CT	AA	GA	GG	*3/*3
F62			CC	AC	GG	GG	*3/*3
F63	CC	GT	CC	AA	GG	GG	*3/*3
F64	CT	GG	CT	AA	GG	GG	*3/*3

References

1. Evans MJ, Kaufman MH. Establishment in culture of pluripotential cells from mouse embryos. **Nature**. 1981;292:154-156.
2. Martin GR. Isolation of a pluripotent cell line from early mouse embryos cultured in medium conditioned by teratocarcinoma stem cells. **Proc Natl Acad Sci U S A**. 1981;78:7634-7638.
3. Thomson JA, Itskovitz-Eldor J, Shapiro SS et al. Embryonic stem cell lines derived from human blastocysts. **Science**. 1998;282:1145-1147.
4. Takahashi K, Yamanaka S. Induction of Pluripotent Stem Cells from Mouse Embryonic and Adult Fibroblast Cultures by Defined Factors. **Cell**. 2006;126:663-676.
5. Takahashi K, Tanabe K, Ohnuki M et al. Induction of Pluripotent Stem Cells from Adult Human Fibroblasts by Defined Factors. **Cell**. 2007;131:861-872.
6. Lensch MW, Mummery CL. From stealing fire to cellular reprogramming: a scientific history leading to the 2012 Nobel Prize. **Stem Cell Reports**. 2013;1:5-17.
7. World's first clinical trial of human embryonic stem cell therapy cleared. **Regen Med**. 2009;4:161.
8. Alper J. Geron gets green light for human trial of ES cell-derived product. **Nature biotechnology**. 2009;27:213-214.
9. Brindley D, Mason C. Human embryonic stem cell therapy in the post-Geron era. **Regen Med**. 2012;7:17-18.
10. Reardon S, Cyranoski D. Japan stem-cell trial stirs envy. **Nature**. 2014;513:287-288.
11. Chapin RE, Stedman DB. Endless Possibilities: Stem Cells and the Vision for Toxicology Testing in the 21st Century. **Toxicological Sciences**. 2009;112:17-22.
12. Reya T, Morrison SJ, Clarke MF et al. Stem cells, cancer, and cancer stem cells. **Nature**. 2001;414:105-111.
13. Nagy A. Lineage Marking. In: Lanza R, ed. Essentials of Stem Cell Biology, Second ed. London: Elsevier; 2009:429-436.
14. Irion S, Nostro MC, Kattman SJ et al. Directed differentiation of pluripotent stem cells: from developmental biology to therapeutic applications. **Cold Spring Harb Symp Quant Biol**. 2008;73:101-110.
15. Yu J, Vodyanik MA, Smuga-Otto K et al. Induced Pluripotent Stem Cell Lines Derived from Human Somatic Cells. **Science**. 2007;318:1917-1920.
16. Davila JC, Cezar GG, Thiede M et al. Use and application of stem cells in toxicology. **Toxicological sciences : an official journal of the Society of Toxicology**. 2004;79:214-223.
17. Need AC, Motulsky AG, Goldstein DB. Priorities and standards in pharmacogenetic research. **Nature genetics**. 2005;37:671-681.
18. Mandenius CF, Steel D, Noor F et al. Cardiotoxicity testing using pluripotent stem cell-derived human cardiomyocytes and state-of-the-art bioanalytics: a review. **J Appl Toxicol**. 2011;31:191-205.
19. Wobus AM, Loser P. Present state and future perspectives of using pluripotent stem cells in toxicology research. **Archives of toxicology**. 2011;85:79-117.
20. Webb S. The gold rush for induced pluripotent stem cells. **Nature biotechnology**. 2009;27:977-979.
21. Harris K, Aylott M, Cui Y et al. Comparison of electrophysiological data from human-induced pluripotent stem cell-derived cardiomyocytes to functional preclinical safety assays. **Toxicological sciences : an official journal of the Society of Toxicology**. 2013;134:412-426.
22. Chong JJ, Yang X, Don CW et al. Human embryonic-stem-cell-derived cardiomyocytes regenerate non-human primate hearts. **Nature**. 2014;510:273-277.

23. Chi KR. Revolution dawning in cardiotoxicity testing. **Nat Rev Drug Discov**. 2013;12:565-567.
24. Sager PT, Gintant G, Turner JR et al. Rechanneling the cardiac proarrhythmia safety paradigm: a meeting report from the Cardiac Safety Research Consortium. **Am Heart J**. 2014;167:292-300.
25. McKim JM. In Vitro Approaches for Determining Liver-Specific Toxicity of New Drug Candidates. In: Wilson AG, ed. New Horizons in Predictive Toxicology: Current Status and Application. Cambridge: The Royal Society of Chemistry; 2012:157-214.
26. Zhang H, Davis CD, Sinz MW et al. Cytochrome P450 reaction-phenotyping: an industrial perspective. **Expert Opin Drug Metab Toxicol**. 2007;3:667-687.
27. Singh SS. Preclinical pharmacokinetics: an approach towards safer and efficacious drugs. **Current drug metabolism**. 2006;7:165-182.
28. Venkatakrishnan K, Von Moltke LL, Greenblatt DJ. Human drug metabolism and the cytochromes P450: application and relevance of in vitro models. **J Clin Pharmacol**. 2001;41:1149-1179.
29. Guengerich FP. Human Cytochrome P450 Enzymes. In: Montellano PROd, ed. Cytochrome P450: Structure, Mechanism, and Biochemistry, Third ed. New York: Kluwer Academic/Plenum Publishers; 2005:377-530.
30. Ingelman-Sundberg M, Sim SC, Gomez A et al. Influence of cytochrome P450 polymorphisms on drug therapies: Pharmacogenetic, pharmacoepigenetic and clinical aspects. **Pharmacology & Therapeutics**. 2007;116:496-526.
31. Lu AY, Wang RW, Lin JH. Cytochrome P450 in vitro reaction phenotyping: a re-evaluation of approaches used for P450 isoform identification. **Drug metabolism and disposition: the biological fate of chemicals**. 2003;31:345-350.
32. Nedderman AN, Dear GJ, North S et al. From definition to implementation: a cross-industry perspective of past, current and future MIST strategies. **Xenobiotica**. 2011;41:605-622.
33. Lin JH, Lu AY. Role of pharmacokinetics and metabolism in drug discovery and development. **Pharmacological reviews**. 1997;49:403-449.
34. Miners JO, Knights KM, Houston JB et al. In vitro-in vivo correlation for drugs and other compounds eliminated by glucuronidation in humans: pitfalls and promises. **Biochem Pharmacol**. 2006;71:1531-1539.
35. Barros SA, Martin RB. Predictive toxicogenomics in preclinical discovery. **Methods Mol Biol**. 2008;460:89-112.
36. Houston JB. Utility of in vitro drug metabolism data in predicting in vivo metabolic clearance. **Biochem Pharmacol**. 1994;47:1469-1479.
37. Houston JB, Galetin A. Methods for predicting in vivo pharmacokinetics using data from in vitro assays. **Current drug metabolism**. 2008;9:940-951.
38. Wrighton SA, Ring BJ, Vandenbranden M. The Use of In Vitro Metabolism Techniques in the Planning and Interpretation of Drug Safety Studies. **Toxicologic Pathology**. 1995;23:199-208.
39. Brandon EFA, Raap CD, Meijerman I et al. An update on in vitro test methods in human hepatic drug biotransformation research: pros and cons. **Toxicology and Applied Pharmacology**. 2003;189:233-246.
40. Chandra P, Lecluyse EL, Brouwer KL. Optimization of culture conditions for determining hepatobiliary disposition of taurocholate in sandwich-cultured rat hepatocytes. **In Vitro Cell Dev Biol Anim**. 2001;37:380-385.
41. LeCluyse EL. Human hepatocyte culture systems for the in vitro evaluation of cytochrome P450 expression and regulation. **Eur J Pharm Sci**. 2001;13:343-368.
42. Huang SM, Strong JM, Zhang L et al. New era in drug interaction evaluation: US Food and Drug Administration update on CYP enzymes, transporters, and the guidance process. **J Clin Pharmacol**. 2008;48:662-670.

43. Costa A, Sarmento B, Seabra V. An evaluation of the latest in vitro tools for drug metabolism studies. **Expert Opin Drug Metab Toxicol**. 2014;10:103-119.
44. Lin JH, Chiba M, Baillie TA. Is the role of the small intestine in first-pass metabolism overemphasized? **Pharmacological reviews**. 1999;51:135-158.
45. Paine MF, Hart HL, Ludington SS et al. The human intestinal cytochrome P450 "pie". **Drug metabolism and disposition: the biological fate of chemicals**. 2006;34:880-886.
46. de Waziers I, Cugnenc PH, Yang CS et al. Cytochrome P 450 isoenzymes, epoxide hydrolase and glutathione transferases in rat and human hepatic and extrahepatic tissues. **The Journal of pharmacology and experimental therapeutics**. 1990;253:387-394.
47. Shimada T, Yamazaki H, Mimura M et al. Interindividual variations in human liver cytochrome P-450 enzymes involved in the oxidation of drugs, carcinogens and toxic chemicals: studies with liver microsomes of 30 Japanese and 30 Caucasians. **The Journal of pharmacology and experimental therapeutics**. 1994;270:414-423.
48. Groothuis GM, de Graaf IA. Precision-cut intestinal slices as in vitro tool for studies on drug metabolism. **Current drug metabolism**. 2013;14:112-119.
49. van Breemen RB, Li Y. Caco-2 cell permeability assays to measure drug absorption. **Expert Opin Drug Metab Toxicol**. 2005;1:175-185.
50. Benet LZ, Cummins CL. The drug efflux-metabolism alliance: biochemical aspects. **Adv Drug Deliv Rev**. 2001;50 Suppl 1:S3-11.
51. Pfrunder A, Gutmann H, Beglinger C et al. Gene expression of CYP3A4, ABC-transporters (MDR1 and MRP1-MRP5) and hPXR in three different human colon carcinoma cell lines. **J Pharm Pharmacol**. 2003;55:59-66.
52. Gupta A, Mugundu GM, Desai PB et al. Intestinal human colon adenocarcinoma cell line LS180 is an excellent model to study pregnane X receptor, but not constitutive androstane receptor, mediated CYP3A4 and multidrug resistance transporter 1 induction: studies with anti-human immunodeficiency virus protease inhibitors. **Drug metabolism and disposition: the biological fate of chemicals**. 2008;36:1172-1180.
53. van de Kerkhof EG, Ungell AL, Sjoberg AK et al. Innovative methods to study human intestinal drug metabolism in vitro: precision-cut slices compared with ussing chamber preparations. **Drug metabolism and disposition: the biological fate of chemicals**. 2006;34:1893-1902.
54. Brugmann SA, Wells JM. Building additional complexity to in vitro-derived intestinal tissues. **Stem Cell Res Ther**. 2013;4 Suppl 1:S1.
55. Foulke-Abel J, In J, Kovbasnjuk O et al. Human enteroids as an ex-vivo model of host-pathogen interactions in the gastrointestinal tract. **Exp Biol Med (Maywood)**. 2014;239:1124-1134.
56. Jung P, Sato T, Merlos-Suarez A et al. Isolation and in vitro expansion of human colonic stem cells. **Nat Med**. 2011;17:1225-1227.
57. Sato T, Stange DE, Ferrante M et al. Long-term expansion of epithelial organoids from human colon, adenoma, adenocarcinoma, and Barrett's epithelium. **Gastroenterology**. 2011;141:1762-1772.
58. Watson CL, Mahe MM, Munera J et al. An in vivo model of human small intestine using pluripotent stem cells. **Nat Med**. 2014.
59. McCracken KW, Howell JC, Wells JM et al. Generating human intestinal tissue from pluripotent stem cells in vitro. **Nature protocols**. 2011;6:1920-1928.
60. Spence JR, Mayhew CN, Rankin SA et al. Directed differentiation of human pluripotent stem cells into intestinal tissue in vitro. **Nature**. 2011;470:105-109.
61. Wang A, Sander M. Generating cells of the gastrointestinal system: current approaches and applications for the differentiation of human pluripotent stem cells. **J Mol Med (Berl)**. 2012;90:763-771.

62. Finkbeiner SR, Zeng XL, Utama B et al. Stem cell-derived human intestinal organoids as an infection model for rotaviruses. **MBio**. 2012;3:e00159-00112.
63. Yeung CK, Shen DD, Thummel KE et al. Effects of chronic kidney disease and uremia on hepatic drug metabolism and transport. **Kidney Int**. 2014;85:522-528.
64. Haehner BD, Gorski JC, Vandenbranden M et al. Bimodal distribution of renal cytochrome P450 3A activity in humans. **Mol Pharmacol**. 1996;50:52-59.
65. Kuehl P, Zhang J, Lin Y et al. Sequence diversity in CYP3A promoters and characterization of the genetic basis of polymorphic CYP3A5 expression. **Nature genetics**. 2001;27:383-391.
66. Lin YS, Dowling AL, Quigley SD et al. Co-regulation of CYP3A4 and CYP3A5 and contribution to hepatic and intestinal midazolam metabolism. **Mol Pharmacol**. 2002;62:162-172.
67. Lohr JW, Willsky GR, Acara MA. Renal drug metabolism. **Pharmacological reviews**. 1998;50:107-141.
68. Ryan MJ, Johnson G, Kirk J et al. HK-2: an immortalized proximal tubule epithelial cell line from normal adult human kidney. **Kidney Int**. 1994;45:48-57.
69. Jenkinson SE, Chung GW, van Loon E et al. The limitations of renal epithelial cell line HK-2 as a model of drug transporter expression and function in the proximal tubule. **Pflugers Arch**. 2012;464:601-611.
70. Kelly EJ, Wang Z, Voellinger JL et al. Innovations in preclinical biology: ex vivo engineering of a human kidney tissue microperfusion system. **Stem Cell Res Ther**. 2013;4 Suppl 1:S17.
71. Uzarski JS, Xia Y, Belmonte JC et al. New strategies in kidney regeneration and tissue engineering. **Curr Opin Nephrol Hypertens**. 2014;23:399-405.
72. Lam AQ, Freedman BS, Bonventre JV. Directed differentiation of pluripotent stem cells to kidney cells. **Semin Nephrol**. 2014;34:445-461.
73. Batchelder CA, Lee CC, Matsell DG et al. Renal ontogeny in the rhesus monkey (Macaca mulatta) and directed differentiation of human embryonic stem cells towards kidney precursors. **Differentiation**. 2009;78:45-56.
74. Lin SA, Kolle G, Grimmond SM et al. Subfractionation of differentiating human embryonic stem cell populations allows the isolation of a mesodermal population enriched for intermediate mesoderm and putative renal progenitors. **Stem cells and development**. 2010;19:1637-1648.
75. Song B, Smink AM, Jones CV et al. The directed differentiation of human iPS cells into kidney podocytes. **PLoS ONE**. 2012;7:e46453.
76. Narayanan K, Schumacher KM, Tasnim F et al. Human embryonic stem cells differentiate into functional renal proximal tubular-like cells. **Kidney Int**. 2013;83:593-603.
77. Lam AQ, Freedman BS, Morizane R et al. Rapid and efficient differentiation of human pluripotent stem cells into intermediate mesoderm that forms tubules expressing kidney proximal tubular markers. **J Am Soc Nephrol**. 2014;25:1211-1225.
78. Takasato M, Er PX, Becroft M et al. Directing human embryonic stem cell differentiation towards a renal lineage generates a self-organizing kidney. **Nat Cell Biol**. 2014;16:118-126.
79. Araoka T, Mae S, Kurose Y et al. Efficient and rapid induction of human iPSCs/ESCs into nephrogenic intermediate mesoderm using small molecule-based differentiation methods. **PLoS ONE**. 2014;9:e84881.
80. Hewitt NJ, Gómez Lechón MJ, Houston JB et al. Primary Hepatocytes: Current Understanding of the Regulation of Metabolic Enzymes and Transporter Proteins, and Pharmaceutical Practice for the Use of Hepatocytes in Metabolism, Enzyme Induction, Transporter, Clearance, and Hepatotoxicity Studies. **Drug Metabolism Reviews**. 2007;39:159-234.
81. Medine Claire N, Greenhough S, Hay David C. Role of stem-cell-derived hepatic endoderm in human drug discovery. **Biochemical Society Transactions**. 2010;38:1033.

82. Rambhatla L, Chiu CP, Kundu P et al. Generation of hepatocyte-like cells from human embryonic stem cells. **Cell Transplant**. 2003;12:1-11.
83. Duan Y, Catana A, Meng Y et al. Differentiation and Enrichment of Hepatocyte-Like Cells from Human Embryonic Stem Cells In Vitro and In Vivo. **Stem Cells**. 2007;25:3058-3068.
84. Hay DC, Fletcher J, Payne C et al. Highly efficient differentiation of hESCs to functional hepatic endoderm requires ActivinA and Wnt3a signaling. **Proceedings of the National Academy of Sciences**. 2008;105:12301-12306.
85. Hay DC, Zhao D, Fletcher J et al. Efficient Differentiation of Hepatocytes from Human Embryonic Stem Cells Exhibiting Markers Recapitulating Liver Development In Vivo. **Stem Cells**. 2008;26:894-902.
86. Szkolnicka D, Farnworth SL, Lucendo-Villarin B et al. Deriving functional hepatocytes from pluripotent stem cells. **Curr Protoc Stem Cell Biol**. 2014;30:1G 5 1-1G 5 12.
87. Ek M, Söderdahl T, Küppers-Munther B et al. Expression of drug metabolizing enzymes in hepatocyte-like cells derived from human embryonic stem cells. **Biochemical Pharmacology**. 2007;74:496-503.
88. Duan Y, Ma X, Zou W et al. Differentiation and Characterization of Metabolically Functioning Hepatocytes from Human Embryonic Stem Cells. **Stem Cells**. 2010;28:674-686.
89. Ramasamy TS, Yu JSL, Selden C et al. Application of Three-Dimensional Culture Conditions to Human Embryonic Stem Cell-Derived Definitive Endoderm Cells Enhances Hepatocyte Differentiation and Functionality. **Tissue Engineering Part A**. 2013;19:360-367.
90. Takayama K, Inamura M, Kawabata K et al. Efficient Generation of Functional Hepatocytes From Human Embryonic Stem Cells and Induced Pluripotent Stem Cells by HNF4α Transduction. **Molecular Therapy**. 2011;20:127-137.
91. Takayama K, Inamura M, Kawabata K et al. Generation of metabolically functioning hepatocytes from human pluripotent stem cells by FOXA2 and HNF1α transduction. **Journal of Hepatology**. 2012;57:628-636.
92. Takayama K, Kawabata K, Nagamoto Y et al. 3D spheroid culture of hESC/hiPSC-derived hepatocyte-like cells for drug toxicity testing. **Biomaterials**. 2013;34:1781-1789.
93. Ogawa S, Surapisitchat J, Virtanen C et al. Three-dimensional culture and cAMP signaling promote the maturation of human pluripotent stem cell-derived hepatocytes. **Development**. 2013;140:3285-3296.
94. Nakamura N, Saeki K, Mitsumoto M et al. Feeder-free and serum-free production of hepatocytes, cholangiocytes, and their proliferating progenitors from human pluripotent stem cells: application to liver-specific functional and cytotoxic assays. **Cell Reprogram**. 2012;14:171-185.
95. Magner NL, Jung Y, Wu J et al. Insulin and igfs enhance hepatocyte differentiation from human embryonic stem cells via the PI3K/AKT pathway. **Stem Cells**. 2013;31:2095-2103.
96. Cai J, Zhao Y, Liu Y et al. Directed differentiation of human embryonic stem cells into functional hepatic cells. **Hepatology**. 2007;45:1229-1239.
97. Hay DC, Zhao D, Ross A et al. Direct Differentiation of Human Embryonic Stem Cells to Hepatocyte-like Cells Exhibiting Functional Activities. **Cloning and Stem Cells**. 2007;9:51-62.
98. Sullivan GJ, Hay DC, Park IH et al. Generation of functional human hepatic endoderm from human induced pluripotent stem cells. **Hepatology**. 2010;51:329-335.
99. Shan J, Schwartz RE, Ross NT et al. Identification of small molecules for human hepatocyte expansion and iPS differentiation. **Nat Chem Biol**. 2013;9:514-520.
100. Miki T, Ring A, Gerlach J. Hepatic differentiation of human embryonic stem cells is promoted by three-dimensional dynamic perfusion culture conditions. **Tissue Eng Part C Methods**. 2011;17:557-568.

101. Subramanian K, Owens DJ, Raju R et al. Spheroid culture for enhanced differentiation of human embryonic stem cells to hepatocyte-like cells. **Stem cells and development**. 2014;23:124-131.
102. Hannan NR, Segeritz CP, Touboul T et al. Production of hepatocyte-like cells from human pluripotent stem cells. **Nature protocols**. 2013;8:430-437.
103. Zhao D, Chen S, Duo S et al. Promotion of the efficient metabolic maturation of human pluripotent stem cell-derived hepatocytes by correcting specification defects. **Cell Res**. 2013;23:157-161.
104. Brolen G, Sivertsson L, Bjorquist P et al. Hepatocyte-like cells derived from human embryonic stem cells specifically via definitive endoderm and a progenitor stage. **J Biotechnol**. 2010;145:284-294.
105. Kia R, Sison RL, Heslop J et al. Stem cell-derived hepatocytes as a predictive model for drug-induced liver injury: are we there yet? **Br J Clin Pharmacol**. 2013;75:885-896.
106. Basma H, Soto–Gutiérrez A, Yannam GR et al. Differentiation and Transplantation of Human Embryonic Stem Cell–Derived Hepatocytes. **Gastroenterology**. 2009;136:990-999.e994.
107. Zhang S, Chen S, Li W et al. Rescue of ATP7B function in hepatocyte-like cells from Wilson's disease induced pluripotent stem cells using gene therapy or the chaperone drug curcumin. **Hum Mol Genet**. 2011;20:3176-3187.
108. Yildirimman R, Brolen G, Vilardell M et al. Human embryonic stem cell derived hepatocyte-like cells as a tool for in vitro hazard assessment of chemical carcinogenicity. **Toxicological sciences : an official journal of the Society of Toxicology**. 2011;124:278-290.
109. Johansson I, Ingelman-Sundberg M. Genetic Polymorphism and Toxicology--With Emphasis on Cytochrome P450. **Toxicological Sciences**. 2010;120:1-13.
110. Davila JC. Use and Application of Stem Cells in Toxicology. **Toxicological Sciences**. 2004;79:214-223.
111. Godoy P, Hewitt NJ, Albrecht U et al. Recent advances in 2D and 3D in vitro systems using primary hepatocytes, alternative hepatocyte sources and non-parenchymal liver cells and their use in investigating mechanisms of hepatotoxicity, cell signaling and ADME. **Archives of toxicology**. 2013;87:1315-1530.
112. Szkolnicka D, Zhou W, Lucendo-Villarin B et al. Pluripotent Stem Cell–Derived Hepatocytes: Potential and Challenges in Pharmacology. **Annual Review of Pharmacology and Toxicology**. 2013;53:147-159.
113. Evans WE. Pharmacogenomics: Translating Functional Genomics into Rational Therapeutics. **Science**. 1999;286:487-491.
114. Wienkers LC, Heath TG. Predicting in vivo drug interactions from in vitro drug discovery data. **Nature Reviews Drug Discovery**. 2005;4:825-833.
115. Paine MF, Khalighi M, Fisher JM et al. Characterization of interintestinal and intraintestinal variations in human CYP3A-dependent metabolism. **J Pharmacol Exp Ther**. 1997;283:1552-1562.
116. Vogel G. Stem cells. Wisconsin to distribute embryonic cell lines. **Science**. 2000;287:948-949.
117. Chiao E, Elazar M, Xing Y et al. Isolation and Transcriptional Profiling of Purified Hepatic Cells Derived from Human Embryonic Stem Cells. **Stem Cells**. 2008;26:2032-2041.
118. Agarwal S, Holton KL, Lanza R. Efficient Differentiation of Functional Hepatocytes from Human Embryonic Stem Cells. **Stem Cells**. 2008;26:1117-1127.
119. Bukong TN, Lo T, Szabo G et al. Novel developmental biology-based protocol of embryonic stem cell differentiation to morphologically sound and functional yet immature hepatocytes. **Liver International**. 2012;32:732-741.
120. Ghaedi M, Duan Y, Zern MA et al. Hepatic differentiation of human embryonic stem cells on growth factor-containing surfaces. **Journal of Tissue Engineering and Regenerative Medicine**. 2012:n/a-n/a.

121. Hay DC, Pernagallo S, Diaz-Mochon JJ et al. Unbiased screening of polymer libraries to define novel substrates for functional hepatocytes with inducible drug metabolism. **Stem Cell Research**. 2011;6:92-102.
122. Heo J, Ahn E-K, Jeong H-G et al. Transcriptional characterization of Wnt pathway during sequential hepatic differentiation of human embryonic stem cells and adipose tissue-derived stem cells. **Biochemical and Biophysical Research Communications**. 2013;434:235-240.
123. Touboul T, Hannan NRF, Corbineau S et al. Generation of functional hepatocytes from human embryonic stem cells under chemically defined conditions that recapitulate liver development. **Hepatology**. 2010;51:1754-1765.
124. DeLaForest A, Nagaoka M, Si-Tayeb K et al. HNF4A is essential for specification of hepatic progenitors from human pluripotent stem cells. **Development**. 2011;138:4143-4153.
125. Szkolnicka D, Farnworth SL, Lucendo-Villarin B et al. Accurate prediction of drug-induced liver injury using stem cell-derived populations. **Stem Cells Transl Med**. 2014;3:141-148.
126. Smith H, Eaton, DL, Bammler, TK. Polymorphisms in Xenobiotic Conjugation. In: Costa L, Eaton, DL, ed. Gene-Environment Interactions: The Fundamentals of Ecogenetics. New York: Wiley Press; 2006:127-158.
127. Hoskins JM, Goldberg RM, Qu P et al. UGT1A1*28 Genotype and Irinotecan-Induced Neutropenia: Dose Matters. **JNCI Journal of the National Cancer Institute**. 2007;99:1290-1295.
128. Ghotbi R, Christensen M, Roh H-K et al. Comparisons of CYP1A2 genetic polymorphisms, enzyme activity and the genotype-phenotype relationship in Swedes and Koreans. **European Journal of Clinical Pharmacology**. 2007;63:537-546.
129. Liu L, Mugundu GM, Kirby BJ et al. Quantification of human hepatocyte cytochrome P450 enzymes and transporters induced by HIV protease inhibitors using newly validated LC-MS/MS cocktail assays and RT-PCR. **Biopharmaceutics & Drug Disposition**. 2012;33:207-217.
130. Lucendo-Villarin B, Cameron K, Szkolnicka D et al. Stabilizing hepatocellular phenotype using optimized synthetic surfaces. **J Vis Exp**. 2014.
131. Raimundo S. A novel intronic mutation, 2988G>A, with high predictivity for impaired function of cytochrome P450 2D6 in white subjects*1. **Clinical Pharmacology & Therapeutics**. 2004;76:128-138.
132. Toscano C, Klein K, Blievernicht J et al. Impaired expression of CYP2D6 in intermediate metabolizers carrying the *41 allele caused by the intronic SNP 2988G>A: evidence for modulation of splicing events. **Pharmacogenet Genomics**. 2006;16:755-766.
133. Rau T, Diepenbruck S, Diepenbruck I et al. The 2988G>A polymorphism affects splicing of a CYP2D6 minigene. **Clin Pharmacol Ther**. 2006;80:555-558; author reply 558-560.
134. Wrighton SA, Stevens JC. The human hepatic cytochromes P450 involved in drug metabolism. **Crit Rev Toxicol**. 1992;22:1-21.
135. Siller R, Greenhough S, Naumovska E et al. Small-molecule-driven hepatocyte differentiation of human pluripotent stem cells. **Stem Cell Reports**. 2015;4:939-952.
136. Tasnim F, Phan D, Toh YC et al. Cost-effective differentiation of hepatocyte-like cells from human pluripotent stem cells using small molecules. **Biomaterials**. 2015;70:115-125.
137. McLean AB, D'Amour KA, Jones KL et al. Activin a efficiently specifies definitive endoderm from human embryonic stem cells only when phosphatidylinositol 3-kinase signaling is suppressed. **Stem Cells**. 2007;25:29-38.
138. Gripon P, Rumin S, Urban S et al. Infection of a human hepatoma cell line by hepatitis B virus. **Proc Natl Acad Sci U S A**. 2002;99:15655-15660.
139. Aninat C, Piton A, Glaise D et al. Expression of cytochromes P450, conjugating enzymes and nuclear receptors in human hepatoma HepaRG cells. **Drug metabolism and disposition: the biological fate of chemicals**. 2006;34:75-83.

140. Hart SN, Li Y, Nakamoto K et al. A comparison of whole genome gene expression profiles of HepaRG cells and HepG2 cells to primary human hepatocytes and human liver tissues. **Drug metabolism and disposition: the biological fate of chemicals**. 2010;38:988-994.
141. Li H, Wang H. Activation of xenobiotic receptors: driving into the nucleus. **Expert Opin Drug Metab Toxicol**. 2010;6:409-426.
142. Tolson AH, Wang H. Regulation of drug-metabolizing enzymes by xenobiotic receptors: PXR and CAR. **Adv Drug Deliv Rev**. 2010;62:1238-1249.
143. Jover R, Bort R, Gomez-Lechon MJ et al. Cytochrome P450 regulation by hepatocyte nuclear factor 4 in human hepatocytes: a study using adenovirus-mediated antisense targeting. **Hepatology**. 2001;33:668-675.
144. Fluck CE, Mullis PE, Pandey AV. Reduction in hepatic drug metabolizing CYP3A4 activities caused by P450 oxidoreductase mutations identified in patients with disordered steroid metabolism. **Biochem Biophys Res Commun**. 2010;401:149-153.
145. Pandey AV, Fluck CE. NADPH P450 oxidoreductase: structure, function, and pathology of diseases. **Pharmacol Ther**. 2013;138:229-254.
146. Langton S, Gudas LJ. CYP26A1 knockout embryonic stem cells exhibit reduced differentiation and growth arrest in response to retinoic acid. **Dev Biol**. 2008;315:331-354.
147. Gudas LJ, Wagner JA. Retinoids regulate stem cell differentiation. **J Cell Physiol**. 2011;226:322-330.
148. Lutsenko S, Efremov RG, Tsivkovskii R et al. Human copper-transporting ATPase ATP7B (the Wilson's disease protein): biochemical properties and regulation. **J Bioenerg Biomembr**. 2002;34:351-362.
149. Yokoi T, Nakajima M. microRNAs as mediators of drug toxicity. **Annu Rev Pharmacol Toxicol**. 2013;53:377-400.
150. Yokoi T, Nakajima M. Toxicological implications of modulation of gene expression by microRNAs. **Toxicological sciences : an official journal of the Society of Toxicology**. 2011;123:1-14.
151. Lagos-Quintana M, Rauhut R, Meyer J et al. New microRNAs from mouse and human. **RNA**. 2003;9:175-179.
152. Lagos-Quintana M, Rauhut R, Lendeckel W et al. Identification of novel genes coding for small expressed RNAs. **Science**. 2001;294:853-858.
153. Lau NC, Lim LP, Weinstein EG et al. An abundant class of tiny RNAs with probable regulatory roles in Caenorhabditis elegans. **Science**. 2001;294:858-862.
154. Lee RC, Ambros V. An extensive class of small RNAs in Caenorhabditis elegans. **Science**. 2001;294:862-864.
155. Reinhart BJ, Weinstein EG, Rhoades MW et al. MicroRNAs in plants. **Genes Dev**. 2002;16:1616-1626.
156. Ha M, Kim VN. Regulation of microRNA biogenesis. **Nat Rev Mol Cell Biol**. 2014;15:509-524.
157. Bartel DP. MicroRNAs: target recognition and regulatory functions. **Cell**. 2009;136:215-233.
158. Kim VN, Han J, Siomi MC. Biogenesis of small RNAs in animals. **Nat Rev Mol Cell Biol**. 2009;10:126-139.
159. Krol J, Loedige I, Filipowicz W. The widespread regulation of microRNA biogenesis, function and decay. **Nat Rev Genet**. 2010;11:597-610.
160. Bartel DP. MicroRNAs: genomics, biogenesis, mechanism, and function. **Cell**. 2004;116:281-297.
161. Carthew RW, Sontheimer EJ. Origins and Mechanisms of miRNAs and siRNAs. **Cell**. 2009;136:642-655.
162. Ambros V. The functions of animal microRNAs. **Nature**. 2004;431:350-355.
163. Fabian MR, Sonenberg N, Filipowicz W. Regulation of mRNA translation and stability by microRNAs. **Annu Rev Biochem**. 2010;79:351-379.

164. Friedman RC, Farh KK, Burge CB et al. Most mammalian mRNAs are conserved targets of microRNAs. **Genome Res**. 2009;19:92-105.
165. Vasudevan S, Tong Y, Steitz JA. Switching from repression to activation: microRNAs can up-regulate translation. **Science**. 2007;318:1931-1934.
166. Chekulaeva M, Filipowicz W. Mechanisms of miRNA-mediated post-transcriptional regulation in animal cells. **Curr Opin Cell Biol**. 2009;21:452-460.
167. Orom UA, Nielsen FC, Lund AH. MicroRNA-10a binds the 5'UTR of ribosomal protein mRNAs and enhances their translation. **Mol Cell**. 2008;30:460-471.
168. Henke JI, Goergen D, Zheng J et al. microRNA-122 stimulates translation of hepatitis C virus RNA. **EMBO J**. 2008;27:3300-3310.
169. Jopling CL, Yi M, Lancaster AM et al. Modulation of hepatitis C virus RNA abundance by a liver-specific MicroRNA. **Science**. 2005;309:1577-1581.
170. Lagos-Quintana M, Rauhut R, Yalcin A et al. Identification of tissue-specific microRNAs from mouse. **Curr Biol**. 2002;12:735-739.
171. Houbaviy HB, Murray MF, Sharp PA. Embryonic Stem Cell-Specific MicroRNAs. **Developmental Cell**. 2003;5:351-358.
172. Lee RC, Feinbaum RL, Ambros V. The C. elegans heterochronic gene lin-4 encodes small RNAs with antisense complementarity to lin-14. **Cell**. 1993;75:843-854.
173. Wightman B, Ha I, Ruvkun G. Posttranscriptional regulation of the heterochronic gene lin-14 by lin-4 mediates temporal pattern formation in C. elegans. **Cell**. 1993;75:855-862.
174. Reinhart BJ, Slack FJ, Basson M et al. The 21-nucleotide let-7 RNA regulates developmental timing in Caenorhabditis elegans. **Nature**. 2000;403:901-906.
175. Slack FJ, Basson M, Liu Z et al. The lin-41 RBCC gene acts in the C. elegans heterochronic pathway between the let-7 regulatory RNA and the LIN-29 transcription factor. **Mol Cell**. 2000;5:659-669.
176. Pasquinelli AE, Reinhart BJ, Slack F et al. Conservation of the sequence and temporal expression of let-7 heterochronic regulatory RNA. **Nature**. 2000;408:86-89.
177. Ambros V, Bartel B, Bartel DP et al. A uniform system for microRNA annotation. **RNA**. 2003;9:277-279.
178. Griffiths-Jones S, Grocock RJ, van Dongen S et al. miRBase: microRNA sequences, targets and gene nomenclature. **Nucleic Acids Res**. 2006;34:D140-144.
179. Rieger JK, Klein K, Winter S et al. Expression variability of absorption, distribution, metabolism, excretion-related microRNAs in human liver: influence of nongenetic factors and association with gene expression. **Drug metabolism and disposition: the biological fate of chemicals**. 2013;41:1752-1762.
180. Abba M, Mudduluru G, Allgayer H. MicroRNAs in cancer: small molecules, big chances. **Anticancer Agents Med Chem**. 2012;12:733-743.
181. Volinia S, Calin GA, Liu CG et al. A microRNA expression signature of human solid tumors defines cancer gene targets. **Proc Natl Acad Sci U S A**. 2006;103:2257-2261.
182. Kloosterman WP, Plasterk RH. The diverse functions of microRNAs in animal development and disease. **Dev Cell**. 2006;11:441-450.
183. Calin GA, Dumitru CD, Shimizu M et al. Frequent deletions and down-regulation of micro- RNA genes miR15 and miR16 at 13q14 in chronic lymphocytic leukemia. **Proc Natl Acad Sci U S A**. 2002;99:15524-15529.
184. Calin GA, Sevignani C, Dumitru CD et al. Human microRNA genes are frequently located at fragile sites and genomic regions involved in cancers. **Proc Natl Acad Sci U S A**. 2004;101:2999-3004.
185. Ciafre SA, Galardi S, Mangiola A et al. Extensive modulation of a set of microRNAs in primary glioblastoma. **Biochem Biophys Res Commun**. 2005;334:1351-1358.

186. Lu J, Getz G, Miska EA et al. MicroRNA expression profiles classify human cancers. **Nature**. 2005;435:834-838.
187. Alvarez-Garcia I, Miska EA. MicroRNA functions in animal development and human disease. **Development**. 2005;132:4653-4662.
188. He L, Thomson JM, Hemann MT et al. A microRNA polycistron as a potential human oncogene. **Nature**. 2005;435:828-833.
189. Michael MZ, SM OC, van Holst Pellekaan NG et al. Reduced accumulation of specific microRNAs in colorectal neoplasia. **Mol Cancer Res**. 2003;1:882-891.
190. Metzler M, Wilda M, Busch K et al. High expression of precursor microRNA-155/BIC RNA in children with Burkitt lymphoma. **Genes Chromosomes Cancer**. 2004;39:167-169.
191. Johnson SM, Grosshans H, Shingara J et al. RAS is regulated by the let-7 microRNA family. **Cell**. 2005;120:635-647.
192. Takamizawa J, Konishi H, Yanagisawa K et al. Reduced expression of the let-7 microRNAs in human lung cancers in association with shortened postoperative survival. **Cancer Res**. 2004;64:3753-3756.
193. Garzon R, Calin GA, Croce CM. MicroRNAs in Cancer. **Annu Rev Med**. 2009;60:167-179.
194. Lee YS, Dutta A. MicroRNAs in cancer. **Annu Rev Pathol**. 2009;4:199-227.
195. He L, He X, Lim LP et al. A microRNA component of the p53 tumour suppressor network. **Nature**. 2007;447:1130-1134.
196. Raver-Shapira N, Marciano E, Meiri E et al. Transcriptional activation of miR-34a contributes to p53-mediated apoptosis. **Mol Cell**. 2007;26:731-743.
197. Chang TC, Wentzel EA, Kent OA et al. Transactivation of miR-34a by p53 broadly influences gene expression and promotes apoptosis. **Mol Cell**. 2007;26:745-752.
198. Chang TC, Yu D, Lee YS et al. Widespread microRNA repression by Myc contributes to tumorigenesis. **Nature genetics**. 2008;40:43-50.
199. Dews M, Homayouni A, Yu D et al. Augmentation of tumor angiogenesis by a Myc-activated microRNA cluster. **Nature genetics**. 2006;38:1060-1065.
200. Bueno MJ, Perez de Castro I, Gomez de Cedron M et al. Genetic and epigenetic silencing of microRNA-203 enhances ABL1 and BCR-ABL1 oncogene expression. **Cancer Cell**. 2008;13:496-506.
201. Saito Y, Liang G, Egger G et al. Specific activation of microRNA-127 with downregulation of the proto-oncogene BCL6 by chromatin-modifying drugs in human cancer cells. **Cancer Cell**. 2006;9:435-443.
202. Yanaihara N, Caplen N, Bowman E et al. Unique microRNA molecular profiles in lung cancer diagnosis and prognosis. **Cancer Cell**. 2006;9:189-198.
203. Lawrie CH, Gal S, Dunlop HM et al. Detection of elevated levels of tumour-associated microRNAs in serum of patients with diffuse large B-cell lymphoma. **Br J Haematol**. 2008;141:672-675.
204. Mitchell PS, Parkin RK, Kroh EM et al. Circulating microRNAs as stable blood-based markers for cancer detection. **Proc Natl Acad Sci U S A**. 2008;105:10513-10518.
205. Szafranska AE, Davison TS, John J et al. MicroRNA expression alterations are linked to tumorigenesis and non-neoplastic processes in pancreatic ductal adenocarcinoma. **Oncogene**. 2007;26:4442-4452.
206. Chen X, Ba Y, Ma L et al. Characterization of microRNAs in serum: a novel class of biomarkers for diagnosis of cancer and other diseases. **Cell Res**. 2008;18:997-1006.
207. Kumar MS, Lu J, Mercer KL et al. Impaired microRNA processing enhances cellular transformation and tumorigenesis. **Nature genetics**. 2007;39:673-677.
208. Joshi PM, Riddle MR, Djabrayan NJ et al. Caenorhabditis elegans as a model for stem cell biology. **Dev Dyn**. 2010;239:1539-1554.

209. Newman MA, Thomson JM, Hammond SM. Lin-28 interaction with the Let-7 precursor loop mediates regulated microRNA processing. **RNA**. 2008;14:1539-1549.
210. Heo I, Joo C, Cho J et al. Lin28 mediates the terminal uridylation of let-7 precursor MicroRNA. **Mol Cell**. 2008;32:276-284.
211. Viswanathan SR, Daley GQ, Gregory RI. Selective blockade of microRNA processing by Lin28. **Science**. 2008;320:97-100.
212. Piskounova E, Viswanathan SR, Janas M et al. Determinants of microRNA processing inhibition by the developmentally regulated RNA-binding protein Lin28. **J Biol Chem**. 2008;283:21310-21314.
213. Mallanna SK, Rizzino A. Emerging roles of microRNAs in the control of embryonic stem cells and the generation of induced pluripotent stem cells. **Dev Biol**. 2010;344:16-25.
214. Hinton A, Hunter S, Reyes G et al. From pluripotency to islets: miRNAs as critical regulators of human cellular differentiation. **Adv Genet**. 2012;79:1-34.
215. Bracken CP, Gregory PA, Kolesnikoff N et al. A double-negative feedback loop between ZEB1-SIP1 and the microRNA-200 family regulates epithelial-mesenchymal transition. **Cancer Res**. 2008;68:7846-7854.
216. Gregory PA, Bert AG, Paterson EL et al. The miR-200 family and miR-205 regulate epithelial to mesenchymal transition by targeting ZEB1 and SIP1. **Nat Cell Biol**. 2008;10:593-601.
217. Grishok A, Pasquinelli AE, Conte D et al. Genes and mechanisms related to RNA interference regulate expression of the small temporal RNAs that control C. elegans developmental timing. **Cell**. 2001;106:23-34.
218. Hatfield SD, Shcherbata HR, Fischer KA et al. Stem cell division is regulated by the microRNA pathway. **Nature**. 2005;435:974-978.
219. Bernstein E, Kim SY, Carmell MA et al. Dicer is essential for mouse development. **Nature genetics**. 2003;35:215-217.
220. Kanellopoulou C, Muljo SA, Kung AL et al. Dicer-deficient mouse embryonic stem cells are defective in differentiation and centromeric silencing. **Genes Dev**. 2005;19:489-501.
221. Murchison EP, Partridge JF, Tam OH et al. Characterization of Dicer-deficient murine embryonic stem cells. **Proc Natl Acad Sci U S A**. 2005;102:12135-12140.
222. Leaman D, Chen PY, Fak J et al. Antisense-mediated depletion reveals essential and specific functions of microRNAs in Drosophila development. **Cell**. 2005;121:1097-1108.
223. Hinton A, Afrikanova I, Wilson M et al. A distinct microRNA signature for definitive endoderm derived from human embryonic stem cells. **Stem cells and development**. 2010;19:797-807.
224. Ivey KN, Muth A, Arnold J et al. MicroRNA regulation of cell lineages in mouse and human embryonic stem cells. **Cell Stem Cell**. 2008;2:219-229.
225. Wang Y, Baskerville S, Shenoy A et al. Embryonic stem cell-specific microRNAs regulate the G1-S transition and promote rapid proliferation. **Nature genetics**. 2008;40:1478-1483.
226. Bar M, Wyman SK, Fritz BR et al. MicroRNA discovery and profiling in human embryonic stem cells by deep sequencing of small RNA libraries. **Stem Cells**. 2008;26:2496-2505.
227. Suh MR, Lee Y, Kim JY et al. Human embryonic stem cells express a unique set of microRNAs. **Dev Biol**. 2004;270:488-498.
228. Morin RD, O'Connor MD, Griffith M et al. Application of massively parallel sequencing to microRNA profiling and discovery in human embryonic stem cells. **Genome Res**. 2008;18:610-621.
229. Card DA, Hebbar PB, Li L et al. Oct4/Sox2-regulated miR-302 targets cyclin D1 in human embryonic stem cells. **Mol Cell Biol**. 2008;28:6426-6438.
230. Anokye-Danso F, Trivedi CM, Juhr D et al. Highly efficient miRNA-mediated reprogramming of mouse and human somatic cells to pluripotency. **Cell Stem Cell**. 2011;8:376-388.

231. Marson A, Levine SS, Cole MF et al. Connecting microRNA genes to the core transcriptional regulatory circuitry of embryonic stem cells. **Cell**. 2008;134:521-533.
232. O'Donnell KA, Wentzel EA, Zeller KI et al. c-Myc-regulated microRNAs modulate E2F1 expression. **Nature**. 2005;435:839-843.
233. Wilson KD, Venkatasubrahmanyam S, Jia F et al. MicroRNA profiling of human-induced pluripotent stem cells. **Stem cells and development**. 2009;18:749-758.
234. Lakshmipathy U, Love B, Goff LA et al. MicroRNA expression pattern of undifferentiated and differentiated human embryonic stem cells. **Stem cells and development**. 2007;16:1003-1016.
235. Laurent LC, Chen J, Ulitsky I et al. Comprehensive microRNA profiling reveals a unique human embryonic stem cell signature dominated by a single seed sequence. **Stem Cells**. 2008;26:1506-1516.
236. Stadler B, Ivanovska I, Mehta K et al. Characterization of microRNAs involved in embryonic stem cell states. **Stem cells and development**. 2010;19:935-950.
237. Ribeiro AO, Schoof CR, Izzotti A et al. MicroRNAs: modulators of cell identity, and their applications in tissue engineering. **Microrna**. 2014;3:45-53.
238. Gangaraju VK, Lin H. MicroRNAs: key regulators of stem cells. **Nat Rev Mol Cell Biol**. 2009;10:116-125.
239. Guo WT, Wang XW, Wang Y. Micro-management of pluripotent stem cells. **Protein Cell**. 2014;5:36-47.
240. Tay Y, Zhang J, Thomson AM et al. MicroRNAs to Nanog, Oct4 and Sox2 coding regions modulate embryonic stem cell differentiation. **Nature**. 2008;455:1124-1128.
241. Tay YM, Tam WL, Ang YS et al. MicroRNA-134 modulates the differentiation of mouse embryonic stem cells, where it causes post-transcriptional attenuation of Nanog and LRH1. **Stem Cells**. 2008;26:17-29.
242. Choi YJ, Lin CP, Ho JJ et al. miR-34 miRNAs provide a barrier for somatic cell reprogramming. **Nat Cell Biol**. 2011;13:1353-1360.
243. Xu N, Papagiannakopoulos T, Pan G et al. MicroRNA-145 regulates OCT4, SOX2, and KLF4 and represses pluripotency in human embryonic stem cells. **Cell**. 2009;137:647-658.
244. O'Loghlen A, Munoz-Cabello AM, Gaspar-Maia A et al. MicroRNA regulation of Cbx7 mediates a switch of Polycomb orthologs during ESC differentiation. **Cell Stem Cell**. 2012;10:33-46.
245. Zhong X, Li N, Liang S et al. Identification of microRNAs regulating reprogramming factor LIN28 in embryonic stem cells and cancer cells. **J Biol Chem**. 2010;285:41961-41971.
246. Kwon C, Han Z, Olson EN et al. MicroRNA1 influences cardiac differentiation in Drosophila and regulates Notch signaling. **Proc Natl Acad Sci U S A**. 2005;102:18986-18991.
247. Zhao Y, Samal E, Srivastava D. Serum response factor regulates a muscle-specific microRNA that targets Hand2 during cardiogenesis. **Nature**. 2005;436:214-220.
248. Zhao Y, Ransom JF, Li A et al. Dysregulation of cardiogenesis, cardiac conduction, and cell cycle in mice lacking miRNA-1-2. **Cell**. 2007;129:303-317.
249. Chen JF, Mandel EM, Thomson JM et al. The role of microRNA-1 and microRNA-133 in skeletal muscle proliferation and differentiation. **Nature genetics**. 2006;38:228-233.
250. Nemir M, Croquelois A, Pedrazzini T et al. Induction of cardiogenesis in embryonic stem cells via downregulation of Notch1 signaling. **Circ Res**. 2006;98:1471-1478.
251. Lowell S, Benchoua A, Heavey B et al. Notch promotes neural lineage entry by pluripotent embryonic stem cells. **PLoS Biol**. 2006;4:e121.
252. Anderson C, Catoe H, Werner R. MIR-206 regulates connexin43 expression during skeletal muscle development. **Nucleic Acids Res**. 2006;34:5863-5871.
253. McCarthy JJ. MicroRNA-206: the skeletal muscle-specific myomiR. **Biochim Biophys Acta**. 2008;1779:682-691.

254. Wong CF, Tellam RL. MicroRNA-26a targets the histone methyltransferase Enhancer of Zeste homolog 2 during myogenesis. **J Biol Chem**. 2008;283:9836-9843.
255. Caretti G, Di Padova M, Micales B et al. The Polycomb Ezh2 methyltransferase regulates muscle gene expression and skeletal muscle differentiation. **Genes Dev**. 2004;18:2627-2638.
256. Krichevsky AM, King KS, Donahue CP et al. A microRNA array reveals extensive regulation of microRNAs during brain development. **RNA**. 2003;9:1274-1281.
257. Smirnova L, Grafe A, Seiler A et al. Regulation of miRNA expression during neural cell specification. **Eur J Neurosci**. 2005;21:1469-1477.
258. Krichevsky AM, Sonntag KC, Isacson O et al. Specific microRNAs modulate embryonic stem cell-derived neurogenesis. **Stem Cells**. 2006;24:857-864.
259. Yeo M, Lee SK, Lee B et al. Small CTD phosphatases function in silencing neuronal gene expression. **Science**. 2005;307:596-600.
260. Visvanathan J, Lee S, Lee B et al. The microRNA miR-124 antagonizes the anti-neural REST/SCP1 pathway during embryonic CNS development. **Genes Dev**. 2007;21:744-749.
261. Tzur G, Levy A, Meiri E et al. MicroRNA expression patterns and function in endodermal differentiation of human embryonic stem cells. **PLoS ONE**. 2008;3:e3726.
262. Kim N, Kim H, Jung I et al. Expression profiles of miRNAs in human embryonic stem cells during hepatocyte differentiation. **Hepatol Res**. 2011;41:170-183.
263. Chen Y, Zhou H, Sarver AL et al. Hepatic differentiation of liver-derived progenitor cells and their characterization by microRNA analysis. **Liver Transpl**. 2010;16:1086-1097.
264. Fu H, Tie Y, Xu C et al. Identification of human fetal liver miRNAs by a novel method. **FEBS Lett**. 2005;579:3849-3854.
265. Tzur G, Israel A, Levy A et al. Comprehensive gene and microRNA expression profiling reveals a role for microRNAs in human liver development. **PLoS ONE**. 2009;4:e7511.
266. Doddapaneni R, Chawla YK, Das A et al. Overexpression of microRNA-122 enhances in vitro hepatic differentiation of fetal liver-derived stem/progenitor cells. **Journal of Cellular Biochemistry**. 2013;114:1575-1583.
267. Haussecker D, Kay MA. miR-122 continues to blaze the trail for microRNA therapeutics. **Mol Ther**. 2010;18:240-242.
268. Gebert LF, Rebhan MA, Crivelli SE et al. Miravirsen (SPC3649) can inhibit the biogenesis of miR-122. **Nucleic Acids Res**. 2014;42:609-621.
269. Lanford RE, Hildebrandt-Eriksen ES, Petri A et al. Therapeutic silencing of microRNA-122 in primates with chronic hepatitis C virus infection. **Science**. 2010;327:198-201.
270. Krutzfeldt J, Rajewsky N, Braich R et al. Silencing of microRNAs in vivo with 'antagomirs'. **Nature**. 2005;438:685-689.
271. Esau C, Davis S, Murray SF et al. miR-122 regulation of lipid metabolism revealed by in vivo antisense targeting. **Cell Metab**. 2006;3:87-98.
272. Elmen J, Lindow M, Schutz S et al. LNA-mediated microRNA silencing in non-human primates. **Nature**. 2008;452:896-899.
273. Janssen HL, Reesink HW, Lawitz EJ et al. Treatment of HCV infection by targeting microRNA. **N Engl J Med**. 2013;368:1685-1694.
274. Tsuchiya Y, Nakajima M, Takagi S et al. MicroRNA regulates the expression of human cytochrome P450 1B1. **Cancer Res**. 2006;66:9090-9098.
275. Takagi S, Nakajima M, Mohri T et al. Post-transcriptional regulation of human pregnane X receptor by micro-RNA affects the expression of cytochrome P450 3A4. **J Biol Chem**. 2008;283:9674-9680.
276. Pan YZ, Gao W, Yu AM. MicroRNAs regulate CYP3A4 expression via direct and indirect targeting. **Drug metabolism and disposition: the biological fate of chemicals**. 2009;37:2112-2117.

277. Kida K, Nakajima M, Mohri T et al. PPARalpha is regulated by miR-21 and miR-27b in human liver. **Pharm Res**. 2011;28:2467-2476.
278. Ji J, Zhang J, Huang G et al. Over-expressed microRNA-27a and 27b influence fat accumulation and cell proliferation during rat hepatic stellate cell activation. **FEBS Lett**. 2009;583:759-766.
279. Karbiener M, Fischer C, Nowitsch S et al. microRNA miR-27b impairs human adipocyte differentiation and targets PPARgamma. **Biochem Biophys Res Commun**. 2009;390:247-251.
280. Jennewein C, von Knethen A, Schmid T et al. MicroRNA-27b contributes to lipopolysaccharide-mediated peroxisome proliferator-activated receptor gamma (PPARgamma) mRNA destabilization. **J Biol Chem**. 2010;285:11846-11853.
281. Ramamoorthy A, Li L, Gaedigk A et al. In silico and in vitro identification of microRNAs that regulate hepatic nuclear factor 4alpha expression. **Drug metabolism and disposition: the biological fate of chemicals**. 2012;40:726-733.
282. Takagi S, Nakajima M, Kida K et al. MicroRNAs regulate human hepatocyte nuclear factor 4alpha, modulating the expression of metabolic enzymes and cell cycle. **J Biol Chem**. 2010;285:4415-4422.
283. Mohri T, Nakajima M, Fukami T et al. Human CYP2E1 is regulated by miR-378. **Biochem Pharmacol**. 2010;79:1045-1052.
284. Yu D, Green B, Tolleson WH et al. MicroRNA hsa-miR-29a-3p modulates CYP2C19 in human liver cells. **Biochem Pharmacol**. 2015.
285. Fukushima T, Hamada Y, Yamada H et al. Changes of micro-RNA expression in rat liver treated by acetaminophen or carbon tetrachloride--regulating role of micro-RNA for RNA expression. **J Toxicol Sci**. 2007;32:401-409.
286. Wang K, Zhang S, Marzolf B et al. Circulating microRNAs, potential biomarkers for drug-induced liver injury. **Proc Natl Acad Sci U S A**. 2009;106:4402-4407.
287. Zhang Y, Jia Y, Zheng R et al. Plasma microRNA-122 as a biomarker for viral-, alcohol-, and chemical-related hepatic diseases. **Clin Chem**. 2010;56:1830-1838.
288. Moffat ID, Boutros PC, Celius T et al. microRNAs in adult rodent liver are refractory to dioxin treatment. **Toxicological sciences : an official journal of the Society of Toxicology**. 2007;99:470-487.
289. Zhao Y, Srivastava D. A developmental view of microRNA function. **Trends Biochem Sci**. 2007;32:189-197.
290. Landgraf P, Rusu M, Sheridan R et al. A Mammalian microRNA Expression Atlas Based on Small RNA Library Sequencing. **Cell**. 2007;129:1401-1414.
291. Kuppusamy KT, Jones DC, Sperber H et al. Let-7 family of microRNA is required for maturation and adult-like metabolism in stem cell-derived cardiomyocytes. **Proc Natl Acad Sci U S A**. 2015;112:E2785-2794.
292. Tan W, Li Y, Lim SG et al. miR-106b-25/miR-17-92 clusters: polycistrons with oncogenic roles in hepatocellular carcinoma. **World J Gastroenterol**. 2014;20:5962-5972.

VITAE

Jenna Voellinger was born in Rochester, New York. In 2008, she graduated from the State University of New York at Buffalo with a B.S./M.S. degree in Pharmaceutical Science. She then joined the Department of Pharmaceutics at the University of Washington as a graduate student, and in 2009 she joined Dr. Edward Kelly's lab. Jenna was the recipient of an NIH training grant in the Pharmacological Sciences, and an NIH TL1 Multidisciplinary Clinical Research training grant.